NANOPARTICLE-BASED PLATFORM FOR EXTRACTION AND DETECTION OF CARBAPENEM-RESISTANT *E. COLI* FROM FOODS AND WATER

By

Oznur Caliskan-Aydogan

A DISSERTATION

Submitted to
Michigan State University
in partial fulfillment of the requirements
for the degree of

Biosystems Engineering – Doctor of Philosophy

2024

ABSTRACT

Antimicrobial resistance (AMR) is a growing global concern, and carbapenem-resistant *Enterobacterales* (CRE) are one of the most urgent threats due to limited antibiotic therapies. CRE, specifically carbapenemase-producing (CP) strains, are found in clinical, environmental, and food samples worldwide, causing many hospitalizations and deaths. Early detection is crucial in minimizing and controlling their detrimental impact. However, many detection techniques usually require pure culture after retrieving the pathogens from matrices, which takes several days. Thus, rapid detection of the causative bacteria directly from samples is needed for outbreak prevention. In this study, two nanoparticles, glycan-coated magnetic nanoparticles (gMNPs) and dextrin-coated gold nanoparticles (dGNPs), were used to extract and detect, respectively, CP *E. coli*, particularly those harboring *Klebsiella pneumoniae carbapenemase* (KPC), from spiked tap water and food samples. Experiments for magnetic extraction and plasmonic detection were first conducted using pure cultures of resistant *E. coli* (R) isolates and susceptible *E. coli* (S) acting as reference, followed by applying them in *E. coli*-contaminated matrices.

The gMNPs offer rapid and cost-effective extraction and concentration of bacteria. A confocal laser scanning microscopy and transmission electron microscopy (TEM) initially confirmed the binding of gMNPs to bacterial cells in a buffer solution. The gMNP-cell binding capacity was expressed as concentration factor (CF), quantified through the standard plating method. Results showed that the CF of all *E. coli* (R) isolates was lower than that of *E. coli* (S). This study further illustrated that the lower CF could be the effect of cell surface characteristics of *E. coli* (R) isolates, where they displayed heterogeneous cell shape (rod and round cells) and lower negative zeta potential (cell surface charge). In addition, bacterial load and solution pH on gMNP-cell interaction were evaluated. Results showed that the higher bacterial load and pH environment resulted in lower CF of both *E. coli* (R) and *E. coli* (S) isolates. Further, the effectiveness of gMNPs in large-volume water and food samples was tested. The gMNPs successfully extracted *E. coli* (R) and *E. coli* (S) isolates from buffer solution, tap water, and food samples (raw chicken breast, ground beef, and romaine lettuce), as confirmed by TEM and the selective plating method. The CF of both *E. coli* (R) and *E. coli* (S) in buffer solution and tap water was higher than in food samples. The variable CF in food samples could be the effect of food microparticles and natural microflora, where non-selective gMNPs may bind to plant and animal tissues and natural microflora. Whereas the gMNPs successfully extracted bacterial cells from foods and water, their

specific and rapid detection is also significant. To achieve this, a plasmonic biosensor was designed for feasibility.

Gold nanoparticle-based plasmonic biosensors have recently drawn attention due to their unique surface plasmon resonance (SPR) properties. GNPs change color upon aggregation or agglomeration, allowing for simple use without expensive and complex equipment and data analysis. This work utilized highly stable dextrin-coated GNPs to detect CP bacteria, specifically *Klebsiella pneumoniae* carbapenemase (KPC)-producing bacteria, targeting the bla_{KPC} gene. The assay only requires dGNPs, an oligonucleotide probe specific to bla_{KPC}, and DNA samples to detect the target DNA within 30 min without PCR amplification. The stability of dGNPs under an acidic environment indicates the presence of target DNA due to probe-binding and dGNPs' protection, maintaining their red appearance. The absence of target DNA was indicated by the aggregation of dGNPs, corresponding to a color change from red to blue or purple. The stability and aggregation of dGNPs were further confirmed by TEM and quantified by a shift in absorbance spectra. The plasmonic biosensor was tested in 47 bacterial isolates: 14 KPC-producing target bacteria and 33 non-target bacteria. The biosensor successfully detected and differentiated bla_{KPC}-positive bacteria, regardless of bacterial type. The diagnostic sensitivity and specificity were 79% and 97%, respectively, along with a detection limit of 2.5 ng/μL. For specific bacterial (*E. coli*) detection, an earlier developed plasmonic biosensor with a *uidA* probe was further used.

Finally, the two biosensor platforms were implemented to detect KPC-producing *E. coli* from water and food samples. Magnetically extracted bacteria from the artificially contaminated tap water, romaine lettuce, ground beef, and chicken breast samples were followed by short enrichment and DNA extraction. The plasmonic biosensors successfully detected KPC-producing *E. coli* from each sample by parallel detection targeting of *uidA* and bla_{KPC} genes, with no false positives for the samples contaminated with non-target bacteria. The biosensor successfully detected the target organism, where the original concentration prior to magnetic extraction was 10^3 CFU/mL. The biosensor results were further verified with the standard PCR test. As proof-of-concept, these findings indicate promising applications of the integrated platform for cost-effective and rapid bacterial detection from complex matrices within <7 h. The gained insights may facilitate future application of this platform; recommendations for further optimizations and studies have also been identified.

Dedicated to my beloved daughter, Sare.

ACKNOWLEDGEMENTS

First, I would like to thank my advisor, Dr. Evangelyn Alocilja, for her support and guidance during my Ph. D program. I would also like to thank my research supervisory committee members, Dr. Teresa Bergholz, Dr. Shannon Manning, Dr. Jade Mitchell, and Dr. Frances Downes (guest member) who gave their attention, knowledge, and constructive feedback throughout my study. I also specifically thank Dr. Downes for her assistance in obtaining bacterial isolates from the Michigan Department of Health and Human Services (MDHHS).

Further, I would like to thank all members of Nano-Biosensors Laboratory for their inspiration and support and help in adjusting to the lab. My special thanks go to Saad Sharief for his friendship, helpful conversations and discussion in research, assistance in PCR work and reviewing manuscripts. I would also like to thank Chloe, who helped me in taking microscopic images in this work. I also would like to thank Emma, Chelsie, Regina, and James for their helpful discussion and positive lab atmosphere, which made me enjoy my research. I would like to thank the academic specialist, Dr. Alicia Withrow, for their assistance in taking TEM images. Also, I would like to express my appreciation to the BAE family, specifically graduate program coordinator Dr. Steven Safferman and graduate secretaries Barb DeLong, Sarah Eubanks, Tara Miller, and Kate Balgoyen for being helpful during my Ph. D program.

Further, I am grateful for the scholarship that I was awarded by the Ministry of the National Education of Turkey for financial support of my doctoral program at Michigan State University. Also, this research supplies and materials were supported by the Targeted Support Grant for Technology Development (TSGTD), Michigan State University Foundation; the USDA Hatch MICL 02782; USDA Hatch Multistate NC1194 MICL 04233; and the USDA-NIFA project 2022-67017-36982.

Finally, I would like to thank my family back home and friends across the US and Turkey for their endless love, guidance, and support throughout my life. I truly thank my husband, Beytullah Aydogan, for his support. I am so thankful to have my little daughter Sare since the beginning of the Ph. D. journey. She deserves the biggest thanks; her unconditional love and energy encourage me to manage my academic and family life during this long journey.

TABLE OF CONTENTS

CHAPTER 1: INTRODUCTION AND LITERATURE REVIEW

Some parts of section 1.1 and all sections from 1.2.1 to 1.2.4.5 were published in a review article, "A Review of Carbapenem Resistance in *Enterobacterales* and Its Detection Techniques" *Microorganisms*, 2023 (10.3390/microorganisms11061491). Herein, section 1.2.1.1 of this chapter from the published paper is modified.

1.1. Problem Statement

Infectious disease outbreaks have killed thousands of people with severe negative global economic impacts. Among these, antimicrobial resistance (AMR) is a major growing concern [1]. Several microorganisms have been identified as a cause of severe common infections due to acquired resistance to one or more antimicrobials on the market [2]. Due to antimicrobial-resistant infections, it was estimated that approximately 700,000 people die each year worldwide [3], 35,000 people in the USA [4] and 33,000 people in Europe [5]. Among these, 39% of the cases were linked with last-resort antimicrobial-resistant bacteria (ARB) [5].

Carbapenems, a subclass of β-lactam antibiotics, are used as the last line of defense against severe infections, especially multi-resistant infections in healthcare [1,6]. Inevitably, the emergence and spread of carbapenem-resistant bacteria have globally increased at an alarming rate since early 2010 [6]. Carbapenem-resistant *Enterobacteriaceae* (CRE) has a higher mortality rate in humans due to a lack of alternative antibiotic treatments [6]. Based on recent reports from the World Health Organization (WHO) and the Centers for Disease Control and Prevention (CDC), CRE is on the global priority list of infections caused by ARB [1,4]. The emergence and spread of CRE are mainly a result of the rapid dissemination of carbapenemase enzymes through horizontal gene transfer (HGT). This enables the development of carbapenemase-producing (CP) bacteria cases in humans who are not using the antibiotic or are hospitalized but interact with environments and hosts colonized with CP bacteria [3].

Carbapenems, as with many antibiotics, are not entirely metabolized in the body, resulting in the transfer of residues from human excreta into hospital sewage. Due to the low concentration of antibiotics, bacteria in hospital effluent may acquire resistance, which could be accelerated through HGT [1]. Inappropriate or missing regulatory status and practices in waste water treatment plan (WWTP) systems, contaminated urban wastewater, and sewage sludge result in their accumulation and spread to the environment [5]. Thus, CP bacteria have been

reported not only in clinical samples but also in the environment. Several studies reported that CP bacteria were found in hospital and municipal wastewater, drinking water, surface and groundwater, agricultural environments, food animals, and retail food products [1,5,7–11]. Water sources and global food trade have the most direct relationship to human activities for the export of CP bacteria and their genes [7,12]. Thus, several countries have had a zero-tolerance policy and international ban on selling food items contaminated with CP bacteria [1].

In the last two decades, global surveillance programs have targeted animal-based food products that are potential sources of resistant organisms. These surveillance programs mostly focus on tracing pathogenic indicator bacteria such as *Salmonella*, *E. coli*, *Campylobacter*, and *Enterococcus* on meat products (e.g., beef, poultry, and pork) and food animals [13,14]. The surveillance has been extended to tracking CP bacteria in food animals and meat products since 2016 in the U.S. and Europe [6,13,14]. Thus, rapid identification of CP bacteria in the food chain and implementation of surveillance programs are important to prevent and control future possible endemic or pandemic outbreaks.

The current methods for the detection of ARB have multiple obstacles. Traditional antimicrobial susceptibility testing (AST) requires pure cultures of the target pathogen before testing for their resistance to different antimicrobial concentrations, taking days to weeks [15–17]. Efforts have been made to develop rapid methods to prevent and control such infections more effectively. Many rapid phenotypic (e.g., colorimetric and spectrometry-based techniques) and molecular methods (e.g., PCR-based techniques, microarrays) have been implemented to reduce detection time from days to hours with higher specificity and sensitivity [15,16,18]. However, these techniques require advanced laboratory equipment, costly reagents, data analysis, and trained personnel [15,16,18], which limits their use in low-resource settings. As antimicrobial-resistant infections are a global concern, rapid detection of the causative bacteria is paramount. Other rapid detection methods, including immunological assays and a variety of biosensors, have been developed. However, these assays are sometimes associated with costly equipment needs or may have low specificity or sensitivity once implemented in foods and clinical matrices [18–22]. Gold nanoparticles (GNPs) based colorimetric methods have been recently popular because of their simplicity, rapidity, and cost-effectiveness [23,24]; their use for the detection of ARB needs attention. Thus, this study proposed the use of GNPs to detect carbapenem-resistant bacteria.

In addition to concerns about accessible detection assays, pre-analytical sample processing (separation, enrichment, and purification) of bacteria from matrices is often a significant challenge before detection. This is typically necessary to ensure the presence of a minimum number of cells required for successful detection [25]. Traditional sample processing methods, including physical methods (e.g., centrifugation and filtration), require incubation in selective media for the isolation of target bacteria, but time-consuming. Thus, chemical and biological methods (e.g., dielectrophoresis, metal hydroxides, and immunomagnetic particles) have been developed and implemented as rapid bacterial extraction and concentration techniques directly from matrices. In practice, bacterial separation and concentration methods directly from food matrices could reduce time or the need for culture incubation (enrichment), removal of inhibitors from matrices, and applicability of separation techniques for large sample volumes [25,26]. However, these methods still face some challenges in terms of the limit of bacterial concentration and ineffective separation from complex matrices [26–28]. Among some primary alternatives, magnetic nanoparticles (MNPs) have recently been used for rapid and effective concentration of bacteria from complex samples due to their simplicity. Immunomagnetic separation (IMS) has conventionally been used to concentrate and extract target bacteria based on antigen-antibody conjugation. However, it is not efficient in many food matrices due to the blocking of the antibody by food debris and is associated with higher costs and specific storage conditions, limiting their application [28]. Recently, carbohydrate-functionalized MNPs have been used as simple, cost-effective, and rapid alternatives to IMS [26,29]. For instance, glycan-coated MNPs (gMNPs) have successfully extracted and concentrated several bacteria (e.g., *E.coli*, *Salmonella*, *Bacillus*, *Listeria*) from a variety of food matrices including milk, juice, egg, and flour [23,29,30]. However, their use for the extraction of ARB requires further attention.

The extraction of ARB from various matrices has not explicitly been documented well. While some examples exist for separating ARB from pure cultures and clinical samples [31–34], data is scare for food matrices. The antimicrobial-resistant profile of bacteria is mostly tested on pure cultures after retrieving and identifying them, which takes several days. Rapid and efficient extraction of ARB directly from matrices is needed for their rapid detection. Therefore, this study proposed the use of carbohydrate (glycan)-coated MNPs to extract carbapenem-resistant bacteria rapidly. The MNP-bacterial cell adhesion relies on cell surface characteristics: surface charge, hydrophobic or hydrophilic interactions, and receptor-ligand interaction (antibody or

lectin binding sites) [26,35,36]. Thus, cell surface characteristics are also important in understanding cell adhesion mechanisms for bacterial extraction and detection.

Cell surface characteristics of ARB have been investigated in several studies. For instance, some studies showed that the biochemical components of ARB are different from those of susceptible bacteria based on distinct fingerprint patterns. Raman Spectrum is one example where bacterial differentiation or detection was achieved using this pattern. [37,38]. Also, a variety of studies showed that alteration in the biosynthesis of cell wall material, membrane components, and cytoplasmic contents may result in changes in cell surface characteristics, including cell morphology and cell surface charge [39–43]. These cell characteristics are utilized for cell attachment, bacterial capture, and detection techniques [15–17,41,42,44,45]. The changes in cell surface characteristics might impact their adhesion or attachment to substrate surfaces on their interactions with environmental factors as well as their detection [41]. Therefore, cell surface characteristics of carbapenem-resistant bacteria need further attention in terms of cell adhesion mechanisms for the development of rapid extraction and detection assays.

This research mainly seeks to address the limitations of current bacterial extraction and detection methods by designing rapid and cost-effective assays for carbapenem-resistant bacteria. To achieve this:

- Glycan-coated magnetic nanoparticles (gMNPs) were used to extract and concentrate carbapenem-resistant bacteria (CP *E. coli*) along with cell surface characterization in terms of morphology and surface charges.
- Dextrin-coated gold nanoparticles (dGNPs)-based colorimetric (plasmonic) biosensors were used for the detection of carbapenem-resistant bacteria (CP bacteria).

The end goal of this research is to analyze the effectiveness of the two combined methodologies, capture and biosensing, for the detection of carbapenem-resistant *E. coli* directly from artificially contaminated foods and water.

The summary of the proposed study is outlined in Figure 1.1; how ARBs emerge and spread into the environment, animals, foods, and humans; foods (vegetable crops and animal-derived foods), and water as major routes affecting humans; detection of contaminated foods with ARB, specifically CP *E. coli*, using carbohydrate-coated magnetic and gold nanoparticles (bacterial extraction by gMNPs and detection by dGNPs) to make food safe and save the lives.

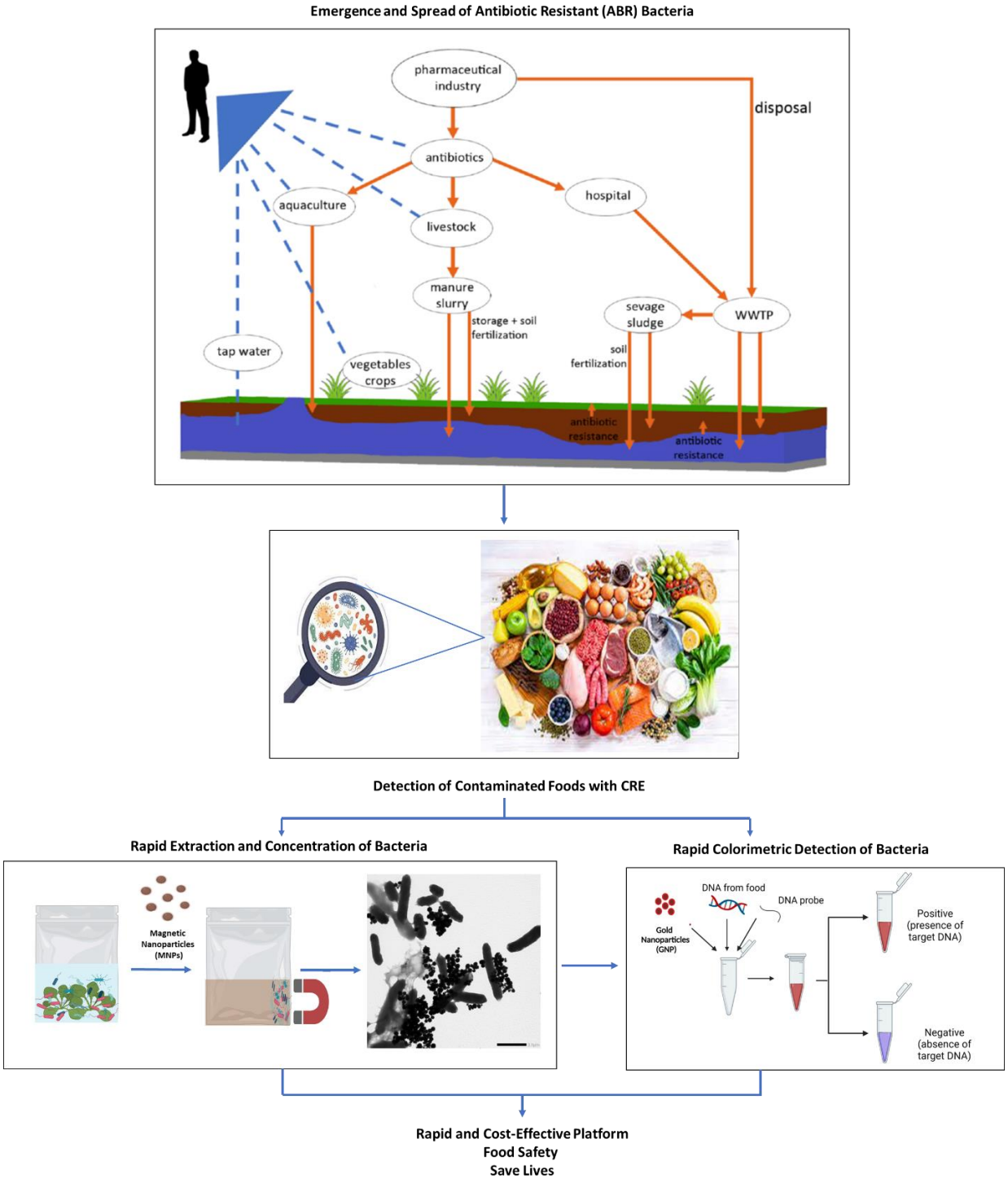

Figure 1.1. Graphical outline of the proposed study; the emergence and spread of antimicrobial-resistant bacteria (ARB) into the environment and humans; foods as a route affecting human health; detection of the contaminated foods with CRE using magnetic and gold nanoparticles as the rapid and cost-effective platform. Acknowledgment: The image above is from a study [5]; the images in the middle are from Google; the images at the bottom, along with TEM images, were created using BioRender.com.

1.2. Relevant Background

This section is divided into several sections, namely: (1) current issues with AMR, specifically carbapenem-resistant bacteria and their rapid dissemination in the environment, animals, and foods; (2) antimicrobial-resistance tracking systems; (3) current detection methods and techniques for ARB including CRE, along with their limitations and advantages; (4) gold nanoparticle-based plasmonic biosensors; (5) limitation and advantages of the current bacterial separation and extraction methods; (6) glycan-coated magnetic nanoparticle-based extraction; 7) cell surface characteristics of ARB; (8) and conclusion and knowledge gaps.

1.2.1. Introduction-Antimicrobial Resistance

Antimicrobial resistance (AMR) is acquired when microorganisms grow or survive in the presence of antimicrobials or drugs designed to kill them [4]. AMR threatens the effective prevention and treatment of a wide range of infections caused by pathogenic bacteria, viruses, parasites, and fungi. AMR has been a serious threat to public health since the beginning of the last decades [2,4,46–48].

AMR has a high potential to increase costs and destabilize the health infrastructure. A recent report by the Centers for Disease Control and Prevention (CDC) in 2019 stated that AMR kills at least 1.27 million people worldwide and is associated with approximately 5 million deaths [4,46]. In the United States (US), the CDC reported that AMR causes more than 2.8 million infections and 35,000 deaths annually [4], with a predicted annual cost of approximately USD 55 billion [49]. In Europe, AMR results in an estimated 25,000 deaths and a cost of EUR 1.5 billion in health expenditures each year [47]. In accordance with recent estimates, infections by antimicrobial-resistant microorganisms will annually result in 10 million deaths, along with USD 100 trillion in costs, by the year 2050 [50]. The problem of AMR is particularly urgent due to the high presence of unregulated antibiotics in the market [2,4,51]. The misuse and overuse of antibiotics enable the emergence and spread of resistance in bacteria, leading to more difficulty in controlling and treating infections [48].

1.2.1.1. Development of Antibiotic Resistance and Their Mechanisms

The first antibiotic, penicillin, was found by Alexander Fleming in 1928. With its release into the market in 1941, penicillin-resistant bacteria (*Staphylococcus aureus*) increased in the following year [4,52]. There has been a continued discovery of new antibiotics coupled with the

emergence of resistance, since bacteria find ways to survive and resist new antibiotics, resulting in less-effective drugs. Antibiotics have different strategies and mechanisms of action for bacterial death [4,52,53]. Accordingly, bacteria have become resistant to antibiotics through different mechanisms, and they are listed as follows: (1) restriction on the access of the antibiotic by changing the entry pathways or limiting their number, (2) activation of efflux pumps in their cell walls to remove the antibiotics that enter the cell, (3) changing or destroying the antibiotic with enzymes, (4) alteration of the targets for the antibiotic by modification of intracellular enzymes so that they can no longer latch onto it, and (5) the development of a new cell process to bypass the effects of the antibiotic [2,47,54–56]. Bacteria can also mediate tolerance to antibiotics by forming biofilms on surfaces to prevent antibiotics from penetrating through the outer cell membrane, allowing the natural growth of the bacteria [57]. Thus, once microorganisms are exposed to antibiotics, they adapt and grow in the presence of antibiotics, similar to their adaptation to a new environment[47,51].

To understand the problem of antibiotic resistance, it is helpful to discuss how antibiotic resistance is developed in a bacterial population. Development of resistance to antibiotics may be due to intrinsic (natural) or acquired resistance mechanisms or both. Intrinsic resistance is a generalizable trait that is universally found within the genome of a bacterial species, which is independent of antibiotic selective pressure [56,58,59]. In contrast, acquired resistance develops once a new trait is expressed due to a genetic change by selection in the setting of antibiotic exposure [56,60]. Herein, this review deals with acquired resistance in a bacterial population originally susceptible to antimicrobial agents. From an evolutionary perspective, bacteria acquire resistance through two major genetic strategies: 1) mutations in chromosomal genes, which are subsequently transmitted vertically as bacteria divide, and 2) acquisition of new DNA coding for resistance determinants through horizontal gene transfer (HGT) [56,60,61].

In the former route, a subset of bacterial cells from susceptible populations in the presence of antibiotics can develop mutations in genes that are often associated with the mechanism of action of the antibiotic agent, allowing preserved cell survival. When a resistant mutation emerges, the antibiotic agent eliminates the susceptible population and resistant subpopulations become dominant in size [56,58,60]. The mutational resistance is only maintained if needed in the presence of the antibiotic agent [60].

In the second way, the transmission of external genetic materials by HGT occurs through three main routes: (1) transformation (incorporation of naked DNA), where the bacterium takes infree DNA from the environment; (2) transduction (phage-mediated), where bacteriophages move short pieces of chromosomal DNA from infected bacterium to another bacterium; and (3) conjugation (cell-to-cell contact), the transfer of plasmids (circular DNA) from one bacterium to another. Conjugation is the most efficient and common way to share genetic information, always leaving behind a copy of the resistant gene, resulting in the emergence and spread of AMR [54,56–58]. HGT typically involves genes harbored on mobile genetic elements (MGEs) such as transposons and plasmids. Transposons, specialized fragments of DNA, carry several resistant genes but cannot replicate by themselves. They can move within the genome, facilitating resistant gene migration from the chromosome to the plasmid [57,58]. Finally, integrons as genetic elements can play a role in the acquisition and expression of several resistant genes but are not movable. Thus, encoding mechanisms are based on the capture of resistant genes and the excision of genes within and from the integrons. This is one of the efficient mechanisms of the accumulation of resistant genes. Integrons also provide a mechanism for adding new genes into the bacterial chromosome and are mostly carried in plasmids, increasing the horizontal mobility of the antibiotic-resistant genes [56,58,61]. Overall, HGT play a primary role in the acquisition, accumulation, and dissemination of antibiotic resistant genes in bacteria [56–58,62,63]. There is growing evidence that the presence of antibiotics or antimicrobial treatment can further induce HGT, impacting the rise of AMR [63].

1.2.1.2. Factors Converging Emergence and Transmission of Antibiotic Resistance

The development of antibiotic resistance worldwide is increasing due to the misuse and excessive use of antibiotics and antifungals, global trade networks, medical tourism, poor sanitation conditions, improper waste management systems, and urbanization [1,5,6,62,64,65]. Remarkably, the overuse and misuse of antibiotics in healthcare, veterinary medicine, agriculture, and aquaculture and their release to the environment contribute to the emergence and spread of AMR [1,5,62,64,65]. Significant sources of antimicrobial-resistant bacteria include healthcare settings and the environment. AMR can be transmitted through contact with people, animals, and contaminated water or foods [66]. In addition, intestinal commensal bacteria have been reported as a significant reservoir of antimicrobial-resistant bacteria and genes (ARGs). Due to HGT and the prior use of antibiotics, the commensal flora of humans and animals can

acquire ARGs; the fecal carriage of resistant bacteria and ARGs leads to their emergence and spreads in the community, environment, animal, and foods [66,67]. For example, the surveillance of human fecal carriage has shown a significant increase in intestinal ARG carriage worldwide [66]. In another example, animal guts can contaminate its products during animal slaughtering and food processing. The handling and consumption of contaminated food or contact with animals or their surroundings (fertilizer) cause the spread of AMR in the community and environment (soil and water), along with fruits, vegetables, etc. [4]. Thus, wastewater from human activities, healthcare services, and general population-collected wastewater treatment plants (WWTP) are sources of antimicrobials, commensal and pathogen bacteria, antibiotic-resistant bacteria, and ARGs [5]. Due to inefficient, inappropriate, or missing regulatory status and practices on WWTP systems, contaminated urban wastewater, sewage sludge, manure, sediment, and reclaimed water result in their accumulation and spread in the environment and community [5,54]. As seen in Figure 1.2, everything is connected in a complex web; the health of people is connected to the health of animals and the environment. Hence, communities, healthcare facilities, environments, food, farms, and animals are all impacted, affecting progress in healthcare and life expectancy [4,5].

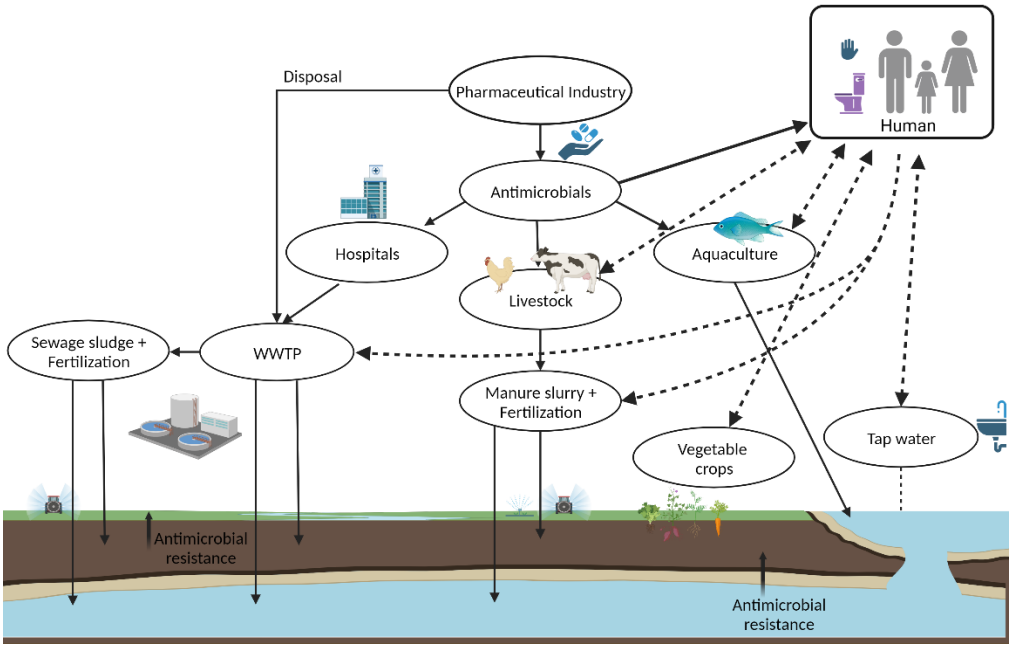

Figure 1.2. The complex web of the emergence and spread of antimicrobial resistance, which is adapted by study [5] (created with BioRender.com, accessed on 18 May 2023). WWTP: Wastewater Treatment Plant.

AMR causes threats to anyone regardless of age, to immunocompromised people, and to people with chronic illnesses [4,68]. AMR also puts at risk those who receive modern healthcare advances, such as joint replacements, organ transplants, cancer therapy, etc. These procedures have a risk of infection, and effective antibiotics may not be available [4,69]. AMR is a global crisis, and new forms of resistance emerge and rapidly spread across countries and continents through people, goods, and animals. One billion people travel through international borders every year, and a global effort is necessary to slow the emergence and spread of AMR [4,48].

1.2.2. Urgent Threat of Infections by Antimicrobial-Resistant Bacteria: Carbapenem-Resistant Bacteria

The World Health Organization (WHO) and CDC reported the current and future threat of infections by antimicrobial-resistant microorganisms with a high level of concern [4,70]. Carbapenem-resistant *Acinetobacter baumannii* (CRA), carbapenem-resistant *Pseudomonas aeruginosa* (CRP), and carbapenem-resistant *Enterobacterales* (CRE) have been listed as critical priority pathogens by the WHO [70]. In addition, CRE and CRA have been reported as the most urgent threats by the CDC since 2019 [4]. Particularly, CRE results in 1100 deaths and 13,100 infections in the USA [4], with a high fraction of these infections potentially resulting in death due to limited antibiotic therapies [4,6,69].

Carbapenems, a broad-spectrum β-lactam antibiotic, are structurally related to penicillin [71]. Carbapenems have a carbon instead of a sulfone at the fourth position of the β-lactam ring, differing from other β-lactams. The unique structure plays a major role in their stability against β-lactamases [72]. Carbapenems are not easily diffusible through the cell wall, but they enter the bacteria through outer membrane proteins (porins). Then, carbapenems degrade the cell wall at the penicillin-binding proteins (PBPs) via the β-lactam ring. The mode of action weakens the glycan backbone in the cell wall due to autolysis, and the cell is destroyed because of osmotic pressure [71–73].

Carbapenems have been used as last-line agents against Gram-negative, Gram-positive, and anaerobic bacteria [72]. The last-resort antibiotics were approved for clinical use in humans and released into the market in 1985 [4,8,74]. Carbapenems may occasionally be used for pets under certain conditions, according to the Animal Medicinal Drug Use Clarification Act (AMDUCA) [10,75]. Among carbapenems, ertapenem and panipenem have limited use against non-fermentative Gram-negative bacteria but are appropriate for community-acquired infections.

Carbapenems, including imipenem, meropenem, doripenem, and biapenem, have been widely used in hospital-acquired infections. These carbapenems are typically reserved for use in patients infected with multi-drug resistant (MDR) bacteria, including extended-spectrum β-lactamase (ESBL)-producing and ampicillinase C (AmpC)-producing bacterial infections [1,6,73], such as complicated intraabdominal and urinary infections, bloodstream and skin infections, community-acquired and nosocomial pneumonia, meningitis, and febrile pneumonia [8,76,77].

Carbapenem-resistant bacteria were first described in 1996 with the identification of carbapenemase-producing *Klebsiella pneumoniae* [1,54]. In the last decade, the emergence and spread of carbapenem-resistant bacteria have globally increased. For example, many infections caused by CRE are mostly seen in patients in hospitals, long-term care facilities, and long-term acute care hospitals [78–80]. Such infections are high risk for patients using ventilators, urinary catheters, intravenous catheters, and long-term antibiotic treatment and for immunocompromised patients [78]. A significant fraction of these infections result in death due to limited treatment options [4,6,69,81]. Specifically, bloodstream infection by CRE causes a high mortality rate in pediatric populations [77,82]. The characteristics, mechanisms, and outcomes of carbapenem-resistant bacteria are thus crucial to prevent and manage such infections [83].

CRE are *Enterobacterales* resistant to at least one of the carbapenem antibiotics based on their antibiotic susceptibility profile (phenotypic definition) [78]. There are different mechanisms (e.g., genotypic); carbapenem resistance mainly develops when bacteria (1) acquire structural changes in penicillin-binding proteins (PBPs), (2) show a decrease or loss of specific outer membrane porins that filter carbapenems from reaching their site of action, (3) activate the efflux pumps to remove the antibiotics and regulate the intramembrane environment, and (4) acquire β-lactamases and carbapenemases to degrade or hydrolyze carbapenems and other β-lactam antibiotics (e.g., penicillins and cephalosporins) [71–73,78]. In addition, carbapenem resistance can be acquired by a combination of CTX-M (activity against cefotaxime) and AmpC enzymes, allowing low-level carbapenem resistance. Further, the combination of the β-lactamase expression and porin gene mutations is associated with high-level carbapenem resistance, attenuating therapy responses [84].

Overall, CRE can become resistant through chromosomal mutations in the porin gene (non-carbapenemase-producing CRE) and/or the production of carbapenem hydrolyzing-enzymes (carbapenemase-producing (CP) CRE) [78]. The presence or expression of the gene

coding carbapenemase is usually sufficient for carbapenem resistance, covering 30% of CRE. Thus, CP-CRE is a subset of all CRE [6,78]. These genes are often on mobile genetic elements, leading to their rapid spread and resulting in infections and colonization [4,57,78,85]. Many CRE-colonized individuals do not develop infections; however, they can still spread the bacteria [78]. Similarly, the transfer of genetic elements can occur in the food chain and the environment [4,57,78]. Therefore, routine tests for these carbapenemases through the Antibiotic Resistance Laboratory Network and CDC laboratories are conducted to prevent and control their emergence and spread [78].

1.2.2.1. Carbapenemases

A large variety of carbapenemases have been classified into three groups: Ambler Classes A, B, and D β-lactamases, based on hydrolytic and inhibitor profiles using active catalytic substrates of serine or zinc [1,56,71,73,86]. The characteristics of the three most common classes of carbapenemases are detailed and listed in Table 1.1 [1,86,87].

Class A enzymes, serine β-lactamases, hydrolyze a broad variety of β-lactam antibiotics, including carbapenems, cephalosporins, penicillin, and aztreonam [86]. These enzymes were identified as chromosomally encoded and plasmid-encoded types [86]. Some of the chromosomally encoded genes are NmcA (not metalloenzyme carbapenemase A), SME (*Serratia marcescencens* enzyme), IMI-1 (imipenem hydrolyzing β-lactamase), and SFC-1 (*Serratia fonticola* carbapenemase-1). The plasmid-encoded genes are KPC (*Klebsiella pneumoniae* carbapenemase), IMI (Imipenem-hydrolyzing beta-lactamase), and GES (Guiana extended spectrum) [1,71]. Among these, the KPC type is the most prevalent enzyme and causes outbreaks in many Asian, African, North American, and European countries [1,71]. KPC gene is mainly located within a 10-kb length, mobile transposon Tn4401, frequently established on conjugative plasmids. The link of bla_{KPC} with plasmids and transposons assists in intraspecies gene transfer and the dissemination of the gene [88]. Several KPC variants have rapidly increased, and 84 KPC alleles have been recorded in the GenBank database [89]. Of these, KPC-2 and -3 are the most common enzymes worldwide, and 22 KPC variants have also conferred ESBL-, CTX-M-, or ceftazidime-avibactam (CZA)-resistance in their gene position. For example, the KPC-2 gene was carried on the NTE_{KPC}-Ib transposon on plasmids with a 15-bp insertion, which also harbored the resistance gene, CZA resistance [84,89]. Overall, KPC types are mostly found in *Klebsiella pneumoniae*, *Klebsiella oxytoca*, *E. coli*, and *Serratia marcescens*,

as well as in *Enterobacter*, *Salmonella*, and *Proteus* species [1,56,71]. Their rapid spread and diverse variants severely threaten human health and impact therapeutic efficacy [56,71,89].

Class B enzymes are known as Metallo-β-lactamases (MBL) since they utilize metal ions (usually Zinc) as a cofactor to attack the enzyme's active site (β-lactam ring). There are 10 types of MBLs; the most important ones include New Delhi Metallo-beta-lactamase (NDM), Verona Integron-Encoded Metallo-beta-lactamase (VIM), and Imipenemase (IMP) [1,71,78,90]. They hydrolyze all current β-lactam antibiotics, except for monobactams (e.g., aztreonam) [87]. IMP was first reported in Japan in *S. marcescens* in the early 1990s [56], and over 85 sequence variants have been described [87]. IMP variants are found in *Acinetobacter* and *Pseudomonas* species, as well as in the *Enterobacteriaceae* family [56,71]. VIM was then identified in *P. auregionasa* in Verona, Italy, in late 1997, and over 69 variants have been described [87]. VIM variants are mostly found in *Pseudomonas*, *Acinetobacter*, and *Enterobacteriaceae* species, which are globally distributed [56,71,87]. Recently, NDM was the most prevalent MBL, first identified in *Klebsiellea pneumoniae* and *E. coli* isolated from a patient who traveled from India to Sweden in 2008 [56,87]. There have been 29 NDM variants described, and NDM-1 is the most prevalent type. NDM variants are generally dominant in *Klebsiella pneumoniae*, *E. coli*, *Acinetobacter baumannii*, and *Pseudomonas aeruginosa* [71,87,90].

Class B enzymes are usually found in plasmid vectors or other mobile genetic elements [86]. For instance, IMP and VIM are mostly integron-associated; they are encoded by gene cassettes within class 1 or 3 integrons that may be embedded in transposons, allowing insertion into the bacterial plasmids [87]. NDM is not integron-associated; it has been observed in plasmids rapidly disseminated worldwide [87,90]. Additionally, NDM-producing bacteria can have both NDM-1 and a type IV secretion system (T4SS) gene cluster in plasmids, showing high virulence [90]. Further, NDM-producing bacteria may harbor other carbapenemases in plasmids (e.g., KPC, VIM, and OXA types) and ESBLs [56,78,84,90]. Thus, the emergence of NDM-producing bacteria with increasing variants is a significant threat to public health.

Class D enzymes, serine β-lactamases, are oxacillinase or oxacillin-hydrolyzing enzymes (OXA), comprising over 200 enzymes. OXA rapidly mutates and expands its spectrum activity; the most prevalent carbapenem-hydrolyzing enzymes are OXA-48 and OXA-181 in over 40 carbapenemase variants [74]. OXA-48 was first identified in *Klebsiella pneumoniae* in Turkey in 2001 [91,92]. Plasmids are the primary genetic elements for the transmission and propagation of

the genes; the most frequent hosts for OXA-48 are self-conjugative 60- to 70-kb plasmids [92]. Currently, OXA-48 and OXA-101 variants are mostly dominant in *Klebsiella pneumoniae* in Turkey, the Middle East, North Africa, and Europe [56,71,74,92]. However, it should be noted that OXA-producing bacteria often have low-level resistance due to weak expression, which is risky for false positive detection and suitable treatment options [92].

Table 1.1. The most common carbapenemases in bacteria with their gene location [1,86,87].

Ambler Class	Representative Gene	No of Variants	Gene Location	Bacterial Origins
A	KPC (Klebsiella pneumoniae carbapenemase)	>84	Plasmid	*K. pneumoniae*
	GES (Guiana extended spectrum)	>27	Plasmid	*P. aeruginosa*
	IMI (Imipenem-hydrolysing beta-lactamase)	>9	Chromosome	*E. cloacae*
	SME (*Serratia marcescencens* enzyme)	>5	Chromosome	*S. marcescencens*
	SFC (*Serratia fonticola* carbapenemase-1)	>1	Chromosome	*S. fonticola*
	NMC-A (not metalloenzyme carbapenemase A)	>1	Chromosome	*E. cloacae*
B	NDM (New Delhi metallo-lactamase)	>29	Plasmid	*K. pneumoniae*
	VIM (Verona integron-encoded metallo-lactamase)	>69	Plasmid	*P. aeruginosa*
	IMP (Imipenemase),	>85	Plasmid	*S. marcescencens*
	GIM (German imipenemase)	>2	Plasmid	*P. aeruginosa*
	SIM (Seoul imipenemase)	>1	Plasmid	*P. aeruginosa*
D	OXA (Oxacillin-hydrolyzing carbapenemase)	>40	Plasmid	*K. pneumoniae*

The genes coding carbapenemase in β-lactamase (*bla*) are defined as bla_{KPC}, bla_{NDM}, bla_{OXA-48}, bla_{VIM}, and bla_{IMP} [13,56,73]. These genes are found in many bacteria, such as *E. coli*, *K. pneumoniae*, *Salmonella*, *Acinetobacter*, and *Pseudomonas*. These bacteria are isolated not only from humans but also animals, food supplies, and water sources worldwide [1,85,93], detailed in the next section.

1.2.2.2. Dissemination of the Carbapenemases in Humans, Animals, Foods, and Environment

Several studies have shown that healthcare settings can lead to the spread of CP pathogens in humans [1,68,94]. Frequent hospital visits and long-term stays in healthcare facilities represent a high risk of colonization and infection development with CP bacteria, particularly with CP-CRE [1,68]. For instance, KPC-producing *K. pneumoniae* caused hospital outbreaks in many European countries such as Greece, Italy, Spain, France, and Germany [95–97]; NDM and KPC-producing *K. pneumoniae* were identified in transplanted patients in Brazil [98]; CP-CRE were found to spread in hospital and community settings in Africa [99–101] and Asia [94,102,103]. Another factor of CP-CRE spread is international travel and medical tourism

[1]. For instance, KPC-producing *K. pneumoniae* and *E. cloacae* were isolated from patients in New York who had recently traveled from France and Greece [104,105]. In another example, NDM-producing *K. pneumoniae* and *E. coli* were isolated from Sweden and UK patients who recently traveled to India [106,107].

Among CP-CRE, *E. coli* and *K. pneumoniae* have been disseminated globally at an alarming rate in the medical community as critical human pathogens [108,109]. For instance, KPC-producing *K. pneumoniae* has been found in more than 100 different sequence types (STs). Particularly, *K. pneumoniae* ST258 is predominant and primarily associated with KPC-2 and KPC-3 production. ST258 comprises two distinct lineages, clades I and II, and ST258 is a hybrid clonal complex created by a large recombination event between ST11 and ST442 [109]. Further, ST11, ST340, and ST512 are single-locus variants of ST258 and harbor carbapenemases. ST11 is closely related to ST258, which is associated with KPC, NDM, VIM, IMP, and OXA-48 production [109].

Further, carbapenem resistance in pathogenic *E. coli* is a major concern because of limited therapy. For instance, *E. coli* ST131, causing severe urinary infections, has been linked to the rapid global increase in AMR among *E. coli* strains [108]. Further, FimH30 lineage and virotype C are the common lineage among ST131, contributing to the spread of ST131 associated with carbapenemases. ST131 is most likely responsible for the global distribution of *E.coli* with KPC, NDM, and OXA-48 production [108]. These sequence types of *E. coli* and *K. pneumoniae* pose a major threat to public health because of their worldwide distribution [108,109].

Additionally, hospitals or health-care settings are a reservoir for CP bacteria. Carbapenem residues in human excreta can get into hospital sewage. Due to the selection of a low concentration of antibiotics, bacteria in hospital effluent can become resistant to carbapenems [1]. Hospital sewage may act as a reservoir for resistance genes, where bacteria likely acquire resistance through HGT [1,68]. Likewise, antibiotic residues and resistant genes released into municipal wastewater could contribute to the selection of CRE and their dissemination to ground and surface water, spreading them to the environment [1]. For example, CP *E. coli*, *E. cloacae*, *K. pneumoniae*, and *Citrobacter freundii* were found in the river and hospital sewage in Portugal [110], China [111], Vietnam [112], and Australia [113,114]. VIM- and KPC-producing *E. coli* were found in seven waste water treatment plants in the USA [115];

OXA-48 carrying CRE in tap water was found in six states in the USA [114]. In addition, KPC-producing *Salmonella* was found in human feces, hospital sewage, and effluent in the USA and Brazil [116,117].

Another possible way of CP bacteria transmission to animals and farms is through direct contact with colonized hosts (human and animal) and a contaminated environment (surface water, ground water, soil) [1]. CP bacteria *(E. coli*, *K. pneumoniae*, *Salmonella*, *Acinetobacter*, *Pseudomonas*) have been detected in farm animals, poultry, fish, mollusks, and wild birds and animals [1,85,93,118–124]. The transmission of CP bacteria also alerts food safety, particularly CRE in the food-chain. For instance, CP bacteria were isolated in meat (beef, chicken, pork), seafood (clam, fish, prawn), and vegetables (lettuce, spinach, Chinese cabbage, roselle) [79,125–130]. These studies showed major carbapenemases (NDM, VIM, and KPC) present in foods. The presence of CP bacteria in the food chain mainly contributes to their spread worldwide due to the global food trade, posing a risk to human health [129].

Various environmental, microbiological, and clinical investigations have shown that CP-CRE can widely spread in the community, animal and agricultural products, and the environment [1,7,10,12,119,131]. For the early detection and optimal management of the spread and emergence of CRE, some recommendations include (1) the necessity of screening and rapid diagnostic tools for patients who may have visited countries or hospitals with frequent infection by CRE, (2) specific policies and prioritizing funding for the control and management of infections by CRE, (3) clear strategies indicating the use of carbapenems, and 4) international co-operation to reduce the global spread of CRE [132]. Due to the major threat of CP-CRE infections and the colonization to public health with global economic and security implications, their rapid diagnostic surveillance is of utmost importance [6,13,14].

1.2.3. Surveillance Systems for Control of Antimicrobial Resistance (AMR) Including CRE

The WHO initiated the Global Antimicrobial Resistance and Surveillance System (GLASS) in 2015 to strengthen knowledge and develop strategies against AMR [133]. The GLASS has supported a standardized approach for collecting, analyzing, and sharing data regarding antimicrobial resistance at global, national, regional, and local levels. The system provides surveillance approaches with epidemiological, clinical, and population-level data. It incorporates data on AMR in humans, antimicrobial medicines, and AMR in the food chain and the environment [133].

The GLASS has partnerships with the WHO AMR Surveillance and Quality Assessment Collaborating Centers Network (WHO AMR Surveillance CC Network) [133]. This network has a strong collaboration with AMR regional networks, such as the Central Asian and European Surveillance of Antimicrobial Resistance (CAESAR), the European Antimicrobial Resistance Surveillance Network (EARS-Net), the Latin American Network for Antimicrobial Resistance Surveillance (Rede Latinoamericana de Vigilancia de la Resistencia a los Antimicrobianos (ReLAVRA)), and the Western Pacific Regional Antimicrobial Consumption Surveillance System (WPRACSS) [133].

The CDC also tracks AMR threats and collects data on human infections, pathogens, and risk factors with domestic and international partners. This allows for strengthening and sharing among networks of the collected data submitted to WHO [13]. AMR tracking systems of the CDC are the National Antimicrobial Resistance and Monitoring Systems for Enteric Bacteria (NARMS) and the Antibiotic Resistance Laboratory Network (AR Lab Network). The NARM was established in 1996 by the CDC, FDA, and the United States Department of Agriculture (USDA) in partnership with the government to track antibiotic resistance in pathogens from humans, retail meats, and food-producing animals (42,121). The AR Lab Network was established in 2016, which supports lab testing in healthcare, community, food, and the environment (e.g., water and soil) [13]. The Global Antimicrobial Resistance Laboratory and Response Network (Global AR Lab and Response Network) of the CDC was established in 2021 to improve the detection of existing and emerging AMR threats in humans, foods, animals, and the environment globally [13].

The CDC tracks resistant bacteria (*Salmonella*, *Shigella*, *Campylobacter*, *Vibrio*, and *E. coli* O157) in infected patients [13]. The FDA checks retail meats from grocery stores (chicken, ground beef, ground turkey, pork, shrimp, tilapia, and salmon) for *Salmonella*, *E. coli*, *Campylobacter*, *Vibrio*, *Enterococcus*, and *Aeromonas*. The USDA, along with FSIS and Agricultural Research Services (ARS), tracks *Salmonella*, *E.coli*, *Campylobacter*, *Vibrio*, and *Enterococcus* in food animals at slaughter (chickens, turkeys, cattle, swine) [13,134]. The CDC tests these specified bacterial isolates to determine their resistance profile and routinely tests 12 classes of antibiotics depending on the bacterial type. Among the antibiotics, aminoglycosides, penicillin, carbapenems, macrolides, β-lactam combination agents, cephems, and tetracyclines

are commonly used for resistant profile testing. Recently, carbapenems have been added to the list to screen the AMR profile in *Salmonella*, *Shigella*, *E.coli*, and *Vibrio* [13].

The surveillance programs also aid in preventing and controlling possible future outbreaks from food and water sources; foodborne pathogens and their resistant profile, including CP bacteria, are tracked in many countries [6,13,14]. As infections caused by particularly CRE are a global concern, the rapid detection of the causative bacteria is of utmost importance [10,83,132].

1.2.4. Current and Emerging Detection Techniques of CRE

Diagnostic tests assist in screening or monitoring specific infections or conditions to control and prevent CRE spread in the community. However, diagnostic AST protocols usually start with identifying the bacteria species in selective media, followed by growth in the presence of antibiotics (carbapenem) for determining their antibiotic-resistant profile [4,135]. However, each hour of delay in obtaining a correct diagnosis and appropriate antibiotic treatment of infections by CRE increases the mortality rate by approximately 8% [136]. For instance, delayed diagnosis and treatment in CP-CRE raise the mortality risk from 0.9% to 3.7%, hospital cost from ~USD 10,000 to ~USD 25,000, and hospital stay from 5.1 days to 8.5 days [80,137]. Thus, rapid and accurate detection is a significant step in controlling and preventing such microbial infections. Several culture-based, rapid phenotypic, genotypic methods, and biosensors have been developed to detect carbapenem resistance, including carbapenem-hydrolyzing enzymes, detailed in this section with advantages and limitations.

1.2.4.1. Culture-Based Methods

Antimicrobial susceptibility testing (AST) is widely used in clinical and public health laboratories to assess the antimicrobial resistance profiles of target microorganisms. The standard culture-based AST methods include broth and agar dilution tests, disk diffusion, and E-tests. These tests, approved by the Food and Drug Administration (FDA), involve the isolation of pure cultures of the potential pathogens, followed by testing these bacteria on media with minimum inhibitory concentration (MIC) levels [15–17,135]. Specifically, disk diffusion is a gold standard for AST; bacteria are inoculated on agar plates with a single antibiotic disk and then incubated to determine the resistant profile. Among carbapenems, imipenem, meropenem, and ertapenem have been commonly used for the early detection of carbapenem resistance; ertapenem has been

described as the most sensitive indicator [138]. To determine the susceptible, intermediate, and resistant profile of tested bacteria, the most widely used standard interpretation of AST and breakpoints are recommended by the Clinical and Laboratory Standards Institute (CLSI) and European Committee for Antimicrobial Susceptibility Testing (EUCAST) [139].

AST disk diffusion and E-test combination with specific inhibitors have been used to differentiate the carbapenem-hydrolyzing enzymes from two main types, KPC and MBLs [140]. Examples of this are the addition of chelating agents, such as EDTA, in the broth microdilution and E-test aids in confirming the presence of MBLs with binding zinc ions and inhibiting MBL activities [86,141]. The sensitivity and specificity of this test are reported to be >82% and >97%, respectively [140]. Similarly, phenyl-boronic acid (PBA) is incorporated into the E-test for KPC identification by the inhibition of KPC activity. This test's sensitivity and specificity are reported as 92% and 100%, respectively [140]. Multidisc diffusion tests with inhibitors of specific enzyme types, including clavulanate for ESBL and cloxacillin for AmpC, are also used to differentiate enzymes [71,140,141].

Modified Hodge Test (MHT) was developed to identify the presence of carbapenemases [142,143]. The MHT was first introduced in 2010 for detecting carbapenemase genes and was widely used because of its ability to detect KPC producers. In this method, the suspected bacteria are inoculated by swabbing a straight line from the edge of the meropenem disk on Mueller Hilton Agar (MHA) that is pre-inoculated with susceptible *E. coli*. The plates are incubated overnight, and the cloverleaf-like zone is observed for CP isolates. The use of this method was recommended by CLSI in 2009. It has good sensitivity for other carbapenemases (VIM, IMP, and OXA-48), although its performance in detecting NDM enzymes was found to be lower [141,143]. Overall, its sensitivity and specificity were found to be 69% [143] and 93–98% [140], respectively.

Carbapenemase inactivation method (CIM) has been recently introduced by CLSI (2016) with higher accuracy and accessibility [140,141,144]. This method is initiated by a suspension of bacteria in a broth and incubation with a meropenem disk (2–4 h); if the isolate produces the enzymes, the meropenem in the disk is degraded. The disk in the broth can then be placed on MHA streaked with susceptible *E. coli* and incubated, which detects carbapenemase activity with no zone or a narrow zone diameter of <19 nm [140,141,144]. This method showed high concordance with results obtained by a PCR test, which is used in many clinical and public

health laboratories [140,141]. The sensitivity and specificity of the CIM method were over 95% [140,144].

Specific media have also been designed for CP strain screening [71,145,146]. For example, Chromogenic Media and Brilliance CRE Agar are used for the initial detection of CRE strains in colonized and infected patients, with 76.5% sensitivity. CHROM agar KPC is used to screen for KPC and VIM-producing *Enterobacteriaceae*, but it can detect high-level resistance with 43% sensitivity. SUPERCARBA medium is mainly used for KPC and OXA-48 producers and is applicable to detect low-level resistance with higher sensitivity (96.5%) [145–147]. ID Carba and Colorex KPC media were designed for CP Enterobacteriaceae [145]. All these selective media are directly applicable to patient samples; however, they have lower specificity (>50%) depending on the enzyme type [145,147,148].

The mentioned culture-based methods are cost-effective and widely applicable. Among these methods, the CIM has a higher sensitivity and specificity in identifying and typing carbapenemases. However, they are labor-intensive and require time-consuming steps to isolate pure cultures, taking days to weeks to determine the resistance profile of the suspected bacteria [15,16,135].

1.2.4.2. Rapid Phenotypic Methods

Automated AST systems, which are rapid culture-based methods, have been developed to shorten the required time to detect antimicrobial resistance [16,138]. For example, FDA-approved commercial automated instruments are MicroScanWalkAway and Vitek-1/Vitek-2, which measure bacterial growth in the presence of antibiotics by recording bacterial turbidity using a photometer [16,71]. Further, BD Phoenix measures bacterial growth in the presence of antibiotics by recording bacterial turbidity and colorimetric changes. Sensititrere records bacterial growth with antibiotics by measuring fluorescence [16]. Besides imaging-based technologies, automated microscopes, such as multiplexed automated digital microscopy (MADM) that is FDA approved, single cell-morphological analysis (SCMA), oCelloscope, Fluorescence microscopy, and cell lysis-based methods are also used. These automated microscopes measure the phenotypic response, changes in bacterial growth rate, and the cellular morphology and structure profile of bacteria in the presence of antibiotics [16,17,71].

Optical techniques have also been developed, which measure the physical and biochemical profile of bacterial cells [149]. For example, forward laser light scatters (FLLS) and

rapid electro-optical technology have been used to measure bacterial numbers by optical density and to estimate cell density and size using light scattering of the cell particles in a liquid [16,135,150]. Another optical technique, flow cytometry (FC), is used for cell counting and the detection of a biomarker using changes in morpho-functional and physiological characteristics of cells [16,151,152]. Additionally, Raman spectroscopic analysis has been recently used to measure and compare the spectra of bacteria in the presence of antibiotics to distinguish resistant strains [17,22,135]. Further, several miniaturized lab-on-a-chip systems have also been fabricated using microfluidic techniques, substituting agar to measure the growth of pure bacteria in the presence of antibiotics for rapid testing [16,135]. An ultraviolet (UV) spectrophotometric method was developed to measure the carbapenem imipenem hydrolysis activity of CP bacteria [153]. Lastly, bioluminescence-based detection assays (BCDA) have also been developed for CP bacteria based on adenosine triphosphate (ATP) level differences in culture media. Such assays are rapid (<2.5 h) and accurate, with higher specificity and sensitivity [154]. However, the applicability of this technique in matrices is low due to reduced sensitivity [18,141,153,154].

Matrix-assisted laser desorption/ionization time-of-flight mass spectrometry (MALDI-TOF MS) in optical techniques has recently become popular for identifying pathogens and resistant bacteria due to its distinct fingerprint spectra [17,151]. To determine the antimicrobial resistant profile in pathogens, MALDI-TOF MS identifies (1) the antimicrobial-resistant clonal group (e.g., carbapenem-resistant *E. coli*), the modified antimicrobial drug (e.g., carbapenemase activity), the modified antimicrobial target (e.g., lipid A modification), the direct detection of the AMR determinant (e.g., KPC-2 β-lactamases), and biomarkers co-expressed with the AMR determinants (e.g., bla_{KPC} carrying plasmid)[155]. This technique identifies specific resistant profiles (e.g., KPC and MBLs) of bacteria at the species and genus level from single isolated colonies within 1–4 h, with 72.5–100% sensitivity and 98–100% specificity; however, it has issues regarding OXA-48 identification [18,77,155]. Further, the combination of automation and the implementation of a user-friendly interface recently made MALDI-TOF MS popular in clinical laboratories [18,156–158].

Colorimetric assays have also been developed as rapid, simple, and cost-effective phenotypic methods for detecting CP bacteria based on their carbapenemase hydrolytic activity [96,140,141]. The Carba NP test (2 h) measures the hydrolysis of imipenem, leading to changes in pH and resulting in a color change from red to yellow/orange. The sensitivity of this test was

found to be 73–100% for most carbapenemases, but it performed poorly in the detection of the OXA-48 enzyme [96,140,141]. The Carba NP test has been recommended for use as a first-line test for screening carbapenemase activity by the CLSI in the US. The RAPIDEC Carba NP test (first commercial test), β-CARBA test, Rapid CARB screen, Rapid Carb Blue kit, and Neo-CARB kit have been used to detect CP bacteria within 2 h, with varying sensitivity (>70%) and specificity (>89%) from the pure culture [18,141,159]. However, these assays require pure cultures and are dependent on the growth rate of the bacteria [18].

Many of these rapid phenotypic techniques and automated systems still require pure cultures; thus, sample preparation and pre-treatment steps require several hours to days [18,149]. Last but not least, these techniques require costly equipment, complex data analysis, and skilled personnel, which limits their applicability in low-resource setting laboratories [16,17,135,151].

1.2.4.3. Genotypic Methods

Molecular AST methods are effective techniques to detect specific resistant genes in a short time from matrices without the need for a tedious bacterial culture and a long incubation time [18,149]. Among these, PCR-based methods, DNA microarray and chips, whole genome sequencing (WGS), loop-mediated isothermal amplification (LAMP), and fluorescence in situ hybridization (FISH) methods are the main techniques used for the detection of the antimicrobial-resistant profile [17,135,151].

PCR-based methods are among the most efficient and widely used rapid molecular tools to quantify and profile genes encoding resistance in species and genus levels. This method amplifies the target nucleic acid sequence using specific primers that anneal to single-stranded DNA after denaturing the target DNA at a high temperature [160,161]. Advancements in PCR offer a more rapid and robust variation of this technique, such as real-time or quantitative PCR (qPCR), reverse transcriptase PCR (RT-PCR), digital PCR, multiplex PCR (mPCR), and automated PCR. For instance, mPCR offers the advantage of the simultaneous detection of multiple resistant genes through the use of multiple sets of primers [18,135,151,162]. Real-time PCR, or qPCR, allows for the rapid simultaneous detection and quantification of amplified PCR products using fluorescent dyes, eliminating gel electrophoresis [135,163,164]. Automated systems of PCR or qPCR are commercially available and automatically purify the sample, concentrate DNA, and amplify and detect major bacterial genes, confirming antibiotic resistance in less than two hours [135,165].

For two decades, PCR-based techniques have been used as the gold standard for the detection of β-lactam resistant genes in *Enterobacteriaceae*. For example, multiplex PCR was developed to detect 11 acquired genes encoding carbapenemase (*bla*$_{IMP}$, *bla*$_{VIM,}$ *bla*$_{NDM}$, *bla*$_{SPM}$, *bla*$_{AIM}$, *bla*$_{DIM}$, *bla*$_{GIM}$, *bla*$_{SIM}$ *bla*$_{KPC,}$ *bla*$_{BIC}$, and *bla*$_{OXA-48}$) using three different multiplex reaction mixtures [18,141,166]. Several automated systems were also developed to identify the target genes [18,141,166]. Real-time multiplex PCR or qPCR systems allow a combination of amplification and detection in a single step, limiting contamination risks. GeneXpert is an automated real-time PCR platform that uses the Carba-R assay and can detect and quantify numerous bacterial species and several carbapenemase genes from rectal samples [18,167]. The Check-Direct assay has a panel of different multiplex real-time PCR kits using several probes, including narrow and broad-spectrum B-lactamase genes [18,141,168]. A broad range of multiplex PCR panels was developed to increase their analytical performance without requiring skilled personnel. However, these PCR-based tests are expensive, limiting their use in low-resource laboratories [18].

Other molecular methods such as FISH, microarray, WGS, and LAMP assays have also been used for detecting carbapenem resistance [135,151,169]. FISH is a technique for detecting specific RNA or DNA sequences using dye-labeled oligonucleotide probes visualized by fluorescence microscopy [170]. Microarray-based methods utilize multiple spots on a solid support chip for different oligonucleotides corresponding to resistant genes to detect labeled DNA fragments in a single assay [171]. In the whole genome sequencing (WGS) technique, a whole bacterial sequence is screened for antibiotic-resistant genes and compared with known genes in publicly available databases, allowing the prediction of existing and emerging phenotypic and genotypic resistance [172]. Lastly, the LAMP assay is a simple amplification technique that resolves PCR temperature cycling using a single temperature for target gene amplification. This method produces a large number of DNA copies in a short period [173,174]. LAMP has been used as an alternative to PCR due to its simplicity and cost-effectiveness, especially in low-resource setting laboratories. However, the technique still requires a complex primer design [17,135,169].

Emerging molecular techniques and automated systems have been improved to reduce costs and the detection system for β-lactam resistant genes [18,141]. Luminex tech, for example, is a well-established approach based on a colored microsphere-based flow cytometry

assay. The method can detect specific alleles, antibodies, or peptides from a single colony [175]. The multiplex oligonucleotide ligation-PCR procedure assists in detecting β-lactam resistant genes and their variations with higher sensitivity and specificity (100% and 99.4%) within 5 h [18]. Further, the LAMP method, using hydroxy naphtol blue dye (LAMP-HNB) and microarray techniques, detects genes encoding carbapenemase with higher specificity and sensitivity at 100% and >90%, respectively [135,141,173,174]. Multiplexed paper-based Bac-PAC is another assay used to categorize the AMR profile of individual strains of CRE by providing a colorimetric readout [176]. The RNA-targeted molecular approach, NucliSENS EasyQKPC test, has also been used for detecting bla_{KPC} variants within 2 h, at a 93.3% sensitivity and 99% specificity [177]. Another technique, PCR amplification coupled with electrospray ionization mass spectrometry (PCR-ESI-MS), has been used to accurately measure exact molecular masses. With advanced software, the sequence of DNA fragments is reconstructed for accurate identification as well as subtyping of the resistant genes. This technique has been used to identify bla_{KPC} genes directly from clinical samples in 4–6 h [178]. Lastly, whole genome sequencing methods have been used as the most reliable technique to detect carbapenemase, but the high cost, longer turn-around time, and complex data management limit their use [135,141,179].

Genotypic methods generally offer key advantages, including higher sensitivity and specificity in a short time, increasing their real-world applicability. However, these methods require costly reagents and equipment and need skilled operators [16,135,149,180]. In addition, their sensitivity and selectivity can be affected by specimen debris, resulting in the inhibition of the reaction or false positives [18,135]. Another limitation of many molecular assays is that only known genes can be targeted; phenotypic resistance may be missed by molecular assays, but WGS can help discover novel genes [17,135,149,160]. Further, the limited number of targeted genes is a challenge in molecular tests due to the diversity of carbapenemase-encoding genes. Thus, the target gene is mainly based on the most relevant variant in each geographical area. For example, several commercial kits stated have been developed to detect bla_{KPC}, the most prevalent carbapenemase in the USA, and may not be used for other genes [18].

1.2.4.4. Rapid Serological (Immunological) Methods

Immunological assays rely on antibody–antigen reactions to detect bacteria, providing rapid results at a moderate cost [181]. A few methods, including latex agglutination and immunochromatographic assays, have generally been used for the detection of methicillin-

resistant *Staphylococcus aureus* (MRSA) [135]. Enzyme-linked immunosorbent assay (ELISA) has also been used to detect either genes or proteins by the combination of the PCR amplification of samples [135,169], which aids in detecting MRSA and CRE [135]. Additionally, a lateral-flow immunochromatographic assay, OXA-48K-SeT, was designed based on the immunological capture of two epitopes that are specific to OXA-48 variants, using colloidal GNPs in 15 min. It has 100% sensitivity and specificity with a detection limit of 10^6 CFU/mL [181]. In another study, a lateral-flow immunochromatographic assay was used to detect the carbapenem-resistant gene, $bla_{OXA\text{-}23\text{-}like}$, using multiple cross displacement amplification from pure culture as well as clinical sputum samples [182].

Further, a multiplex immunochromatographic test, ICT RESIST-4 O.K.N.V. K-SeT, uses monoclonal antibodies to rapidly detect OXA-48 variants, KPC, NDM, and VIM carbapenemases. This assay has 99.2% sensitivity and 100% specificity from pure culture on Mueller Hilton Agar (MHA) [21]. The immunological assays depend on the level of protein production; accurate results require an enrichment of 18 h [21,181]. However, the diversity of carbapenemase can prevent further developments since initially designed antibodies may not be applicable for targeted antigenic site modification [18]. Although it is a rapid test, it is still costly [18,21], with lower sensitivity and specificity in complex matrices [18,135,169].

1.2.4.5. Biosensing Techniques

Biosensors, as analytical devices, have emerged as alternative techniques for simple, rapid, cost-effective, and reliable pathogen detection. Biosensors utilize biological or chemical reactions and convert the recognition event into measurable signals for the detection of the target analyte [183,184]. Biosensor types are classified based on their data output system, target analyte, and label dependence [185]. Mainly, biosensors are classified as thermal, mechanical, electrochemical, and optical based on their operating mechanism [151]. Several biosensor applications, particularly electrochemical and optical biosensors, are well documented, but few studies have been developed for antibiotic resistance, especially for carbapenem-resistant bacteria. Biosensor platforms often share the same mechanism, advantages, and disadvantages, and for the purpose of this brief overview, popular electrochemical and optical biosensors are elaborated on. Examples of antibiotic-resistant detection studies are discussed.

Electrochemical biosensors utilize the electrical response of bacterial cells; the immobilized bio-recognition element on an electrode interacts with the target, resulting in an

electrical signal. Various recognition elements (antibody, phage, aptamer, DNA, etc.), nanoparticles, and signal processing techniques have been used [151,185]. For example, DNA-based biosensors typically use single-stranded DNA immobilized on an electrode with a sequence complementary to the target DNA. The difference between the electrical properties of single-stranded DNA and hybridized double-stranded DNA assists in the detection of the specific target using cyclic voltammetry [186]. Numerous electrochemical biosensors have been used to detect antibiotic resistance. Examples include a study that combined nitrogen-doped graphene with GNPs to detect the human multidrug-resistant gene *MDR1* [187]. In another study, an electrochemical DNA-sensing system identified MRSA based on a MNP/DNA/AuNP hybridization complex using a chronoamperometric signal [188]. Another electrochemical sensor utilized an antibody conjugated with MNPs to detect MRSA from nasal swabs [33]. A label-free electrochemical biosensor detected a PCR amplified bla_{NDM} gene in carbapenem-resistant *Citrobacter freundii* using impedance spectroscopy [189]. In another study, bla_{KPC} detection was achieved in *K. pneumoniae* and *E. coli* using voltammetry techniques and sandwich hybridization assays in 45 min at a level of 10^4 CFU/mL [80].

Optical biosensors are widely used platforms for bacterial detection and rely on measuring absorbance, fluorescence, Raman scattering, surface plasmon resonance (SPR), and colorimetry [151]. These biosensors are highly sensitive but can be costly. Surface plasmon resonance (SPR) is the most commonly used assay, which utilizes refractive index measurements due to the excitation of the surface plasmon waves by the interaction of an analyte with its ligand [190]. The technique mainly uses antibodies or DNA as a recognition element. For example, the immobilized single-stranded DNA sequences on the surface bind to their complementary sequence upon hybridization, resulting in a change in plasmon resonance [190]. Raman scattering techniques are also common and measure molecular vibrational, rotational, and low-frequency modes, providing characteristic information about carbohydrates, lipids, proteins, and nucleic acids [22,151,169]. However, they require a higher bacterial concentration and are limited in differentiating closer spectral signals. Recently, the Surface-Enhanced Raman Scattering technique (SERS) has been developed using nanoparticles that enhance Raman signals [22]. This assay can differentiate strains of carbapenem-resistant and susceptible *E.coli* using silver nanoparticles [22], gold nanostars [191], and gold and silver nanorods [192] by comparing

their SERS spectral signature with higher specificity and sensitivity. However, these optical biosensors require complex and multivariate data analysis.

The performance of these optical and electrochemical biosensors often depends on the detection limit, sensitivity, specificity, reproducibility, interference response, response time, storage, and operational stability [183,184]. These platforms are highly rapid and often sensitive to their target bacteria. They also reduce or eliminate isolation and culture times, allowing direct measurements from clinical and biological samples [151,169]. However, sensitivity at low-level bacterial loads is still challenging for many biosensor platforms, along with their costly and complex techniques for signal measurements and analysis [151].

Plasmonic biosensors that allow colorimetric detection are noteworthy; they offer rapid and simple visual detection within one hour without the necessity of complex and costly equipment [23,193,194]. For example, a study used a plasmonic nanosensor for the colorimetric detection of CP pathogens using gold nanoparticles (GNP) based on carbapenemase activity and pH changes [19]. Here, the GNPs changed color in response to pH and turned to purple, blue, or gray, from red, within 15 min. CRE was detected at a concentration of more than 10^5 CFU/mL directly from urine and sputum samples within 2.5–3 h. The results were easily distinguished visually and confirmed quantitatively using vis-NIR spectroscopy [19]. Further, DNA-based plasmonic biosensors using GNPs have extensively been used to detect target bacterial DNA. For instance, thiol-capped GNPs were used to detect *Klebsiella pneumoniae* within one hour using an amplified K2A gene [193] and the unamplified DNA of uropathogenic *E. coli* [195]. Dextrin-coated GNPs (dGNPs) were used earlier to detect the unamplified DNA of *E. coli* O157:H7 [23], *E.coli* [196], Salmonella *Enteritidis* [197], and *Pseudoperonospora cubensis* [198] within 30 min. Plasmonic biosensors allow the detection of pathogens in a short time without complex and costly equipment requirements. However, further attention is needed to detect ARB to improve their accessibility and applicability.

Table 1.2. The advantages and limitations of the current and emerging detection techniques for the most common carbapenemases (carbapenem-hydrolyzing enzymes).

Techniques	Advantages	Limitations
Culture-based methods	**Simple and cost-effective**	**Time-consuming (>24 h)**
1. Improved AST tests: E-test or disk diffusion test [71,140,141]	Detect KPC and MBLs with good sensitivity (>82%) and specificity (>95%)	Insufficient for OXA-48 Require specific reagents and pure culture
2. Modified Hodge Test (MHT) * [141,143]	Detects KPC with good sensitivity (>69% and specificity (>90%)	Insufficient for MBLs Requires pure culture
3. Carbapenem-inactivation methods (CIM) * [140,141]	Detect all carbapenemases with higher sensitivity (>90%) and specificity (>95%)	Require pure culture
4. Selective media: SUPERCARBA, Colorex KPC, ID Carba, CHROM agar KPC, etc. [145–147]	Detect carbapenemases from direct patient samples SUPERCARBA has higher sensitivity (>96.5%)	Variable sensitivity (40–96.5%) and specificity (>50%)
Rapid phenotypic methods	**Rapid (<24 h)**	**Costly equipment**
1. Colorimetric assay: CarbaNP test and its automated kits * [96,140,141]	Detect carbapenemases with good sensitivity (>70%) and specificity (>80%) Simple, rapid (<2 h), and cost-effective No equipment requirement	Insufficient for OXA-48 Require pure culture
2. MALDI-TOF MS * [18,156,157]	Rapidly (1–4 h) detects KPC and MBLs with good sensitivity (>72.5%) and specificity (>95%) Low-measurement cost and simple	Requires data analysis Insufficient for OXA-48 Requires single isolated colonies
3. Emerging techniques: BCDA, FC, microfluidic techniques, and Raman spectroscopic techniques [18,22,149,152,154]	Simple and rapid (<4 h) Good sensitivity (>80%) and specificity (>90%) from pure culture	Lower applicability on specimens Insufficient work on carbapenemases

Table 1.2 (cont'd)

Genotypic methods	**Rapid and highly specific (>90%) and sensitive (>90%)**	**Costly and complex equipment**
1. PCR-based methods: qPCR, RT-PCR, mPCR, automated PCR (Xpert system, Check-Direct, and Carba-R-assay) [18,162,166] *	Gold standard and rapid (<4 h) Detect and type all carbapenemases directly from specimens	High technical requirements and specific reagents High measurement cost
2. Loop-mediated isothermal amplification (LAMP) [18,173]	Simple and moderate cost Applicable in low-resource settings	Specific reagents and complex primer design
3. Whole genome sequencing (WGS) [18,172] *	Discovers a new resistance mechanism	Longer turn-around time Complex data management
4. Emerging techniques: FISH, microarray techniques, PCR-ESI-MS, and NucliSENS EasyQKPC [18,149,174]	Rapid (<6 h) Detect carbapenemases	Require specific equipment and reagents Insufficient work on carbapenemases
Immunological methods Enzyme-linked immunosorbent assay (ELISA), an Immunochromatographic assay [18,135,169,182]	Rapid and moderate cost Poor sensitivity and specificity directly from specimens	Complex and difficult antibody design due to antigenic site modification
Biosensors: Emerging technology	**Rapid, simple, and cost-effective**	**Specific equipment**
1. Electrochemical assays: Impedimetric, potentiometric, and voltammetric [80,186,189] **2.** Optical assays: Raman scattering, SPR, and SERS [22,151,169,190]	Detect carbapenemases Moderate cost	Require equipment for signal processing and data analysis Insufficient work on AMR and carbapenemase detection from pure culture and specimens
2.1. Plasmonic biosensors [19]	Rapid, simple, and cost-effective No equipment requirement	Insufficient work on AMR and carbapenemase detection from pure culture and specimens

*Techniques have been used in diagnostic laboratories (clinical and public health laboratories). AST: antibiotic susceptibility test, MALDI-TOF MS: matrix-assisted laser desorption/ionization time-of-flight mass spectrometry, BCDA: bioluminescence-based detection assays, FC: flow cytometry, FISH: fluorescence in situ hybridization, PCR-ESI-MS: PCR amplification coupled with electrospray ionization mass spectrometry, NucliSENS EasyQKPC: RNA-targeted molecular approach, SPR: surface plasmon resonance; SERS: Surface-Enhanced Raman Scattering technique.

Overall, several phenotypic and genotypic methods and biosensors have been developed to detect ARB, including CP bacteria, with advancements in automation and nanotechnology. All these techniques have advantages and disadvantages in cost, rapidity, simplicity, reliability, and applicability (Table 1.2). However, these detection techniques need to be developed further by improving their sensitivity, specificity, and testing on clinical and biological samples to increase their real-world applicability and accessibility. The plasmonic biosensors typically do not require highly trained personnel, as is usually the case with conventional and rapid phenotypic and molecular techniques. This enhances their applicability in low-resource settings for on-site detection [23,197]. Such rapid and cost-effective techniques as screening/diagnostic tests should be implemented in clinical and public health and agricultural and food testing laboratories, especially in low-resource laboratories.

1.2.4.6. Gold Nanoparticle-Based Plasmonic Biosensor

1.2.4.6.1. Properties of Gold Nanoparticles (GNP)

Various biosensor platforms have used several nanomaterials to enhance sensor sensitivity by increasing capture efficiency or amplifying detection signals due to their unique optical, electric, and magnetic properties [199]. Among these, GNPs extensively offer capturing, sensing, detecting, and imaging applications for chemical and biological samples. Their size-dependent chemical, electric, and optical properties as well as pertinent physical properties, including a high surface area to volume ratio are primary advantages [200–202]. In addition, GNPs are chemically stable and easily modified for biosensor applications [199,201,202]. Further, GNPs have simple preparation methods and the most common synthesis methods, such as the Turkevich-Frens and Brust-Schiffrin methods, which are detailed by Zhao and coworkers [203]. Briefly, the Turkevich-Frens methods produce spherical GNPs using sodium citrate as a result of a single-phase metal salt redox reaction. The Brust-Schiffrin method utilizes a thiolate for GNP stabilization in a two-phase reduction reaction [203]. The GNPs' properties and simple preparation techniques have stimulated their popularity and use in recent years [199,201,202].

The unique optical properties of GNPs, depending on their shape or size, have been used in many biosensor platforms [201,202]. Free electrons of GNPs in colloidal solutions induce coherent oscillation once the light frequency matches the electron frequency, producing a strong SPR band. The SPR band is strongly distance-dependent, transforming from a monodispersed

state to an aggregated state in a liquid solution, resulting in a visible color change [200–202]. Small monodispersed GNPs have SPR absorption peak at around 520 nm, with a red color, shifted to a longer wavelength with the aggregated particles or the increase of particle size that leads to a change from red color to blue or purple [23,199,204]. These properties of GNPs are utilized in many biosensor platforms, including fluorescence sensing, SERS sensing, and electrochemical biosensing discussed in the previous section, as well as in colorimetric sensing.

1.2.4.6.2. Colorimetric DNA Detection

A colorimetric biosensor is widely applicable due to its ease of use, cost-effectiveness, rapidity, and sensitivity. A visual system that allows detection without complicated equipment can offer an ideal solution [151]. As with many biosensor platforms, colorimetric biosensors have also been implemented to detect a variety of bacterial targets such as DNA, proteins, antigens, and other small molecules [23,193,194,204,205]. GNPs have been extensively used to detect target DNA from several bacteria. A platform using GNPs conjugated with oligonucleotide probes for the detection of DNA was first developed in 1996 [206]. In this method, the thiol-capped oligonucleotide probe attaches to GNP surfaces, and then the specific probe adheres to the target DNA upon denaturation and hybridization. The detection is achieved through the addition of salt after DNA hybridization, resulting in color change because of GNP aggregation [206]. This method is still commonly used for target DNA detection [193–195,207].

GNP colorimetric biosensor relies on the aggregation of GNPs, resulting in a visible color change, as stated previously. GNP colorimetric biosensor methods utilizing DNA probes typically have been used in two separate concepts upon GNP aggregation of target sample (TA) and non-target samples (NTA), illustrated in Figure 1.3 [23]. The first approach, crosslinking assay, usually uses two probes and attaches them to GNPs to form a polymeric network with target DNA. This network leads to the aggregation of GNPs and a color change; therefore, target samples show blue, while nontarget samples display red [23,200]. In the other TA approach, GNPs are not functionalized with the oligonucleotide probe; target DNA is hybridized with the probe, and the GNP is free, while the unhybridized probe in the absence of target DNA adsorbs to the GNP surfaces. Thus, the free or non-surrounded GNP aggregates upon salt application, turning blue in color, whereas non-target samples protect GNP from aggregate, remaining red color [23,193,200]. In NTA assay, an oligonucleotide probe is typically attached to GNPs and then binds to target DNA through hybridization. GNP-probe-DNA complexes protected GNP

from aggregation upon salt application, remaining red in color, while non-target DNA samples are free, and GNP is not protected from aggregation, turning blue [23,194,200,207,208]. This approach was used in this study for the detection of the target bacteria.

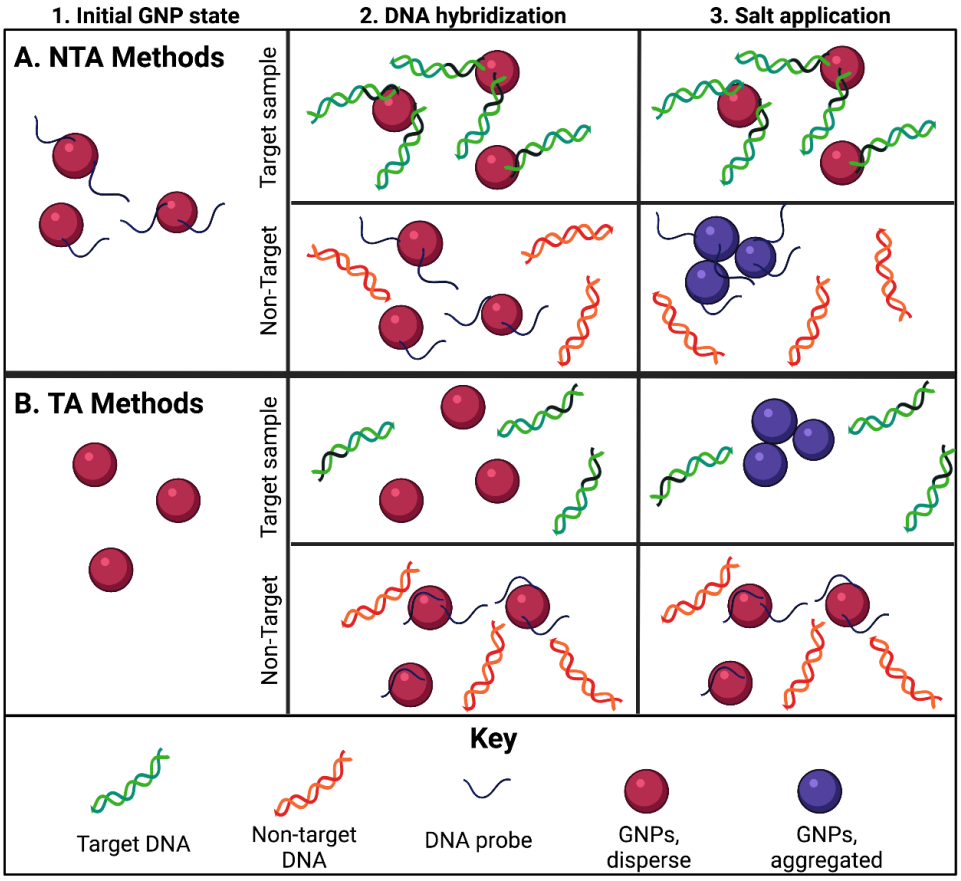

Figure 1.3. Schematic illustration of GNP biosensor concepts, which is from a study [23].

GNP biosensors with both TA and NTA approaches have been developed for target bacteria detection from different matrices. For instance, a GNP colorimetric biosensor with the NTA approach detected target bacteria (*E. coli* O157:H7) against non-target DNA samples (*E.coli* C3K, *S. Enteritidis*, *L. monocytogenes*, and *B. cereus*) from pure culture and flour sample within 30 min [23]. Multiple strains of *Salmonella* spp. (10 CFU/mL) were concentrated from raw chicken and blueberries using immunomagnetic separation, followed by 6 h incubation, and then detected using a GNP biosensor with the NTA approach [194]. Alternatively, PCR amplified product from food samples has also been used to detect *Salmonella* spp. from food samples [209]. GNP biosensors may require some additional pretreatment steps, and culturing may be required to detect the bacteria from matrices [23,194]. Further, DNA extraction may also

increase the assay cost using extraction kits; however, using simple methods such as boiling can eliminate this need [23,193,194].

The applicability of the GNP-based plasmonic (colorimetric) biosensor for the detection of target bacteria from matrices increases its accessibility. Thus, this promising assay was further developed to detect carbapenem-resistant bacteria from pure cultures and matrices (water and foods) in this study. For the rapid and accurate detection, isolation (extraction) of bacteria from matrices is equally essential.

1.2.5. Current Separation or Extraction Methods

Preanalytical sample processing, extraction, and concentration of bacteria from matrices is an important and essential step to ensure sufficient numbers of cells for rapid detection [25,26,136]. The current bacterial separation techniques in food and clinical matrices, including physical methods such as centrifugation and filtration, and chemical and biological methods such as dielectrophoresis, metal hydroxides, and magnetic nanoparticles, were detailed.

1.2.5.1. Physical Methods: Filtration and Centrifugation

Bacterial separation by filtration and centrifugation is commonly used with food and clinical matrices [26,27,210]. These techniques are primarily based on bacterial characteristics (e.g., bacterial size and density) and solution density for separation from matrices. In the filtration technique, bacterial separation relies on passing suspended particles through filters with various pore sizes. The size difference between cells and matrix particles assists in removing interfering components for efficient bacterial separation [26,27,210]. While this method is inexpensive and quick (1-10 min) [26,27], its effectiveness is sometimes limited and remediated by the multiple filtration steps due to clogging filters. This may occur due to large food particles or blood cells and platelets in clinical samples [26,27,210]. Extensive cleaning and removal of the clogged food debris can help to remove the matrix interference, but it may also remove previously trapped bacteria. Thus, the two-step filtration process with overnight enrichment (6-18 h) is often needed for PCR-based detection of bacteria [27].

The filtration technique is often combined with centrifugation to increase bacterial capture capacity. Centrifugation is used to pelletize bacterial cells, and supernatant is removed. Samples can then be resuspended in a smaller volume of solution, effectively concentrating bacteria [26,27]. Centrifugation is typically rapid (5-30 min); however, it may require multiple

steps and washes, which reduce bacterial concentration. In addition, centrifugation techniques such as continuous flow centrifugation (CFC) and buoyant-density centrifugations (BDC) have been developed to improve the efficient extraction and concentration of bacteria from food matrices [26,27]. For instance, BDC techniques have successfully concentrated food-borne pathogens and removed PCR-inhibiting food debris, followed by target DNA detection without sample culturing [211]. In addition, CFC has improved the effective concentration of bacteria from large volumes of samples, contributing to higher total bacteria capture [212]. However, centrifugation techniques still face several limitations when used for complex matrices, such as inefficient bacterial extraction, lower bacterial capture, and labor-intensive steps [26,27,211,212].

1.2.5.2. Chemical and Biological Methods

Chemical or biological methods are based on adsorption and make use of naturally occurring biological or chemical interactions between affinity ligands and specific surface substrates on solid support [25–27]. Affinity agents can be antibodies, bacteriophages, proteins, aptamers, carbohydrates, and charged particles that interact through physicochemical interactions, including Van der Waal's forces, electrostatic interactions, and hydrogen bonding [25,26]. These methods can be nonspecific or specific to a target [26,27].

Metal hydroxide-based techniques have been used for nonspecific separation of bacteria from food and clinical samples [26,27]. In this method, metal hydroxides, including zirconium hydroxide and/or titanium hydroxide, can immobilize bacterial cells through a chelation process; amino acid ligands on bacterial surfaces bind with hydroxyl groups of metal hydroxides by covalent bonds [26,27]. First, bacterial separation from the sample matrix is employed through a high-speed centrifugation step. Then, resuspended bacterial cells in small-volume solutions are concentrated by immobilization with metal hydroxide at low-speed centrifugation, all within one hour [27]. However, most studies still include a 4-8 hour enrichment period before detection using PCR [213] or mass spectrometry [214]. Although metal hydroxide immobilization is an inexpensive and rapid technique for the non-specific extraction of viable bacteria from matrices, its use in food samples is limited since non-selective metal hydroxide may bind to food components. In addition, this technique also requires centrifugation, leading to additional equipment costs [26,27,213,214].

Dielectrophoresis (DEP)-based techniques utilize a nonuniform electrical field polarization that induces bacterial cell migration towards the electrodes; this has separated bacteria from food and clinical matrices [26,27,210]. This method mainly utilizes non-specific affinity, separating a variety of bacterial cells with negatively charged bacteria adhering to positively charged residues [26,210,215]. This technique is also employed for screening antibiotic susceptibility using charge differences resulting from antibiotic-induced cell wall inhibition and cell lysis [216]. Dielectrophoresis has been used to extract bacteria from food and clinical matrices with a combination of mechanical filtration, centrifugation, nanoparticles as well as some biosensors and biochips to enhance detection [26,27,210,215]. The key advantage of this method is rapidity (<30 min) with minimal cell damage and the capability of separating viable and nonviable cells. However, the detection limit of dielectrophoresis-based techniques is generally higher (>10^6 CFU/mL) and highly variable depending on device design. Also, complex matrices present problems because of the high conductivity of food particles, limiting their use in food samples [26,27,210].

Magnetic nanoparticles (MNPs)-based extraction has commonly been used for rapid and effective separation techniques without the use of centrifugation and filtration [217,218]. MNPs can theoretically improve bacterial capture because of their large surface area/volume ratio for the attachment of ligands. Their small size can assist in moving faster than larger particles; multiple particles penetrate matrix interstices and interact with bacterial cells, increasing their capture efficiency [25,26]. Further, MNPs draw attention because of their low-cost, unique properties (non-toxic, physically and chemically stable, safe, biocompatible, large surface area/volume ratio, and superparamagnetic), and functionalization with recognition moieties [26,180,217,218]. One of the most significant advantages of MNPs is their superparamagnetic properties at a particle size of 10-200nm. This property helps rapidly disperse MNPs in liquids; an external magnetic field can still be magnetized and manipulated [26,180,219,220]. Another beneficial property is their high surface area/volume ratio, which gives higher adsorption capacity, leading to potentially high binding capacity with the target. In addition to these properties of MNPs that are based on the metallic core, surface coating and functionalization of MNPs can help control their stability and selectivity [26,220]. MNP surface can be functionalized with recognition moieties (antibodies, phages, antibiotics, carbohydrate and proprotein groups) to enable higher bacterial capture at low concentrations [25,180,220,221].

1.2.5.3. MNP-Based Extraction Techniques

Antibody-conjugated MNPs can bind to antigens on the surface of bacteria, enabling target bacterial separation and concentration. The efficiency of antibody-based magnetic separation or immunomagnetic separation (IMS) can be influenced by several factors, including particle composition/size and concentration, bacteria concentration, and incubation time of immunomagnetic particles with target bacteria [25,26,32]. This technique has commonly been employed to separate pathogens and ABR bacteria from food and clinical matrices with a variety of detection methods, including electrochemical and spectrometric techniques [32,37,222–224], electrochemical sensors [33], and GNP-based colorimetric biosensors [194]. IMS has also been implemented with immune-based assays or sensors by analyzing proteins, enzymes, and genes of target pathogens and ABR bacteria [135,169,181]. In comparison to other techniques mentioned above, the advantages of IMS are its high specificity and exclusion of natural microflora. The separation process can be successfully implemented in under 2 hours, reducing purification steps required before detection. Also, IMS allows for processing large-volume samples; the separated sample can be resuspended in a low volume, leading to a significant concentration of bacteria [26]. However, food debris can block the antibody, preventing the separation and concentration of bacteria [26,27]. IMS is also costly compared to conventional methods; antibody production and conjugation with MNP can be time-consuming and expensive, along with low-temperature storage requirements, limiting their use in low-resource settings [26].

Bacteriophage-based MNPs have recently been applied for rapid separation of specific bacteria of interest from complex environments [27,225,226]. Bacteriophages are used as recognition probes to bind specific receptors on the host surface. A few examples exist in the literature where phage-based magnetic particles have been used for bacterial separation from water and foods such as lettuce, milk, cheese, and salmon, among others [227,228]. However, the method has limitations regarding the tedious and lengthy process of coating magnetic particles with phages [25,225]. Further, issues related to desiccation and low density of capture elements on magnetic particles, undesired damage of target cells, and degradation of DNA are common concerns [25,27,229].

Biomolecule (e.g., carbohydrate, protein, antibiotics) functionalized MNPs offer inexpensive, simple, and rapid solutions compared to antibody and phage functionalized MNPs. Functionalizing MNPs with biomolecules may lead to either specific or non-specific binding

bacteria [25]. For example, an antibiotic agent (e.g., vancomycin, daptomycin, and gentamicin) on MNPs can successfully recognize the cell surface of gram-positive and gram-negative bacteria [180,221]. Vancomycin-functionalized MNPs have been shown to detect vancomycin-resistant *Enterococci* [230]. Vancomycin-functionalized and gold-coated MNPs were used to separate and concentrate carbapenem-resistant *E. coli* and *K. pneumoniae* [34]. However, the antibiotic-conjugated methods are limited because of MNP's size and conjugation techniques as well as its specificity and binding capacity [25,180,230]. In other studies, amine-functionalized magnetic nanoparticles were used to extract bacteria from water, green tea, and grape juice, achieving high capture efficiencies [231]. Recently, glycan-coated magnetic nanoparticles (gMNPs) successfully extracted and concentrated several bacteria from large-volume food samples, including milk [29,232], thick and complex liquid (beef juice, apple cider, and homogenized eggs) [30], sausage, deli ham, lettuce, spinach, chicken salad, and flour [232]. The gMNPs are promising as they offer cost-effective, rapid, and efficient bacterial separation from various food matrices [29,30,232]; however, gMNPs need further attention for bacterial separation, specifically for ARB, including CRE.

1.2.5.4. Glycan-Coated Magnetic Nanoparticles

1.2.5.4.1. Synthesis and Surface Coating of Magnetic Nanoparticles (MNPs)

Several materials, including pure metals (Fe, Co, Ti, Ni), metal oxides, ferrites, and metal alloys can be used to synthesize MNPs. Among these, iron oxides, such as magnetite (Fe3O4) and maghemite (Fe_2O_3), are commonly used for magnetic core. Various physical, chemical, and biological methods can be used to synthesize MNP, including co-coprecipitation, high-temperature thermal decomposition, hydrothermal processes, and microemulsion, among many others [26,180,233]. These synthesis methods and MNP's applications are comprehensively reviewed in the literature [180,233].

As mentioned previously, the metallic core of MNPs shows magnetic properties, and surface coatings assist in controlling MNP selectivity and stability. Several materials can be used as MNP coatings for stabilization and modification of active groups to produce core-shell-formation by physical adsorption or covalent binding [25,26,180,233]. As common MNP coatings, surfactant molecules, including silica, colloidal gold, glycan, or complex carbohydrates, have been used [26,233,234]. Coating can be accomplished during MNP

synthesis or as a post-synthetic functionalization step, as reviewed by Fratila and coworkers [234]. For instance, glycan coatings are achieved through the presence of carbohydrates during MNP synthesis, allowing for ligand adsorption onto the MNP surface. For post-synthetic methods, the functionalized carbohydrates are introduced to the MNP surface, and ligand exchange, covalent linking, or non-covalent functionalization can be achieved [26,234]. Many carbohydrate surfactants or glycans, such as mannose, galactose, glucose, caprylic acid cysteine, and chitosan, have been employed as MNP coatings [25,26,29,180,234]. Further, gMNPs may include other materials, such as amino groups, to improve capture efficiency [30]. The primary advantages associated with using the gMNPs are their stability at room temperature, one-pot synthesis, scalable production, rapid capture, and biosensor compatibility [26].

1.2.5.4.2. Magnetic Extraction in Foods

MNP-based bacterial extraction from food matrices in most studies follows similar methods regardless of the surface coating [26,29,180,235], as demonstrated in Figure 1.4 [26]. In this methodology, the MNPs are applied to liquified food samples that are naturally or artificially inoculated with one or more bacterial species. After MNP has dispersed into the liquid, the sample is incubated to allow for MNP-cell attachment. The incubation time usually depends on MNP surface coating and specific methodology, varying from one minute to hours. After the incubation, an external magnet is applied to concentrate the MNP-bacteria complexes, and the supernatant is removed. The remaining samples are then resuspended in a lower sample volume [26,29,180,235]. These concentrated MNP-bacteria samples can then be detected using various methods, including biosensors [26,29,30,194].

The non-specific nature of MNPs may lead to complications in extraction from complex food matrices and those with a high level of natural microflora. MNP-bacteria, bacteria-food matrix, and MNP-food matrix interactions in liquified samples are possible due to their attachment preference to food particles as a result of hydrophobic or hydrophilic surfaces and electrostatic force difference [35]. However, most of the food matrix (free-food matrix and bacteria-food matrix) in the liquefied samples is removed with the supernatant [26]. This methodology assists in reducing the food matrix from the sample and does not significantly affect the detection. For instance, gMNPs efficiently extracted bacteria directly from a thick, nutritionally rich, and chemically complex matrix (e.g., egg, beef juice, sausage, lettuce, flour, and Vitamin D milk), with little loss in capture capacity [30,232,236]. This further confirms that

interferences of the food matrix did not significantly prevent the detection of target DNA [23]. However, in some cases, the food matrix may affect subsequent detection based on the method employed. Thus, employing multiple washing steps with PBS following supernatant removal can assist in removing food particles [26,29,180,235].

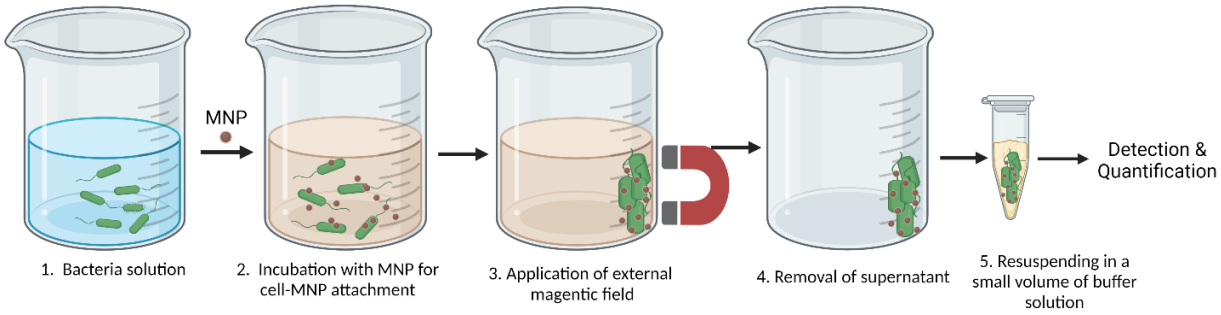

Figure 1.4. Schematic representation of the magnetic separation of bacteria (created with BioRender), which is adapted from studies [26,180].

The gMNPs offer many advantages against other methods; the gMNPs cost four times less than antibody-based assays and do not require special storage conditions [30], reducing overall expenses compared to IMS [26]. The gMNPs can also be stable for a long time; for instance, MNPs coated with alginate or chitosan were suspended in buffer solutions and stored at room temperature for six months; flocculation or settling of the MNP was not observed [237]. Further, bacterial extraction and concentration using gMNPs can be done within 15 min [26,30,235]. Thus, the economical, efficient, and rapid nature of gMNPs and their storage conditions increase their use and accessibility for bacterial separation, particularly in low-resource settings. Therefore, the gMNPs harbor a potential for separation of ARB from various matrices.

1.2.5.4.3. Mechanism of MNP-Cell Attachment

Bacterial attachment or adherence to host surfaces is facilitated by adhesins. Adhesins can be polypeptides (fimbrial (pili) or afimbrial) or polysaccharides (usually components of the bacterial cell membrane, cell wall, and capsule). The mechanism of adhesin binding is receptor-ligand interaction and is based on protein-protein or protein-carbohydrate interactions [35,238]. Carbohydrates or glycan have a key role in many cellular mechanisms of bacterial attachment and host infections by interacting mainly between surface proteins (e.g., lectins) and glycans [25,32].

The biological process of glycan-protein interaction has been utilized for bacterial capture and detection. Here, gMNPs can take over the role of cell surface glycan and attach to proteins (e.g., lectins) on bacterial surfaces through non-covalent and electrostatic interactions [26,235,239]. These interactions mainly include van der Waals interactions and hydrogen bonds between hydroxyl and amino groups present on carbohydrate and microbial protein surfaces [25,26,180,235]. The MNP-bacterial cell adhesion has also been shown through microscopic imaging [26,29,240]. In this MNP-cell adhesion, the superparamagnetic property of MNPs assists in the rapid extraction of the MNP-bacteria complexes using an external magnetic field. In many studies, gMNPs have been successfully applied for bacterial extraction and concentration from different matrices [26,29,240,241].

Non-specific MNP capture of bacterial cells using gMNPs can also be enhanced by their positively charged nature since both gram-positive and gram-negative bacteria are negatively charged because of their cell wall components. The generalized electrostatic force between the oppositely charged components promotes close proximity between glycan and bacterial lectins for more effective cell attachment [26,180]. For instance, chitosan is a natural hydrophilic, biocompatible, nontoxic biopolymer with two hydroxyl groups (-OH) and amino group (-NH2), assisting MNP suspension in aqueous solution and improving the proximity between surface markers of bacteria and polycationic structure of MNPs [220,239]. Also, chitosan becomes positively charged at pH (5-7) through the protonation of these amino groups and is more effective in cell attachment [220,239]. The positively charged gMNPs may facilitate the adhesion with bacteria by reducing electrostatic repulsion [26,239].

MNP-cell interaction might differ in bacterial types due to differences in cell wall components. For instance, in a study of the extraction of gram-positive and gram-negative pathogens from various milk types using the glycan-coated MNPs, the capture capacity was higher for gram-positive bacteria (*B. cereus*) compared to gram-negative bacteria (*E. coli* and *Salmonella* Enteritidis) [29]. Further, recent work suggested MNP binding capacity (concentration factor) to be higher in gram-positive bacteria (*Bacillus*, *S. aureus*, and *Listeria*) compared to gram-negative bacteria (*E. coli*, *Salmonella* species), hypothesizing the influence of surface charge [232]. The cell surface components or characteristics help to understand the attachment mechanism [26,242]. Thus, this study aims to investigate the cell surface properties of carbapenem-resistant bacteria for further insights on their cell attachment properties.

1.2.6. Phenotypic Cell Properties or Characteristics of Antibiotic-Resistant Bacteria

As previously mentioned, the misuse and overuse of antibiotics in human medicine, veterinary medicine, and agriculture during the last 70-80 years and their release into the environment have created selective pressure on bacteria [5,62,243]. While a high level of antibiotic concentrations is therapeutically used in humans, about half of all antibiotics are excreted in an unchanged active form mainly via urine into wastewater, manure, run-off water, various aquatic environments, and soil [5,244]. The low-level of antibiotics in the environment does not kill all susceptible bacteria and can slow down their growth. This promotes the evolution of *de novo* resistance, the selection of antibiotic-resistant mutants, and the transfer of resistant genes [62,64,243–245]. Once the population remains exposed to antibiotics for a long time, the possibility of genetic mutations increases, and the resistance becomes stable in the absence of antibiotics [243,246].

The long-term subinhibitory antibiotic exposure modulates bacterial gene expression at the transcription level of about 5-10% of genes linked with the cellular process (e.g., protein synthesis, carbohydrate metabolism, target modification) [5]. This serves as an expression of adaptation to new and unfavorable conditions and the emergence of new microbial phenotypes, which contribute to the induction of several types of responses to environmental stressors [5,244]. This also accelerates the horizontal transfer of the genes to non-pathogenic and pathogenic microbes in the environment [5]. Due to the adaptive mechanisms that are conserved and transmitted to other microorganisms vertically or horizontally, bacteria can subsequently adapt and survive at high-levels of antibiotics, above the minimum inhibitory concentration (MIC) [64,151,243,245].

In addition, several studies showed antibiotic exposure can cause differences in bacterial phenotypic properties such as cell morphology, cell adhesion, and cell motility abilities. The cell wall, which plays a crucial role in protection, morphological characterization, stability, and adhesion to surfaces, is primarily affected [39,40,247,248]. Thus, it is a target for many antibiotics, especially β-lactams, which affect the susceptibility of the organism by increasing the possibility of peptidoglycan biosynthesis disruptions [40,247]. In various studies, morphological and ultrastructural changes in bacterial cells under antibiotic exposure were observed, attributed to cell wall synthesis disruption (deficiency in cell wall materials and cell lysis) [39,41,249–253] as well as alteration membrane components and cytoplasmic contents [254,255]. These

disruptions and changes are also a strategy to protect the bacteria against cell walls targeting antibiotics [256], resulting in the change of cell morphology [39,247] and alterations in electrostatic surface charge [41,43,257–259].

1.2.6.1. Cell Morphological Characteristics

The morphological and ultrastructural changes under antibiotic stress depend on the antibiotic types and concentrations, type of bacteria, and cell wall structure [39]. Changes in cell shape under antibiotic exposure are mainly characterized as spherical, elongated, or filamented types. A spherical shape occurs as a result of the loss of the peptidoglycan layer that provides rigid, shape-determining structure and membrane tension to cells. Cell elongation or filaments occur when rod-shaped bacterial cells become abnormally long by producing peptidoglycan for the lateral wall instead of the septal wall [39]. Several studies highlighted that β-lactam-induced elongation and spheroplast formation were observed in many gram-negative and some of gram-positive bacteria species [39,253,260,261].

The shape formation with carbapenem exposure is detailed in the literature. Carbapenem first initiates its mode of action by penetrating the bacteria cell wall and binding to enzymes for Penicillin-binding proteins (PBPs) [39,260,261]. The affinity of PBP-1, PBP-2, and PBP-3 in Gram-negative bacillus-shaped bacteria results in spheroplast and filamentous-shaped organisms [39,260,261]. Researchers also stated that the heterogeneity in morphological changes was a result of binding with more than one PBP. For example, imipenem, panipenem, and biapenem have a high affinity for PBP-1 or PBP-2, resulting in spheroplast forms. Meropenem, alternatively, binds with PBP-2 and/or PBP-3 and causes elongation or filament form depending on exposure period and antibiotic concentrations [39,260–262]. Also, low-level antibiotic concentrations cause filament forms, while high concentrations tend to produce spheroplast form due to more intense cell damage with increasing antibiotic concentrations and exposure time [39,253]. In a study, Cross and co-workers (2019) highlighted the occurrence of cell wall-deficient/spheroplast forms in clinical Gram-negative pathogens upon exposure to meropenem (6 h) in vitro and in vivo. This spheroplast form of the bacteria can mediate antibiotic tolerance of pathogenic bacteria and cause treatment failure, increasing the possibility of mutation and broad resistance to other antibiotics [263].

Morphological characteristics of bacteria can impact their Brownian forces and cell attachment to surfaces [247]. For example, in a MNP-based separation technique, MNP-cell

binding characteristics of gram-negative and gram-positive bacteria were visualized; both individual and clusters of *Listeria* and *E.coli* cells attached to MNPs at mostly specific locations along with different attachment capacity [26,232]. Thus, cell morphological characteristics of ARB can also be needed for further aspects of their cell-MNP binding properties.

1.2.6.2. Cell Surface Charge Characteristics

Cell surface characteristics play a significant role in maintaining cellular function. Zeta potential, the electrical potential of the interfacial region between the bacterial surface and the aqueous environment, indirectly provides information about cell surface characteristics [42], [44]. Surface charges are associated with multiple factors, including the outer membrane compounds on the cell wall, the tridimensional structure of the cell surface, growth conditions, pH, and ionic strength, among others [42,44]. Zeta potential is mainly linked with negatively charged functional groups accompanied by peptidoglycan, teichoic acid, and teichuronic acid on the surface of gram-positive bacteria, while it is linked with lipopolysaccharide, phospholipids and proteins on the surface of gam-negative bacteria [44,264]. It has been applied for the characterization of pathogen strains, biofilm formation, physiologic state of bacteria, interaction of several compounds with the bacterial surface, and to study the effect on permeability of bacteria [42]. For example, the zeta potential of *E. coli*, *Salmonella* Newport, and *Pseudomonas* had lower negative charge under minimal media compared to bacteria in rich media. They also found that the cell types and sizes of the starved bacteria were different [265]. Colistin-susceptible *Acinetobacter baumannii* cells had a greater negative charge than colistin-resistant *Acinetobacter baumannii* [43]. The chemical nature of cells or environmental conditions leads to differences in cell wall composition, growth rate, cell morphology, anion and cationic balance on the cell surface, and electrical potential differences [40–42,44,264].

In addition, electrostatic surface charges are primed for the evolution of the bacterial adhesion process. Particularly, electrostatic surface charges can impact overall polarity to maintain the degree of surface hydrophilicity for optimal cell function [42]. The cell wall is associated with the adhesion to surfaces in the presence of adhesins, which are macromolecules such as extracellular proteins and polysaccharides responsible for specific or non-specific adhesive interactions at the interface [35]. Charges are a result of acidic and basic functional groups on the cell wall and membrane (such as carboxylic, phosphoric, hydroxyl, and amine groups) and their disassociation or protonation [42,44]. Thus, the difference in cell wall

compositions resulting in different surface charges can affect their adhesion or attachment to surfaces. This adhesion mechanism related to electrostatic surface charge are utilized for interaction between bacteria and nanoparticles in many areas (pharmacology, biotechnology, chemistry, nanomedicine, etc.) [41,264] as well as efficient bacterial extraction and detection in different matrices [26,41,180]. For example, negatively charged bacteria can attach to positively charged nanoparticles using electrostatic force [31,220,264].

The attachment mechanism with MNPs is commonly used for efficient separation, concentration, and detection of cells in different matrices [26,180]. This attachment may result from electrostatic forces that assist close proximity between the positively charged MNPs and negatively charged bacterial cells [26,30,266]. While the surface charge contributes towards cell attachment, glycan-protein binding also plays a significant role [29,232]. Additionally, differences in the cell wall composition of bacterial species can affect their cell adhesion properties (surface charges and specific binding locations) [26,29,30,180,266].

Studies on surface charges of ARB and their cell adhesion properties are limited. As previously mentioned, cell wall compositions of antibiotic-exposed or antibiotic- resistant bacteria can be different from antibiotic-susceptible bacteria; this may affect their cell adhesion properties as well as their separation and detection. Thus, this study aimed to investigate morphological and surface charge characteristics of carbapenem-susceptible and carbapenem-resistant bacteria in the absence and presence of carbapenem stress for further insights into their cell attachment properties.

1.3. Conclusions and Knowledge Gaps

The emergence and spread of ARB, including carbapenem-resistant bacteria, are a global health issue. Even though carbapenems are used in human medicine, several studies widely showed that carbapenem-resistant bacteria are found in food-producing animals, foods, water sources, etc., due to antibiotic selection in the environment and rapid dissemination of the resistant genes in a complex web. There have been continuing efforts to develop rapid and cost-effective detection methods to prevent and control their spread in the community. Thus, this study mainly aimed to develop a rapid, simple, and cost-effective assay for the detection of carbapenem-resistant bacteria. Herein, this study proposed to investigate the efficacy of carbohydrate-coated magnetic and gold nanoparticles to detect carbapenem-resistant *E. coli* from water and foods.

To improve rapid and reliable detection, separation and concentration techniques play major roles. Specific separation techniques have not been documented well for ARB since resistance profiles are tested after pathogen identification. Current methods for bacterial separation and concentration have been documented and discussed with their advantages and limitations. The efficient separation, short-assay times, and cost-effectiveness of MNP-based methods allow their applicability to low-resource environments. Magnetic separation, especially immunomagnetic separation, has commonly been used for rapid selective separation. However, the lack of standardization, high experimental cost, and their storage conditions are primary limitations. The gMNPs offer a cost-effective alternative to IMS techniques. Their simple synthesis and functionalization procedure and room-temperature storage conditions illustrate their potential for cost-effective, rapid, and efficient bacteria extraction from matrices. The gMNPs have been successful in the extraction of pathogens from a variety of foods, as seen in the literature. As stated previously, these techniques have not been specified for ARB isolation from pure culture or matrices. Further studies must be performed to investigate the effectiveness of the promising gMNPs on ARB to both confirm current elements of this MNP-cell mechanism theory and discover possible factors.

To better understand this theory, factors affecting MNP-cell interaction must be evaluated. Earlier studies showed differences in phenotypic cell surface characteristics of ARB and utilized these properties for further insights into the development of bacterial capture and detection methods. Notably, differences in cell surface characteristics have been used for many applications for bacterial capture (chemical and biological) techniques. There has still been ongoing research on understanding the cell characteristics of ARB to discover new potential factors. In particular, cell properties of carbapenem-resistant bacteria have not been documented well. Thus, further studies are necessary to evaluate cell properties of carbapenem-susceptible and carbapenem-resistant bacteria. These cell properties may shed light on the MNP-cell adhesion mechanisms for bacterial capture or separation techniques.

Further, many detection techniques have been explored to detect ARB, including CP-CRE. The most widely used AST cultural assays are time-consuming, taking days to a week. Many current rapid phenotypic and genotypic methods and biosensors often require pure culture, costly and complex equipment, data analysis, and skilled personnel. In particular, GNP-based plasmonic biosensors have recently shown profound promise as a cost-effective, rapid, and

simple detection technique by eliminating complex and costly equipment. The plasmonic biosensor has successfully implemented pathogen detection from pure culture, clinical matrices, and food matrices in the literature. The biosensor can become an accessible and rapid detection method, especially in low-resource settings. Hence, further research must be conducted to develop a plasmonic biosensor for detecting and differentiating carbapenem-resistant bacteria from pure culture and matrices.

Many extraction and detection techniques have not been well documented in testing real samples. A few studies showed the GNP biosensor was implemented to detect pathogens from matrices; however, limited works are conducted with DNA extract directly from extraction, and enrichment time is still required. Studies mostly use overnight enrichment to achieve the detection. Thus, further research must be conducted into reducing the duration of enrichment time as well as investigating the effective detection of target bacteria extracted from matrices. The successful rapid detection from matrices increases accessibility and applicability.

Foods and water are one of the major routes and reservoirs of pathogens and resistant bacteria. Thus, in many countries, particularly in Europe and North America, food-borne pathogens and their resistant profile are tracked to ensure safe food for consumers. CDC and EFSA include CP-CRE tracking in food animals and retail meats. However, non-animal products also need attention. Since several studies showed, these bacteria are also found in fresh produce. Thus, studies must also focus on non-animal products, animal products, and environmental samples.

REFERENCES

[1] Taggar, G., Rheman, M. A., Boerlin, P., and Diarra, M. S., "Molecular Epidemiology of Carbapenemases in Enterobacteriales from Humans, Animals, Food and the Environment," Antibiotics, 2020, 9(10), pp. 1–22, DOI: 10.3390/antibiotics9100693.

[2] Prestinaci, F., Pezzotti, P., and Pantosti, A., "Antimicrobial Resistance: A Global Multifaceted Phenomenon," Pathog. Glob. Health, 2015, 109(7), pp. 309–318, DOI: 10.1179/2047773215Y.0000000030.

[3] Capozzi, C., Maurici, M., and Panà, A., "[Antimicrobial Resistance: It Is a Global Crisis, 'a Slow Tsunami']," Ig. Sanita Pubbl., 2019, 75(6), p. 429—450.

[4] Antimicrobial Resistance: CDC's Antibiotic Resistance Threats in the United States, 2019. Available online:https://www.cdc.gov/drugresistance/pdf/threatsreport/2019-ar-threats-report-508.pdf (Accessed:06-September-2022).

[5] Serwecińska, L., "Antimicrobials and Antibiotic-Resistant Bacteria: A Risk to the Environment and to Public Health," Water, 2020, 12(12), p. 3313, DOI: 10.3390/w12123313.

[6] Dankittipong, N., Fischer, E. A. J., Swanenburg, M., Wagenaar, J. A., Stegeman, A. J., and de Vos, C. J., "Quantitative Risk Assessment for the Introduction of Carbapenem-Resistant Enterobacteriaceae (CPE) into Dutch Livestock Farms," Antibiotics, 2022, 11(2), p. 281, DOI: 10.3390/antibiotics11020281.

[7] Mills, M. C., and Lee, J., "The Threat of Carbapenem-Resistant Bacteria in the Environment: Evidence of Widespread Contamination of Reservoirs at a Global Scale," Environ. Pollut., 2019, 255, p. 113143, DOI: 10.1016/j.envpol.2019.113143.

[8] Bonardi, S., and Pitino, R., "Carbapenemase-Producing Bacteria in Food-Producing Animals, Wildlife and Environment: A Challenge for Human Health," Ital. J. Food Saf., 2019, 8(2), DOI: 10.4081/ijfs.2019.7956.

[9] Köck, R., Daniels-Haardt, I., Becker, K., Mellmann, A., Friedrich, A. W., Mevius, D., Schwarz, S., and Jurke, A., "Carbapenem-Resistant Enterobacteriaceae in Wildlife, Food-Producing, and Companion Animals: A Systematic Review," Clin. Microbiol. Infect., 2018, 24(12), pp. 1241–1250, DOI: 10.1016/j.cmi.2018.04.004.

[10] Woodford, N., Wareham, D. W., Guerra, B., and Teale, C., "Carbapenemase-Producing Enterobacteriaceae and Non-Enterobacteriaceae from Animals and the Environment: An Emerging Public Health Risk of Our Own Making?," J. Antimicrob. Chemother., 2014, 69(2), pp. 287–291, DOI: 10.1093/jac/dkt392.

[11] Guerra, B., Fischer, J., and Helmuth, R., "An Emerging Public Health Problem: Acquired Carbapenemase-Producing Microorganisms Are Present in Food-Producing Animals, Their Environment, Companion Animals and Wild Birds," Vet. Microbiol., 2014, 171(3–4), pp. 290–297, DOI: 10.1016/j.vetmic.2014.02.001.

[12] Morrison, B. J., and Rubin, J. E., “Carbapenemase Producing Bacteria in the Food Supply Escaping Detection,” PLoS One, 2015, 10(5), DOI: 10.1371/journal.pone.0126717.

[13] CDC, “Antimicrobial Resistance;Tracking Antibiotic Resistance,” CDC (Centers Dis. Control Prev. Dis. Control Prev., 2021, [Online]. Available: https://www.cdc.gov/drugresistance/tracking.html. [Accessed: 05-May-2022].

[14] ECDC: EARS-Net, “Annual Report of The European Antimicrobial Resistance Surveillance Network (EARS-Net),” Surveill. Report; ECDC, 2017, [Online]. Available: https://www.ecdc.europa.eu/en/publications-data/surveillance-antimicrobial-resistance-europe-2017.

[15] McLain, J. E., Cytryn, E., Durso, L. M., and Young, S., “Culture-based Methods for Detection of Antibiotic Resistance in Agroecosystems: Advantages, Challenges, and Gaps in Knowledge,” J. Environ. Qual., 2016, 45(2), pp. 432–440.

[16] Syal, K., Mo, M., Yu, H., Iriya, R., Jing, W., Guodong, S., Wang, S., Grys, T. E., Haydel, S. E., and Tao, N., “Current and Emerging Techniques for Antibiotic Susceptibility Tests,” Theranostics, 2017, 7(7), pp. 1795–1805, DOI: 10.7150/thno.19217.

[17] Khan, Z. A., Siddiqui, M. F., and Park, S., “Current and Emerging Methods of Antibiotic Susceptibility Testing,” Diagnostics, 2019, 9(2), p. 49, DOI: 10.3390/diagnostics9020049.

[18] Decousser, J.-W., Poirel, L., and Nordmann, P., “Recent Advances in Biochemical and Molecular Diagnostics for the Rapid Detection of Antibiotic-Resistant Enterobacteriaceae : A Focus on ß-Lactam Resistance,” Expert Rev. Mol. Diagn., 2017, 17(4), pp. 327–350, DOI: 10.1080/14737159.2017.1289087.

[19] Santopolo, G., Rojo-Molinero, E., Clemente, A., Borges, M., Oliver, A., and de la Rica, R., “Bedside Detection of Carbapenemase-Producing Pathogens with Plasmonic Nanosensors,” Sensors Actuators, B Chem., 2021, 329(October 2020), DOI: 10.1016/j.snb.2020.129059.

[20] Tominaga, T., “Rapid Detection of Klebsiella Pneumoniae, Klebsiella Oxytoca, Raoultella Ornithinolytica and Other Related Bacteria in Food by Lateral-Flow Test Strip Immunoassays,” J. Microbiol. Methods, 2018, 147(February), pp. 43–49, DOI: 10.1016/j.mimet.2018.02.015.

[21] Greissl, C., Saleh, A., and Hamprecht, A., “Rapid Detection of OXA-48-like, KPC, NDM, and VIM Carbapenemases in Enterobacterales by a New Multiplex Immunochromatographic Test,” Eur. J. Clin. Microbiol. Infect. Dis., 2019, 38(2), pp. 331–335, DOI: 10.1007/s10096-018-3432-2.

[22] Bashir, S., Nawaz, H., Majeed, M. I., Mohsin, M., Abdullah, S., Ali, S., Rashid, N., Kashif, M., Batool, F., Abubakar, M., Ahmad, S., and Abdulraheem, A., “Rapid and Sensitive Discrimination among Carbapenem Resistant and Susceptible E. Coli Strains Using Surface Enhanced Raman Spectroscopy Combined with Chemometric Tools,” Photodiagnosis Photodyn. Ther., 2021, 34(March), DOI: 10.1016/j.pdpdt.2021.102280.

[23] Dester, E., Kao, K., and Alocilja, E. C., "Detection of Unamplified E. Coli O157 DNA Extracted from Large Food Samples Using a Gold Nanoparticle Colorimetric Biosensor," Biosensors, 2022, 12(5), p. 274, DOI: 10.3390/bios12050274.

[24] Quintela, I. A., de los Reyes, B. G., Lin, C.-S., and Wu, V. C. H., "Simultaneous Colorimetric Detection of a Variety of Salmonella Spp. in Food and Environmental Samples by Optical Biosensing Using Oligonucleotide-Gold Nanoparticles," Front. Microbiol., 2019, 10, DOI: 10.3389/fmicb.2019.01138.

[25] Suh, S. H., Jaykus, L. A., and Brehm-Stecher, B., *Advances in Separation and Concentration of Microorganisms from Food Samples*, Woodhead Publishing Limited, 2013, DOI: 10.1533/9780857098740.3.173.

[26] Dester, E., and Alocilja, E., "Current Methods for Extraction and Concentration of Foodborne Bacteria with Glycan-Coated Magnetic Nanoparticles: A Review," Biosensors, 2022, 12(2), p. 112, DOI: 10.3390/bios12020112.

[27] Benoit, P. W., and Donahue, D. W., "Methods for Rapid Separation and Concentration of Bacteria in Food That Bypass Time-Consuming Cultural Enrichment," J. Food Prot., 2003, 66(10), pp. 1935–1948, DOI: 10.4315/0362-028X-66.10.1935.

[28] Dwivedi, H. P., and Jaykus, L.-A., "Detection of Pathogens in Foods: The Current State-of-the-Art and Future Directions," Crit. Rev. Microbiol., 2011, 37(1), pp. 40–63, DOI: 10.3109/1040841X.2010.506430.

[29] Matta, L. L., and Alocilja, E. C., "Carbohydrate Ligands on Magnetic Nanoparticles for Centrifuge-Free Extraction of Pathogenic Contaminants in Pasteurized Milk," J. Food Prot., 2018, 81(12), pp. 1941–1949, DOI: 10.4315/0362-028X.JFP-18-040.

[30] Matta, L. L., Harrison, J., Deol, G. S., and Alocilja, E. C., "Carbohydrate-Functionalized Nanobiosensor for Rapid Extraction of Pathogenic Bacteria Directly from Complex Liquids with Quick Detection Using Cyclic Voltammetry," IEEE Trans. Nanotechnol., 2018, 17(5), pp. 1006–1013, DOI: 10.1109/TNANO.2018.2841320.

[31] Li, Z., Ma, J., Ruan, J., and Zhuang, X., "Using Positively Charged Magnetic Nanoparticles to Capture Bacteria at Ultralow Concentration," Nanoscale Res. Lett., 2019, 14, DOI: 10.1186/s11671-019-3005-z.

[32] Kearns, H., Goodacre, R., Jamieson, L. E., Graham, D., and Faulds, K., "SERS Detection of Multiple Antimicrobial-Resistant Pathogens Using Nanosensors," Anal. Chem., 2017, 89(23), pp. 12666–12673, DOI: 10.1021/acs.analchem.7b02653.

[33] Nemr, C. R., Smith, S. J., Liu, W., Mepham, A. H., Mohamadi, R. M., Labib, M., and Kelley, S. O., "Nanoparticle-Mediated Capture and Electrochemical Detection of Methicillin-Resistant Staphylococcus Aureus," Anal. Chem., 2019, DOI: 10.1021/acs.analchem.8b04792.

[34] Wang, J., Yang, W., Peng, Q., Han, D., Kong, L., Fan, L., Zhao, M., and Ding, S., "Rapid

Detection of Carbapenem-Resistant Enterobacteriaceae Using PH Response Based on Vancomycin-Modified Fe3O4@Au Nanoparticle Enrichment and the Carbapenemase Hydrolysis Reaction," Anal. Methods, 2019, 12(1), pp. 104–111, DOI: 10.1039/c9ay02196e.

[35] Frank, J. F., "Microbial Attachment to Food and Food Conctact Surfaces," *Advances Innnnnnnn Food and Nutrition Research Vol 43,* Academic press, 2001, ISBN: 0-12-016443-4.

[36] Payne, M. J., and Kroll, R. G., "Methods for the Separation and Concentration of Bacteria from Foods," Trends Food Sci. Technol., 1991, 2, pp. 315–319, DOI: 10.1016/0924-2244(91)90734-Z.

[37] Wang, K., Li, S., Petersen, M., Wang, S., and Lu, X., "Detection and Characterization of Antibiotic-Resistant Bacteria Using Surface-Enhanced Raman Spectroscopy," Nanomaterials, 2018, 8(10), DOI: 10.3390/nano8100762.

[38] Galvan, D. D., and Yu, Q., "Surface-Enhanced Raman Scattering for Rapid Detection and Characterization of Antibiotic-Resistant Bacteria," Adv. Healthc. Mater., 2018, 7(13), pp. 1–27, DOI: 10.1002/adhm.201701335.

[39] Cushnie, T. P. T., O'Driscoll, N. H., and Lamb, A. J., "Morphological and Ultrastructural Changes in Bacterial Cells as an Indicator of Antibacterial Mechanism of Action," Cell. Mol. Life Sci., 2016, 73(23), pp. 4471–4492, DOI: 10.1007/s00018-016-2302-2.

[40] Yang, D. C., Blair, K. M., and Salama, N. R., "Staying in Shape: The Impact of Cell Shape on Bacterial Survival in Diverse Environments," Microbiol. Mol. Biol. Rev., 2016, 80(1), pp. 187–203.

[41] Nishino, M., Matsuzaki, I., Musangil, F. Y., Takahashi, Y., Iwahashi, Y., Warigaya, K., Kinoshita, Y., Kojima, F., and Murata, S., "Measurement and Visualization of Cell Membrane Surface Charge in Fixed Cultured Cells Related with Cell Morphology," PLoS One, 2020, 15(7 July), DOI: 10.1371/journal.pone.0236373.

[42] Ferreyra Maillard, A. P. V., Espeche, J. C., Maturana, P., Cutro, A. C., and Hollmann, A., "Zeta Potential beyond Materials Science: Applications to Bacterial Systems and to the Development of Novel Antimicrobials," Biochim. Biophys. Acta - Biomembr., 2021, 1863(6), p. 183597, DOI: 10.1016/j.bbamem.2021.183597.

[43] Soon, R. L., Nation, R. L., Cockram, S., Moffatt, J. H., Harper, M., Adler, B., Boyce, J. D., Larson, I., and Li, J., "Different Surface Charge of Colistin-Susceptible and -Resistant Acinetobacter Baumannii Cells Measured with Zeta Potential as a Function of Growth Phase and Colistin Treatment," J. Antimicrob. Chemother., 2011, 66(1), pp. 126–133, DOI: 10.1093/jac/dkq422.

[44] Wilson, W. W., Wade, M. M., Holman, S. C., and Champlin, F. R., "Status of Methods for Assessing Bacterial Cell Surface Charge Properties Based on Zeta Potential Measurements," J. Microbiol. Methods, 2001, 43(3), pp. 153–164, DOI: 10.1016/S0167-

7012(00)00224-4.

[45] Kumar, N., Wang, W., Ortiz-Marquez, J. C., Catalano, M., Gray, M., Biglari, N., Hikari, K., Ling, X., Gao, J., van Opijnen, T., and Burch, K. S., "Dielectrophoresis Assisted Rapid, Selective and Single Cell Detection of Antibiotic Resistant Bacteria with G-FETs," Biosens. Bioelectron., 2020, 156(February), p. 112123, DOI: 10.1016/j.bios.2020.112123.

[46] Ferri, M., Ranucci, E., Romagnoli, P., and Giaccone, V., "Antimicrobial Resistance: A Global Emerging Threat to Public Health Systems," Crit. Rev. Food Sci. Nutr., 2017, 57(13), pp. 2857–2876, DOI: 10.1080/10408398.2015.1077192.

[47] Morehead, M. S., and Scarbrough, C., "Emergence of Global Antibiotic Resistance," Prim. Care - Clin. Off. Pract., 2018, 45(3), pp. 467–484, DOI: 10.1016/j.pop.2018.05.006.

[48] WHO, "Antimicrobial Resistance," WHO (World Heal. Organ., 2021, [Online]. Available: https://www.who.int/news-room/fact-sheets/detail/antimicrobial-resistance. [Accessed: 05-Oct-2022].

[49] Smith, R., and Coast, J., "The True Cost of Antimicrobial Resistance," BMJ, 2013, 346(7899), DOI: 10.1136/bmj.f1493.

[50] Littmann, J., Buyx, A., and Cars, O., "Antibiotic Resistance: An Ethical Challenge," Int. J. Antimicrob. Agents, 2015, 46(4), pp. 359–361, DOI: 10.1016/j.ijantimicag.2015.06.010.

[51] Rodríguez-Rojas, A., Rodríguez-Beltrán, J., Couce, A., and Blázquez, J., "Antibiotics and Antibiotic Resistance: A Bitter Fight against Evolution," Int. J. Med. Microbiol., 2013, 303(6–7), pp. 293–297, DOI: 10.1016/j.ijmm.2013.02.004.

[52] Hutchings, M. I., Truman, A. W., and Wilkinson, B., "Antibiotics: Past, Present and Future," Curr. Opin. Microbiol., 2019, 51, pp. 72–80, DOI: 10.1016/j.mib.2019.10.008.

[53] Davies, J., and Davies, D., "Origins and Evolution of Antibiotic Resistance," Microbiol. Mol. Biol. Rev., 2010, 74(3), pp. 417–433, DOI: 10.1128/MMBR.00016-10.

[54] CDC (Centers for Disease Control and Prevention), "Antimicrobial Resistance," CDC, [Online]. Available: https://www.cdc.gov/drugresistance/about/how-resistance-happens.html.

[55] Moore, D. W., "Antibiotic Classification & Mechanism," Ortho Bullets, [Online]. Available: https://www.orthobullets.com/basic-science/9059/antibiotic-classification-and-mechanism.

[56] Munita, J. M., and Arias, C. A., "Mechanisms of Antibiotic Resistance," Virulence Mech. Bact. Pathog., 2016, 4(2), pp. 481–511, DOI: 10.1128/9781555819286.ch17.

[57] Capita, R., and Alonso-Calleja, C., "Antibiotic-Resistant Bacteria: A Challenge for the Food Industry," Crit. Rev. Food Sci. Nutr., 2013, 53(1), pp. 11–48, DOI: 10.1080/10408398.2010.519837.

[58] Holmes, A. H., Moore, L. S. P., Sundsfjord, A., Steinbakk, M., Regmi, S., Karkey, A., Guerin, P. J., and Piddock, L. J. V., "Understanding the Mechanisms and Drivers of Antimicrobial Resistance," Lancet, 2016, 387(10014), pp. 176–187, DOI: 10.1016/S0140-6736(15)00473-0.

[59] Cox, G., and Wright, G. D., "Intrinsic Antibiotic Resistance: Mechanisms, Origins, Challenges and Solutions," Int. J. Med. Microbiol., 2013, 303(6–7), pp. 287–292, DOI: 10.1016/j.ijmm.2013.02.009.

[60] Culyba, M. J., Mo, C. Y., and Kohli, R. M., "Targets for Combating the Evolution of Acquired Antibiotic Resistance," Biochemistry, 2015, 54(23), pp. 3573–3582, DOI: 10.1021/acs.biochem.5b00109.

[61] Van Hoek, A. H. A. M., Mevius, D., Guerra, B., Mullany, P., Roberts, A. P., and Aarts, H. J. M., "Acquired Antibiotic Resistance Genes: An Overview," Front. Microbiol., 2011, 2(SEP), DOI: 10.3389/fmicb.2011.00203.

[62] Sandegren, L., "Selection of Antibiotic Resistance at Very Low Antibiotic Concentrations," Ups. J. Med. Sci., 2014, 119(2), pp. 103–107.

[63] Liu, G., Thomsen, L. E., and Olsen, J. E., "Antimicrobial-Induced Horizontal Transfer of Antimicrobial Resistance Genes in Bacteria: A Mini-Review," J. Antimicrob. Chemother., 2022, 77(3), pp. 556–567, DOI: 10.1093/jac/dkab450.

[64] Andersson, D. I., and Hughes, D., "Evolution of Antibiotic Resistance at Non-Lethal Drug Concentrations," Drug Resist. Updat., 2012, 15(3), pp. 162–172.

[65] Wellington, E. M. H., Boxall, A. B. A., Cross, P., Feil, E. J., Gaze, W. H., Hawkey, P. M., Johnson-Rollings, A. S., Jones, D. L., Lee, N. M., and Otten, W., "The Role of the Natural Environment in the Emergence of Antibiotic Resistance in Gram-Negative Bacteria," Lancet Infect. Dis., 2013, 13(2), pp. 155–165.

[66] Hu, Y., Matsui, Y., and W. Riley, L., "Risk Factors for Fecal Carriage of Drug-Resistant Escherichia Coli: A Systematic Review and Meta-Analysis," Antimicrob. Resist. Infect. Control, 2020, 9(1), p. 31, DOI: 10.1186/s13756-020-0691-3.

[67] Ouchar Mahamat, O., Tidjani, A., Lounnas, M., Hide, M., Benavides, J., Somasse, C., Ouedraogo, A.-S., Sanou, S., Carrière, C., Bañuls, A.-L., Jean-Pierre, H., Dumont, Y., and Godreuil, S., "Fecal Carriage of Extended-Spectrum β-Lactamase-Producing Enterobacteriaceae in Hospital and Community Settings in Chad," Antimicrob. Resist. Infect. Control, 2019, 8(1), p. 169, DOI: 10.1186/s13756-019-0626-z.

[68] Band, V. I., and Weiss, D. S., "Heteroresistance: A Cause of Unexplained Antibiotic Treatment Failure?," PLOS Pathog., 2019, 15(6), p. e1007726, DOI: 10.1371/journal.ppat.1007726.

[69] Rebold, N., Lagnf, A. M., Alosaimy, S., Holger, D. J., Witucki, P., Mannino, A., Dierker, M., Lucas, K., Kunz Coyne, A. J., El Ghali, A., Caniff, K. E., Veve, M. P., and Rybak, M.

J., “Risk Factors for Carbapenem-Resistant Enterobacterales Clinical Treatment Failure,” Microbiol. Spectr., 2023, 11(1), DOI: 10.1128/spectrum.02647-22.

[70] World Health Organization (WHO), “WHO Publishes List of Bacteria for Which New Antibiotics Are Urgently Needed,” WHO, [Online]. Available: https://www.who.int/news/item/27-02-2017-who-publishes-list-of-bacteria-for-which-new-antibiotics-are-urgently-needed. [Accessed: 06-Sep-2022].

[71] Codjoe, F., and Donkor, E., “Carbapenem Resistance: A Review,” Med. Sci., 2017, 6(1), p. 1, DOI: 10.3390/medsci6010001.

[72] Papp-Wallace, K. M., Endimiani, A., Taracila, M. A., and Bonomo, R. A., “Carbapenems: Past, Present, and Future,” Antimicrob. Agents Chemother., 2011, 55(11), pp. 4943–4960, DOI: 10.1128/AAC.00296-11.

[73] Smith, H. Z., and Kendall, B., “Carbapenem Resistant Enterobacteriaceae,” StatPearls [Internet]. StatPearls Publ., 2021.

[74] Kopotsa, K., Osei Sekyere, J., and Mbelle, N. M., “Plasmid Evolution in Carbapenemase-producing Enterobacteriaceae : A Review,” Ann. N. Y. Acad. Sci., 2019, 1457(1), pp. 61–91, DOI: 10.1111/nyas.14223.

[75] Michael, G. B., Freitag, C., Wendlandt, S., Eidam, C., Feßler, A. T., Lopes, G. V., Kadlec, K., and Schwarz, S., “Emerging Issues in Antimicrobial Resistance of Bacteria from Food-Producing Animals,” Future Microbiol., 2015, 10(3), pp. 427–443, DOI: 10.2217/FMB.14.93.

[76] Mallick, A., Roy, A., Sarkar, S., Mondal, K. C., and Das, S., “Customized Molecular Diagnostics of Bacterial Bloodstream Infections for Carbapenem Resistance: A Convenient and Affordable Approach,” Pathog. Glob. Health, 2023, pp. 1–8, DOI: 10.1080/20477724.2023.2201982.

[77] Liu, Y.-C., Lu, C.-Y., Yen, T.-Y., Chang, L.-Y., Chen, J.-M., Lee, P.-I., and Huang, L.-M., “Clinical Characteristics and Outcomes of Carbapenem-Resistant Enterobacterales Bacteremia in Pediatric Patients,” J. Microbiol. Immunol. Infect., 2023, 56(1), pp. 84–92, DOI: 10.1016/j.jmii.2022.09.010.

[78] CDC, “Healthcare-Associated Infections (HAIs):CRE Technical Information,” CDC (Centers Dis. Control Prev., 2019, [Online]. Available: https://www.cdc.gov/hai/organisms/cre/technical-info.html. [Accessed: 08-Jun-2022].

[79] Liu, B.-T., Zhang, X.-Y., Wan, S.-W., Hao, J.-J., Jiang, R.-D., and Song, F.-J., “Characteristics of Carbapenem-Resistant Enterobacteriaceae in Ready-to-Eat Vegetables in China,” Front. Microbiol., 2018, 9(JUN), DOI: 10.3389/fmicb.2018.01147.

[80] Gordon, N., Bawa, R., and Palmateer, G., “Carbapenem-Resistant Enterobacteriaceae Testing in 45 Minutes Using an Electronic Sensor,” *Current Issues in Medicine: Diagnosis and Imaging*, 2021, pp. 1–18.

[81] Rabaan, A. A., Eljaaly, K., Alhumaid, S., Albayat, H., Al-Adsani, W., Sabour, A. A., Alshiekheid, M. A., Al-Jishi, J. M., Khamis, F., Alwarthan, S., Alhajri, M., Alfaraj, A. H., Tombuloglu, H., Garout, M., Alabdullah, D. M., Mohammed, E. A. E., Yami, F. S. Al, Almuhtaresh, H. A., Livias, K. A., Mutair, A. Al, Almushrif, S. A., Abusalah, M. A. H. A., and Ahmed, N., "An Overview on Phenotypic and Genotypic Characterisation of Carbapenem-Resistant Enterobacterales," Medicina (B. Aires)., 2022, 58(11), p. 1675, DOI: 10.3390/medicina58111675.

[82] Armin, S., Azimi, L., Shariatpanahi, G., Shirvani, A., and Almasian Tehrani, N., "The Prevalence of Colonization with Carbapenem-Resistant Enterobacteriaceae, E. Coli, Klebsiella and Enterobacter, and Related Risk Factors in Children," Arch. Pediatr. Infect. Dis., 2023, In Press(In Press), DOI: 10.5812/pedinfect-134518.

[83] Zeng, M., Xia, J., Zong, Z., Shi, Y., Ni, Y., Hu, F., Chen, Y., Zhuo, C., Hu, B., Lv, X., Li, J., Liu, Z., Zhang, J., Yang, W., Yang, F., Yang, Q., Zhou, H., Li, X., Wang, J., Li, Y., Ren, J., Chen, B., Chen, D., Wu, A., Guan, X., Qu, J., Wu, D., Huang, X., Qiu, H., Xu, Y., Yu, Y., and Wang, M., "Guidelines for the Diagnosis, Treatment, Prevention and Control of Infections Caused by Carbapenem-Resistant Gram-Negative Bacilli," J. Microbiol. Immunol. Infect., 2023, DOI: 10.1016/j.jmii.2023.01.017.

[84] Eichenberger, E. M., and Thaden, J. T., "Epidemiology and Mechanisms of Resistance of Extensively Drug Resistant Gram-Negative Bacteria," Antibiotics, 2019, 8(2), p. 37, DOI: 10.3390/antibiotics8020037.

[85] Guerra, B., Fischer, J., and Helmuth, R., "An Emerging Public Health Problem: Acquired Carbapenemase-Producing Microorganisms Are Present in Food-Producing Animals, Their Environment, Companion Animals and Wild Birds," Vet. Microbiol., 2014, 171(3–4), pp. 290–297, DOI: 10.1016/j.vetmic.2014.02.001.

[86] Queenan, A. M., and Bush, K., "Carbapenemases: The Versatile β-Lactamases," Clin. Microbiol. Rev., 2007, 20(3), pp. 440–458, DOI: 10.1128/CMR.00001-07.

[87] Boyd, S. E., Livermore, D. M., Hooper, D. C., and Hope, W. W., "Metallo-β-Lactamases: Structure, Function, Epidemiology, Treatment Options, and the Development Pipeline," Antimicrob. Agents Chemother., 2020, 64(10), DOI: 10.1128/AAC.00397-20.

[88] Cheruvanky, A., Stoesser, N., Sheppard, A. E., Crook, D. W., Hoffman, P. S., Weddle, E., Carroll, J., Sifri, C. D., Chai, W., Barry, K., Ramakrishnan, G., and Mathers, A. J., "Enhanced Klebsiella Pneumoniae Carbapenemase Expression from a Novel Tn 4401 Deletion," Antimicrob. Agents Chemother., 2017, 61(6), DOI: 10.1128/AAC.00025-17.

[89] Wu, Y., Yang, X., Liu, C., Zhang, Y., Cheung, Y. C., Wai Chi Chan, E., Chen, S., and Zhang, R., "Identification of a KPC Variant Conferring Resistance to Ceftazidime-Avibactam from ST11 Carbapenem-Resistant Klebsiella Pneumoniae Strains," Microbiol. Spectr., 2022, 10(2), DOI: 10.1128/spectrum.02655-21.

[90] Farhat, N., and Khan, A. U., "Evolving Trends of New Delhi Metallo-Betalactamse (NDM) Variants: A Threat to Antimicrobial Resistance," Infect. Genet. Evol., 2020, 86, p.

104588, DOI: 10.1016/j.meegid.2020.104588.

[91] Poirel, L., Héritier, C., Tolün, V., and Nordmann, P., "Emergence of Oxacillinase-Mediated Resistance to Imipenem in Klebsiella Pneumoniae," Antimicrob. Agents Chemother., 2004, 48(1), pp. 15–22, DOI: 10.1128/AAC.48.1.15-22.2004.

[92] Boyd, S. E., Holmes, A., Peck, R., Livermore, D. M., and Hope, W., "OXA-48-Like β-Lactamases: Global Epidemiology, Treatment Options, and Development Pipeline," Antimicrob. Agents Chemother., 2022, 66(8), DOI: 10.1128/aac.00216-22.

[93] Nair, D. V. T., Venkitanarayanan, K., and Johny, A. K., "Antibiotic-Resistant Salmonella in the Food Supply and the Potential Role of Antibiotic Alternatives for Control," Foods, 2018, 7(10), DOI: 10.3390/foods7100167.

[94] Farzana, R., Jones, L. S., Rahman, M. A., Sands, K., van Tonder, A. J., Portal, E., Criollo, J. M., Parkhill, J., Guest, M. F., Watkins, W. J., Pervin, M., Boostrom, I., Hassan, B., Mathias, J., Kalam, M. A., and Walsh, T. R., "Genomic Insights Into the Mechanism of Carbapenem Resistance Dissemination in Enterobacterales From a Tertiary Public Heath Setting in South Asia," Clin. Infect. Dis., 2023, 76(1), pp. 119–133, DOI: 10.1093/cid/ciac287.

[95] Grundmann, H., Livermore, D. M., Giske, C. G., Cantón, R., Rossolini, G. M., Campos, J., Vatopoulos, A., Gniadkowski, M., Toth, A., Pfeifer, Y., Jarlier, V., Carmeli, Y., and the CNSE Working Group, C., "Carbapenem-Non-Susceptible Enterobacteriaceae in Europe: Conclusions from a Meeting of National Experts," Eurosurveillance, 2010, 15(46), DOI: 10.2807/ese.15.46.19711-en.

[96] Nordmann, P., Poirel, L., and Dortet, L., "Rapid Detection of Carbapenemase-Producing Enterobacteriaceae," Emerg. Infect. Dis., 2012, 18(9), pp. 1503–1507, DOI: 10.3201/eid1809.120355.

[97] Souli, M., Galani, I., Antoniadou, A., Papadomichelakis, E., Poulakou, G., Panagea, T., Vourli, S., Zerva, L., Armaganidis, A., Kanellakopoulou, K., and Giamarellou, H., "An Outbreak of Infection Due to B-Lactamase Klebsiella Pneumoniae Carbapenemase 2–Producing K. Pneumoniae in a Greek University Hospital: Molecular Characterization, Epidemiology, and Outcomes," Clin. Infect. Dis., 2010, 50(3), pp. 364–373, DOI: 10.1086/649865.

[98] Raro, O. H. F., da Silva, R. M. C., Filho, E. M. R., Sukiennik, T. C. T., Stadnik, C., Dias, C. A. G., Oteo Iglesias, J., and Pérez-Vázquez, M., "Carbapenemase-Producing Klebsiella Pneumoniae From Transplanted Patients in Brazil: Phylogeny, Resistome, Virulome and Mobile Genetic Elements Harboring BlaKPC–2 or BlaNDM–1," Front. Microbiol., 2020, 11(July), pp. 1–16, DOI: 10.3389/fmicb.2020.01563.

[99] Manenzhe, R. I., Zar, H. J., Nicol, M. P., and Kaba, M., "The Spread of Carbapenemase-Producing Bacteria in Africa: A Systematic Review," J. Antimicrob. Chemother., 2015, 70(1), pp. 23–40, DOI: 10.1093/jac/dku356.

[100] Tula, M., Enabulele, O., Ophori, E., Aziegbemhin, A., Iyoha, O., and Filgona, J., "A Systematic Review of the Current Status of Carbapenem Resistance in Nigeria: Its Public Health Implication for National Intervention," Niger. Postgrad. Med. J., 2023, 30(1), p. 1, DOI: 10.4103/npmj.npmj_240_22.

[101] Taha, M. S., Hagras, M. M., Shalaby, M. M., Zamzam, Y. A., Elkolaly, R. M., Abdelwahab, M. A., and Maxwell, S. Y., "Genotypic Characterization of Carbapenem-Resistant Klebsiella Pneumoniae Isolated from an Egyptian University Hospital," Pathogens, 2023, 12(1), p. 121, DOI: 10.3390/pathogens12010121.

[102] Munny, N. N., Shamsuzzaman, S. M., Hossain, T., Khatun, S., and Johora, F. T., "Prevalence and Phenotypic Detection of Carbapenem-Resistant Enterobacter Species from the Clinical Specimens of a Tertiary Care Hospital in Bangladesh," Updat. Dent. Coll. J., 2023, 13(1), pp. 17–22, DOI: 10.3329/updcj.v13i1.64051.

[103] Huang, Y., Li, J., Wang, Q., Tang, K., Cai, X., and Li, C., "Detection of Carbapenem-Resistant Hypervirulent Klebsiella Pneumoniae ST11-K64 Co-Producing NDM-1 and KPC-2 in a Tertiary Hospital in Wuhan," J. Hosp. Infect., 2023, 131, pp. 70–80, DOI: 10.1016/j.jhin.2022.09.014.

[104] Cuzon, G., Naas, T., Demachy, M. C., and Nordmann, P., "Plasmid-Mediated Carbapenem-Hydrolyzing β-Lactamase KPC-2 in Klebsiella Pneumoniae Isolate from Greece," Antimicrob. Agents Chemother., 2008, 52(2), pp. 796–797, DOI: 10.1128/AAC.01180-07.

[105] Naas, Thierry, Patrice Nordmann, Gérard Vedel, and C. P., "Plasmid-Mediated Carbapenem-Hydrolyzing ℕ -Lactamase KPC in a Klebsiella Pneumoniae Isolate from France," Antimicrob. Agents Chemother., 2005, 49(10), pp. 4423–4424, DOI: 10.1128/AAC.49.10.4423.

[106] Kumarasamy, K. K., Toleman, M. A., Walsh, T. R., Bagaria, J., Butt, F., Balakrishnan, R., Chaudhary, U., Doumith, M., Giske, C. G., Irfan, S., Krishnan, P., Kumar, A. V, Maharjan, S., Mushtaq, S., Noorie, T., Paterson, D. L., Pearson, A., Perry, C., Pike, R., Rao, B., Ray, U., Sarma, J. B., Sharma, M., Sheridan, E., Thirunarayan, M. A., Turton, J., Upadhyay, S., Warner, M., Welfare, W., Livermore, D. M., and Woodford, N., "Emergence of a New Antibiotic Resistance Mechanism in India, Pakistan, and the UK: A Molecular, Biological, and Epidemiological Study," Lancet Infect. Dis., 2010, 10(9), pp. 597–602, DOI: 10.1016/S1473-3099(10)70143-2.

[107] Bij, A. K. Van Der, and Pitout, J. D. D., "The Role of International Travel in the Worldwide Spread of Multiresistant Enterobacteriaceae," 2012, (June), pp. 2090–2100, DOI: 10.1093/jac/dks214.

[108] Peirano, G., Bradford, P. A., Kazmierczak, K. M., Badal, R. E., Hackel, M., Hoban, D. J., and Pitout, J. D. D., "Global Incidence of Carbapenemase-Producing Escherichia Coli ST131," Emerg. Infect. Dis., 2014, 20(11), pp. 1928–1931, DOI: 10.3201/eid2011.141388.

[109] Pitout, J. D. D., Nordmann, P., and Poirel, L., "Carbapenemase-Producing Klebsiella Pneumoniae, a Key Pathogen Set for Global Nosocomial Dominance," Antimicrob. Agents Chemother., 2015, 59(10), pp. 5873–5884, DOI: 10.1128/AAC.01019-15.

[110] Poirel, L., Barbosa-Vasconcelos, A., Simões, R. R., Da Costa, P. M., Liu, W., and Nordmann, P., "Environmental KPC-Producing Escherichia Coli Isolates in Portugal," Antimicrob. Agents Chemother., 2012, 56(3), pp. 1662–1663, DOI: 10.1128/AAC.05850-11.

[111] Zhang, X., Lü, X., and Zong, Z., "Enterobacteriaceae Producing the KPC-2 Carbapenemase from Hospital Sewage," Diagn. Microbiol. Infect. Dis., 2012, 73(2), pp. 204–206, DOI: 10.1016/j.diagmicrobio.2012.02.007.

[112] Isozumi, R., Yoshimatsu, K., Yamashiro, T., Hasebe, F., Nguyen, B. M., Ngo, T. C., Yasuda, S. P., Koma, T., Shimizu, K., and Arikawa, J., "Bla NDM-1 –Positive Klebsiella Pneumoniae from Environment, Vietnam," Emerg. Infect. Dis., 2012, 18(8), DOI: 10.3201/eid1808.111816.

[113] Lepuschitz, S., Schill, S., Stoeger, A., Pekard-Amenitsch, S., Huhulescu, S., Inreiter, N., Hartl, R., Kerschner, H., Sorschag, S., Springer, B., Brisse, S., Allerberger, F., Mach, R. L., and Ruppitsch, W., "Whole Genome Sequencing Reveals Resemblance between ESBL-Producing and Carbapenem Resistant Klebsiella Pneumoniae Isolates from Austrian Rivers and Clinical Isolates from Hospitals," Sci. Total Environ., 2019, 662, pp. 227–235, DOI: 10.1016/j.scitotenv.2019.01.179.

[114] Tanner, W. D., VanDerslice, J. A., Goel, R. K., Leecaster, M. K., Fisher, M. A., Olstadt, J., Gurley, C. M., Morris, A. G., Seely, K. A., Chapman, L., Korando, M., Shabazz, K.-A., Stadsholt, A., VanDeVelde, J., Braun-Howland, E., Minihane, C., Higgins, P. J., Deras, M., Jaber, O., Jette, D., and Gundlapalli, A. V., "Multi-State Study of Enterobacteriaceae Harboring Extended-Spectrum Beta-Lactamase and Carbapenemase Genes in U.S. Drinking Water," Sci. Rep., 2019, 9(1), p. 3938, DOI: 10.1038/s41598-019-40420-0.

[115] Hoelle, J., Johnson, J. R., Johnston, B. D., Kinkle, B., Boczek, L., Ryu, H., and Hayes, S., "Survey of US Wastewater for Carbapenem-Resistant Enterobacteriaceae," J. Water Health, 2019, 17(2), pp. 219–226, DOI: 10.2166/wh.2019.165.

[116] Miriagou, V., Tzouvelekis, L. S., Rossiter, S., Tzelepi, E., Angulo, F. J., and Whichard, J. M., "Imipenem Resistance in a Salmonella Clinical Strain Due to Plasmid-Mediated Class A Carbapenemase KPC-2," Antimicrob. Agents Chemother., 2003, 47(4), pp. 1297–1300, DOI: 10.1128/AAC.47.4.1297-1300.2003.

[117] Chagas, T. P. G., Seki, L. M., da Silva, D. M., and Asensi, M. D., "Occurrence of KPC-2-Producing Klebsiella Pneumoniae Strains in Hospital Wastewater," J. Hosp. Infect., 2011, 77(3), p. 281, DOI: 10.1016/j.jhin.2010.10.008.

[118] Hamza, D., Dorgham, S., Ismael, E., El-Moez, S. I. A., Elhariri, M., Elhelw, R., and Hamza, E., "Emergence of β-Lactamase- and Carbapenemase- Producing Enterobacteriaceae at Integrated Fish Farms," Antimicrob. Resist. Infect. Control, 2020,

9(1), p. 67, DOI: 10.1186/s13756-020-00736-3.

[119] Fischer, J., Schmoger, S., Jahn, S., Helmuth, R., and Guerra, B., "NDM-1 Carbapenemase-Producing Salmonella Enterica Subsp. Enterica Serovar Corvallis Isolated from a Wild Bird in Germany," J. Antimicrob. Chemother., 2013, 68(12), pp. 2954–2956, DOI: 10.1093/jac/dkt260.

[120] Shaheen, B. W., Nayak, R., and Boothe, D. M., "Emergence of a New Delhi Metallo-β-Lactamase (NDM-1)-Encoding Gene in Clinical Escherichia Coli Isolates Recovered from Companion Animals in the United States," Antimicrob. Agents Chemother., 2013, 57(6), pp. 2902–2903, DOI: 10.1128/AAC.02028-12.

[121] Stolle, I., Prenger-Berninghoff, E., Stamm, I., Scheufen, S., Hassdenteufel, E., Guenther, S., Bethe, A., Pfeifer, Y., and Ewers, C., "Emergence of OXA-48 Carbapenemase-Producing Escherichia Coli and Klebsiella Pneumoniae in Dogs," J. Antimicrob. Chemother., 2013, 68(12), pp. 2802–2808, DOI: 10.1093/jac/dkt259.

[122] Fischer, J., Rodriguez, I., Schmoger, S., Friese, A., Roesler, U., Helmuth, R., and Guerra, B., "Escherichia Coli Producing VIM-1 Carbapenemase Isolated on a Pig Farm," J. Antimicrob. Chemother., 2012, 67(7), pp. 1793–1795, DOI: 10.1093/jac/dks108.

[123] Fischer, J., Rodríguez, I., Schmoger, S., Friese, A., Roesler, U., Helmuth, R., and Guerra, B., "Salmonella Enterica Subsp. Enterica Producing VIM-1 Carbapenemase Isolated from Livestock Farms," J. Antimicrob. Chemother., 2013, 68(2), pp. 478–480, DOI: 10.1093/jac/dks393.

[124] Vikram, A., and Schmidt, J. W., "Functional Bla KPC-2 Sequences Are Present in U.S. Beef Cattle Feces Regardless of Antibiotic Use," Foodborne Pathog. Dis., 2018, 15(7), pp. 444–448, DOI: 10.1089/fpd.2017.2406.

[125] Sugawara, Y., Hagiya, H., Akeda, Y., Aye, M. M., Myo Win, H. P., Sakamoto, N., Shanmugakani, R. K., Takeuchi, D., Nishi, I., Ueda, A., Htun, M. M., Tomono, K., and Hamada, S., "Dissemination of Carbapenemase-Producing Enterobacteriaceae Harbouring BlaNDM or BlaIMI in Local Market Foods of Yangon, Myanmar," Sci. Rep., 2019, 9(1), p. 14455, DOI: 10.1038/s41598-019-51002-5.

[126] Roschanski, N., Guenther, S., Vu, T. T. T., Fischer, J., Semmler, T., Huehn, S., Alter, T., and Roesler, U., "VIM-1 Carbapenemase-Producing Escherichia Coli Isolated from Retail Seafood, Germany 2016," Eurosurveillance, 2017, 22(43), pp. 1–7, DOI: 10.2807/1560-7917.ES.2017.22.43.17-00032.

[127] Wang, J., Yao, X., Luo, J., Lv, L., Zeng, Z., and Liu, J. H., "Emergence of Escherichia Coli Coproducing NDM-1 and KPC-2 Carbapenemases from a Retail Vegetable, China," J. Antimicrob. Chemother., 2018, 73(1), pp. 252–254, DOI: 10.1093/jac/dkx335.

[128] Touati, A., Mairi, A., Baloul, Y., Lalaoui, R., Bakour, S., Thighilt, L., Gharout, A., and Rolain, J.-M., "First Detection of Klebsiella Pneumoniae Producing OXA-48 in Fresh Vegetables from Béjaïa City, Algeria," J. Glob. Antimicrob. Resist., 2017, 9, pp. 17–18,

DOI: 10.1016/j.jgar.2017.02.006.

[129] Yao, X., Doi, Y., Zeng, L., Lv, L., and Liu, J.-H., "Carbapenem-Resistant and Colistin-Resistant Escherichia Coli Co-Producing NDM-9 and MCR-1," Lancet Infect. Dis., 2016, 16(3), pp. 288–289, DOI: 10.1016/S1473-3099(16)00057-8.

[130] Chaalal, N., Touati, A., Bakour, S., Aissa, M. A., Sotto, A., Lavigne, J. P., and Pantel, A., "Spread of OXA-48 and NDM-1-Producing Klebsiella Pneumoniae ST48 and ST101 in Chicken Meat in Western Algeria," Microb. Drug Resist., 2021, 27(4), pp. 492–500, DOI: 10.1089/mdr.2019.0419.

[131] Fernández, J., Guerra, B., and Rodicio, M. R., "Resistance to Carbapenems in Non-Typhoidal Salmonella Enterica Serovars from Humans, Animals and Food," Vet. Sci., 2018, 5(2), DOI: 10.3390/vetsci5020040.

[132] Bedos, J. P., Daikos, G., Dodgson, A. R., Pan, A., Petrosillo, N., Seifert, H., Vila, J., Ferrer, R., and Wilson, P., "Early Identification and Optimal Management of Carbapenem-Resistant Gram-Negative Infection," J. Hosp. Infect., 2021, 108, pp. 158–167, DOI: 10.1016/j.jhin.2020.12.001.

[133] World Health Organization (WHO), "Global Antimicrobial Resistance and Use Surveillance System (GLASS)," [Online]. Available: https://www.who.int/initiatives/glass.

[134] FDA, "The National Antimicrobial Resistance Monitoring System, NARMS," FDA, 2023, [Online]. Available: https://www.fda.gov/animal-veterinary/antimicrobial-resistance/national-antimicrobial-resistance-monitoring-system.

[135] Sutherland, J. B., Rafii, F., Lay, J. O., and Williams, A. J., "Rapid Analytical Methods to Identify Antibiotic-Resistant Bacteria," *Antibiotic Drug Resistance*, Wiley, September 9, 2019, pp. 533–566, DOI: 10.1002/9781119282549.ch21.

[136] Alizadeh, M., Wood, R. L., Buchanan, C. M., Bledsoe, C. G., Wood, M. E., McClellan, D. S., Blanco, R., Ravsten, T. V., Husseini, G. A., Hickey, C. L., Robison, R. A., and Pitt, W. G., "Rapid Separation of Bacteria from Blood – Chemical Aspects," Colloids Surfaces B Biointerfaces, 2017, 154, pp. 365–372, DOI: 10.1016/j.colsurfb.2017.03.027.

[137] Buehler, S. S., Madison, B., Snyder, S. R., Derzon, J. H., Cornish, N. E., Saubolle, M. A., Weissfeld, A. S., Weinstein, M. P., Liebow, E. B., and Wolk, D. M., "Effectiveness of Practices To Increase Timeliness of Providing Targeted Therapy for Inpatients with Bloodstream Infections: A Laboratory Medicine Best Practices Systematic Review and Meta-Analysis," Clin. Microbiol. Rev., 2016, 29(1), pp. 59–103, DOI: 10.1128/CMR.00053-14.

[138] Al-Zahrani, I. A., "Routine Detection of Carbapenem-Resistant Gram-Negative Bacilli in Clinical Laboratories," Saudi Med. J., 2018, 39(9), pp. 861–872, DOI: 10.15537/smj.2018.9.22840.

[139] Cusack, T. P., Ashley, E. A., Ling, C. L., Rattanavong, S., Roberts, T., Turner, P., Wangrangsimakul, T., and Dance, D. A. B., "Impact of CLSI and EUCAST Breakpoint Discrepancies on Reporting of Antimicrobial Susceptibility and AMR Surveillance," Clin. Microbiol. Infect., 2019, 25(7), pp. 910–911, DOI: 10.1016/j.cmi.2019.03.007.

[140] Lutgring, J. D., and Limbago, B. M., "The Problem of Carbapenemase-Producing-Carbapenem-Resistant-Enterobacteriaceae Detection," J. Clin. Microbiol., 2016, 54(3), pp. 529–534, DOI: 10.1128/JCM.02771-15.

[141] Cui, X., Zhang, H., and Du, H., "Carbapenemases in Enterobacteriaceae: Detection and Antimicrobial Therapy," Front. Microbiol., 2019, 10(August), pp. 1–12, DOI: 10.3389/fmicb.2019.01823.

[142] Takayama, Y., Adachi, Y., Nihonyanagi, S., and Okamoto, R., "Modified Hodge Test Using Mueller-Hinton Agar Supplemented with Cloxacillin Improves Screening for Carbapenemase-Producing Clinical Isolates of Enterobacteriaceae," J. Med. Microbiol., 2015, 64(7), pp. 774–777, DOI: 10.1099/jmm.0.000068.

[143] Amjad, A., Ia, M., Sa, A., Farwa, U., Malik, N., and Zia, F., "Modified Hodge Test : A Simple and Effective Test for Detection of Carbapenemase Production The Isolates Which Showed Intermediate or Susceptible Zones for Imipenem Were Tested for Carbapenemase Modified Hodge Test , as CL Recommends the MHT to Be Perform," Iran. J. Microbiol., 2011, 3(4), pp. 189–193.

[144] Saito, K., Nakano, R., Suzuki, Y., Nakano, A., Ogawa, Y., Yonekawa, S., Endo, S., Mizuno, F., Kasahara, K., Mikasa, K., Kaku, M., and Yano, H., "Suitability of Carbapenem Inactivation Method (CIM) for Detection of IMP Metallo-β-Lactamase-Producing Enterobacteriaceae," J. Clin. Microbiol., 2017, 55(4), pp. 1220–1222, DOI: 10.1128/JCM.02275-16.

[145] Alizadeh, N., Rezaee, M. A., Kafil, H. S., Barhaghi, M. H. S., Memar, M. Y., Milani, M., Hasani, A., and Ghotaslou, R., "Detection of Carbapenem-Resistant Enterobacteriaceae by Chromogenic Screening Media," J. Microbiol. Methods, 2018, 153(September), pp. 40–44, DOI: 10.1016/j.mimet.2018.09.001.

[146] Nordmann, P., and Poirel, L., "Strategies for Identification of Carbapenemase-Producing Enterobacteriaceae," J. Antimicrob. Chemother., 2013, 68(3), pp. 487–489, DOI: 10.1093/jac/dks426.

[147] Nordmann, P., Girlich, D., and Poirel, L., "Detection of Carbapenemase Producers in Enterobacteriaceae by Use of a Novel Screening Medium," J. Clin. Microbiol., 2012, 50(8), pp. 2761–2766, DOI: 10.1128/JCM.06477-11.

[148] Girlich, D., Poirel, L., and Nordmann, P., "Comparison of the SUPERCARBA, CHROMagar KPC, and Brilliance CRE Screening Media for Detection of Enterobacteriaceae with Reduced Susceptibility to Carbapenems," Diagn. Microbiol. Infect. Dis., 2013, 75(2), pp. 214–217, DOI: 10.1016/j.diagmicrobio.2012.10.006.

[149] Somily, A. M., Garaween, G. A., Abukhalid, N., Absar, M. M., and Senok, A. C., "Comparison of Molecular and Phenotypic Methods for the Detection and Characterization of Carbapenem Resistant Enterobacteriaceae," Acta Microbiol. Immunol. Hung., 2016, 63(1), pp. 69–81, DOI: 10.1556/030.63.2016.1.5.

[150] Maugeri, G., Lychko, I., Sobral, R., and Roque, A. C. A., "Identification and Antibiotic-Susceptibility Profiling of Infectious Bacterial Agents: A Review of Current and Future Trends," Biotechnol. J., 2019, 14(1), p. 1700750, DOI: 10.1002/biot.201700750.

[151] Reynoso, E. C., Laschi, S., Palchetti, I., and Torres, E., "Advances in Antimicrobial Resistance Monitoring Using Sensors and Biosensors: A Review," Chemosensors, 2021, 9(8), DOI: 10.3390/chemosensors9080232.

[152] Silva, A. P., Faria-Ramos, I., Ricardo, E., Miranda, I. M., Espinar, M. J., Costa-de-Oliveira, S., Cantón, R., Rodrigues, A. G., and Pina-Vaz, C., "Rapid Flow Cytometry Test for Identification of Different Carbapenemases in Enterobacteriaceae," Antimicrob. Agents Chemother., 2016, 60(6), pp. 3824–3826, DOI: 10.1128/AAC.02947-15.

[153] Bernabeu, S., Poirel, L., and Nordmann, P., "Spectrophotometry-Based Detection of Carbapenemase Producers among Enterobacteriaceae," Diagn. Microbiol. Infect. Dis., 2012, 74(1), pp. 88–90, DOI: 10.1016/j.diagmicrobio.2012.05.021.

[154] van Almsick, V., Ghebremedhin, B., Pfennigwerth, N., and Ahmad-Nejad, P., "Rapid Detection of Carbapenemase-Producing Acinetobacter Baumannii and Carbapenem-Resistant Enterobacteriaceae Using a Bioluminescence-Based Phenotypic Method," J. Microbiol. Methods, 2018, 147(February), pp. 20–25, DOI: 10.1016/j.mimet.2018.02.004.

[155] Bianco, G., Comini, S., Boattini, M., Ricciardelli, G., Guarrasi, L., Cavallo, R., and Costa, C., "MALDI-TOF MS-Based Approaches for Direct Identification of Gram-Negative Bacteria and BlaKPC-Carrying Plasmid Detection from Blood Cultures: A Three-Year Single-Centre Study and Proposal of a Diagnostic Algorithm," Microorganisms, 2022, 11(1), p. 91, DOI: 10.3390/microorganisms11010091.

[156] Knox, J., Jadhav, S., Sevior, D., Agyekum, A., Whipp, M., Waring, L., Iredell, J., and Palombo, E., "Phenotypic Detection of Carbapenemase-Producing Enterobacteriaceae by Use of Matrix-Assisted Laser Desorption Ionization–Time of Flight Mass Spectrometry and the Carba NP Test," J. Clin. Microbiol., 2014, 52(11), pp. 4075–4077, DOI: 10.1128/JCM.02121-14.

[157] Gato, E., Anantharajah, A., Arroyo, M. J., Artacho, M. J., Caballero, J. de D., Candela, A., Chudějová, K., Constanso, I. P., Elías, C., Fernández, J., Jiménez, J., Lumbreras, P., Méndez, G., Mulet, X., Pérez-Palacios, P., Rodríguez-Sánchez, B., Cantón, R., Hrabák, J., Mancera, L., Martínez-Martínez, L., Oliver, A., Pascual, Á., Verroken, A., Bou, G., and Oviaño, M., "Multicenter Performance Evaluation of MALDI-TOF MS for Rapid Detection of Carbapenemase Activity in Enterobacterales: The Future of Networking Data Analysis With Online Software," Front. Microbiol., 2022, 12, DOI: 10.3389/fmicb.2021.789731.

[158] Yu, J., Lin, Y.-T., Chen, W.-C., Tseng, K.-H., Lin, H.-H., Tien, N., Cho, C.-F., Huang, J.-Y., Liang, S.-J., Ho, L.-C., Hsieh, Y.-W., Hsu, K.-C., Ho, M.-W., Hsueh, P.-R., and Cho, D.-Y., "Direct Prediction of Carbapenem-Resistant, Carbapenemase-Producing, and Colistin-Resistant Klebsiella Pneumoniae Isolates from Routine MALDI-TOF Mass Spectra Using Machine Learning and Outcome Evaluation," Int. J. Antimicrob. Agents, 2023, p. 106799, DOI: 10.1016/j.ijantimicag.2023.106799.

[159] Eltahlawi, R. A., Jiman-Fatani, A., Gad, N. M., Ahmed, S. H., Al-Rabia, M. W., Zakai, S., Kharaba, A., and El-Hossary, D., "Detection of Carbapenem-Resistance in CRE by Comparative Assessment of RAPIDEC® CARBA NP and Xpert^{TM}Carba-R Assay," Infect. Drug Resist., 2023, Volume 16, pp. 1123–1131, DOI: 10.2147/IDR.S393739.

[160] Woodford, N., and Sundsfjord, A., "Molecular Detection of Antibiotic Resistance: When and Where?," J. Antimicrob. Chemother., 2005, 56(2), pp. 259–261, DOI: 10.1093/jac/dki195.

[161] Rijpens, N. P., and Herman, L. M. F., "Molecular Methods for Identification and Detection of Bacterial Food Pathogens," J. AOAC Int., 2002, 85(4), pp. 984–995, DOI: 10.1093/jaoac/85.4.984.

[162] Smiljanic, M., Kaase, M., Ahmad-Nejad, P., and Ghebremedhin, B., "Comparison of In-House and Commercial Real Time-PCR Based Carbapenemase Gene Detection Methods in Enterobacteriaceae and Non-Fermenting Gram-Negative Bacterial Isolates," Ann. Clin. Microbiol. Antimicrob., 2017, 16(1), p. 48, DOI: 10.1186/s12941-017-0223-z.

[163] Probst, K., Boutin, S., Späth, I., Scherrer, M., Henny, N., Sahin, D., Heininger, A., Heeg, K., and Nurjadi, D., "Direct-PCR from Rectal Swabs and Environmental Reservoirs: A Fast and Efficient Alternative to Detect BlaOXA-48 Carbapenemase Genes in an Enterobacter Cloacae Outbreak Setting," Environ. Res., 2022, 203, p. 111808, DOI: 10.1016/j.envres.2021.111808.

[164] Naas, T., Ergani, A., Carrër, A., and Nordmann, P., "Real-Time PCR for Detection of NDM-1 Carbapenemase Genes from Spiked Stool Samples," Antimicrob. Agents Chemother., 2011, 55(9), pp. 4038–4043, DOI: 10.1128/AAC.01734-10.

[165] Hlousek, L., Voronov, S., Diankov, V., Leblang, A. B., Wells, P. J., Ford, D. M., Nolling, J., Hart, K. W., Espinoza, P. A., Bristol, M. R., Tsongalis, G. J., Yen-Lieberman, B., Slepnev, V. I., Kong, L. I., and Lee, M.-C., "Automated High Multiplex QPCR Platform for Simultaneous Detection and Quantification of Multiple Nucleic Acid Targets," Biotechniques, 2012, 52(5), pp. 316–324, DOI: 10.2144/0000113852.

[166] Poirel, L., Walsh, T. R., Cuvillier, V., and Nordmann, P., "Multiplex PCR for Detection of Acquired Carbapenemase Genes," Diagn. Microbiol. Infect. Dis., 2011, 70(1), pp. 119–123, DOI: 10.1016/j.diagmicrobio.2010.12.002.

[167] Dortet, L., Fusaro, M., and Naas, T., "Improvement of the Xpert Carba-R Kit for the Detection of Carbapenemase-Producing Enterobacteriaceae," Antimicrob. Agents Chemother., 2016, 60(6), pp. 3832–3837, DOI: 10.1128/AAC.00517-16.

[168] Lau, A. F., Fahle, G. A., Kemp, M. A., Jassem, A. N., Dekker, J. P., and Frank, K. M., "Clinical Performance of Check-Direct CPE, a Multiplex PCR for Direct Detection of Bla KPC , Bla NDM and/or Bla VIM , and Bla OXA-48 from Perirectal Swabs," J. Clin. Microbiol., 2015, 53(12), pp. 3729–3737, DOI: 10.1128/JCM.01921-15.

[169] Wu, S., and Hulme, J. P., "Recent Advances in the Detection of Antibiotic and Multi-Drug Resistant Salmonella: An Update," Int. J. Mol. Sci., 2021, 22(7), DOI: 10.3390/ijms22073499.

[170] Frickmann, H., Zautner, A. E., Moter, A., Kikhney, J., Hagen, R. M., Stender, H., and Poppert, S., "Fluorescence in Situ Hybridization (FISH) in the Microbiological Diagnostic Routine Laboratory: A Review," Crit. Rev. Microbiol., 2017, 43(3), pp. 263–293, DOI: 10.3109/1040841X.2016.1169990.

[171] Frye, J. G., Jesse, T., Long, F., Rondeau, G., Porwollik, S., McClelland, M., Jackson, C. R., Englen, M., and Fedorka-Cray, P. J., "DNA Microarray Detection of Antimicrobial Resistance Genes in Diverse Bacteria," Int. J. Antimicrob. Agents, 2006, 27(2), pp. 138–151, DOI: 10.1016/j.ijantimicag.2005.09.021.

[172] Marimuthu, K., Venkatachalam, I., Koh, V., Harbarth, S., Perencevich, E., Cherng, B. P. Z., Fong, R. K. C., Pada, S. K., Ooi, S. T., Smitasin, N., Thoon, K. C., Tambyah, P. A., Hsu, L. Y., Koh, T. H., De, P. P., Tan, T. Y., Chan, D., Deepak, R. N., Tee, N. W. S., Kwa, A., Cai, Y., Teo, Y.-Y., Thevasagayam, N. M., Prakki, S. R. S., Xu, W., Khong, W. X., Henderson, D., Stoesser, N., Eyre, D. W., Crook, D., Ang, M., Lin, R. T. P., Chow, A., Cook, A. R., Teo, J., and Ng, O. T., "Whole Genome Sequencing Reveals Hidden Transmission of Carbapenemase-Producing Enterobacterales," Nat. Commun., 2022, 13(1), p. 3052, DOI: 10.1038/s41467-022-30637-5.

[173] Nakano, R., Nakano, A., Ishii, Y., Ubagai, T., Kikuchi-Ueda, T., Kikuchi, H., Tansho-Nagakawa, S., Kamoshida, G., Mu, X., and Ono, Y., "Rapid Detection of the Klebsiella Pneumoniae Carbapenemase (KPC) Gene by Loop-Mediated Isothermal Amplification (LAMP)," J. Infect. Chemother., 2015, 21(3), pp. 202–206, DOI: 10.1016/j.jiac.2014.11.010.

[174] Wu, B., Tong, X., Chen, B., Yuan, W., Fu, M., Yang, X., Chen, H., Zhang, G., Wu, G., and Xu, B., "Development of Microfluidic Chip-Based Loop-Mediated Isothermal Amplification (LAMP) Method for Detection of Carbapenemase Producing Bacteria," Microbiol. Spectr., 2022, 10(5), DOI: 10.1128/spectrum.00322-22.

[175] Ceyssens, P.-J., Garcia-Graells, C., Fux, F., Botteldoorn, N., Mattheus, W., Wuyts, V., De Keersmaecker, S., Dierick, K., and Bertrand, S., "Development of a Luminex XTAG ® Assay for Cost-Effective Multiplex Detection of β-Lactamases in Gram-Negative Bacteria," J. Antimicrob. Chemother., 2016, 71(9), pp. 2479–2483, DOI: 10.1093/jac/dkw201.

[176] Oeschger, T., Kret, L., and Erickson, D., "Multiplexed Paper-Based Assay for Personalized Antimicrobial Susceptibility Profiling of Carbapenem-Resistant Enterobacteriaceae Performed in a Rechargeable Coffee Mug," Sci. Rep., 2022.

[177] McEwan, A. S., Derome, A., Meunier, D., Burns, P. J., Woodford, N., and Dodgson, A. R., "Evaluation of the NucliSENS EasyQ KPC Assay for Detection of Klebsiella Pneumoniae Carbapenemase-Producing Enterobacteriaceae," J. Clin. Microbiol., 2013, 51(6), pp. 1948–1950, DOI: 10.1128/JCM.00057-13.

[178] Laffler, T. G., Cummins, L. L., McClain, C. M., Quinn, C. D., Toro, M. A., Carolan, H. E., Toleno, D. M., Rounds, M. A., Eshoo, M. W., Stratton, C. W., Sampath, R., Blyn, L. B., Ecker, D. J., and Tang, Y.-W., "Enhanced Diagnostic Yields of Bacteremia and Candidemia in Blood Specimens by PCR-Electrospray Ionization Mass Spectrometry," J. Clin. Microbiol., 2013, 51(11), pp. 3535–3541, DOI: 10.1128/JCM.00876-13.

[179] Zankari, E., Hasman, H., Kaas, R. S., Seyfarth, A. M., Agersø, Y., Lund, O., Larsen, M. V., and Aarestrup, F. M., "Genotyping Using Whole-Genome Sequencing Is a Realistic Alternative to Surveillance Based on Phenotypic Antimicrobial Susceptibility Testing," J. Antimicrob. Chemother., 2013, 68(4), pp. 771–777, DOI: 10.1093/jac/dks496.

[180] Bohara, R. A., and Pawar, S. H., "Innovative Developments in Bacterial Detection with Magnetic Nanoparticles," Appl. Biochem. Biotechnol., 2015, 176(4), pp. 1044–1058, DOI: 10.1007/s12010-015-1628-9.

[181] Wareham, D. W., Shah, R., Betts, J. W., Phee, L. M., and Momin, M. H. F. A., "Evaluation of an Immunochromatographic Lateral Flow Assay (OXA-48 K -SeT) for Rapid Detection of OXA-48-Like Carbapenemases in Enterobacteriaceae," J. Clin. Microbiol., 2016, 54(2), pp. 471–473, DOI: 10.1128/JCM.02900-15.

[182] Hu, S., Niu, L., Zhao, F., Yan, L., Nong, J., Wang, C., Gao, N., Zhu, X., Wu, L., Bo, T., Wang, H., and Gu, J., "Identification of Acinetobacter Baumannii and Its Carbapenem-Resistant Gene BlaOXA-23-like by Multiple Cross Displacement Amplification Combined with Lateral Flow Biosensor," Sci. Rep., 2019, 9(1), p. 17888, DOI: 10.1038/s41598-019-54465-8.

[183] Perumal, V., and Hashim, U., "Advances in Biosensors: Principle, Architecture and Applications," J. Appl. Biomed., 2014, 12(1), pp. 1–15, DOI: 10.1016/j.jab.2013.02.001.

[184] Ahmed, A., Rushworth, J. V., Hirst, N. A., and Millner, P. A., "Biosensors for Whole-Cell Bacterial Detection," Clin. Microbiol. Rev., 2014, 27(3), pp. 631–646, DOI: 10.1128/CMR.00120-13.

[185] Ahmed, M. U., Zourob, M., and Tamiya, E., "Introduction to Food Biosensors," Food Biosens., 2017, pp. 1–21, ISBN: 978-1-5231-2621-7.

[186] Drummond, T. G., Hill, M. G., and Barton, J. K., "Electrochemical DNA Sensors," Nat. Biotechnol., 2003, 21(10), pp. 1192–1199, DOI: 10.1038/nbt873.

[187] Chen, M., Hou, C., Huo, D., Bao, J., Fa, H., and Shen, C., "An Electrochemical DNA Biosensor Based on Nitrogen-Doped Graphene/Au Nanoparticles for Human Multidrug Resistance Gene Detection," Biosens. Bioelectron., 2016, 85, pp. 684–691, DOI: 10.1016/j.bios.2016.05.051.

[188] Watanabe, K., Kuwata, N., Sakamoto, H., Amano, Y., Satomura, T., and Suye, S. I., "A Smart DNA Sensing System for Detecting Methicillin-Resistant Staphylococcus Aureus Using Modified Nanoparticle Probes," Biosens. Bioelectron., 2015, 67, pp. 419–423, DOI: 10.1016/j.bios.2014.08.075.

[189] Huang, J. M.-Y., Henihan, G., Macdonald, D., Michalowski, A., Templeton, K., Gibb, A. P., Schulze, H., and Bachmann, T. T., "Rapid Electrochemical Detection of New Delhi Metallo-Beta-Lactamase Genes To Enable Point-of-Care Testing of Carbapenem-Resistant Enterobacteriaceae," Anal. Chem., 2015, 87(15), pp. 7738–7745, DOI: 10.1021/acs.analchem.5b01270.

[190] Homola, J., "Present and Future of Surface Plasmon Resonance Biosensors," Anal. Bioanal. Chem., 2003, 377(3), pp. 528–539, DOI: 10.1007/s00216-003-2101-0.

[191] Wong, Y. L., Kang, W. C. M., Reyes, M., Teo, J. W. P., and Kah, J. C. Y., "Rapid Detection of Carbapenemase-Producing Enterobacteriacae Based on Surface-Enhanced Raman Spectroscopy with Gold Nanostars," ACS Infect. Dis., 2020, 6(5), pp. 947–953, DOI: 10.1021/acsinfecdis.9b00318.

[192] Li, J., Wang, C., Kang, H., Shao, L., Hu, L., Xiao, R., Wang, S., and Gu, B., "Label-Free Identification Carbapenem-Resistant Escherichia Coli Based on Surface-Enhanced Resonance Raman Scattering," RSC Adv., 2018, 8(9), pp. 4761–4765, DOI: 10.1039/C7RA13063E.

[193] Ahmadi, S., Kamaladini, H., Haddadi, F., and Sharifmoghadam, M. R., "Thiol-Capped Gold Nanoparticle Biosensors for Rapid and Sensitive Visual Colorimetric Detection of Klebsiella Pneumoniae," J. Fluoresc., 2018, 28(4), pp. 987–998, DOI: 10.1007/s10895-018-2262-z.

[194] Quintela, I. A., De Los Reyes, B. G., Lin, C. S., and Wu, V. C. H., "Simultaneous Colorimetric Detection of a Variety of Salmonella Spp. In Food and Environmental Samples by Optical Biosensing Using Oligonucleotide-Gold Nanoparticles," Front. Microbiol., 2019, 10(MAY), pp. 1–12, DOI: 10.3389/fmicb.2019.01138.

[195] Bakthavathsalam, P., Rajendran, V. K., and Baquir Mohammed, J. A., "A Direct Detection of Escherichia Coli Genomic DNA Using Gold Nanoprobes," J. Nanobiotechnology, 2012, 10(1), p. 8, DOI: 10.1186/1477-3155-10-8.

[196] Sharief, S. A., Caliskan-Aydogan, O., and Alocilja, E., "Carbohydrate-Coated Magnetic and Gold Nanoparticles for Point-of-Use Food Contamination Testing," Biosens. Bioelectron. X, 2023, 13(November 2022), p. 100322, DOI: 10.1016/j.biosx.2023.100322.

[197] Sharief, S. A., Caliskan-Aydogan, O., and Alocilja, E. C., "Carbohydrate-Coated Nanoparticles for PCR-Less Genomic Detection of Salmonella from Fresh Produce," Food Control, 2023, 150(January), p. 109770, DOI: 10.1016/j.foodcont.2023.109770.

[198] Baetsen-Young, A. M., Vasher, M., Matta, L. L., Colgan, P., Alocilja, E. C., and Day, B., "Direct Colorimetric Detection of Unamplified Pathogen DNA by Dextrin-Capped Gold

Nanoparticles," Biosens. Bioelectron., 2018, 101(August 2017), pp. 29–36, DOI: 10.1016/j.bios.2017.10.011.

[199] Wang, Y., and Alocilja, E. C., "Gold Nanoparticle-Labeled Biosensor for Rapid and Sensitive Detection of Bacterial Pathogens," J. Biol. Eng., 2015, 9(1), pp. 1–7, DOI: 10.1186/s13036-015-0014-z.

[200] Aldewachi, H., Chalati, T., Woodroofe, M. N., Bricklebank, N., Sharrack, B., and Gardiner, P., "Gold Nanoparticle-Based Colorimetric Biosensors," Nanoscale, 2018, 10(1), pp. 18–33, DOI: 10.1039/C7NR06367A.

[201] Li, Y., Schluesener, H. J., and Xu, S., "Gold Nanoparticle-Based Biosensors," Gold Bull., 2010, 43(1), pp. 29–41, DOI: 10.1007/BF03214964.

[202] Zeng, S., Yong, K.-T., Roy, I., Dinh, X.-Q., Yu, X., and Luan, F., "A Review on Functionalized Gold Nanoparticles for Biosensing Applications," Plasmonics, 2011, 6(3), pp. 491–506, DOI: 10.1007/s11468-011-9228-1.

[203] Zhao, P., Li, N., and Astruc, D., "State of the Art in Gold Nanoparticle Synthesis," Coord. Chem. Rev., 2013, 257(3–4), pp. 638–665, DOI: 10.1016/j.ccr.2012.09.002.

[204] Hua, Z., Yu, T., Liu, D., and Xianyu, Y., "Recent Advances in Gold Nanoparticles-Based Biosensors for Food Safety Detection," Biosens. Bioelectron., 2021, 179(February), p. 113076, DOI: 10.1016/j.bios.2021.113076.

[205] Mohamed A. Abdou Mohamed, Kozlowski, H. N., Kim, J., Zagorovsky, K., Kantor, M., Feld, J. J., Mubareka, S., Mazzulli, T., and Chan, W. C. W., "Diagnosing Antibiotic Resistance UsingNucleic Acid Enzymes and Gold Nanoparticles," 2021.

[206] Mirkin, C. A., Letsinger, R. L., Mucic, R. C., and Storhoff, J. J., "A DNA-Based Method for Rationally Assembling Nanoparticles into Macroscopic Materials," Nature, 1996, 382(6592), pp. 607–609, DOI: 10.1038/382607a0.

[207] Osmani Bojd, M., Kamaladini, H., Haddadi, F., and Vaseghi, A., "Thiolated AuNP Probes and Multiplex PCR for Molecular Detection of Staphylococcus Epidermidis," Mol. Cell. Probes, 2017, 34, pp. 30–36, DOI: 10.1016/j.mcp.2017.04.006.

[208] Hua, Z., Yu, T., Liu, D., and Xianyu, Y., "Recent Advances in Gold Nanoparticles-Based Biosensors for Food Safety Detection," Biosens. Bioelectron., 2021, 179(January), p. 113076, DOI: 10.1016/j.bios.2021.113076.

[209] Prasad, D., Shankaracharya, and Vidyarthi, A. S., "Gold Nanoparticles-Based Colorimetric Assay for Rapid Detection of Salmonella Species in Food Samples," World J. Microbiol. Biotechnol., 2011, 27(9), pp. 2227–2230, DOI: 10.1007/s11274-011-0679-5.

[210] Pitt, W. G., Alizadeh, M., Husseini, G. A., McClellan, D. S., Buchanan, C. M., Bledsoe, C. G., Robison, R. A., Blanco, R., Roeder, B. L., Melville, M., and Hunter, A. K., "Rapid Separation of Bacteria from Blood-Review and Outlook," Biotechnol. Prog., 2016, 32(4),

pp. 823–839, DOI: 10.1002/btpr.2299.

[211] Fukushima, H., Katsube, K., Hata, Y., Kishi, R., and Fujiwara, S., "Rapid Separation and Concentration of Food-Borne Pathogens in Food Samples Prior to Quantification by Viable-Cell Counting and Real-Time PCR," Appl. Environ. Microbiol., 2007, 73(1), pp. 92–100, DOI: 10.1128/AEM.01772-06.

[212] Agoston, R., Soni, K. A., McElhany, K., Cepeda, M. L., Zuckerman, U., Tzipori, S., ... & Pillai, S. D., "Rapid Concentration of Bacillus and Clostridium Spores from Large Volumes of Milk, Using Continuous Flow Centrifugation," J. Food Prot., 2009, 72(3), pp. 666–668, DOI: 10.4315/0362-028X-72.3.666.

[213] Rathnayaka, U. S. K., & Rakshit, S. K, "Evaluation of Metal Hydroxide Immobilization and Dna Extraction Methods on Detection of Salmonella Enterica from Pork Sausage by Nested Polymerase Chain Reaction," J. Muscle Foods, 2010, 21(4), pp. 801–812, DOI: 10.1111/j.1745-4573.2010.00220.x.

[214] Chen, C.-T., Reddy, P. M., Ma, Y.-R., and Ho, Y.-P., "Mass Spectrometric Identification of Pathogens in Foods Using a Zirconium Hydroxide Immobilization Approach," Int. J. Mass Spectrom., 2012, 312, pp. 45–52, DOI: 10.1016/j.ijms.2011.05.014.

[215] Kumar, N., Wang, W., Ortiz-Marquez, J. C., Catalano, M., Gray, M., Biglari, N., Hikari, K., Ling, X., Gao, J., van Opijnen, T., and Burch, K. S., "Dielectrophoresis Assisted Rapid, Selective and Single Cell Detection of Antibiotic Resistant Bacteria with G-FETs," Biosens. Bioelectron., 2020, 156, p. 112123, DOI: 10.1016/j.bios.2020.112123.

[216] Chung, C.-C., Cheng, I.-F., Chen, H.-M., Kan, H.-C., Yang, W.-H., and Chang, H.-C., "Screening of Antibiotic Susceptibility to β-Lactam-Induced Elongation of Gram-Negative Bacteria Based on Dielectrophoresis," Anal. Chem., 2012, 84(7), pp. 3347–3354, DOI: 10.1021/ac300093w.

[217] Krishna, V. D., Wu, K., Su, D., Cheeran, M. C. J., Wang, J. P., and Perez, A., "Nanotechnology: Review of Concepts and Potential Application of Sensing Platforms in Food Safety," Food Microbiol., 2018, 75, pp. 47–54, DOI: 10.1016/j.fm.2018.01.025.

[218] Lv, M., Liu, Y., Geng, J., Kou, X., Xin, Z., and Yang, D., "Engineering Nanomaterials-Based Biosensors for Food Safety Detection," Biosens. Bioelectron., 2018, 106(January), pp. 122–128, DOI: 10.1016/j.bios.2018.01.049.

[219] Olsvik, Ø., Popovic, T., Skjerve, E., Cudjoe, K. S., Hornes, E., Ugelstad, J., and Uhlén, M., "Magnetic Separation Techniques in Diagnostic Microbiology," Clin. Microbiol. Rev., 1994, 7(1), pp. 43–54, DOI: 10.1128/CMR.7.1.43.

[220] Mohammed, L., Gomaa, H. G., Ragab, D., and Zhu, J., "Magnetic Nanoparticles for Environmental and Biomedical Applications: A Review," Particuology, 2017, 30, pp. 1–14, DOI: 10.1016/j.partic.2016.06.001.

[221] Gu, H., Ho, P. L., Tsang, K. W. T., Yu, C. W., and Xu, B., "Using Biofunctional Magnetic

Nanoparticles to Capture Gram-Negative Bacteria at an Ultra-Low Concentration," Chem. Commun., 2003, 3(14), pp. 1758–1759, DOI: 10.1039/b305421g.

[222] Xu, M., Wang, R., and Li, Y., "Rapid Detection of Escherichia Coli O157:H7 and Salmonella Typhimurium in Foods Using an Electrochemical Immunosensor Based on Screen-Printed Interdigitated Microelectrode and Immunomagnetic Separation," Talanta, 2016, 148, pp. 200–208, DOI: 10.1016/j.talanta.2015.10.082.

[223] Lai, H., Xu, F., and Wang, L., "A Review of the Preparation and Application of Magnetic Nanoparticles for Surface-Enhanced Raman Scattering," J. Mater. Sci., 2018, 53(12), pp. 8677–8698, DOI: 10.1007/s10853-018-2095-9.

[224] Chen, J., and Park, B., "Effect of Immunomagnetic Bead Size on Recovery of Foodborne Pathogenic Bacteria," Int. J. Food Microbiol., 2018, 267(July 2017), pp. 1–8, DOI: 10.1016/j.ijfoodmicro.2017.11.022.

[225] Guntupalli, R., Sorokulova, I., Olsen, E., Globa, L., Pustovyy, O., and Vodyanoy, V., "Biosensor for Detection of Antibiotic Resistant Staphylococcus Bacteria.," J. Vis. Exp., 2013, (75), pp. 1–11, DOI: 10.3791/50474.

[226] Tawil, N., Mouawad, F., Lévesque, S., Sacher, E., Mandeville, R., and Meunier, M., "The Differential Detection of Methicillin-Resistant, Methicillin-Susceptible and Borderline Oxacillin-Resistant Staphylococcus Aureus by Surface Plasmon Resonance," Biosens. Bioelectron., 2013, 49, pp. 334–340, DOI: 10.1016/j.bios.2013.05.031.

[227] Wang, Z., Wang, D., Kinchla, A. J., Sela, D. A., and Nugen, S. R., "Rapid Screening of Waterborne Pathogens Using Phage-Mediated Separation Coupled with Real-Time PCR Detection," Anal. Bioanal. Chem., 2016, 408(15), pp. 4169–4178, DOI: 10.1007/s00216-016-9511-2.

[228] Kretzer, J. W., Schmelcher, M., and Loessner, M. J., "Ultrasensitive and Fast Diagnostics of Viable Listeria Cells by CBD Magnetic Separation Combined with A511::LuxAB Detection," Viruses, 2018, 10(11), DOI: 10.3390/v10110626.

[229] Bayat, F., Didar, T. F., and Hosseinidoust, Z., "Emerging Investigator Series: Bacteriophages as Nano Engineering Tools for Quality Monitoring and Pathogen Detection in Water and Wastewater," Environ. Sci. Nano, 2021, 8(2), pp. 367–389, DOI: 10.1039/d0en00962h.

[230] "Gu et Al_2003_Using Biofunctional Magnetic Nanoparticles to Capture Vancomycin-Resistant Enterococci and Other Gram-Positive Bacteria at Ultralow Concentration.Pdf."

[231] Zheng, Q., Liu, H., and Zhu, J., "Amine-Functionalized Fe3O4 Magnetic Nanoparticles for Rapid Capture and Removal of Bacterial Pathogens," J. Chinese Inst. Food Sci. Technol., 2014, 14(6), pp. 200–207.

[232] Dester, E. F., "Extraction, Concentration, and Detection of Foodborne Pathogens Using Glycan-Coated Magnetic Nanoparticles and a Gold Nanoparticle Colorimetric Biosensor,"

Michigan State University.

[233] Cardoso, V. F., Francesko, A., Ribeiro, C., Bañobre-López, M., Martins, P., and Lanceros-Mendez, S., "Advances in Magnetic Nanoparticles for Biomedical Applications," Adv. Healthc. Mater., 2018, 7(5), p. 1700845, DOI: 10.1002/adhm.201700845.

[234] Fratila, R. M., Moros, M., and de la Fuente, J. M., "Recent Advances in Biosensing Using Magnetic Glyconanoparticles," Anal. Bioanal. Chem., 2016, 408(7), pp. 1783–1803, DOI: 10.1007/s00216-015-8953-2.

[235] El-Boubbou, K., Gruden, C., and Huang, X., "Magnetic Glyco-Nanoparticles: A Unique Tool for Rapid Pathogen Detection, Decontamination, and Strain Differentiation," J. Am. Chem. Soc., 2007, 129(44), pp. 13392–13393, DOI: 10.1021/ja076086e.

[236] Matta, L. L., "Biosensing Total Bacterial Load in Liquid Matrices to Improve Food Supply Chain Safety Using Carbohydrate-Functionalized Magnetic Nanoparticles for Cell Capture and Gold Nanoparticles for Signaling," 2018.

[237] Castelló, J., Gallardo, M., Busquets, M. A., and Estelrich, J., "Chitosan (or Alginate)-Coated Iron Oxide Nanoparticles: A Comparative Study," Colloids Surfaces A Physicochem. Eng. Asp., 2015, 468, pp. 151–158, DOI: 10.1016/j.colsurfa.2014.12.031.

[238] Wilson, J. W., Schurr, M. J., LeBlanc, C. L., Ramamurthy, R., Buchanan, K. L., and Nickerson, C. A., "Mechanisms of Bacterial Pathogenicity," Postgrad. Med. J., 2002, 78(918), pp. 216–224, DOI: 10.1136/pmj.78.918.216.

[239] Matta, L. L., and Alocilja, E. C., "Emerging Nano-Biosensing with Suspended MNP Microbial Extraction and EANP Labeling," Biosens. Bioelectron., 2018, 117(July), pp. 781–793, DOI: 10.1016/j.bios.2018.07.007.

[240] Briceno, R. K., Sergent, S. R., Benites, S. M., and Alocilja, E. C., "Nanoparticle-Based Biosensing Assay for Universally Accessible Low-Cost Tb Detection with Comparable Sensitivity as Culture," Diagnostics, 2019, 9(4), DOI: 10.3390/diagnostics9040222.

[241] Karuppuswami, S., Matta, L. L., Alocilja, E. C., and Chahal, P., "A Wireless RFID Compatible Sensor Tag Using Gold Nanoparticle Markers for Pathogen Detection in the Liquid Food Supply Chain," IEEE Sensors Lett., 2018, 2(2), pp. 1–4, DOI: 10.1109/lsens.2018.2822305.

[242] Boodoo, C., Dester, E., Sharief, S. A., and Alocilja, E. C., "Influence of Biological and Environmental Factors in the Extraction and Concentration of Foodborne Pathogens Using Glycan-Coated Magnetic Nanoparticles," J. Food Prot., 2023, 86(4), p. 100066, DOI: 10.1016/j.jfp.2023.100066.

[243] Gullberg, E., Cao, S., Berg, O. G., Ilbäck, C., Sandegren, L., Hughes, D., and Andersson, D. I., "Selection of Resistant Bacteria at Very Low Antibiotic Concentrations," PLoS Pathog., 2011, 7(7), pp. 1–9, DOI: 10.1371/journal.ppat.1002158.

[244] Hughes, D., and Andersson, D. I., "Environmental and Genetic Modulation of the Phenotypic Expression of Antibiotic Resistance," FEMS Microbiol. Rev., 2017, 41(3), pp. 374–391.

[245] Ter Kuile, B. H., Kraupner, N., and Brul, S., "The Risk of Low Concentrations of Antibiotics in Agriculture for Resistance in Human Health Care," FEMS Microbiol. Lett., 2016, 363(19), DOI: 10.1093/femsle/fnw210.

[246] Olofsson, S. K., and Cars, O., "Optimizing Drug Exposure to Minimize Selection of Antibiotic Resistance," Clin. Infect. Dis., 2007, 45(Supplement_2), pp. S129–S136.

[247] Young, K. D., "Bacterial Morphology: Why Have Different Shapes?," Curr. Opin. Microbiol., 2007, 10(6), pp. 596–600.

[248] Silhavy, T. J., Kahne, D., and Walker, S., "The Bacterial Cell Envelope," Cold Spring Harb. Perspect. Biol., 2010, 2(5), pp. a000414–a000414, DOI: 10.1101/cshperspect.a000414.

[249] Capita, R., Riesco-Peláez, F., Alonso-Hernando, A., and Alonso-Calleja, C., "Exposure of Escherichia Coli ATCC 12806 to Sublethal Concentrations of Food-Grade Biocides Influences Its Ability to Form Biofilm, Resistance to Antimicrobials, and Ultrastructure," Appl. Environ. Microbiol., 2014, 80(4), pp. 1268–1280, DOI: 10.1128/AEM.02283-13.

[250] Lorian, V., "Low Concentrations of Antibiotics," J. Antimicrob. Chemother., 1985, 15(SUPPL. A), pp. 15–26, DOI: 10.1093/jac/15.suppl_a.15.

[251] O'Driscoll, N. H., Cushnie, T. P. T., Matthews, K. H., and Lamb, A. J., "Colistin Causes Profound Morphological Alteration but Minimal Cytoplasmic Membrane Perforation in Populations of Escherichia Coli and Pseudomonas Aeruginosa," Arch. Microbiol., 2018, 200(5), pp. 793–802, DOI: 10.1007/s00203-018-1485-3.

[252] Furchtgott, L., Wingreen, N. S., and Huang, K. C., "Mechanisms for Maintaining Cell Shape in Rod-shaped Gram-negative Bacteria," Mol. Microbiol., 2011, 81(2), pp. 340–353.

[253] Chang, T.-W., and Weinstein, L., "Morphological Changes in Gram-Negative Bacilli Exposed to Cephalothin," J. Bacteriol., 1964, 88(6), pp. 1790–1797.

[254] Toyofuku, M., Nomura, N., and Eberl, L., "Types and Origins of Bacterial Membrane Vesicles," Nat. Rev. Microbiol., 2019, 17(1), pp. 13–24.

[255] Wojnicz, D., Kłak, M., Adamski, R., and Jankowski, S., "Influence of Subinhibitory Concentrations of Amikacin and Ciprofloxacin on Morphology and Adherence Ability of Uropathogenic Strains," Folia Microbiol. (Praha)., 2007, 52(4), pp. 429–436.

[256] Shen, J. P., and Chou, C. F., "Morphological Plasticity of Bacteria-Open Questions," Biomicrofluidics, 2016, 10(3), p. 031501, DOI: 10.1063/1.4953660.

[257] Domingues, M. M., Silva, P. M., Franquelim, H. G., Carvalho, F. A., Castanho, M. A. R. B., and Santos, N. C., "Antimicrobial Protein RBPI21-Induced Surface Changes on Gram-Negative and Gram-Positive Bacteria," Nanomedicine Nanotechnology, Biol. Med., 2014, 10(3), pp. 543–551, DOI: 10.1016/j.nano.2013.11.002.

[258] King, T., Osmond-McLeod, M. J., and Duffy, L. L., "Nanotechnology in the Food Sector and Potential Applications for the Poultry Industry," Trends Food Sci. Technol., 2018, 72(September 2017), pp. 62–73, DOI: 10.1016/j.tifs.2017.11.015.

[259] Fonseca, A. P., and Sousa, J. C., "Effect of Antibiotic-Induced Morphological Changes on Surface Properties, Motility and Adhesion of Nosocomial Pseudomonas Aeruginosa Strains under Different Physiological States," J. Appl. Microbiol., 2007, 103(5), pp. 1828–1837, DOI: 10.1111/j.1365-2672.2007.03422.x.

[260] Horii, T., Kobayashi, M., Sato, K., Ichiyama, S., and Ohta, M., "An In-Vitro Study of Carbapenem-Induced Morphological Changes and Endotoxin Release in Clinical Isolates of Gram-Negative Bacilli.," J. Antimicrob. Chemother., 1998, 41(4), pp. 435–442.

[261] Codjoe, F., and Donkor, E., "Carbapenem Resistance: A Review," Med. Sci., 2017, 6(1), p. 1, DOI: 10.3390/medsci6010001.

[262] Bernabeu-Wittel, M., García-Curiel, A., Pichardo, C., Pachon-Ibanez, M. E., Jimenez-Mejias, M. E., and Pachón, J., "Morphological Changes Induced by Imipenem and Meropenem at Sub-Inhibitory Concentrations in Acinetobacter Baumannii," Clin. Microbiol. Infect., 2004, 10(10), pp. 931–934.

[263] Cross, Trevor, Brett Ransegnola, Jung-Ho Shin, Anna Weaver, Kathy Fauntleroy, Michael S. VanNieuwenhze, Lars F. Westblade, and T. D., "Spheroplast-Mediated Carbapenem Tolerance in Gram-Negative Pathogens.," Antimicrob. Agents Chemother., 63(9), pp. e00756-19.

[264] Pajerski, W., Ochonska, D., Brzychczy-Wloch, M., Indyka, P., Jarosz, M., Golda-Cepa, M., Sojka, Z., and Kotarba, A., "Attachment Efficiency of Gold Nanoparticles by Gram-Positive and Gram-Negative Bacterial Strains Governed by Surface Charges," J. Nanoparticle Res., 2019, 21(8), DOI: 10.1007/s11051-019-4617-z.

[265] Soni, K. A., Balasubramanian, A. K., Beskok, A., and Pillai, S. D., "Zeta Potential of Selected Bacteria in Drinking Water When Dead, Starved, or Exposed to Minimal and Rich Culture Media," Curr. Microbiol., 2008, 56(1), pp. 93–97, DOI: 10.1007/s00284-007-9046-z.

[266] Matta, L. L., and Alocilja, E. C., "Emerging Nano-Biosensing with Suspended MNP Microbial Extraction and EANP Labeling," Biosens. Bioelectron., 2018, 117(July), pp. 781–793, DOI: 10.1016/j.bios.2018.07.007.

CHAPTER 2: RESEARCH HYPOTHESES, OBJECTIVES, AND EXPERIMENTAL DESIGN

The primary goal of this research is to successfully extract and detect carbapenem-resistant *E. coli* using carbohydrate-coated nanoparticles from water and foods. The research hypothesis, objectives with specific tasks, and experimental designs are presented in this chapter.

2.1. Hypotheses

This research had two primary hypotheses.

Hypothesis 1: The glycan-coated magnetic nanoparticles (gMNPs) can extract carbapenem-resistant *E. coli* from buffer solution and foods and water.

Hypothesis 2: The dextrin-coated gold nanoparticles (dGNPs)-based plasmonic biosensor can detect the gMNP-extracted carbapenem-resistant *E. coli* from foods and water.

Each hypothesis has two main objectives, as discussed below.

2.2. Objectives and Specific Tasks

The objectives and related tasks, along with the current state-of-the-art (study approaches), are summarized in Table 1.

Objective 1: Evaluation of gMNPs for capturing carbapenem-resistant *E. coli* from buffer solutions. The gMNPs have previously been found to be effective in bacterial capture from buffer solution and complex liquid and solid food matrices in a simple, rapid, and cost-effective manner. However, the efficacy of the gMNPs in ARB, including CRE, has not been documented from buffer or any matrices. The resistant bacteria isolates, specifically carbapenem-resistant *E. coli*, are considered in this study due to their association with various outbreaks worldwide. The binding efficacy of gMNPs with carbapenem-resistant *E. coli* (R*) along* with susceptible *E. coli* (S) (as reference bacterium) was assessed. To further understand the gMNPs-cell interaction, the effect of cell surface characteristics of the resistant bacteria in the absence and presence of carbapenem stress was also evaluated and compared with the *E. coli* (S)

Objective 2: Extraction of the carbapenem-resistant *E. coli* from the selected foods and water using gMNPs. CRE, including CP *E. coli* isolates, have been found not only in clinical samples but also in environmental and food samples. However, their isolation from biological samples has not been documented well. The focus of this objective was to extract these bacteria

from their commonly associated biological matrix (water and complex solid foods). The KPC and NDM-producing *E. coli* isolates were chosen as focused bacteria, as they have been mostly found in samples worldwide. Thus, the effectiveness of gMNPs for extracting *E. coli* (R: KPC and NDM-producing isolates) from large-volume water and food samples was evaluated. The possible factors, such as bacterial concentration and environment pH, impacting gMNP-cell interaction were also evaluated. The effects of food matrices, such as the presence of natural microflora and food microparticles, were further discussed.

Objective 3: Develop a DNA-based plasmonic biosensor platform for carbapenem-resistant bacteria (KPC-producing bacteria). Genomic-based identification methods confer specificity against non-target bacteria, but they are complex and costly. Dextrin-coated gold nanoparticles (dGNPs) offer rapid, simple, and cost-effective solutions for specific DNA sequence detection. Its application for the detection of ARB, including CRE, needs attention. The focused target gene *(bla_{KPC})* was chosen for the detection of all KPC-producing isolates, as KPC is the most common carbapenemase type worldwide. The biosensor was optimized for the detection of the target gene sequence and followed by determining the analytical sensitivity and specificity of the biosensor. Lastly, the detection of the KPC gene using the designed plasmonic biosensor was further verified with a standard PCR test.

Objective 4: Detection of gMNPs- extracted carbapenem-resistant bacteria (KPC-producing *E. coli*) from the water and food samples using the plasmonic biosensor. The direct detection of ARB, including CRE from matrices, specifically from food samples, has not been documented; many techniques use pure cultures after identifying target bacteria for their resistant profile. Thus, the application of techniques for target detection from matrices needs attention. The biosensor platform was implemented for the detection of KPC-producing *E. coli* following their isolation using gMNPs and short enrichment (5 h). Herein, two biosensors were parallelly used to detect *invA* gene (*E. coli* isolates) and bla_{KPC} gene (KPC-producing isolates) to identify KPC-producing *E. coli*. The apparel detection was also verified with the PCR test.

Table 2.1. Primary objectives and related tasks along with the current state-of-the-art (study approaches).

Objectives and Their Specific Tasks	Limitations of Current Approach or Technology	Study Approach	Ref.
Objective 1: Evaluation of the gMNPs for capturing carbapenem-resistant *E. coli* from buffer solution			
Confirmation and elaboration of the gMNPs-bacteria interaction: 1-carbapenem-resistant *E. coli* vs. susceptible *E. coli* 2-Carbapenem-exposed *E. coli* vs non-exposed *E. coli*	MNP-cell interaction, in theory, is well-studied, but their optimized application is rare and not documented in ARB capture.	Confocal laser microscopy (CLM) and Transmission Electron Microscope (TEM) for confirmation of gMNP-cell binding in buffer solution. Standard plating method to quantify their binding capacity (concentration factor).	[1–6]
Factors affecting MNP-cell interaction: examination of cell surface characteristics. 1-Observation of initial cell morphology and cell surface charges of carbapenem-resistant and -susceptible *E. coli.* 2- Observation of the carbapenem-exposed and non-exposed *E. coli* at low, medium, and high-level carbapenem concentrations after long-term cycles.	The cell surface characteristic plays a main role in MNP-cell attachment. 1-The cell morphology and surface charge of ARB have not been documented well. 2-The cell morphology of the exposed bacterial cells is easily affected and documented during the short period of antibiotic exposure (1-6 h). Observation of these cell characteristics is hardly seen under long-term antibiotic exposure.	1-Evaluation and comparison of cell morphology and surface charge of carbapenem-resistant *E. coli* with susceptible *E. coli* in the absence of antibiotic stress. 2-Evaluation of the cell surface characteristics of carbapenem-exposed *E. coli*, comparing them with (non-exposed *E. coli*).	[5,7–10]
Objective 2: Evaluation of the effectiveness of gMNPs for extracting carbapenem-resistant *E. coli* from large-volume food and water samples			
Factors affecting gMNP-bacteria binding capacity	Studies with MNPs have shown the effect of bacterial concentration and solution pH on MNP-bacteria binding, but the known effect on ARB is limited.	MNP-bacteria binding experiments with varying bacterial concentrations and different pH buffer solutions; analyze their effect on MNP-cell binding capacity.	[5,11–15]
Investigation of the efficacy of gMNP-based bacterial extraction from large-volume samples.	A few studies have been conducted to extract ARB from matrices. The gMNPs-based extractions of ARB, including CRE, from biological matrices have not been documented.	The application of gMNPs extraction of the resistant *E. coli* from artificially contaminated foods and water in large volumes (100 mL)	[3,14,15]

Table 2.1 (cont'd)

Objective 3: Development of a DNA-based plasmonic biosensor platform for carbapenem-resistant bacteria			
Optimization of detectable color difference between target and non-target samples	The cost-effective, simple, and rapid GNP-based colorimetric detection has not been tested or optimized for ARB.	Spectrum absorbance measurements and visual results are utilized to optimize the assay for easy and rapid detection.	[16–18]
Determine the specificity and sensitivity of the plasmonic biosensor	Many current methods for resistant bacteria detection often face issues with accessibility, selectivity, and sensitivity.	Measuring absorbance of target and non-target samples at varying bacterial species and DNA concentrations, confirming with PCR test.	[16,19,20]
Objective 4: Parallel plasmonic biosensor platform for detection of gMNPs-extracted carbapenem-resistant *E. coli* from water and food samples			
Short-enrichment step after magnetic extraction for enough DNA sample (5h).	A long enrichment step with > 6-9 h of extracted sample incubation is mostly required.	Extract DNA from the gMNPs-bacteria mixture from water and food samples after 5 h incubation.	[16,20,21]
Implementation of the biosensor assay on DNA samples extracted from foods and water. Two biosensors parallelly target all *E. coli* and KPC-producing bacteria.	A few GNP colorimetric biosensors have been used for the detection of target DNA extracted from matrices but not for direct CRE detection from biological matrices.	Examine the detection of target DNAs from different matrices. Verify the detection with PCR tests.	[16,17,20,22]

2.3. Experimental Design

The detailed experimental design of each objective was further depicted in flowcharts, consisting of research questions, independent and dependent variables for the experiment plan, and data analysis for hypothesis testing. All detailed information, methods, results and discussion of each objective were provided in the following chapters.

2.3.1. Experimental Design of Evaluating the Efficiency of gMNPs for Bacterial Capture

The first objective (Chapter 3) was to assess the effectiveness of glycan-coated MNPs for capturing and concentrating carbapenem-resistant *E.* coli; Figure 2.1 illustrates the experimental design. The underlying hypothesis of gMNPs-bacteria interaction relies on the cell surface characteristics or cell wall components (such as cell morphology, cell surface charge, and receptor-ligand interaction). Thus, this study further explored cell surface characteristics, specifically cell morphology and surface charge, to better understand the gMNP-cell interaction.

In this objective, there were two groups of bacteria: 1) carbapenem-resistant *E. coli* (R) isolates vs. carbapenem-susceptible *E. coli* (S) and 2) carbapenem-exposed *E. coli* vs. non-exposed *E. coli*. Initial gMNPs cell interaction along with cell surface characteristics (surface charge and cell morphology) of the bacteria (group 1) in the absence of the antibiotic were evaluated. Then, the *E. coli* (S) were subsequently exposed to carbapenem concentrations (from low-inhibitory to high-level concentrations) for a long time to mimic low-level, medium-level, and high-level phenotypic resistance. A selected *E. coli* (R) was also exposed to the carbapenem concentrations to investigate the effect of carbapenem on resistant and susceptible cells. Their gMNPs-cell interaction and cell surface characteristics were also evaluated.

The successful binding of gMNPs with these bacterial cells was confirmed using both transmission electron microscopy (TEM) and confocal laser microscopy (CLM). The gMNPs-cell binding capacity was tested in a small-volume buffer solution using the standard plating method. Cell morphology was visualized by the TEM and CLM, and cell surface charge (zeta potential) was measured by a Zetasizer. Finally, all collected data were statically analyzed and discussed in terms of their similarities and differences; the hypothesis was tested and discussed. Part of the discussion included extensive literature research to understand these bacterial cell characteristics with respect to cell binding/attachment properties with the gMNPs.

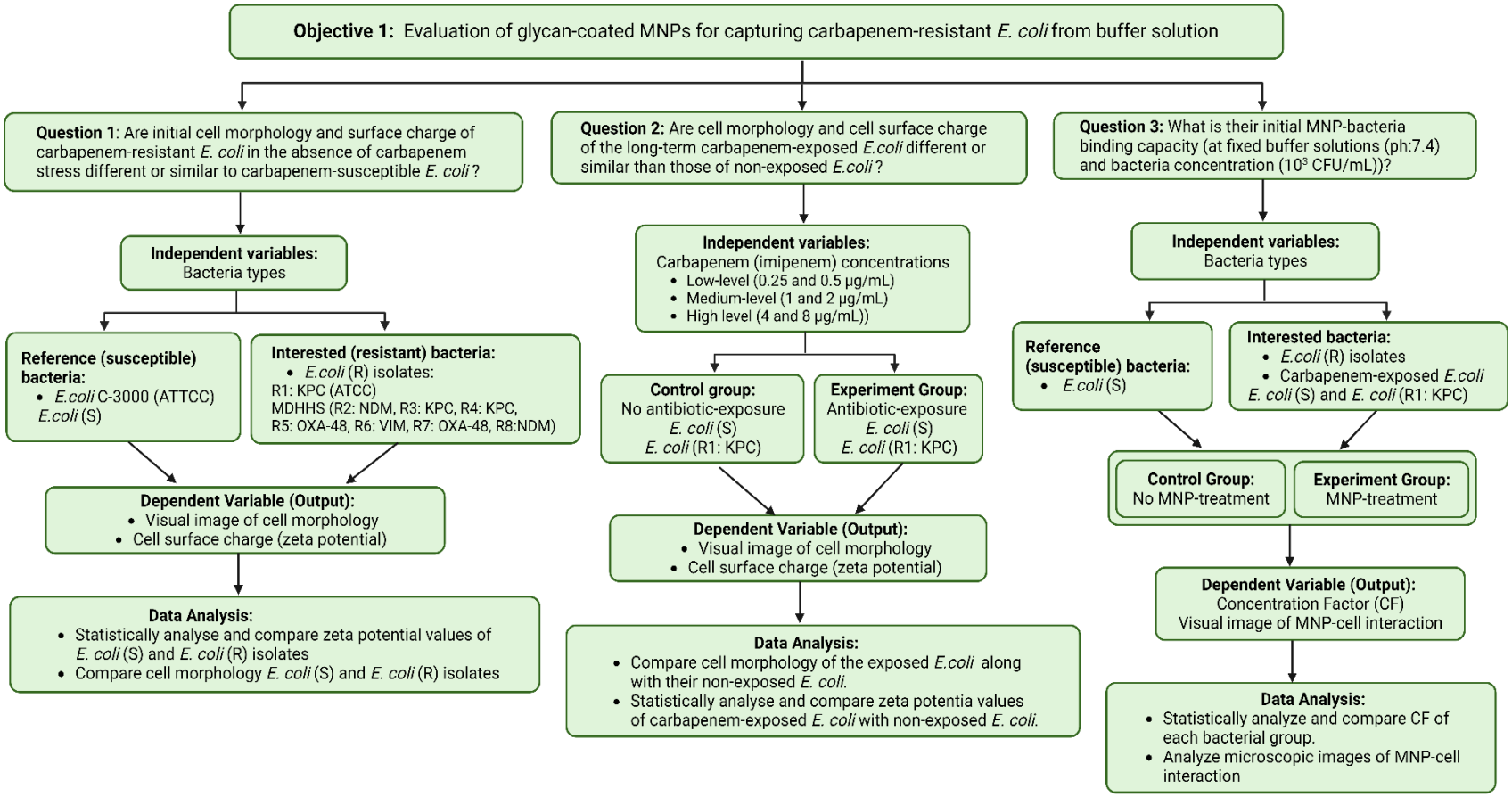

Figure 2.1. Flowchart of experimental design of objective 1 in the research (created with Biorender).

2.3.2. Experimental Design of Bacterial Extraction from Foods and Water Using gMNPs

The gMNPs binding with *E. coli* I isolates from buffer solution were assessed compared to E. coli (S). The second objective (Chapter 4) was to further evaluate the effectiveness of gMNPs for extracting the focused *E. coli* I isolates from large-volume samples (water and foods). Figure 2.2 depicts the flowchart of the experimental design of this objective.

In this objective, three *E. coli* isolates (KPC- and NDM-producing resistant *E. coli* isolates and the susceptible *E. coli*) were focused. The applicability and efficiency of gMNPs from large-volume samples are paramount; thereby, factors such as environmental pH and bacterial loads can impact their efficiency. The gMNPs-cell binding under optimal conditions was first analyzed with different bacterial concentrations and different pH buffer solutions in small volumes (1 mL). The application of gMNPs for bacterial extraction from artificially contaminated water and food samples (100 ml) and uninoculated samples (100 mL) was tested through the selective plating method. Results indicated viable capture of target cells and natural microflora from all matrices. Further gMNP-bacteria binding from samples was also visualized under TEM. All collected data were analyzed and discussed in terms of their similarities and differences; the hypothesis was tested and discussed. Part of the discussion included the literature research to assess the extraction of bacteria from matrices in the presence of natural microflora and food microparticles.

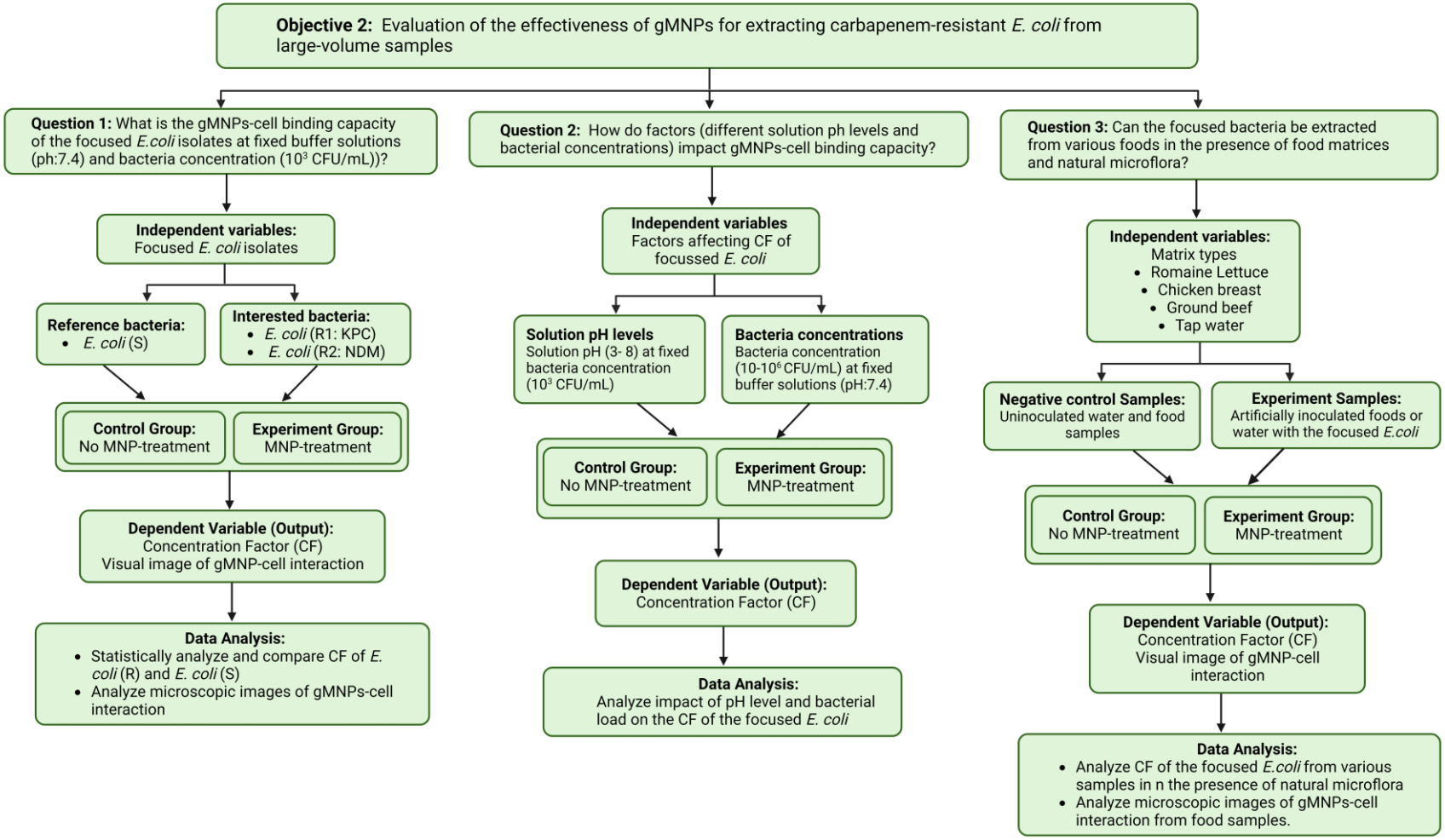

Figure 2.2. Flowchart of experimental design of objective 2 in the research (created with Biorender).

2.3.3. Experimental Design of Development of Plasmonic Biosensor

The third objective (Chapter 5) is to design a plasmonic biosensor platform for rapid detection of carbapenem-resistant bacteria (KPC-producing bacteria). This is a colorimetric biosensor utilizing the surface plasmon resonance of the GNPs. The simple assay only requires GNPs, DNA probes for target bacteria, and DNA samples. The biosensor procedure developed at the Nano-Biosensors Laboratory, MSU, was employed in this study for the detection of carbapenem-resistant bacteria. First, the dextrin-coated GNPs (dGNPs) were synthesized, and their characterization and stability were first tested. In this biosensor, the dGNPs were then functionalized with 11-mercaptoundecanoic acid (MUDA) using thiol-gold chemistry. This enables instantaneous non-covalent interaction of -COOH groups on the coat with amine groups on the probe. The samples were heated in a thermocycler for hybridization (95 °C for 5 min for denaturation and 55 °C for 10 min for annealing). In the absence of target DNA, no hybridization takes place. The addition of HCl induces dGNP aggregation by distributing their electrostatic repulsion. However, the presence of target DNA binds to the dGNPs-probe prevents dGNPs from aggregation; thus, samples with target DNA remained red and peak wavelength closer to 520 nm, while non-target samples allow GNPs aggregation and results in color change (purple or blue) and right shift to higher peak wavelengths farther from 520 nm.

The principle of the biosensor was Initially proved for the detection of the target DNA. First, a specific DNA probe for the carbapenem-resistant gene (bla_{KPC}) was designed, and this assay was optimized in HCl acid volume (5-10 µL) and incubation (response) time (5-10 min) for the target detection. The optimal HCl amount was determined through qualitative and quantitative analysis. The different amounts of HCl (0.1 M) were added to the negative control (nuclease-free water) and target (10 ng/µL of KPC-producing *E. coli* from ATCC), and non-target (10 ng/µL of E.coli (S): *E. coli* C-3000)) tubes and incubated until the time of the aggregation of the control and non-target and without aggregation of the target tube, which is visually observable. The measured absorbance spectra were statistically analyzed; the optimized procedure has a significant and consistent peak shift difference between target and non-target samples.

Further, the optimized biosensor was used to test for biosensor sensitivity with different DNA concentrations and specificity tests with several carbapenem-resistant bacteria harboring carbapenemase genes and carbapenem-susceptible bacteria, as depicted in Figure 2.3.

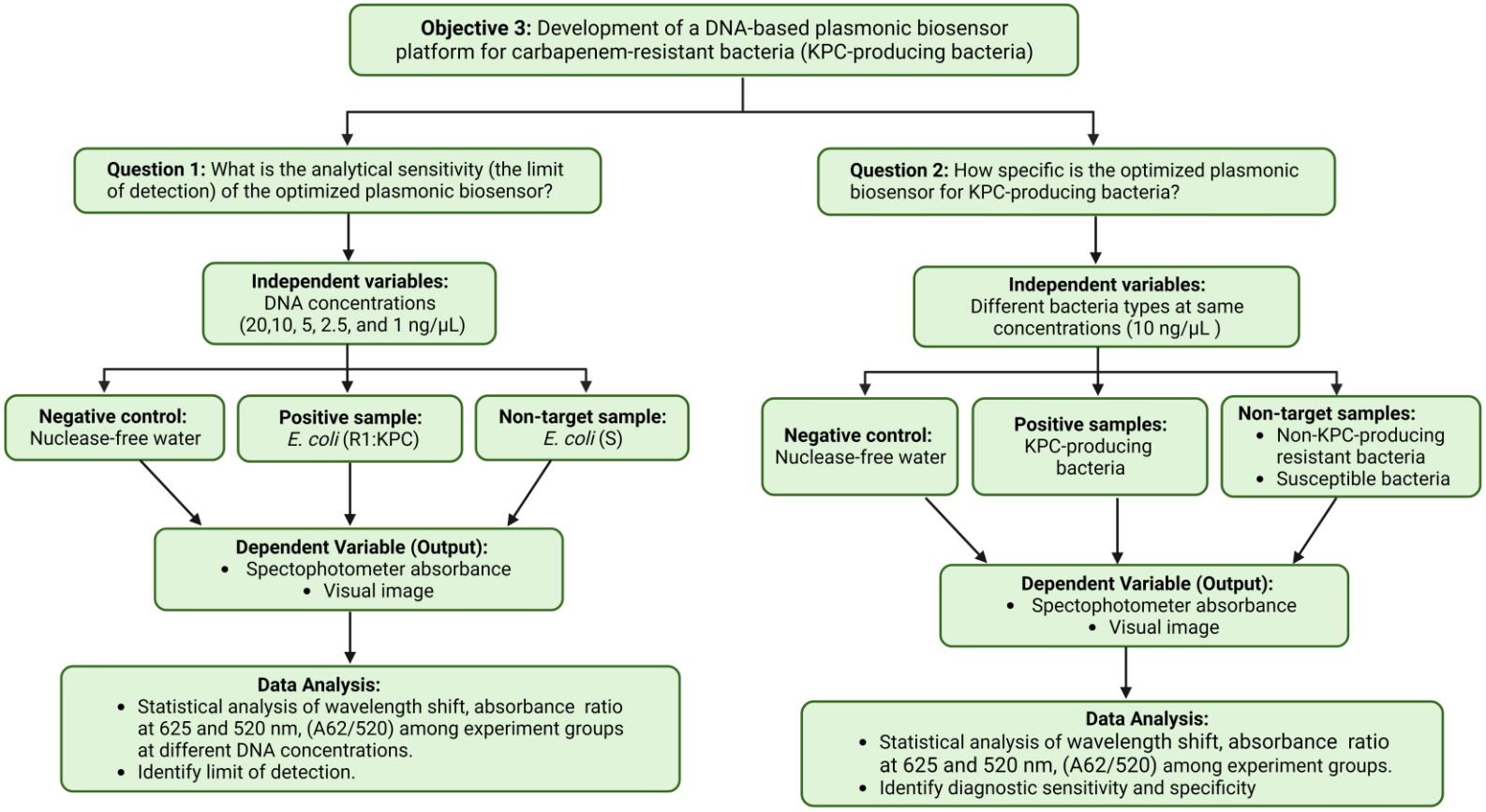

Figure 2.3. Flowchart of experimental design of objective 3 in the research (created with Biorender).

The biosensor results were further verified with PCR tests, and the diagnostic sensitivity and specificity were calculated. This designed platform was further assessed with current techniques in the discussion part.

2.3.4. Detection of KPC-producing *E. coli* from Water and Food Samples

The fourth objective (chapter 6) was to implement the developed biosensor platforms to detect the extracted KPC-producing *E. coli* from water and foods using the gMNP-based extraction procedure. The plating method needs overnight incubation, and the detection of the extracted bacteria with the plasmonic biosensor was tested, which can significantly reduce the detection time.

In this objective, the designed biosensor using a *uidA* probe for *E. coli* detection (developed in our previous) and the developed biosensor (bla_{KPC}) for KPC-producing bacteria in this research were implemented to detect and differentiate KPC-producing *E. coli*. First, the developed *uidA* biosensor was tested for all E. coli detection from pure culture, regardless of susceptibility status. Then, the biosensor was tested in DNA samples extracted from water and food samples, along with the KPC biosensor. Figure 2.4 illustrates the flowchart of the experimental design of this objective.

In this parallel detection, the first task was the short enrichment of the gMNPs-bacteria mixture from food and water samples, followed by DNA extraction. The gMNPs-bacteria mixture (0.5 mL) for target-inoculated, nontarget-inoculated, and uninoculated (control) samples of each matrix were first transferred to TSB (4.5 mL) and incubated for 5 hours at 37 C. Then, DNA extraction was performed using the QIAamp kit, and their DNA concentrations were quantified using Nanodrop. The concentrations of all DNA samples extracted from samples were standardized to similar DNA concentrations on the basis of the lowest DNA concentration of any samples or uninoculated samples. Task 2 detects and differentiates KPC-producing *E. coli* from water and food samples by parallelly targeting the *uidA* and bla_{KPC} genes. Finally, PCR tests were parallelly conducted on the same DNA samples to confirm the biosensor results. All biosensor and PCR results were discussed, and the hypothesis was tested. The efficiency and applicability of the combined assay were further discussed.

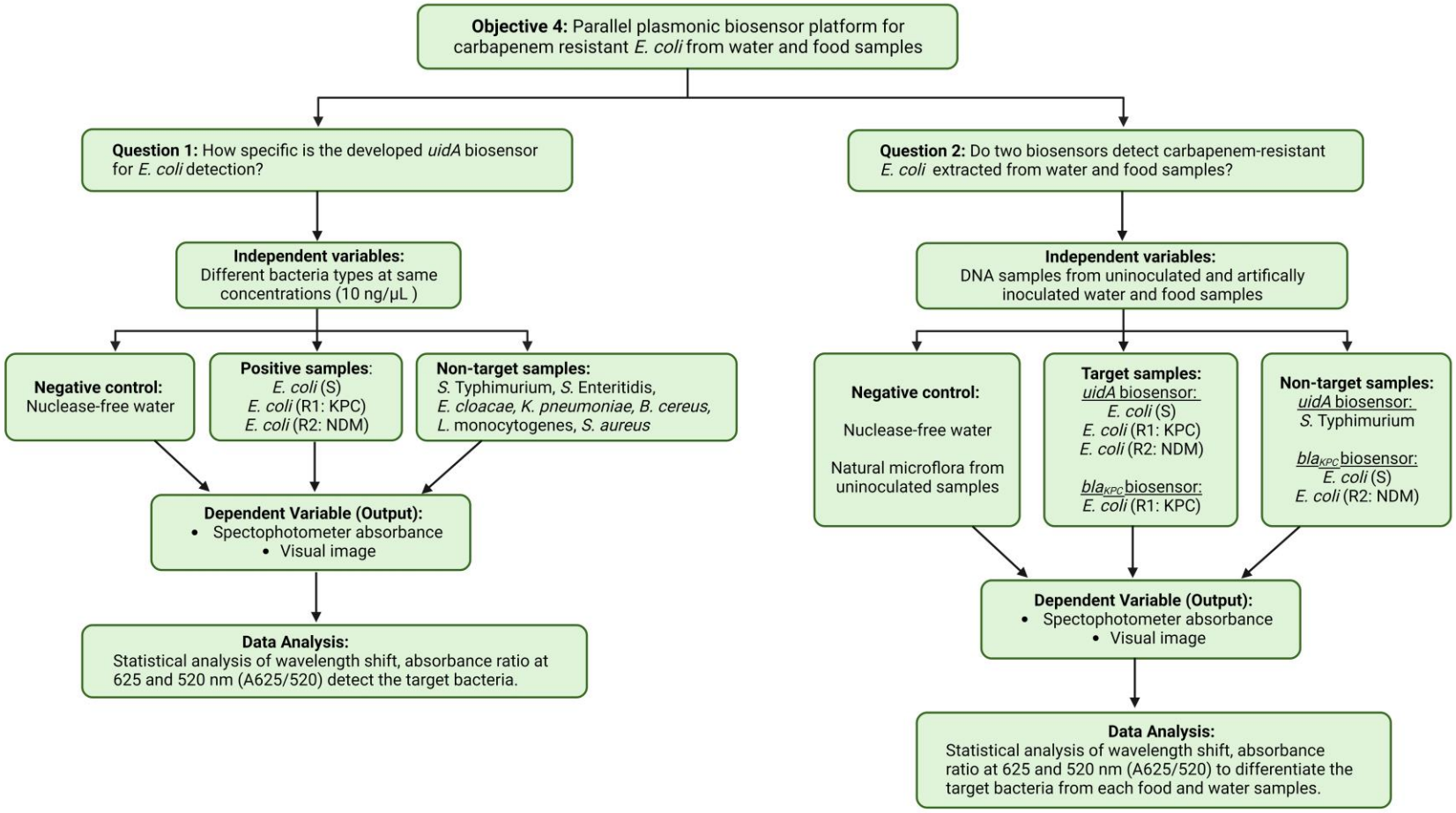

Figure 2.4. Flowchart of experimental design of objective 4 in the research (created with Biorender).

2.4. Data Analysis

All experiments of each objective in this study were triplicate. The collected quantitative data in the following chapters were presented with average and standard deviations in bar graphs. All data were statistically analyzed at a 95% confidence interval. First, normality and equality of variance of each data set were tested to decide which statistical tests were applied, such as parametric test (e.g., student-t test or one-way analysis of variance (ANOVA)) or non-parametric test (e.g., Mann-Whitney or Kruskal-Wallis). Differences in measured properties were statistically analyzed and compared with their control or reference groups. All statistical results and each hypothesis of this research were detailed and discussed in their sections (chapters).

REFERENCES

[1] Dester, E., and Alocilja, E., "Current Methods for Extraction and Concentration of Foodborne Bacteria with Glycan-Coated Magnetic Nanoparticles: A Review," Biosensors, 2022, 12(2), p. 112, DOI: 10.3390/bios12020112.

[2] El-Boubbou, K., Gruden, C., and Huang, X., "Magnetic Glyco-Nanoparticles: A Unique Tool for Rapid Pathogen Detection, Decontamination, and Strain Differentiation," J. Am. Chem. Soc., 2007, 129(44), pp. 13392–13393, DOI: 10.1021/ja076086e.

[3] Matta, L. L., "Biosensing Total Bacterial Load in Liquid Matrices to Improve Food Supply Chain Safety Using Carbohydrate-Functionalized Magnetic Nanoparticles for Cell Capture and Gold Nanoparticles for Signaling," 2018.

[4] Bohara, R. A., and Pawar, S. H., "Innovative Developments in Bacterial Detection with Magnetic Nanoparticles," Appl. Biochem. Biotechnol., 2015, 176(4), pp. 1044–1058, DOI: 10.1007/s12010-015-1628-9.

[5] Nishino, M., Matsuzaki, I., Musangil, F. Y., Takahashi, Y., Iwahashi, Y., Warigaya, K., Kinoshita, Y., Kojima, F., and Murata, S., "Measurement and Visualization of Cell Membrane Surface Charge in Fixed Cultured Cells Related with Cell Morphology," PLoS One, 2020, 15(7 July), DOI: 10.1371/journal.pone.0236373.

[6] Briceno, R. K., Sergent, S. R., Benites, S. M., and Alocilja, E. C., "Nanoparticle-Based Biosensing Assay for Universally Accessible Low-Cost Tb Detection with Comparable Sensitivity as Culture," Diagnostics, 2019, 9(4), DOI: 10.3390/diagnostics9040222.

[7] Bernabeu-Wittel, M., García-Curiel, A., Pichardo, C., Pachon-Ibanez, M. E., Jimenez-Mejias, M. E., and Pachón, J., "Morphological Changes Induced by Imipenem and Meropenem at Sub-Inhibitory Concentrations in Acinetobacter Baumannii," Clin. Microbiol. Infect., 2004, 10(10), pp. 931–934.

[8] Horii, T., Kobayashi, M., Sato, K., Ichiyama, S., and Ohta, M., "An In-Vitro Study of Carbapenem-Induced Morphological Changes and Endotoxin Release in Clinical Isolates of Gram-Negative Bacilli.," J. Antimicrob. Chemother., 1998, 41(4), pp. 435–442.

[9] Cushnie, T. P. T., O'Driscoll, N. H., and Lamb, A. J., "Morphological and Ultrastructural Changes in Bacterial Cells as an Indicator of Antibacterial Mechanism of Action," Cell. Mol. Life Sci., 2016, 73(23), pp. 4471–4492, DOI: 10.1007/s00018-016-2302-2.

[10] Gullberg, E., Cao, S., Berg, O. G., Ilbäck, C., Sandegren, L., Hughes, D., and Andersson, D. I., "Selection of Resistant Bacteria at Very Low Antibiotic Concentrations," PLoS Pathog., 2011, 7(7), pp. 1–9, DOI: 10.1371/journal.ppat.1002158.

[11] Li, Z., Ma, J., Ruan, J., and Zhuang, X., "Using Positively Charged Magnetic Nanoparticles to Capture Bacteria at Ultralow Concentration," Nanoscale Res. Lett., 2019, 14, DOI: 10.1186/s11671-019-3005-z.

[12] Nemr, C. R., Smith, S. J., Liu, W., Mepham, A. H., Mohamadi, R. M., Labib, M., and Kelley, S. O., "Nanoparticle-Mediated Capture and Electrochemical Detection of Methicillin-Resistant Staphylococcus Aureus," Anal. Chem., 2019, DOI: 10.1021/acs.analchem.8b04792.

[13] Matta, L. L., and Alocilja, E. C., "Carbohydrate Ligands on Magnetic Nanoparticles for Centrifuge-Free Extraction of Pathogenic Contaminants in Pasteurized Milk," J. Food Prot., 2018, 81(12), pp. 1941–1949, DOI: 10.4315/0362-028X.JFP-18-040.

[14] Dester, E. F., "Extraction, Concentration, and Detection of Foodborne Pathogens Using Glycan-Coated Magnetic Nanoparticles and a Gold Nanoparticle Colorimetric Biosensor," Michigan State University.

[15] Boodoo, C., Dester, E., Asadullah Sharief, S., and Alocilja, E. C., "Influence of Biological and Environmental Factors in the Extraction and Concentration of Foodborne Pathogens Using Glycan-Coated Magnetic Nanoparticles," J. Food Prot., 2023, 86(4), p. 100066, DOI: 10.1016/j.jfp.2023.100066.

[16] Dester, E., Kao, K., and Alocilja, E. C., "Detection of Unamplified E. Coli O157 DNA Extracted from Large Food Samples Using a Gold Nanoparticle Colorimetric Biosensor," Biosensors, 2022, 12(5), p. 274, DOI: 10.3390/bios12050274.

[17] Quintela, I. A., De Los Reyes, B. G., Lin, C. S., and Wu, V. C. H., "Simultaneous Colorimetric Detection of a Variety of Salmonella Spp. In Food and Environmental Samples by Optical Biosensing Using Oligonucleotide-Gold Nanoparticles," Front. Microbiol., 2019, 10(MAY), pp. 1–12, DOI: 10.3389/fmicb.2019.01138.

[18] Bakthavathsalam, P., Rajendran, V. K., and Baquir Mohammed, J. A., "A Direct Detection of Escherichia Coli Genomic DNA Using Gold Nanoprobes," J. Nanobiotechnology, 2012, 10(1), p. 8, DOI: 10.1186/1477-3155-10-8.

[19] Gordon, N., Bawa, R., and Palmateer, G., "Carbapenem-Resistant Enterobacteriaceae Testing in 45 Minutes Using an Electronic Sensor," *Current Issues in Medicine: Diagnosis and Imaging*, 2021, pp. 1–18.

[20] Sharief, S. A., Caliskan-Aydogan, O., and Alocilja, E., "Carbohydrate-Coated Magnetic and Gold Nanoparticles for Point-of-Use Food Contamination Testing," Biosens. Bioelectron. X, 2023, 13(November 2022), p. 100322, DOI: 10.1016/j.biosx.2023.100322.

[21] Sharief, S. A., Caliskan-Aydogan, O., and Alocilja, E. C., "Carbohydrate-Coated Nanoparticles for PCR-Less Genomic Detection of Salmonella from Fresh Produce," Food Control, 2023, 150(January), p. 109770, DOI: 10.1016/j.foodcont.2023.109770.

[22] Ahmadi, S., Kamaladini, H., Haddadi, F., and Sharifmoghadam, M. R., "Thiol-Capped Gold Nanoparticle Biosensors for Rapid and Sensitive Visual Colorimetric Detection of Klebsiella Pneumoniae," J. Fluoresc., 2018, 28(4), pp. 987–998, DOI: 10.1007/s10895-018-2262-z.

CHAPTER 3: ASSESSMENT OF GLYCAN-COATED MAGNETIC NANOPARTICLES FOR RAPID EXTRACTION OF CARBAPENEM-RESISTANT *E. COLI*

Some parts of this chapter are from a published article, "Cell Morphology as Biomarker of Carbapenem Exposure," *The Journal of Antibiotics*, 2024 (10.1038/s41429-024-00749-9).

3.1. Introduction

Antimicrobial resistance (AMR) is a major growing concern in emerging infectious diseases due to rapid demographic, environmental, and agricultural changes [1,2]. The misuse and overuse of antibiotics and their release into the environment have created selective pressure on bacteria [3–5]. The low level of antibiotics in the environment slows their growth and promotes the evolution of *de novo* resistance, selection of antibiotic-resistant mutants, and transfer of their genes [3,5–8]. The long-term sub-inhibitory antibiotic exposure modulates bacterial gene expression of about 5-10% of genes linked with the cellular process (e.g., protein synthesis, carbohydrate metabolism, target modification) [4]. This assists in the adaptation to new and unfavorable conditions and the emergence of new microbial phenotypes [4,6,8] for bacterial survival at above the minimum inhibitory concentration (MIC) [3,6,7,9]. Bacteria can enhance the effects of resistance due to their rapid multiplication (vertical evolution), passing the gene to their generations [10]. This is also accelerated by the horizontal gene transfer (HGT) between strains of the same species or different bacterial species [4,5,10–12]. Thus, the emergence and spread of antimicrobial-resistant bacteria (ARB) at an alarming rate pose severe challenges to the public and the medical community [2,4,13–15].

In the last decade, carbapenem-resistant *Enterobacterales* (CRE) have been listed as critical priority infections by the World Health Organization (WHO) and the Centers for Disease Control and Prevention (CDC) due to limited treatment options [13,16–19]. The emergence and spread of CRE are mainly due to the rapid dissemination of genes encoding carbapenem hydrolyzing enzymes (carbapenemase) through HGT, which covers 30% of CRE [2,20,21]. The most prevalent carbapenemases in CRE are *Klebsiella pneumoniae* carbapenemase (KPC) and New Delhi Metallo-β-lactamase (NDM), Imipenemase (IMP), and Verona Integron-encoded Metallo-β Lactamase (VIM), and Oxacillinase-48 (OXA-48) [2,12,22]. These genes are often located on mobile genetic elements, leading to their rapid spread and resulting in infections and colonization [10,17,21,23]. Several microbiological studies have found carbapenemase-

producing (CP) CRE in clinical and biological samples [2,4,12,24–28]. Thus, the rapid identification of the causative bacteria is of utmost importance in developing and implementing control and management options and treatment with the best antibiotic choices.

Various methods for identifying and characterizing ARB have been developed rapidly and cost-effectively [2,9]. For rapid and accurate identification, pre-analytical sample processing, including the bacterial extraction, enrichment, and purification of bacteria from matrices, is also of utmost importance [29,30]. However, isolation (extraction) of ARB, including CRE, has not been documented well in the literature; thus, extraction of these bacteria needs attention.

The existing methods for bacterial extraction are physical methods (e.g., centrifugation and filtration) and chemical and biological methods (e.g., dielectrophoresis, metal hydroxides, and magnetic nanoparticle (MNP)-based separation) [29–31]. Among these, MNP-based methods have commonly been used to rapidly and effectively extract bacteria; MNPs draw attention due to cost-effectiveness, stability, benign nature, and biocompatibility with detection assays [30,32–34]. One of the most significant advantages of MNPs is their superparamagnetic properties, assisting in rapidly dispersing MNPs in liquids; these can still be magnetized and manipulated by an external magnetic field [30,32,35,36]. Another beneficial property is their high surface area/volume ratio, which gives higher adsorption capacity, leading to potentially high binding capacity with the target. The MNP-bacterial cell attachment relies on adsorption and makes use of naturally occurring biological or chemical interactions between affinity ligands and specific surface substrates on solid support [29,30,37]. Affinity agents can be antibodies, bacteriophages, proteins, carbohydrates, and charged particles that interact through physicochemical interactions, including Van der Waal's forces, electrostatic interactions, and hydrogen bonding [29,30]. These separation techniques can be nonspecific or specific to a target [30,37].

In MNP-based separation, immunomagnetic separation (IMS) has commonly been used for rapid selective separation. However, the lack of standardization, high experimental cost, and their storage conditions are primary limitations [29,30]. Recently, the use of glycan-coated MNPs (gMNPs) offers several advantages: 1) a simple one-pot synthesis, allowing large-scale production abilities; 2) stability at room temperature with longer-shelf life, eliminating issues such as affordability and low-resource accessibility; 3) the glycan-based interaction of gMNPs allows its application in several bacterial types [30], making gMNPs a lucrative alternative.

However, the application of gMNPs for ARB extractions has not been evaluated. Thus, this study aims to investigate the capability of the promising gMNPs on carbapenem-resistant bacteria, CP-CRE, capture.

The gMNPs-bacterial cell binding (capture) relies on bacterial cell surface characteristics, such as morphological characteristics, electrostatic surface charge, hydrophobic or hydrophilic interactions, and glycan-lectin binding sites [30,38,39]. Therefore, cell surface characteristics (morphological and electrostatic surface charge) of bacteria help in understanding their MNP attachment mechanisms.

3.1.1. Platform Novelty

Despite the increasing global burden of CRE infections, there is a considerable knowledge gap on bacterial extraction, including MNP-bacterial cell interactions. Therefore, this study sought to expand the body of knowledge on the interaction of gMNPs with CP-CRE isolates, specifically CP *E. coli,* due to their prevalence worldwide [12,23,40–44].

This study evaluated two groups of *E. coli* isolates to further understand the MNP-cell attachment mechanisms. The first group referred to carbapenem-susceptible *E. coli* (S) versus carbapenem-resistant *E. coli* (R) isolates in the absence of carbapenem stress (exposure); their initial MNP-cell binding capacity, along with the cell surface characteristics were evaluated. The second group was the carbapenem-exposed versus non-exposed *E. coli* isolates (*E. coli* (S) and *E. coli* (R: KPC)); their cell surface characteristics and MNP-cell interaction were also evaluated. For experimental aspects, the cell surface characteristics in terms of cell morphology and surface charge were first examined. MNP-bacterial cell binding (adhesion) was then confirmed under microscopes, and their binding capacity was assessed by concentration factor (CF) using the standard plating method. Further, the MNP-cell interaction of *E. coli* (R) isolates in the absence and presence of carbapenem stress was compared and discussed with that of *E. coli* (S), along with their cell surface characteristics.

3.2. Materials and Methods

3.2.1. Materials

Bacterial strains of susceptible *E. coli* C-3000 (ATCC 15597) and KPC-producing carbapenem (imipenem and ertapenem)-resistant *E. coli* (BAA-2340) were obtained from the American Type Culture Collection (ATCC). A total of 7 CP *E. coli* isolates were obtained from

the Michigan Department of Health and Human Services (MDHHS). The glycan (chitosan)-functionalized MNPs were from Dr. Evangelyn Alocilja's Nano-Biosensors Laboratory at Michigan State University (MSU). Racks for magnetic separation were purchased from Spherotech (Lake Forest, IL). Tryptic Soy Agar (TSA), Tryptic Soy Broth (TSB), and phosphate-buffered saline (PBS, pH 7.4) were purchased from Sigma Aldrich (St. Louis, MO). Imipenem antibiotic was purchased from Cayman Chemical (Ann Arbor, Michigan), and the polyethersulfone filter was purchased from the PES (Vernon Hills, IL). Gram staining materials (Gram iodine, Gram's safranin solution, ethanol, and crystal violet) were purchased from VWR International (Radnor, PA). For imaging, Transmission Electron Microscope (TEM) supplies (glutaraldehyde, uranyl acetate stain, and cacodylate buffer) were provided by the Center for Advanced Microscopy (CAM), MSU. Copper grids for TEM (formvar/carbon 200 mesh copper) were obtained from Electron Microscopy Systems (Hatfield, PA).

3.2.2. Bacterial Groups of This Study (Study Approach)

CP *E. coli* isolates from MDHHS harbors KPC, NDM, VIM, IMP, and OXA-48 genes; their resistant profile or genes were identified by molecular (CARBA-R Cepheid assay and CDC laboratory-developed assay) and growth-based AST methods in MDHHS. Stock cultures of all CP *E. coli* isolates and a susceptible *E. coli* isolate were stored at -80 °C. The resistant and susceptible cultures were refreshed by plating on TSA and incubated for 24-48 h at 37 °C. For each experiment, fresh bacterial cultures are prepared in 9 mL of TSB with 4-6 h incubation at 37 °C.

As previously mentioned, this study was conducted on two groups of bacteria, which were in the presence and absence of the antibiotic, as listed in Table 3.1. The first group did not have any antibiotic exposure, and the second group had antibiotic exposure; their MNP-cell binding capacity, with cell surface characteristics, was assessed.

Carbapenem (imipenem) antibiotic was used for the second group of bacteria. Imipenem is a broad spectrum of carbapenem against gram-positive and gram-negative bacteria and multi-resistant strains [45]. The current break point of imipenem for *Enterobacteriaceae* is defined as < 1 µg/mL for the susceptible, 2 µg/mL for the intermediate, and $\geq$ 4 µg/mL for resistant by the Clinical & Laboratory Standards Institute (CLSI) [46]. Based on the breakpoint levels, the antibiotic concentrations were defined as follows: low-level (0.25 and 0.5 µg/mL), intermediate (1 and 2 µg/mL), and high-level (4 and 8 µg/mL) in this study.

Table 3.1. Tested bacterial groups in this study.

1) Carbapenem-susceptible *E. coli* vs carbapenem-resistant *E. coli*		**2) Carbapenem-exposed *E. coli* vs non-exposed *E. coli***	
Reference bacteria	Resistant bacteria		
E. coli (S)	<u>*E. coli* (R)</u> R1: KPC (ATCC) R2: NDM R3: KPC R4: KPC R5: OXA-48 R6: VIM R7: OXA-48 R8: NDM	<u>No antibiotic-treatment</u> (Control, 0 µg/mL)	<u>Antibiotic-treatment</u> 0.25 and 0.5 µg/mL, 1 and 2 µg/mL, 4 and 8 µg/mL,
		E. coli (S) *E. coli* (R1: KPC)	*E. coli* (S) *E. coli* (R1: KPC)

Carbapenem-exposed *E. coli* was first created through serial long-term exposure of *E. coli* (S) to imipenem to mimic low-level, medium-level, and high-level resistance. Also, *E. coli* (R1: KPC) were exposed to the antibiotic. This study also investigated the physiological response of *E. coli* (S) and *E. coli* (R1: KPC) to increasing imipenem concentrations for a long period (30 growth cycles).

3.2.2.1. Long-Term Serial Carbapenem Exposure

Imipenem was dissolved in a phosphate buffer solution (PBS, pH 7.4). The prepared antibiotic solution was filter sterilized using 0.22 µm pore size polyethersulfone (PES). The sterilized antibiotic solutions were added to each labeled bottle of the cooled molten TSAs (around 40-50 ^{o}C); the bottles were mixed and poured into petri dishes. No antibiotic was added for the control (0 µg/mL, antibiotic-free growth). The plates were allowed to dry for two hours and then used on the day of preparation. Also, uninoculated TSAs with/without antibiotics were verified for the absence of any microorganisms. This preparation technique was adapted from an earlier study [47].

A general overview of the long-term antibiotic exposure is outlined in Scheme 3.1. *E. coli* (S) and *E. coli* (R1: KPC) were serially exposed to imipenem by standard-plating method during the 30 cycles. First, the overnight cultures were plated onto the prepared TSA plates, including different antibiotic concentrations (0, 0.25, 0.5, 1, 2, 4, and 8 µg/mL), and incubated at 37 °C for 24 hours to one week. The growth of *E. coli* (S) at 0.25 µg/mL and 0.5 µg/mL was observed within 24h, while the growth at 1 µg/mL (MIC) was observed within 36-48 h. Once growth was seen on the TSA plates, the surviving cells were transferred onto TSA with the same antibiotic concentration for serial growth cycles. However, there was no growth of *E. coli* (S) at

high levels of MIC antibiotic exposure (2, 4, and 8 µg/mL) during the week-long incubation. In preliminary works, bacteria growing under 1 µg/mL of imipenem at the end of the 5th cycle were able to survive in higher concentration; thus, they were transferred to TSA plates with 2 µg/mL imipenem, and their serial process was started. A similar procedure was applied for 4 and 8 µg/mL of imipenem exposure, which was transferred from the exposed cells at 2 and 4 µg/mL at the end of the 5th cycle, respectively. Their serial exposure cycles were started and continued for 30 cycles. Further, the increasing imipenem exposure was also conducted on *E. coli* (R1: KPC); the cells were able to grow at each concentration, and their serial cycles were continued during 30 growth cycles.

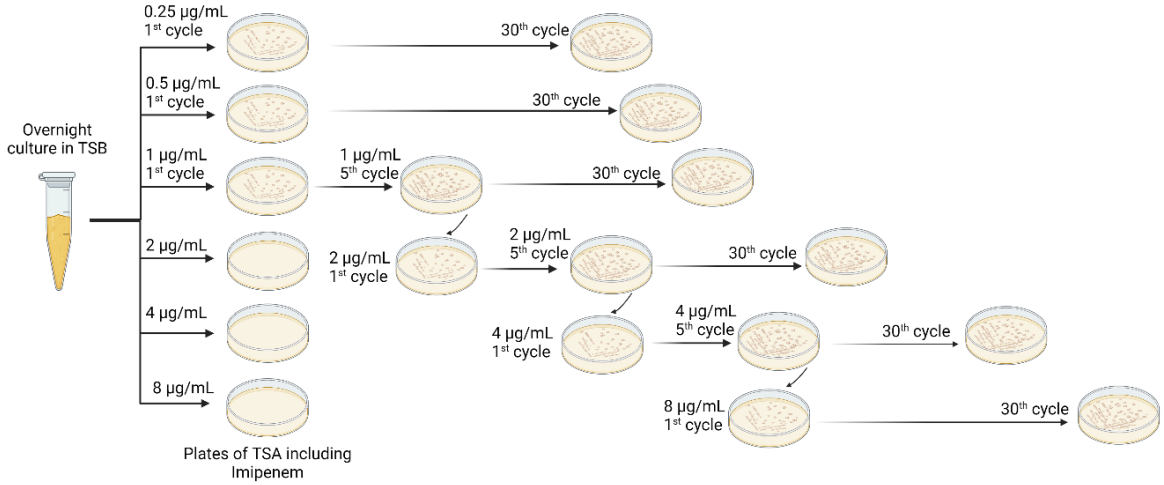

Scheme 3.1. Overview of the experimental procedure for long-term antibiotic exposure on susceptible bacteria (created with BioRender.com, accessed on 10 June 2022).

3.2.3. gMNP Synthesis and MNP-Bacteria Binding Capacity

In-house proprietary chitosan (glycan)-functionalized MNPs were synthesized in the Nano-Biosensor Lab, MSU, following a previously documented procedure [48]. Briefly, iron oxide (III) or magnetite (Fe_3O_4) core with glycan (chitosan) shells was used to make the MNPs. Ferric chloride hexahydrate (as a precursor) in a mixture of ethylene glycol (as a reducing agent), sodium acetate (as porogen), and deacetylated chitosan (5 mg/mL) were used for MNPs synthesis. Chitosan was polymerized to surface-modify the iron oxide nanoparticles. Batches of the gMNPs were stored at room temperature for further use. The gMNPs are stable for at least 3 years; new synthesis was not required for everyday analysis. The gMNPs were suspended in sterile deionized water and sonicated before each experiment.

The gMNPs-cell attachment capacity was quantified through plating (colony counting) on solid growth media, using concentration factor (CF) as depicted in Scheme 3.2, which was adapted from an earlier study [49]. First, 4-6 h spiked bacterial cultures were serially diluted in the PBS (pH:7.4) to a concentration of approximately 10^3 CFU/mL, plated for initial bacterial counts as a control group. For the experiment group, 100 µL of gMNPs was added into 900 µL of the diluted bacterial samples, vortexed for 10-15 seconds, and then incubated for 5 minutes. After 5 minutes of magnetic separation and supernatant removal, it was resuspended in 100 µL of PBS. The final samples were plated on TSA and incubated for 24 h at 37 °C.

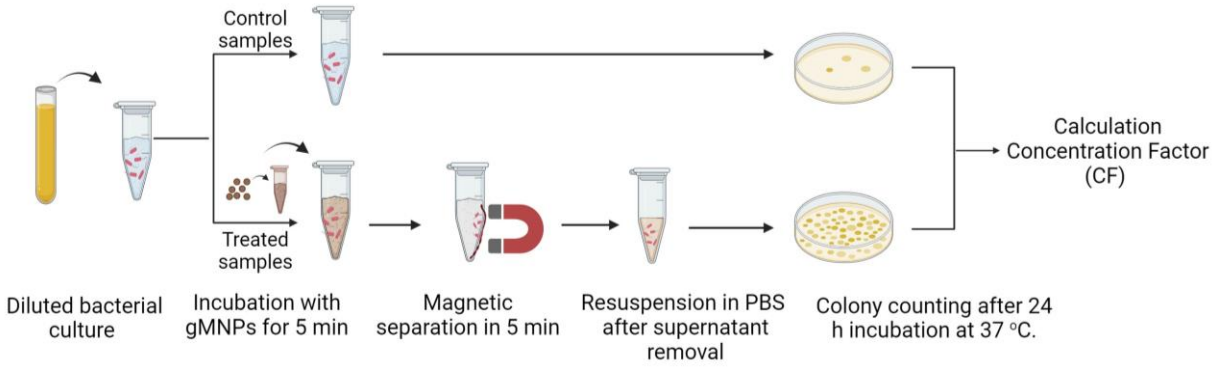

Scheme 3.2. The procedure of gMNPs-bacteria binding capacity (created with BioRender.com, accessed on 10 November 2022).

The MNP-cell binding capacity was determined by concentration factor (CF) through colony counts; only plates with ~20-200 individual colonies were used. The CF was calculated separately for each isolate based on control and treated samples using the following formula (Equation 1).

$$\text{Concentration Factor} = \frac{\text{number of colonies in treated sample}}{\text{number of colonie in control sample}} \quad (1)$$

3.2.4. Cell Surface Charge (Zeta Potential) Measurement

The zeta potential of bacteria was measured using Zetasizer (Zen3600, Malvern, Worcestershire WR14 1XZ, UK), following earlier procedure [49]. The consistency of bacterial concentration of the freshly grown cultures was confirmed using optical density (OD 600: ~0.5) by NanoDrop One C (Thermo Fisher Scientific, Madison, WI). Then, the bacterial culture in TSB was centrifuged at 10000 rpm for 3 minutes (Eppendorf AG, 22331 Hamburg, Germany). After removing the supernatant, the pellet was resuspended in 1 mL of sterile deionized water.

Finally, the resuspended samples were loaded into a folded capillary cuvette and then placed onto the instrument for reading Zeta Potential values. The experiments were performed in triplicates.

3.2.5. Visualization of Bacterial Cells and MNP-Cell Interaction

Visualization of bacterial cells and confirmation of the MNP-cell attachment was assisted by a 3D laser scanning confocal microscope (LSCM) (VK-X1000 Series, Keyence, Osaka, Japan) at Dr. Alocilja's Nano-Biosensors Laboratory, MSU. For visualization of pure bacterial cells using the LSCM, 2-3 of the chosen colonies on the plates were smeared on the microscope slides, and the gram-staining procedure was applied. The LSCM also allowed to visualize the MNP-cell interactions. For the imaging, the final sample of the MNP-cell mixture was resuspended in 100 µL sterile water after magnetic extraction and supernatant removal. A total of 10-20 µL of the final sample was placed on a glass slide, followed by the gram-staining. Optical images of pure bacterial cells and gMNPs-cell interaction from different spots on the slides were taken under 100x magnification.

The ultrastructure of these cells was also observed using a transmission electron microscope (TEM) (JEM-1400 Flash, Jeol, Nieuw-Vennep, Tokyo, Japan) at the CAM, MSU. Briefly, a loop of colonies of the overnight pure culture and gMNP-cell mixture was separately dissolved in the fixative solution (2.5% glutaraldehyde in 0.1M cacodylate buffer) and then dropped onto the grid. After negative staining with uranyl acetate, the grids were loaded into the specimen holder of the TEM, and images were taken in the range of 5000-25000x magnification.

3.2.6. Statistical Analysis

All experiments in this proposed study were triplicate, and quantitative data were presented with average and standard deviations. Differences in the measured values (zeta potential and concentration factor) of each group were statistically analyzed at a 95% confidence interval using the Kruskal-Wallis H test followed by post-hoc Dunn's test.

3.3. Results and Discussion

3.3.1. Visualization of Bacterial Cells

Initial cell morphology (cell shape) of *E. coli* (S) and *E. coli* (R) cells of the first group were monitored using the LSCM, as illustrated in Figure 3.1. The rod shape of *E. coli* (S) was

initially confirmed. The cell structure or shape of *E. coli* (R) isolates were all similar; these cells were heterogeneous with nonperfect rod and round cells, unlike the susceptible cells. Some studies showed that the biochemical components of antibiotic-resistant cells are different from those of susceptible bacteria based on distinct fingerprint patterns. Raman spectroscopy is one example where bacterial differentiation or detection was achieved using this pattern [50,51]. Thus, the cell shape differences in all *E. coli* (R) isolates compared to *E. coli* (S) cells could be the result of alteration in cell wall components.

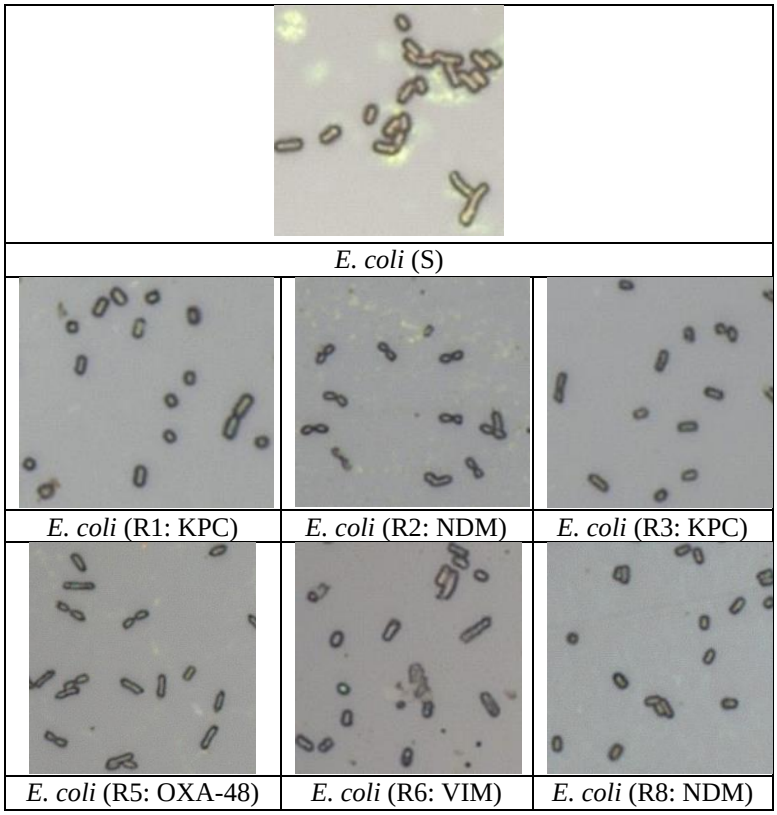

Figure 3.1. The cell shape of carbapenem-susceptible *E. coli* (S) and carbapenem-resistant *E. coli* (R) isolates in the absence of carbapenem exposure (group 1), visualized using a 3D laser scanning confocal microscope (LSCM).

Further, the cell shape of the control (non-exposed) and the exposed *E. coli* cells of the second group at the low, medium, and high-level imipenem concentrations were obtained and illustrated in Fig 3.2. The rod-shaped cells of *E. coli* (S) mostly turned round after carbapenem exposure. The cell morphology was heterogeneous, with imperfect rods and round cells. In addition, the initial cell shape of *E. coli* (R1: KPC), control, was found to be heterogenous (rod and round shapes). Following exposure to imipenem, no major changes in shape were observed (Figure 3.2a). The ultrastructure of the carbapenem-exposed and non-exposed *E. coli* cells was

further visualized using TEM. The images of the control and exposed *E. coli* (S) clearly showed the round shape of the exposed cells at increasing imipenem concentrations. The non-exposed and exposed *E. coli* (R1: KPC) cells similarly had both rod and round cells as clumped forms (Figure 3.2b).

The susceptible bacteria were possibly affected by the antibiotic stress, resulting in their slower growth. Studies suggest that changes in cell components and morphology are interconnected with bacterial growth rate [52–58]. For example, an earlier study evaluated the morphological changes of *Acinetobacter baumannii* induced by imipenem and meropenem. The morphological changes were seen in susceptible and resistant bacteria; however, imipenem showed a stronger effect on susceptible bacteria [59]. Elsewhere, the cell shape of gram-negative bacilli exposed to carbapenems turned to spherical or ovoid cell forms was seen in all strains of *E. coli*, *K. pneumoniae*, *P. aeruginosa*, *Proteus* spp., and *S. marcescens* [60]. In another study, sensitive gram-negative bacilli showed morphological changes with exposure to cephalothin, while naturally resistant bacteria were unaffected [61]. Their study further indicated that no morphological changes in the cells were observed after they were made resistant by repeated subculture (after 24 transfers) in increasing concentrations of antibiotics [61]. Accordingly, the similarities in the shape and stability of the exposed *E. coli* (S) with all *E. coli* (R) isolates might be the reason for acquiring permanent resistance.

The heterogeneous shapes might be due to the effect of carbapenems on the cell wall, disrupting cell wall synthesis. Since carbapenems enter the bacteria through outer membrane proteins (porins) and degrade the penicillin-binding proteins (PBPs) at the cell wall, weakening the glycan backbone in the cell wall [45,62,63]. Several studies highlighted that β-lactam antibiotics induce elongation and spheroplast formation in many species of Gram-negative and some species of Gram-positive bacteria as a result of the loss of peptidoglycan layer that provides rigid, shape-determining structure and membrane tension to cells [58,60,61,64]. Researchers have also stated that the heterogeneity in morphological changes may result from binding with more than one PBP. For example, the affinity to PBP-1 or PBP-2 results in spheroplast forms, while the binding with PBP-2 or PBP-3 causes cell elongation, depending on exposure period and antibiotic concentration [58–60,64].

(a)

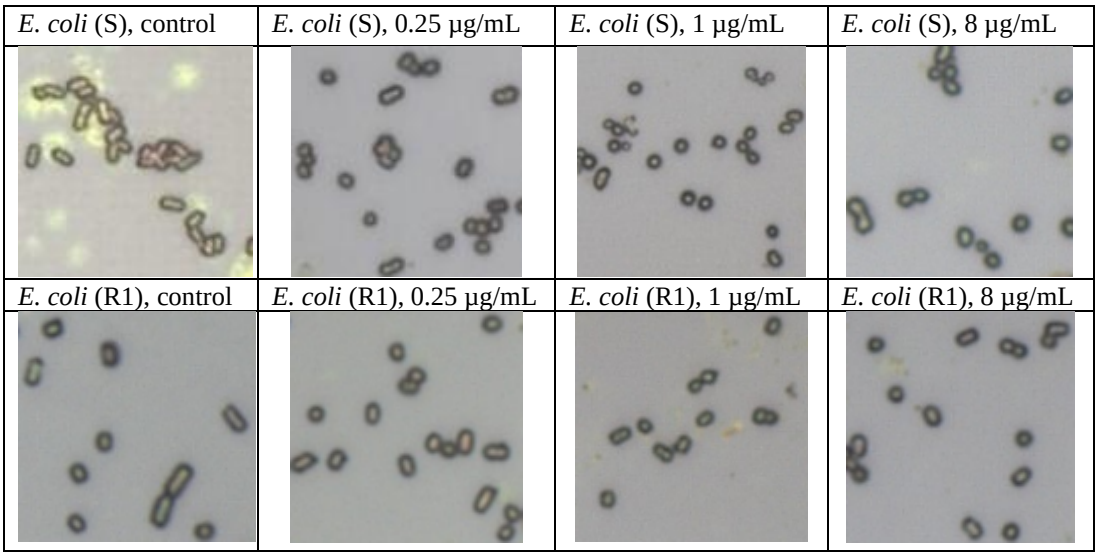

(b)

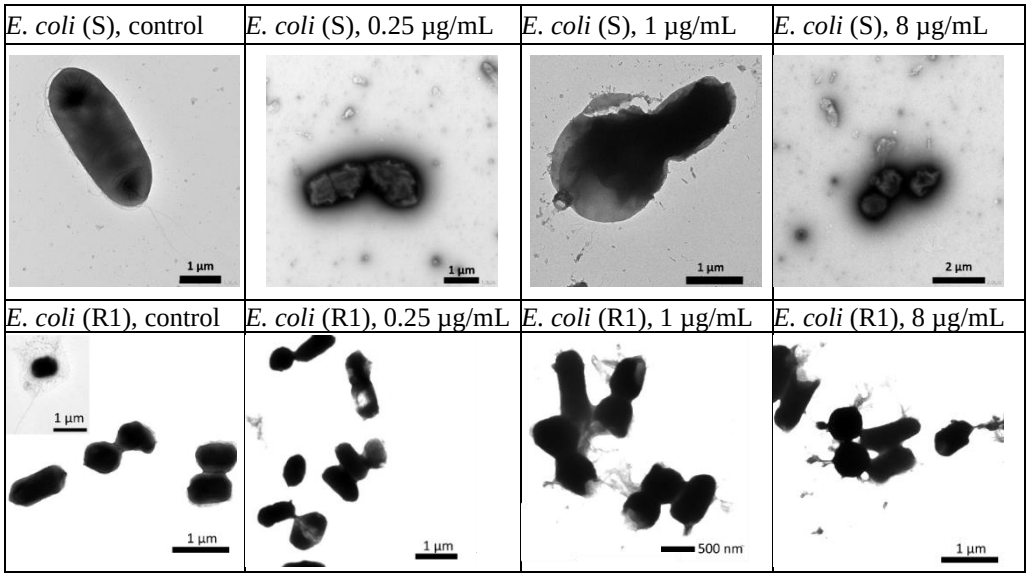

Figure 3.2. Microscopic images of carbapenem-exposed and non-exposed *E. coli* cells at low, medium, and high-level concentration (group 2), using a 3D laser scanning confocal microscope (LSCM) (a) and Transmission Electron Microscopy (TEM) (b).

Further, antibiotics induce endolysin expression and lead to vesicle formation through explosive cell lysis in gram-negative bacteria [65,66]. Also, antibiotic exposure could induce some changes inside the cytoplasm [67]. Various studies showed that alteration in the biosynthesis of cell wall material, membrane components, and cytoplasmic contents may result in disruptions in cell surface characteristics, including cell morphology and surface charge [57,58,68–70]. Differences in the cell wall composition of bacterial species can affect their cell adhesion properties (surface charges and specific binding locations) [30,32,53,71–73]. Thus, the

observed morphological characteristics in this study might impact their motility, cell adhesion, or attachment to substrate surfaces. Cell surface characteristics, therefore, need further attention; the zeta potential of these isolates was also assessed to understand their MNP-cell interaction better.

3.3.2. Cell Surface Charge (Zeta Potential)

Zeta potential values were used as a proxy for cell surface charge. The average zeta potential values of *E. coli* (S) and *E. coli* (R) isolates of the first group are illustrated in Figure 3.3a. The average zeta potential value of *E. coli* (S) was approximately -54 mV, while all *E. coli* (R) isolates were between -20 mV and -43 mV. Overall, *E. coli* (R) cells had significantly lower negative zeta potential values ($p < 0.05$) compared to the reference bacteria (*E. coli* (S)).

The values of the non-exposed and the exposed *E. coli* (S) and *E. coli* (R1: KPC) are illustrated in Figure 3.3b. All exposed *E. coli* (S) cells were between -31 mV and -36 mV, while non-exposed *E. coli* (S) cells were around -54 mV. However, the non-exposed *E. coli* (R) and their exposed cells were in a similar range, approximately -43 mV to -40 mV. The zeta potential values of the non-exposed and exposed *E. coli* were statistically analyzed. The surface charge differences between non-exposed and exposed *E. coli* (S) were significantly different ($p < 0.05$), while there was no significant difference between the non-exposed and exposed *E. coli* (R1: KPC). The long-term exposed *E. coli* (S) showed similar zeta potential values with all *E. coli* (R) samples regardless of carbapenem exposure. It could be concluded that carbapenem exposure can significantly influence the surface charge of susceptible bacteria but not resistant bacteria, similar to the morphological characteristics.

Cell surface charges are associated with multiple factors, including the outer membrane compounds on the cell wall, the tridimensional structure of the cell surface, environment pH, and ionic strength, among others [69,74]. Zeta potential is mainly linked with negatively charged functional groups accompanied by lipopolysaccharide, phospholipids, and proteins on the cell surface of gram-negative bacterial while it is accompanied by peptidoglycan, teichoic acid, and teichuronic acid on the surface of gram-positive bacteria [74,75]. For instance, Soon and coworkers (2011) found that colistin-susceptible *Acinetobacter baumannii* cells exhibited a greater negative charge than colistin-resistant *Acinetobacter baunmannii* cells [70], similar to our findings. They also indicated that the differences might be the result of Lipopolysaccharide (LPS) loss in outer membrane proteins in resistant cells [70]. Further, another study stated that an alteration in the lipid A structure of cell walls reduces the negative charge of the cell, resulting in

the electrostatic repulsion of cationic peptides to the cell wall [8]. Thus, the difference might be the reason for the reduction or loss of outer membrane protein (porins) in carbapenem-resistant bacteria because carbapenems are not easily diffusible through the cell wall, but they enter the bacteria through outer membrane proteins (porins), as stated earlier [2]. Accordingly, the chemical nature of cells and potential modification in cells under any stress (environmental condition) lead to differences in growth rate, affecting cell wall composition, cell morphology, anion and cationic balance on the cell surface, electrical potential differences, and bacterial adhesion properties [57,68,69,74,75].

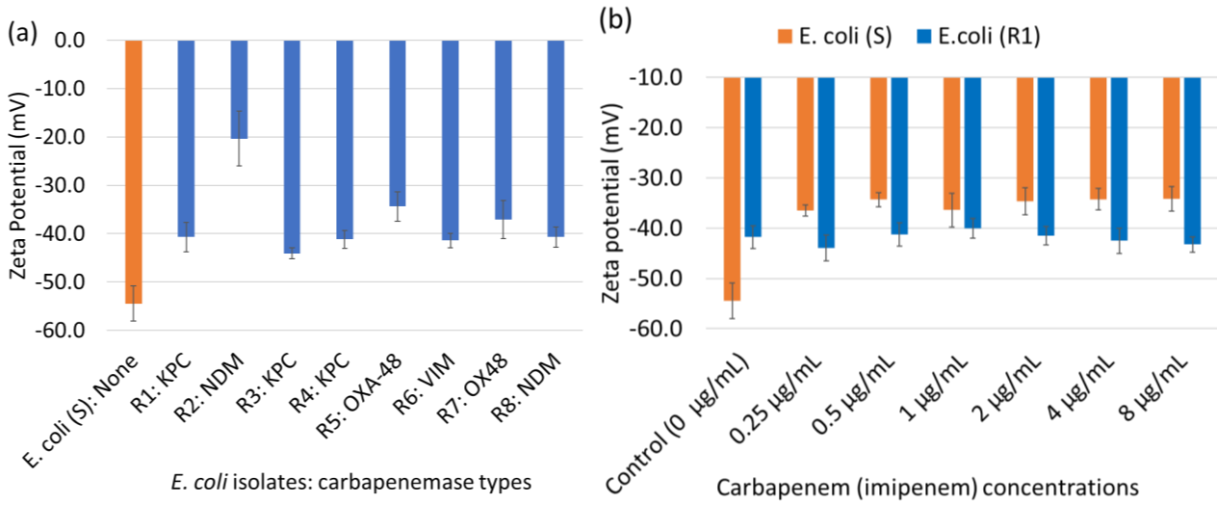

Figure 3.3. The average zeta potential values of *E. coli* isolates (a) *E. coli* (S) versus *E. coli* (R) isolates in the absence of carbapenem exposure (group 1) and (b) carbapenem exposed and non-exposed (control) *E. coli* (S) and *E. coli* (R1) (group 2).

In addition, electrostatic surface charges are primed for the evolution of the bacterial adhesion process [69,74], utilized for interaction between bacteria and nanoparticles in many areas (pharmacology, biotechnology, chemistry, nanomedicine, etc.) [57,75] as well as efficient bacterial extraction and detection in different matrices [30,32,57]. However, studies on surface charges of ARB, including CRE and their cell adhesion properties, are limited. Thus, this study exhibited surface charge characteristics of CRE (CP *E. coli*) compared with reference (susceptible) bacteria for further insights into their cell attachment properties, particularly with nanoparticles.

3.3.3. MNP-Cell Binding Capacity: Concentration Factor

The synthesized gMNPs were first characterized for their size and surface charge using the zeta sizer and TEM. The gMNPs were found to be 40-300 nm in diameter, which provides a

higher surface area-to-volume ratio and superparamagnetic properties, improving bacterial capture [49,76]. Further, gMNPs are positively charged (+20 mV) and create electrostatic interaction with negatively charged bacterial cells for attachment [76].

The efficacy of gMNPs' binding with *E. coli* (S) and all *E. coli* (R) cells of the first group was initially investigated using concentration factor (CF). All *E. coli* (R) isolates showed significantly lower CF (~0.4-1.3) than CF of *E. coli* (S) (~5.3), as seen in Figure 3.4a. Overall, all *E. coli* (R) isolates had much lower bacterial cells compared to *E. coli* (S).

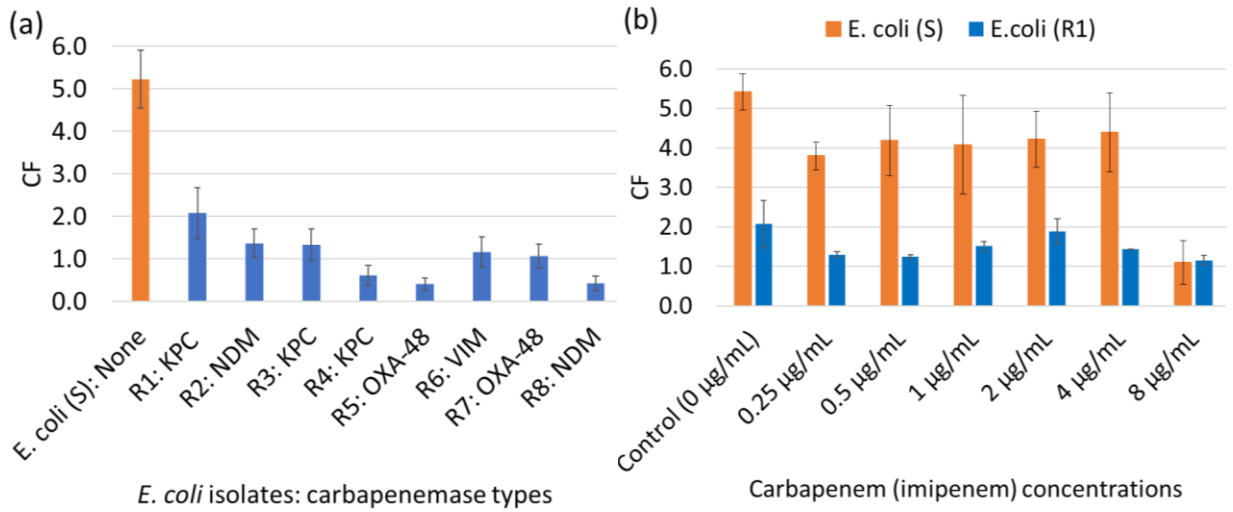

Figure 3.4. The average concentration factor (CF) of *E. coli* isolates: a) *E. coli* (S) versus *E. coli* (R) isolates in the absence of carbapenem exposure (group 1) and (b) carbapenem exposed and non-exposed (control) *E. coli* (S) and *E. coli* (R1) (group 2).

Further, the gMNPs were used to capture the non-exposed and exposed *E. coli* cells; Figure 3.4b illustrates the CF values. The non-exposed *E. coli* (S) had a higher CF value than the exposed *E. coli* (S) in the range of 4.6-1.1. The CF of non-exposed and exposed *E. coli* (R1: KPC) were closer, in the range of 1.6-1.2. Overall, gMNPs captured more *E. coli* (S) cells compared to exposed *E. coli* (S) and all *E. coli* (R) isolates. As previously stated, this might be related to the differences in cell surface characteristics of susceptible bacteria compared with resistant cells and carbapenem-exposed cells since the MNP-cell interaction was hypothesized to be related to the differences in cell wall components in each bacteria type [30,49,53].

Bacterial cell adhesion mainly relies on electrostatic interaction and receptor-ligand interaction, regardless of susceptibility status; bacterial cell attachment to surfaces is facilitated by adhesins (polypeptides (fimbrial (pili)) or polysaccharides (usually components of the bacterial cell membrane, cell wall, and capsule)) [77–80]. Each bacteria type has unique

components and adhesion mechanisms; they mainly use fimbriae for attachment to host cells, but their length, type, and roles are different for each bacterial type, even for their serotypes [77,81,82]. Thus, the chemical nature of cell surface components and the hydrophilic and hydrophobic groups on cell walls led to differences in cell adhesion properties, including nanoparticle-bacterial cell attachment capacity [57].

In studies on comparison of nanoparticle-cell attachment capacity, for example, the gram-positive bacteria showed higher attachment to positively charged gold nanoparticles; the surface charge of gram-positive bacteria was found to be higher negative than that of gram-negative bacteria [75]. In a recent work, glycan-coated MNPs were assessed on gram-negative and gram-positive bacteria: CF of gram-negative bacteria, *E. coli* O157, was lower than those of gram-positive, *L. monocytogenes* and *S. aureus*; the surface charge of *E. coli* O157 was lower negative charge (~-4 mV) than that of *L. monocytogenes* and *S. aureus* (~-35 mV and ~-42 mV, respectively) [49]. In another study, polyethyleneimine-modified magnetic microspheres (Fe3O4@PEI) were assessed to capture bacteria using capture efficiency (CE); the average CE of *S. aureus, A. baumannii*, and *P. aeruginosa* were found to be 97.87% for, 80.57% and 97.25%, respectively, which is in relationship with their zeta potential values -50.4 mV, −23.9 mV, and − 34.6 mV, respectively [83]. In our study, *E. coli* (S) similarly had higher CF, with a lower charge, and *E. coli* (R) had lower CF with a higher charge. Our study further proved the established hypothesis that MNP-cell interaction is inversely related to the zeta potential.

Overall, our study specifically illustrated that gMNPs captured resistant cells. Also, previous studies hypothesized that MNP-bacterial cell interaction is also based on receptor-ligand interaction, including glycan-lectin binding. To further elucidate the MNP-bacteria binding interactions, microscopy was used.

3.3.4. Visualization of gMNPs-Cell Interaction

The gMNPs-bacterial cell interactions were confirmed using the LCSM. Figure 3.5a shows the successful binding of gMNPs to *E. coli* (S) and *E. coli* (R) cells of the first group. Clusters of susceptible and resistant cells surrounded by gMNPs were commonly seen, particularly in *E. coli* (R) isolates. Also, multiple gMNPs are attached to the individual cells.

Further, the gMNPs-cell binding capacity of carbapenem-exposed and non-exposed *E. coli* cells of the second group were visualized using TEM. As observed in the images (Figure 3.5b), the gMNPs similarly bind to carbapenem-exposed and non-exposed bacterial surfaces. The presence of multiple

gMNPs on the cluster or single cells may improve bacterial cell capture. The small size of gMNPs can assist in moving faster than larger particles, interacting with bacterial cells, and increasing their bacterial capture [30,49,76].

(a)

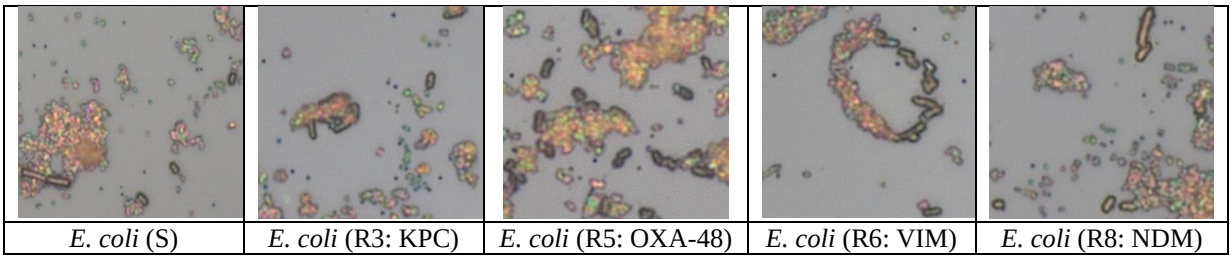

(b)

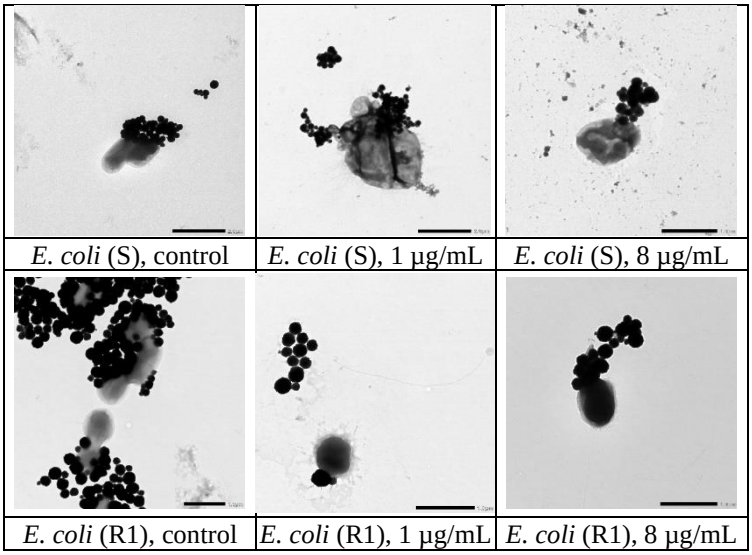

Figure 3.5. Visualization of gMNPs-cell interaction of *E. coli* isolates: (a) *E. coli* (S) versus *E. coli* (R) isolates in the absence of carbapenem exposure (group 1), using a 3D laser scanning confocal microscope (LSCM) and (b) carbapenem exposed and non-exposed (control) *E. coli* (S) and *E. coli* (R1) (group 2), using Transmission Electron Microscopy (TEM).

The LSCM and TEM images further showed that the gMNPs mostly bind to some portions of the cells. This might be due to location-specific glycan–protein interaction. The MNP-bacterial cell interaction based on carbohydrates and cell surface proteins is an established phenomenon. For example, the adhesion FimH, a two-domain protein, binds to terminal mannose residues [84], concanavalin A is another protein, binding to sugar maties in lipopolysaccharide [85], and sugar moieties can bind to C-type Salmo Salar Lectin (SSL) [86]. Site-specific attachment of bacterial cells using microscopic images was further illustrated in several studies [30,73,87].

As previously studied, the MNP-bacteria attachment relies on multiple forces: random Brownian motion, electrostatic interaction, receptor-ligand interaction by van der Waals forces and hydrogen bonds [30,49,88]. This study further showed that these interactions have successfully allowed gMNPs-resistant cell binding, similarly with susceptible cells. However, it should be noted that the lower MNP-cell capture in *E. coli* (R) isolates could be due to the alterations in morphological characteristics, cell surface charges, and the specific-location binding (glycan-protein interaction) [76].

Further, the gMNPs can be used without further surface modification, do not require cold storage, and are chemically stable for three years at room temperature, significantly reducing the cost [2]. The estimated material cost of gMNPs per assay was 0.5 USD [87,89], significantly lower than that of antibody-coated MNPs, which is estimated at 5-10 USD per assay [90]. In addition to its cost-effectiveness, bacterial extraction and concentration using gMNPs can be done within 15 min [30,76]. Overall, the non-selective gMNPs allow the capturing of several bacterial types and resistant bacteria at once, which does not require specific affinity binding and specific preparation for each bacterial type. The economical, efficient, and rapid nature of gMNPs and their storage conditions increase their use and accessibility for bacterial separation, particularly in low-resource settings. However, future works are required to increase its applicability and accessibility.

3.3.5. Future Perspectives

The present study shows that gMNPs can rapidly capture ARB, including CRE (CP *E. coli*). which further elaborate bacterial characteristics and adhesive properties. The findings of the gMNP-cell interaction and cell surface characteristics (cell morphology and cell surface charge) for susceptible and resistant *E. coli* cells further elaborate bacterial characteristics and adhesive properties. While this study assessed several resistant *E. coli* isolates, they were compared by only one susceptible *E. coli*, and further studies with larger sample sizes are required. Each bacterial type/serotype, regardless of susceptibility status, has unique characteristics, adhesive properties, and relationships with hosts, which offer diverse genetic variability [91,92]. For instance, *E. coli* has various pathogen groups and serotypes (O- and H-antigens; >700 serotypes) based on virulent and antigen typing, respectively [93,94], each of which might affect their cell surface characteristics and interaction with surfaces. Thus, this study can be extended to include more susceptible *E. coli* isolates consisting of non-pathogenic

and pathogenic types to elucidate if all susceptible *E. coli* cells behave similarly. In addition, other common carbapenem-resistant bacteria such as *Klebsiella*, *Enterobacter*, *Pseudomonas*, and *Acinetobacter*with their susceptible types and other causative-resistant bacteria (methicillin-resistant Staphylococcus aureus, vancomycin-resistant *Enterococcus*, ampicillin-resistant *Salmonella*, colistin-resistant *E. coli*, etc.) should be assessed to further elucidate the behavior of resistant and susceptible cells.

Although this study showed that gMNPs' binding capacity to carbapenem-resistant and carbapenem-exposed *E. coli* cells was lower compared to susceptible *E. coli*, which could be related to cell wall components, further attention is needed to elucidate the interaction of gMNPs with bacteria and the surrounding environment. For instance, many bacteria can produce biofilm under any stress as their defense mechanism; biofilm is typically a combination of polysaccharides, proteins, lipids, and DNA, and bacterial cells in the biofilm matrix do not have Brownian movement [95,96]. Thus, future studies are needed to test the biofilm formation of bacteria in the absence and presence of antibiotic exposure, along with their interaction with gMNPs. Further, gMNPs can be tested in different matrices such as clinical, environmental, and food samples to understand the effect of matrix components and background microflora on the gMNP-bacteria adhesion mechanism. Moreover, although this magnetic separation using gMNPs is simple, rapid, and cost-effective, its efficiency can be further improved by coating amine groups to increase their positive surface charge, which was shown to be capable of increasing the capture capacity in food matrices [72].

While this study confirmed the differences in cell surface characteristics (cell morphology and cell surface charges) of the antibiotic-exposed and resistant cells; urgent attention is needed to explore their cell characteristics further. Further studies are needed to elucidate the mechanism of antibiotic exposure on bacterial cells. For instance, this study used only one carbapenem (imipenem); studies might be extended to use meropenem, which demonstrates enhanced activity against Gram-negative bacilli [97,98] and different kinds of antibiotics, such as cephalosporins and fluoroquinolones. Moreover, this study showed that long-term serial carbapenem exposure led to changes in cell morphology, which might be due to mutation in PBPs and/or outer membrane protein (porin) relying on the resistant mechanism [11,13,14,63]. The exposed bacteria may be genetically characterized using whole genome sequencing to define emerging resistance.

3.4. Conclusion

This study assessed the applicability of gMNPs for the isolation of carbapenem-resistant *E. coli* compared with susceptible *E. coli*. The cell surface characteristics (cell morphology and surface charge) were further evaluated to understand the MNP-cell binding mechanisms. The gMNPs successfully bound to resistant *E. coli* cells, which was confirmed with microscopic image and standard plating method. This study further showed the differences in cell surface characteristics of the resistant cells, impacting their MNP interaction. In future work, the applicability of the gMNPs can be further tested on larger sample size, including more susceptible cells, CRE isolates and other causative ARB isolates, as well as implemented in clinical and biological samples. These findings can stimulate future research on improving current extraction and diagnostic techniques.

REFERENCES

[1] Wellington, E. M. H., Boxall, A. B. A., Cross, P., Feil, E. J., Gaze, W. H., Hawkey, P. M., Johnson-Rollings, A. S., Jones, D. L., Lee, N. M., and Otten, W., "The Role of the Natural Environment in the Emergence of Antibiotic Resistance in Gram-Negative Bacteria," Lancet Infect. Dis., 2013, 13(2), pp. 155–165.

[2] Caliskan-Aydogan, O., and Alocilja, E. C., "A Review of Carbapenem Resistance in Enterobacterales and Its Detection Techniques," Microorganisms, 2023, 11(6), p. 1491, DOI: 10.3390/microorganisms11061491.

[3] Gullberg, E., Cao, S., Berg, O. G., Ilbäck, C., Sandegren, L., Hughes, D., and Andersson, D. I., "Selection of Resistant Bacteria at Very Low Antibiotic Concentrations," PLoS Pathog., 2011, 7(7), pp. 1–9, DOI: 10.1371/journal.ppat.1002158.

[4] Serwecińska, L., "Antimicrobials and Antibiotic-Resistant Bacteria: A Risk to the Environment and to Public Health," Water, 2020, 12(12), p. 3313, DOI: 10.3390/w12123313.

[5] Sandegren, L., "Selection of Antibiotic Resistance at Very Low Antibiotic Concentrations," Ups. J. Med. Sci., 2014, 119(2), pp. 103–107.

[6] Andersson, D. I., and Hughes, D., "Evolution of Antibiotic Resistance at Non-Lethal Drug Concentrations," Drug Resist. Updat., 2012, 15(3), pp. 162–172.

[7] Ter Kuile, B. H., Kraupner, N., and Brul, S., "The Risk of Low Concentrations of Antibiotics in Agriculture for Resistance in Human Health Care," FEMS Microbiol. Lett., 2016, 363(19), DOI: 10.1093/femsle/fnw210.

[8] Hughes, D., and Andersson, D. I., "Environmental and Genetic Modulation of the Phenotypic Expression of Antibiotic Resistance," FEMS Microbiol. Rev., 2017, 41(3), pp. 374–391.

[9] Reynoso, E. C., Laschi, S., Palchetti, I., and Torres, E., "Advances in Antimicrobial Resistance Monitoring Using Sensors and Biosensors: A Review," Chemosensors, 2021, 9(8), DOI: 10.3390/chemosensors9080232.

[10] Capita, R., and Alonso-Calleja, C., "Antibiotic-Resistant Bacteria: A Challenge for the Food Industry," Crit. Rev. Food Sci. Nutr., 2013, 53(1), pp. 11–48, DOI: 10.1080/10408398.2010.519837.

[11] Munita, J. M., and Arias, C. A., "Mechanisms of Antibiotic Resistance," Virulence Mech. Bact. Pathog., 2016, 4(2), pp. 481–511, DOI: 10.1128/9781555819286.ch17.

[12] Taggar, G., Rheman, M. A., Boerlin, P., and Diarra, M. S., "Molecular Epidemiology of Carbapenemases in Enterobacteriales from Humans, Animals, Food and the Environment," Antibiotics, 2020, 9(10), pp. 1–22, DOI: 10.3390/antibiotics9100693.

[13] Rabaan, A. A., Eljaaly, K., Alhumaid, S., Albayat, H., Al-Adsani, W., Sabour, A. A., Alshiekheid, M. A., Al-Jishi, J. M., Khamis, F., Alwarthan, S., Alhajri, M., Alfaraj, A. H., Tombuloglu, H., Garout, M., Alabdullah, D. M., Mohammed, E. A. E., Yami, F. S. Al, Almuhtaresh, H. A., Livias, K. A., Mutair, A. Al, Almushrif, S. A., Abusalah, M. A. H. A., and Ahmed, N., "An Overview on Phenotypic and Genotypic Characterisation of Carbapenem-Resistant Enterobacterales," Medicina (B. Aires)., 2022, 58(11), p. 1675, DOI: 10.3390/medicina58111675.

[14] Band, V. I., and Weiss, D. S., "Heteroresistance: A Cause of Unexplained Antibiotic Treatment Failure?," PLOS Pathog., 2019, 15(6), p. e1007726, DOI: 10.1371/journal.ppat.1007726.

[15] Abdeta, A., Bitew, A., Fentaw, S., Tsige, E., Assefa, D., Lejisa, T., Kefyalew, Y., Tigabu, E., and Evans, M., "Phenotypic Characterization of Carbapenem Non-Susceptible Gram-Negative Bacilli Isolated from Clinical Specimens," PLoS One, 2021, 16(12 December), pp. 1–18, DOI: 10.1371/journal.pone.0256556.

[16] Dankittipong, N., Fischer, E. A. J., Swanenburg, M., Wagenaar, J. A., Stegeman, A. J., and de Vos, C. J., "Quantitative Risk Assessment for the Introduction of Carbapenem-Resistant Enterobacteriaceae (CPE) into Dutch Livestock Farms," Antibiotics, 2022, 11(2), p. 281, DOI: 10.3390/antibiotics11020281.

[17] Antimicrobial Resistance: CDC's Antibiotic Resistance Threats in the United States, 2019. Available online:https://www.cdc.gov/drugresistance/pdf/threatsreport/2019-ar-threats-report-508.pdf (Accessed:06-September-2022).

[18] Rebold, N., Lagnf, A. M., Alosaimy, S., Holger, D. J., Witucki, P., Mannino, A., Dierker, M., Lucas, K., Kunz Coyne, A. J., El Ghali, A., Caniff, K. E., Veve, M. P., and Rybak, M. J., "Risk Factors for Carbapenem-Resistant Enterobacterales Clinical Treatment Failure," Microbiol. Spectr., 2023, 11(1), DOI: 10.1128/spectrum.02647-22.

[19] World Health Organization (WHO), "WHO Publishes List of Bacteria for Which New Antibiotics Are Urgently Needed," WHO, [Online]. Available: https://www.who.int/news/item/27-02-2017-who-publishes-list-of-bacteria-for-which-new-antibiotics-are-urgently-needed. [Accessed: 06-Sep-2022].

[20] Capozzi, C., Maurici, M., and Panà, A., "[Antimicrobial Resistance: It Is a Global Crisis, 'a Slow Tsunami']," Ig. Sanita Pubbl., 2019, 75(6), p. 429—450.

[21] CDC, "Healthcare-Associated Infections (HAIs):CRE Technical Information," CDC (Centers Dis. Control Prev., 2019, [Online]. Available: https://www.cdc.gov/hai/organisms/cre/technical-info.html. [Accessed: 08-Jun-2022].

[22] Queenan, A. M., and Bush, K., "Carbapenemases: The Versatile β-Lactamases," Clin. Microbiol. Rev., 2007, 20(3), pp. 440–458, DOI: 10.1128/CMR.00001-07.

[23] Guerra, B., Fischer, J., and Helmuth, R., "An Emerging Public Health Problem: Acquired Carbapenemase-Producing Microorganisms Are Present in Food-Producing Animals,

Their Environment, Companion Animals and Wild Birds," Vet. Microbiol., 2014, 171(3–4), pp. 290–297, DOI: 10.1016/j.vetmic.2014.02.001.

[24] Mills, M. C., and Lee, J., "The Threat of Carbapenem-Resistant Bacteria in the Environment: Evidence of Widespread Contamination of Reservoirs at a Global Scale," Environ. Pollut., 2019, 255, p. 113143, DOI: 10.1016/j.envpol.2019.113143.

[25] Bonardi, S., and Pitino, R., "Carbapenemase-Producing Bacteria in Food-Producing Animals, Wildlife and Environment: A Challenge for Human Health," Ital. J. Food Saf., 2019, 8(2), DOI: 10.4081/ijfs.2019.7956.

[26] Köck, R., Daniels-Haardt, I., Becker, K., Mellmann, A., Friedrich, A. W., Mevius, D., Schwarz, S., and Jurke, A., "Carbapenem-Resistant Enterobacteriaceae in Wildlife, Food-Producing, and Companion Animals: A Systematic Review," Clin. Microbiol. Infect., 2018, 24(12), pp. 1241–1250, DOI: 10.1016/j.cmi.2018.04.004.

[27] Woodford, N., Wareham, D. W., Guerra, B., and Teale, C., "Carbapenemase-Producing Enterobacteriaceae and Non-Enterobacteriaceae from Animals and the Environment: An Emerging Public Health Risk of Our Own Making?," J. Antimicrob. Chemother., 2014, 69(2), pp. 287–291, DOI: 10.1093/jac/dkt392.

[28] Guerra, B., Fischer, J., and Helmuth, R., "An Emerging Public Health Problem: Acquired Carbapenemase-Producing Microorganisms Are Present in Food-Producing Animals, Their Environment, Companion Animals and Wild Birds," Vet. Microbiol., 2014, 171(3–4), pp. 290–297, DOI: 10.1016/j.vetmic.2014.02.001.

[29] Suh, S. H., Jaykus, L. A., and Brehm-Stecher, B., *Advances in Separation and Concentration of Microorganisms from Food Samples*, Woodhead Publishing Limited, 2013, DOI: 10.1533/9780857098740.3.173.

[30] Dester, E., and Alocilja, E., "Current Methods for Extraction and Concentration of Foodborne Bacteria with Glycan-Coated Magnetic Nanoparticles: A Review," Biosensors, 2022, 12(2), p. 112, DOI: 10.3390/bios12020112.

[31] Pitt, W. G., Alizadeh, M., Husseini, G. A., McClellan, D. S., Buchanan, C. M., Bledsoe, C. G., Robison, R. A., Blanco, R., Roeder, B. L., Melville, M., and Hunter, A. K., "Rapid Separation of Bacteria from Blood-Review and Outlook," Biotechnol. Prog., 2016, 32(4), pp. 823–839, DOI: 10.1002/btpr.2299.

[32] Bohara, R. A., and Pawar, S. H., "Innovative Developments in Bacterial Detection with Magnetic Nanoparticles," Appl. Biochem. Biotechnol., 2015, 176(4), pp. 1044–1058, DOI: 10.1007/s12010-015-1628-9.

[33] Krishna, V. D., Wu, K., Su, D., Cheeran, M. C. J., Wang, J. P., and Perez, A., "Nanotechnology: Review of Concepts and Potential Application of Sensing Platforms in Food Safety," Food Microbiol., 2018, 75, pp. 47–54, DOI: 10.1016/j.fm.2018.01.025.

[34] Lv, M., Liu, Y., Geng, J., Kou, X., Xin, Z., and Yang, D., "Engineering Nanomaterials-

Based Biosensors for Food Safety Detection," Biosens. Bioelectron., 2018, 106(January), pp. 122–128, DOI: 10.1016/j.bios.2018.01.049.

[35] Olsvik, Ø., Popovic, T., Skjerve, E., Cudjoe, K. S., Hornes, E., Ugelstad, J., and Uhlén, M., "Magnetic Separation Techniques in Diagnostic Microbiology," Clin. Microbiol. Rev., 1994, 7(1), pp. 43–54, DOI: 10.1128/CMR.7.1.43.

[36] Mohammed, L., Gomaa, H. G., Ragab, D., and Zhu, J., "Magnetic Nanoparticles for Environmental and Biomedical Applications: A Review," Particuology, 2017, 30, pp. 1–14, DOI: 10.1016/j.partic.2016.06.001.

[37] Benoit, P. W., and Donahue, D. W., "Methods for Rapid Separation and Concentration of Bacteria in Food That Bypass Time-Consuming Cultural Enrichment," J. Food Prot., 2003, 66(10), pp. 1935–1948, DOI: 10.4315/0362-028X-66.10.1935.

[38] Frank, J. F., "Microbial Attachment to Food and Food Conctact Surfaces," *Advances Innnnnnnn Food and Nutrition Research Vol 43*, Academic press, 2001, ISBN: 0-12-016443-4.

[39] Payne, M. J., and Kroll, R. G., "Methods for the Separation and Concentration of Bacteria from Foods," Trends Food Sci. Technol., 1991, 2, pp. 315–319, DOI: 10.1016/0924-2244(91)90734-Z.

[40] Peirano, G., Bradford, P. A., Kazmierczak, K. M., Badal, R. E., Hackel, M., Hoban, D. J., and Pitout, J. D. D., "Global Incidence of Carbapenemase-Producing Escherichia Coli ST131," Emerg. Infect. Dis., 2014, 20(11), pp. 1928–1931, DOI: 10.3201/eid2011.141388.

[41] Pitout, J. D. D., Nordmann, P., and Poirel, L., "Carbapenemase-Producing Klebsiella Pneumoniae, a Key Pathogen Set for Global Nosocomial Dominance," Antimicrob. Agents Chemother., 2015, 59(10), pp. 5873–5884, DOI: 10.1128/AAC.01019-15.

[42] Hoelle, J., Johnson, J. R., Johnston, B. D., Kinkle, B., Boczek, L., Ryu, H., and Hayes, S., "Survey of US Wastewater for Carbapenem-Resistant Enterobacteriaceae," J. Water Health, 2019, 17(2), pp. 219–226, DOI: 10.2166/wh.2019.165.

[43] Nair, D. V. T., Venkitanarayanan, K., and Johny, A. K., "Antibiotic-Resistant Salmonella in the Food Supply and the Potential Role of Antibiotic Alternatives for Control," Foods, 2018, 7(10), DOI: 10.3390/foods7100167.

[44] Hamza, D., Dorgham, S., Ismael, E., El-Moez, S. I. A., Elhariri, M., Elhelw, R., and Hamza, E., "Emergence of β-Lactamase- and Carbapenemase- Producing Enterobacteriaceae at Integrated Fish Farms," Antimicrob. Resist. Infect. Control, 2020, 9(1), p. 67, DOI: 10.1186/s13756-020-00736-3.

[45] Papp-Wallace, K. M., Endimiani, A., Taracila, M. A., and Bonomo, R. A., "Carbapenems: Past, Present, and Future," Antimicrob. Agents Chemother., 2011, 55(11), pp. 4943–4960, DOI: 10.1128/AAC.00296-11.

[46] Cusack, T. P., Ashley, E. A., Ling, C. L., Rattanavong, S., Roberts, T., Turner, P., Wangrangsimakul, T., and Dance, D. A. B., "Impact of CLSI and EUCAST Breakpoint Discrepancies on Reporting of Antimicrobial Susceptibility and AMR Surveillance," Clin. Microbiol. Infect., 2019, 25(7), pp. 910–911, DOI: 10.1016/j.cmi.2019.03.007.

[47] Andrews, J. M., "Determination of Minimum Inhibitory Concentrations," J. Antimicrob. Chemother., 2001, 48(SUPPL. 1), pp. 5–16, DOI: 10.1093/jac/48.suppl_1.5.

[48] Bhusal, N., Shrestha, S., Pote, N., and Alocilja, E., "Nanoparticle-Based Biosensing of Tuberculosis, an Affordable and Practical Alternative to Current Methods," Biosensors, 2018, 9(1), p. 1, DOI: 10.3390/bios9010001.

[49] Boodoo, C., Dester, E., Sharief, S. A., and Alocilja, E. C., "Influence of Biological and Environmental Factors in the Extraction and Concentration of Foodborne Pathogens Using Glycan-Coated Magnetic Nanoparticles," J. Food Prot., 2023, 86(4), p. 100066, DOI: 10.1016/j.jfp.2023.100066.

[50] Wang, K., Li, S., Petersen, M., Wang, S., and Lu, X., "Detection and Characterization of Antibiotic-Resistant Bacteria Using Surface-Enhanced Raman Spectroscopy," Nanomaterials, 2018, 8(10), DOI: 10.3390/nano8100762.

[51] Galvan, D. D., and Yu, Q., "Surface-Enhanced Raman Scattering for Rapid Detection and Characterization of Antibiotic-Resistant Bacteria," Adv. Healthc. Mater., 2018, 7(13), pp. 1–27, DOI: 10.1002/adhm.201701335.

[52] Schaechter, M., Maaløe, O., and Kjeldgaard, N. O., "Dependency on Medium and Temperature of Cell Size and Chemical Composition during Balanced Growth of Salmonella Typhimurium," Microbiology, 1958, 19(3), pp. 592–606.

[53] Young, K. D., "Bacterial Morphology: Why Have Different Shapes?," Curr. Opin. Microbiol., 2007, 10(6), pp. 596–600.

[54] Young, K. D., "Bacterial Shape: Two-Dimensional Questions and Possibilities," Annu. Rev. Microbiol., 2010, 64, pp. 223–240.

[55] Amir, A., "Cell Size Regulation in Bacteria," Phys. Rev. Lett., 2014, 112(20), p. 208102, DOI: 10.1103/PhysRevLett.112.208102.

[56] Harris, L. K., and Theriot, J. A., "Surface Area to Volume Ratio: A Natural Variable for Bacterial Morphogenesis," Trends Microbiol., 2018, 26(10), pp. 815–832, DOI: 10.1016/j.tim.2018.04.008.

[57] Nishino, M., Matsuzaki, I., Musangil, F. Y., Takahashi, Y., Iwahashi, Y., Warigaya, K., Kinoshita, Y., Kojima, F., and Murata, S., "Measurement and Visualization of Cell Membrane Surface Charge in Fixed Cultured Cells Related with Cell Morphology," PLoS One, 2020, 15(7 July), DOI: 10.1371/journal.pone.0236373.

[58] Cushnie, T. P. T., O'Driscoll, N. H., and Lamb, A. J., "Morphological and Ultrastructural

Changes in Bacterial Cells as an Indicator of Antibacterial Mechanism of Action," Cell. Mol. Life Sci., 2016, 73(23), pp. 4471–4492, DOI: 10.1007/s00018-016-2302-2.

[59] Bernabeu-Wittel, M., García-Curiel, A., Pichardo, C., Pachon-Ibanez, M. E., Jimenez-Mejias, M. E., and Pachón, J., "Morphological Changes Induced by Imipenem and Meropenem at Sub-Inhibitory Concentrations in Acinetobacter Baumannii," Clin. Microbiol. Infect., 2004, 10(10), pp. 931–934.

[60] Horii, T., Kobayashi, M., Sato, K., Ichiyama, S., and Ohta, M., "An In-Vitro Study of Carbapenem-Induced Morphological Changes and Endotoxin Release in Clinical Isolates of Gram-Negative Bacilli.," J. Antimicrob. Chemother., 1998, 41(4), pp. 435–442.

[61] Chang, T.-W., and Weinstein, L., "Morphological Changes in Gram-Negative Bacilli Exposed to Cephalothin," J. Bacteriol., 1964, 88(6), pp. 1790–1797.

[62] Codjoe, F., and Donkor, E., "Carbapenem Resistance: A Review," Med. Sci., 2017, 6(1), p. 1, DOI: 10.3390/medsci6010001.

[63] Smith, H. Z., and Kendall, B., "Carbapenem Resistant Enterobacteriaceae," StatPearls [Internet]. StatPearls Publ., 2021.

[64] Codjoe, F., and Donkor, E., "Carbapenem Resistance: A Review," Med. Sci., 2017, 6(1), p. 1, DOI: 10.3390/medsci6010001.

[65] Toyofuku, M., Nomura, N., and Eberl, L., "Types and Origins of Bacterial Membrane Vesicles," Nat. Rev. Microbiol., 2019, 17(1), pp. 13–24.

[66] Murtha, A. N., Kazi, M. I., Schargel, R. D., Cross, T., Fihn, C., Cattoir, V., Carlson, E. E., Boll, J. M., and Dörr, T., "High-Level Carbapenem Tolerance Requires Antibiotic-Induced Outer Membrane Modifications," PLOS Pathog., 2022, 18(2), p. e1010307, DOI: 10.1371/journal.ppat.1010307.

[67] Wojnicz, D., Kłak, M., Adamski, R., and Jankowski, S., "Influence of Subinhibitory Concentrations of Amikacin and Ciprofloxacin on Morphology and Adherence Ability of Uropathogenic Strains," Folia Microbiol. (Praha)., 2007, 52(4), pp. 429–436.

[68] Yang, D. C., Blair, K. M., and Salama, N. R., "Staying in Shape: The Impact of Cell Shape on Bacterial Survival in Diverse Environments," Microbiol. Mol. Biol. Rev., 2016, 80(1), pp. 187–203.

[69] Ferreyra Maillard, A. P. V., Espeche, J. C., Maturana, P., Cutro, A. C., and Hollmann, A., "Zeta Potential beyond Materials Science: Applications to Bacterial Systems and to the Development of Novel Antimicrobials," Biochim. Biophys. Acta - Biomembr., 2021, 1863(6), p. 183597, DOI: 10.1016/j.bbamem.2021.183597.

[70] Soon, R. L., Nation, R. L., Cockram, S., Moffatt, J. H., Harper, M., Adler, B., Boyce, J. D., Larson, I., and Li, J., "Different Surface Charge of Colistin-Susceptible and -Resistant Acinetobacter Baumannii Cells Measured with Zeta Potential as a Function of Growth

Phase and Colistin Treatment," J. Antimicrob. Chemother., 2011, 66(1), pp. 126–133, DOI: 10.1093/jac/dkq422.

[71] Matta, L. L., and Alocilja, E. C., "Emerging Nano-Biosensing with Suspended MNP Microbial Extraction and EANP Labeling," Biosens. Bioelectron., 2018, 117(July), pp. 781–793, DOI: 10.1016/j.bios.2018.07.007.

[72] Matta, L. L., Harrison, J., Deol, G. S., and Alocilja, E. C., "Carbohydrate-Functionalized Nanobiosensor for Rapid Extraction of Pathogenic Bacteria Directly from Complex Liquids with Quick Detection Using Cyclic Voltammetry," IEEE Trans. Nanotechnol., 2018, 17(5), pp. 1006–1013, DOI: 10.1109/TNANO.2018.2841320.

[73] Matta, L. L., and Alocilja, E. C., "Carbohydrate Ligands on Magnetic Nanoparticles for Centrifuge-Free Extraction of Pathogenic Contaminants in Pasteurized Milk," J. Food Prot., 2018, 81(12), pp. 1941–1949, DOI: 10.4315/0362-028X.JFP-18-040.

[74] Wilson, W. W., Wade, M. M., Holman, S. C., and Champlin, F. R., "Status of Methods for Assessing Bacterial Cell Surface Charge Properties Based on Zeta Potential Measurements," J. Microbiol. Methods, 2001, 43(3), pp. 153–164, DOI: 10.1016/S0167-7012(00)00224-4.

[75] Pajerski, W., Ochonska, D., Brzychczy-Wloch, M., Indyka, P., Jarosz, M., Golda-Cepa, M., Sojka, Z., and Kotarba, A., "Attachment Efficiency of Gold Nanoparticles by Gram-Positive and Gram-Negative Bacterial Strains Governed by Surface Charges," J. Nanoparticle Res., 2019, 21(8), DOI: 10.1007/s11051-019-4617-z.

[76] Caliskan-Aydogan, O., Sharief, S. A., and Alocilja, E. C., "Rapid Isolation of Low-Level Carbapenem-Resistant E. Coli from Water and Foods Using Glycan-Coated Magnetic Nanoparticles," Biosensors, 2023, 13(10), p. 902, DOI: 10.3390/bios13100902.

[77] Wilson, J. W., Schurr, M. J., LeBlanc, C. L., Ramamurthy, R., Buchanan, K. L., and Nickerson, C. A., "Mechanisms of Bacterial Pathogenicity," Postgrad. Med. J., 2002, 78(918), pp. 216–224, DOI: 10.1136/pmj.78.918.216.

[78] Croxen, M. A., and Finlay, B. B., "Molecular Mechanisms of Escherichia Coli Pathogenicity," Nat. Rev. Microbiol., 2010, 8(1), pp. 26–38, DOI: 10.1038/nrmicro2265.

[79] Khan, M. A., and Steiner, T. S., "Mechanisms of Emerging Diarrheagenic Escherichia Coli Infection," Curr. Infect. Dis. Rep., 2002, 4(2), pp. 112–117, DOI: 10.1007/s11908-002-0050-y.

[80] Gomes, T. A. T., Elias, W. P., Scaletsky, I. C. A., Guth, B. E. C., Rodrigues, J. F., Piazza, R. M. F., Ferreira, L. C. S., and Martinez, M. B., "Diarrheagenic Escherichia Coli," Brazilian J. Microbiol., 2016, 47, pp. 3–30, DOI: 10.1016/j.bjm.2016.10.015.

[81] Li, B., Zhao, Y., Liu, C., Chen, Z., and Zhou, D., "Molecular Pathogenesis of Klebsiella Pneumoniae Molecular Pathogenesis of Klebsiella Pneumoniae," 2016, 9(SEPTEMBER 2014), pp. 1071–1081.

[82] Rizi, K. S., Ghazvini, K., and Farsiani, H., "Clinical and Pathogenesis Overview of Enterobacter Infections," Rev. Clin. Med., 2020, 6(4), pp. 146–154, DOI: 10.22038/RCM.2020.44468.1296.

[83] Li, J., Wang, C., Shi, L., Shao, L., Fu, P., Wang, K., Xiao, R., Wang, S., and Gu, B., "Rapid Identification and Antibiotic Susceptibility Test of Pathogens in Blood Based on Magnetic Separation and Surface-Enhanced Raman Scattering," Microchim. Acta, 2019, 186(7), p. 475, DOI: 10.1007/s00604-019-3571-x.

[84] Sauer, M. M., Jakob, R. P., Eras, J., Baday, S., Eriş, D., Navarra, G., Bernèche, S., Ernst, B., Maier, T., and Glockshuber, R., "Catch-Bond Mechanism of the Bacterial Adhesin FimH," Nat. Commun., 2016, 7(1), p. 10738, DOI: 10.1038/ncomms10738.

[85] SAFINA, G., VANLIER, M., and DANIELSSON, B., "Flow-Injection Assay of the Pathogenic Bacteria Using Lectin-Based Quartz Crystal Microbalance Biosensor," Talanta, 2008, 77(2), pp. 468–472, DOI: 10.1016/j.talanta.2008.03.033.

[86] Mi, F., Guan, M., Hu, C., Peng, F., Sun, S., and Wang, X., "Application of Lectin-Based Biosensor Technology in the Detection of Foodborne Pathogenic Bacteria: A Review," Analyst, 2021, 146(2), pp. 429–443, DOI: 10.1039/D0AN01459A.

[87] Briceno, R. K., Sergent, S. R., Benites, S. M., and Alocilja, E. C., "Nanoparticle-Based Biosensing Assay for Universally Accessible Low-Cost Tb Detection with Comparable Sensitivity as Culture," Diagnostics, 2019, 9(4), DOI: 10.3390/diagnostics9040222.

[88] Matta, L. L., and Alocilja, E. C., "Emerging Nano-Biosensing with Suspended MNP Microbial Extraction and EANP Labeling," Biosens. Bioelectron., 2018, 117(July), pp. 781–793, DOI: 10.1016/j.bios.2018.07.007.

[89] Sharief, S. A., Caliskan-Aydogan, O., and Alocilja, E., "Carbohydrate-Coated Magnetic and Gold Nanoparticles for Point-of-Use Food Contamination Testing," Biosens. Bioelectron. X, 2023, 13(November 2022), p. 100322, DOI: 10.1016/j.biosx.2023.100322.

[90] Lau, H. K., Clotilde, L. M., Lin, A. P., Hartman, G. L., and Lauzon, C. R., "Comparison of IMS Platforms for Detecting and Recovering Escherichia Coli O157 and Shigella Flexneri in Foods," SLAS Technol., 2013, 18(2), pp. 178–183, DOI: 10.1177/2211068212468583.

[91] Liu, D., "Escherichia Coli," *Encyclopedia of Microbiology*, T.M. Schmidt, ed., Academic press, 2019.

[92] Yu, D., Banting, G., and Neumann, N. F., "A Review of the Taxonomy, Genetics, and Biology of the Genus Escherichia and the Type Species Escherichia Coli," Can. J. Microbiol., 2021, 67(8), pp. 553–571, DOI: 10.1139/cjm-2020-0508.

[93] Desmarchelier, P., and Fegan, N., "Pathogens in Milk: Escherichia Coli," *Reference Module in Food Science*, Elsevier, 2016, DOI: 10.1016/B978-0-08-100596-5.00989-6.

[94] Rivas, Lucia, Glen E. Mellor, Kari Gobius, and N. F., *Detection and Typing Strategies for Pathogenic Escherichia Coli*, Springer, 2015.

[95] Grande, R., Puca, V., and Muraro, R., "Antibiotic Resistance and Bacterial Biofilm," Expert Opin. Ther. Pat., 2020, 30(12), pp. 897–900, DOI: 10.1080/13543776.2020.1830060.

[96] Uruén, C., Chopo-Escuin, G., Tommassen, J., Mainar-Jaime, R. C., and Arenas, J., "Biofilms as Promoters of Bacterial Antibiotic Resistance and Tolerance," Antibiotics, 2020, 10(1), p. 3, DOI: 10.3390/antibiotics10010003.

[97] El-Gamal, M. I., Brahim, I., Hisham, N., Aladdin, R., Mohammed, H., and Bahaaeldin, A., "Recent Updates of Carbapenem Antibiotics," Eur. J. Med. Chem., 2017, 131, pp. 185–195, DOI: 10.1016/j.ejmech.2017.03.022.

[98] Salmon-Rousseau, A., Martins, C., Blot, M., Buisson, M., Mahy, S., Chavanet, P., and Piroth, L., "Comparative Review of Imipenem/Cilastatin versus Meropenem," Médecine Mal. Infect., 2020, 50(4), pp. 316–322, DOI: 10.1016/j.medmal.2020.01.001.

CHAPTER 4: RAPID ISOLATION OF LOW-LEVEL CARBAPENEM-RESISTANT *E. COLI* FROM WATER AND FOODS USING GLYCAN-COATED MAGNETIC NANOPARTICLES

This chapter has been published in *Biosensors*, 2023 (10.3390/bios13100902).

4.1. Introduction

In the growing global phenomenon of infectious diseases, infections by antimicrobial-resistant bacteria (ARB) are a major concern [1]. The emergence and spread of ARB are linked with the overuse and misuse of antibiotics in healthcare, veterinary medicine, and agriculture, their release into the environment [2–5], and their gene transmission through horizontal gene transfer (HGT) [4–6]. Thus, several microorganisms have been identified as a cause of severe common infections due to acquired resistance to one or more antibiotics on the market, which are found in people, animals, food, plants, and the environment [6,7]. To control and minimize the effect of ARB, there have been great research efforts during the last decade for their rapid detection and to make better-informed antibiotic choices.

Infections related to carbapenem-resistant bacteria have been alarmingly increasing in the last decade and are on the global priority list of ARB [5,8,9]. Even though carbapenems are used as the last line of defense in severe infections in humans, several studies showed that carbapenem-resistant *Enterobacterales* (CRE) are also found in food-producing animals, foods, and water sources, among others [5–7,10–14]. The emergence and spread of CRE are mainly a result of the rapid dissemination of the carbapenemase-producing (CP) gene through HGT [15]. The most prevalent carbapenemases are *Klebsiella pneumoniae* carbapenemase (KPC) and New Delhi metallo-β-lactamase (NDM) [5,16]. To prevent their emergence and spread in the community, antimicrobial resistance (AMR) monitoring systems routinely test the presence of carbapenemases and the resistant profile of specific pathogens in clinical and biological samples [8,17–19].

Rapidly detecting CRE from matrices can assist in preventing or minimizing the associated health and economic consequences [1]. Several phenotypic tests such as matrix-assisted laser desorption/ionization time-of-flight mass spectrometry (MALDI-TOF MS), colorimetric assays (Carba NP tests), amplification-based molecular tests, and biosensors have been implemented to detect CRE in a simple, rapid, and cost-effective manner [7,20–22]. The

detection limit or sensitivity of these techniques was variable with $\geq 10^3$ CFU/mL for MALDI-TOF MS, CarbaNP tests, and electrochemical and optical biosensors, while genotypic methods require 10^1–10^3 CFU/mL [7,22]. However, these techniques have usually used pure or overnight cultures to ensure enough bacterial count for bacterial detection and for determining their resistant profile [7]. Further, the isolation of ARB, including CRE, from various matrices has not explicitly been documented well. A few examples exist for separating CRE from pure cultures and clinical samples [23–26], but data are scarce for food matrices. For rapid and sensitive detection of CRE, their direct extraction (isolation) from matrices in a rapid and simple way is therefore of utmost importance and needs attention.

Overall, current bacterial separation techniques in food and clinical matrices include physical methods such as centrifugation and filtration and biochemical methods such as dielectrophoresis and magnetic nanoparticle (MNP)-based techniques [27–29]. Bacterial separation by filtration and centrifugation is commonly used and is primarily based on bacterial size and solution density [28–30]. While these methods are inexpensive and quick, their effectiveness is sometimes limited and remediated by multiple steps due to large food particles or blood cells and platelets in clinical samples, requiring overnight enrichment [28,30–32]. Biochemical methods for bacterial separation utilize naturally occurring biological or chemical interactions between affinity ligands and specific surface substrates on solid support [27,28,30]. For example, dielectrophoresis (DEP)-based techniques mainly utilize non-specific affinity ligands for separating a variety of bacterial cells, with negatively charged bacteria adhering to positively charged residues [28,29,33]. This technique is also employed for differentiating susceptible bacteria utilizing changes in dielectrophoretic behaviors related to antibiotic-induced cell wall inhibition and cell lysis. [34]. However, separation of ARB from matrices has not been specifically documented. Although this technique has been used for pathogen separation from food and clinical matrices [28–30], complex matrices present problems because of the high conductivity of food particles, limiting their use [28–30,33]. In biochemical methods, MNP-based techniques have recently been used for rapid and effective concentration of bacteria from complex samples due to their low cost, simplicity, and unique properties (large surface area/volume ratio and superparamagnetic) [28,35–37]. MNPs can be functionalized with recognition moieties such as antibodies, phages, carbohydrates, protein groups, and antibiotics for higher bacterial capture at low concentrations [27,35,38,39].

In MNP-based techniques, antibody-based or immunomagnetic separation (IMS) has commonly been used to separate pathogens and resistant bacteria from food and clinical matrices, and often combined with various detection platforms [24,25,40–44]. The IMS has also been implemented with immune-based assays or sensors for analyzing the proteins, enzymes, and genes of target pathogens [45–47]. However, food debris can block the antibody, preventing the separation and concentration of bacteria [28,30]. In addition, antibody production and conjugation with MNPs are time-consuming and expensive, along with low-temperature storage requirements, limiting their use in low-resource settings [28]. In MNP-based methods, bacteriophage-based separation has recently been applied to rapidly separate specific bacteria of interest from complex environments [30,48,49]. For example, phage-based MNPs were used to extract bacteria from water and foods such as lettuce, milk, cheese, and salmon [50,51]. However, the method has limitations with a tedious and lengthy process of coating magnetic particles with phages, undesired damage of target cells, and DNA degradation [27,30,48,52].

Further, MNPs functionalized with biomolecules, such as carbohydrates, proteins, and antibiotics, offer inexpensive, simple, and rapid alternatives to antibody and phage-based MNP separation [27]. For example, vancomycin-coated MNPs can successfully recognize the cell surface of various Gram-positive and Gram-negative bacteria [35,38], including vancomycin-resistant *Enterococci* [53] and carbapenem-resistant *E.coli* and *K. pneumoniae* [26], however, there are concerns about their antibacterial activity [54]. Other MNPs, such as those functionalized with amine groups, have been used to extract bacteria from water, green tea, and grape juice, achieving high capture efficiencies [55], but the functionalization procedure takes several hours. Many carbohydrate surfactants or glycans, such as mannose, galactose, glucose, caprylic acid cysteine, and chitosan, have also been used as MNP coatings [27,28,35,56,57]. In carbohydrate-coated MNPs, glycan (chitosan)-coated MNPs (gMNPs) are promising due to their cost-effective, rapid, and efficient bacterial separation, stability at room temperature, scalable production, and compatibility with many detection techniques [28,57–59]. For example, gMNPs successfully extracted and concentrated several bacteria from large-volume food samples, including milk [57,59], thick and complex liquids (beef juice, apple cider, and homogenized eggs) [58], sausage, deli ham, lettuce, spinach, chicken salad, and flour [60]. However, the use of gMNPs for the isolation of ARB, specifically CRE, from real samples requires attention.

As CRE is a global concern, rapid extraction of the causative bacteria from matrices is equally important as their rapid detection. Water sources and global food trade are among the primary routes for the export of CRE and their genes, posing a significant risk to human health [10,61,62]. Therefore, there has been a zero-tolerance policy and international ban on the sale of foods contaminated with CRE in several countries [5]. Thus, this research aimed to assess the use of gMNPs for rapid extraction of CRE from water and food samples.

4.1.1. Platform Novelty and Applicability

This study aimed to expand the application of gMNPs to rapidly extract ARB, specifically carbapenem-resistant *E. coli* since CP *E. coli* in CRE is commonly found in water sources and foods [5,14,63,64]. The gMNPs were used to extract three *E. coli* isolates: carbapenem-susceptible *E. coli* (S) as a reference (control) bacterium, KPC-producing resistant *E. coli* (R: KPC), and NDM-producing resistant *E. coli* (R: NDM). The gMNPs–bacteria binding capacity in buffer solutions and the effect of cell surface charge were first assessed. Following this, other factors affecting the MNP binding, such as solution pH and bacterial concentrations, were examined to elucidate their potential impact on bacterial capture and binding. Finally, the gMNPs were used to extract these bacteria from a large volume of food and water samples. To our knowledge, this is the first study on the separation of ABR, including CRE, using gMNPs from water and food matrices.

4.2. Material and Methods

4.2.1. Materials

Tryptic Soy Agar (TSA), Tryptic Soy Broth (TSB), Hydrochloric Acid (ACS reagent, 37%), and Phosphate-Buffered Saline (PBS, pH 7.4) were purchased from Sigma Aldrich. Selective media, CHROMagar for *E. coli* and SUPERCARBA for CP bacteria, were purchased from DRG International (Springfield, NJ, USA). Sodium Hydroxide (NaOH) pellets were obtained from VWR International. Transmission Electron Microscope (TEM) supplies (glutaraldehyde, uranyl acetate stain, and cacodylate buffer) were provided by the Center for Advanced Microscopy (CAM), Michigan State University (MSU). Copper grids for TEM (formvar/carbon-coated 200 mesh copper grids) were obtained from Electron Microscopy Systems (Hatfield, PA, USA). Whirl-Pak bags (92 oz. and 18 oz.) were purchased from VWR

International. Racks for magnetic separation were purchased from Spherotech (Lake Forest, IL, USA). All food materials were purchased from a local seller and stored at 4 °C before use.

4.2.2. Bacterial Strains and Culture Conditions

Bacterial strains of susceptible *E. coli* C-3000 (ATCC 15597) and KPC-producing carbapenem (imipenem and ertapenem)-resistant *E. coli* (BAA-2340) were obtained from the American Type Culture Collection (ATCC). A bacterial strain of NDM-producing carbapenem-resistant *E. coli* was obtained from the Michigan Department of Health and Human Services (MDHHS). Stock cultures frozen at –80 °C were refreshed on TSA and TSB and incubated at 37 °C for 24–48 h. Fresh bacterial cultures were grown in 9 mL of TSB for each experiment with an overnight incubation at 37 °C. Then, the fresh cultures were transferred to new 9 mL of TSB for 4–6 h incubation with agitation at 125 rpm before the experiment.

4.2.3. gMNPs Synthesis and Characterization

In-house proprietary glycan (chitosan)-functionalized MNPs were prepared in the Nano-Biosensor Lab, MSU, and synthesized following a previously documented procedure [65]. Briefly, an iron oxide (III) or magnetite (Fe_3O_4) core with chitosan shells was used to make the MNPs. Ferric chloride hexahydrate (as a precursor), in a mixture of ethylene glycol (as a reducing agent) and sodium acetate (as porogen), and deacetylated chitosan (5 mg/mL) were used for the MNP synthesis. Chitosan was polymerized to surface-modify the iron oxide nanoparticles. Batches of the glycan-coated MNPs were stored at room temperature for further use. The gMNPs are stable for at least 3 years; new synthesis was not required for everyday analysis. The gMNPs were suspended in sterile deionized water and sonicated before each experiment.

The gMNPs were further characterized by measuring their size using a Zetasizer (Zen3600, Malvern, Worcestershire WR14 1XZ, UK); 100 µL of gMNPs was suspended in 900 µL of sterile deionized water; a total of 2 mL of gMNPs for sample measurement were taken directly. The morphology of gMNPs was also analyzed using a Transmission Electron Microscope (TEM) (JEM-1400 Flash, Jeol, Tokyo, Japan). The prepared solution of gMNPs (5 µL) was directly dropped onto the copper grid and washed with distilled water, followed by air-drying prior to imaging.

4.2.4. Visualization of gMNPs–Bacteria Binding

Visualization of the gMNPs interaction with bacterial cells was assisted by TEM using a standard negative-staining procedure, as illustrated in Scheme 4.1. For TEM imaging, a few colonies of the overnight culture on TSA were dissolved in 900 µL PBS. After the magnetic incubation and separation, the samples were resuspended in 100 µL fixative solution (2.5% of glutaraldehyde in 0.1 M cacodylate buffer) and followed by staining. The staining procedure used 5 µL of the sample dropped onto the copper grid with a black side for 20–30 s, following which 5 µL of 0.5% uranyl acetate stain was added, and the excess stain was removed. The grids were loaded into the specimen holder of the TEM, and images were taken in the range of 5000–25000× magnification.

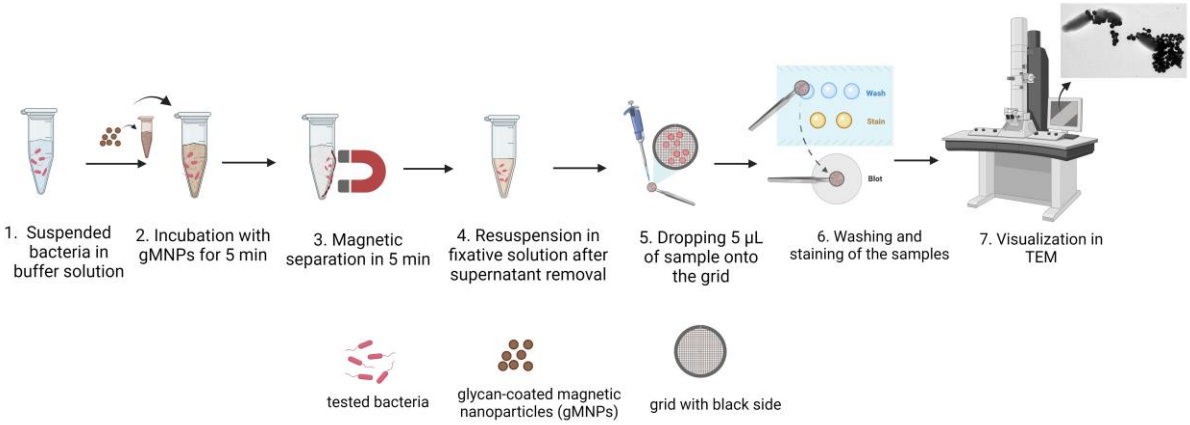

Scheme 4.1**.** The general procedure of TEM imaging; MNP–bacterial cell interaction (created with BioRender.com, accessed on 4 August 2023).

4.2.5. Cell Surface Charge (Zeta Potential) Measurement

The zeta potential of the susceptible and resistant *E. coli* isolates, pure gMNPs, and gMNPs–bacteria conjugation was measured using a Zetasizer. First, the fresh cultures were grown for 4–6 h in TSB, and samples with similar optical density (OD 600) values (~0.5), confirmed using NanoDrop One C, were used. Then, the bacterial culture was centrifuged (Eppendorf AG, 22331 Hamburg, German) at 10,000 rpm for 3 min. After removing the supernatant, the pellet was resuspended in 1 mL of sterile deionized water. For zeta potential measurement of pure gMNPs solution and gMNPs–bacteria conjugation, 100 µL of gMNPs were separately suspended in 900 µL of sterile deionized water and 900 µL of bacteria suspended water, with 5 min incubation. Finally, the resuspended samples were loaded into a folded

capillary cuvette and placed into the instrument for measurements. Experiments were performed in triplicates.

4.2.6. Bacterial Extraction in Buffer Solutions

The gMNP-based bacterial extraction or concentration factor (CF) was quantified through plating (colony counting) on solid growth media [28]. First, 4–6 h spiked bacterial cultures were serially diluted in PBS (pH: 7.4) to a concentration of approximately 10^3 and 10^2 CFU/mL, plated for initial bacterial counts. For the treatment group, 100 µL of gMNPs was added into 900 µL of the diluted bacterial samples (10^3 and 10^2 CFU/mL), vortexed for 10–15 s, and then allowed to stand for 5 min. After 5 min of magnetic separation, the supernatant was removed and resuspended in 100 µL of PBS. Finally, the separated samples were plated on TSA and left for 24 h for incubation at 37 °C. The gMNPs–bacteria binding capacity was determined by CF through colony counts from control samples (no MNP treatment) and MNP-treated samples; only plates with ~20–200 colonies were used. The CF was calculated separately for each serial trial using the following formula (Equation (1)). Experiments were performed in triplicates.

$$\text{Concentration Factor} = \frac{\text{number of colony in gMNPs} - \text{treated samples}}{\text{numebr of colony in control samples}} \qquad (1)$$

Following the confirmation of bacterial extraction, the effect of different bacterial concentrations and PBS adjusted to varying pH levels was conducted with the same procedure. For pH analysis, the PBS pH was first adjusted using HCl or NaOH to 3, 4, 5, 6, 7, and 8, confirmed using a pH meter. The procedure was conducted in triplicate at each pH level with a fixed bacterial load (~10^3 CFU/mL). For the effect of bacterial concentration, fresh 4–6 h spiked bacterial cultures were serially diluted from 10^7 to 10^2 CFU/mL, and CF was determined. The bacterial concentration experiments were conducted in PBS with a fixed pH of 7.4. Each experiment was performed in triplicates.

4.2.7. Bacterial Extraction from Large-Volume Samples (Foods and Water)

Matrices chosen for this study include romaine lettuce, raw chicken breast, ground beef, and tap water. The procedure for magnetic extraction was modified according to the Bacteriological Analytical Manual (BAM) protocols. Scheme 4.2 illustrates the general method used for the extraction. First, 25 g of each food sample or 25 mL of PBS or water in a Whirl-Pak bag were separately inoculated with 1 mL of ~10^5 CFU/mL of fresh bacterial culture. Each

experiment also had an uninoculated negative control group to account for natural microflora. After 1 h of room temperature acclimation of the contaminated samples, 225 mL of PBS was added and homogenized in a stomacher for 2 min. The liquified food matrix was then separated into two Whirl-Pak bags with 100 mL each, one serving as a no gMNPs (control) and the other as a test. To the test sample, 1 mL of gMNPs were added, mixed, and incubated at room temperature for 5 min. After 5 min magnetic separation and supernatant removal, the extracted cells (attached to the bag) were resuspended in 1 mL PBS. The separated gMNPs–bacteria mixture and control samples were plated on the selective media CHROMagar for *E. coli* identification and SUPERCARBA for CP bacteria identification. Also, uninoculated samples were treated with gMNPs; their control and gMNPs-treated samples were plated on both selective and TSA plates to account for natural microflora and confirm the absence of the interested bacteria. The plates were incubated at 37 °C for 24–48 h. For CF of *E. coli* (S), CP *E. coli* (R), and natural microflora from water and food samples, the number of blue colonies on CHROMagar plates, pink colonies on SUPERCARBA plates, and all colonies on TSA plates were used, respectively. The CF values were calculated based on the Equation (1) as described earlier. Each experiment was performed in triplicates.

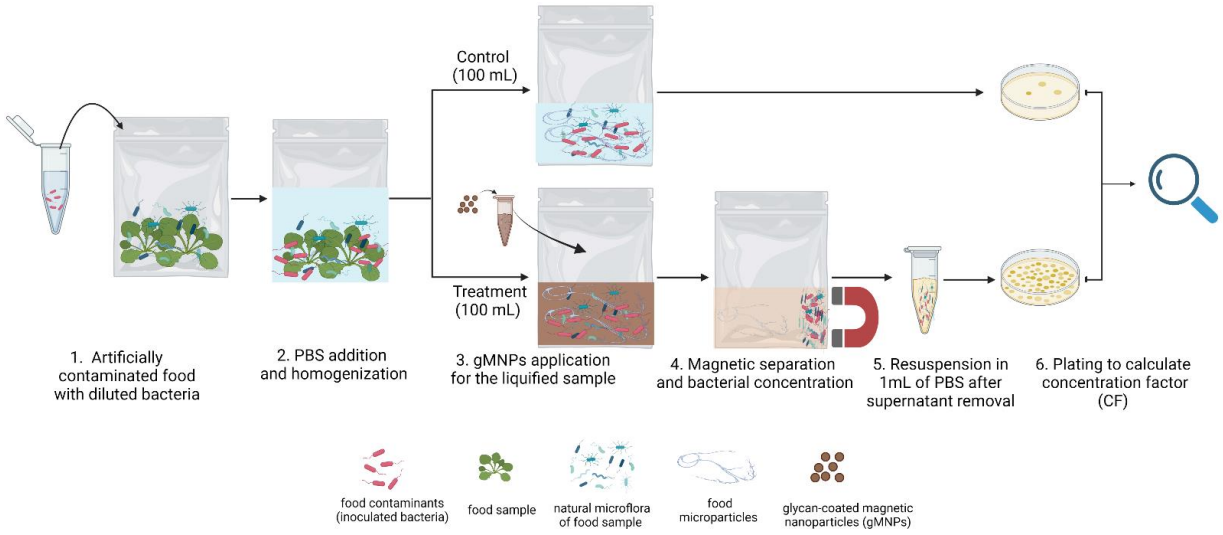

Scheme 4.2**.** The general procedure of gMNP-based bacterial extraction from large-volume samples (created with BioRender.com, accessed on 10 June 2023).

Further, the gMNPs–bacteria interaction from the matrices was visualized using TEM. The extracted gMNPs–cells were resuspended in 100 µL fixative solution (2.5% of

glutaraldehyde in 0.1 M cacodylate buffer). A 5 µL of the mixture was dropped onto the copper grid and followed by the negative staining as described earlier (Scheme 4.1).

4.3. Results and Discussion

4.3.1. Characterization of gMNPs

The synthesized gMNPs were characterized using TEM and Zetasizer. The suspension of gMNPs in sterile deionized water and its electron micrograph are illustrated in Figure 4.1a. All particles were roughly spherical, with multiple gMNPs of varying size, and clumping of particles was usually observed. The size (diameter) of gMNPs in the micrograph was found to be in a range of approximately 40–300 nm, using a measurement tool in TEM software. The mean particle size measured by the Zetasizer was found to be 286.5 ± 5.7 nm. The variation in size obtained from TEM and Zetasizer could probably have resulted from the random clumping of the nanoparticles and surface coating of iron oxide nanoparticles. The nanoparticles' size is critical for their superparamagnetic properties; iron oxide nanoparticles with 50–180 nm showed the highest superparamagnetic properties in an earlier study [66].

Superparamagnetic properties of gMNPs were further confirmed by subjecting the solution to an external magnet for one minute. As seen in Figure 4.1b, the particles were all separated from the solvent and pulled out to the side of the tube, resulting in clear water. The superparamagnetic properties of gMNPs were also confirmed in an earlier study; the gMNPs were observed to be strongly magnetized under an external magnet, further confirmed with their magnetization curves [57].

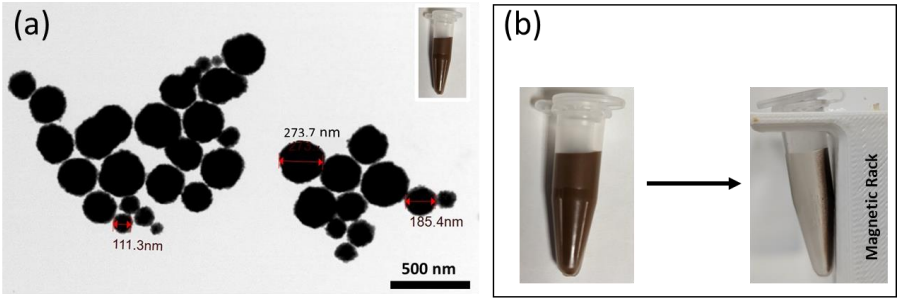

Figure 4.1**.** Characterization of the synthesized gMNPs: (a) TEM micrograph of the gMNPs with an inset tube for gMNPs solution and (b) visualization of superparamagnetic properties of gMNPs under external magnet.

In addition, the smaller size of MNPs has a higher surface area-to-volume ratio, which can assist them in moving faster than larger particles. Multiple particles penetrate matrix

interstices and interact with bacterial cells, improving their bacterial capture [27,28]. In previous studies, the gMNPs successfully extracted several bacteria from various food matrices [28,57,60,67].

4.3.2. Bacterial Extraction from Buffer Solution

4.3.2.1. Concentration Factor (CF)

The efficacy with which gMNPs extract *E. coli* (S), *E. coli* (R: KPC), and *E. coli* (R: NDM) was investigated using CF. Initially, the CF of these bacteria was determined in a small volume of PBS (1 mL) using the standard plating method; results are illustrated in Figure 4.2a. The average CF of resistant *E. coli* (R: KPC) and *E. coli* (R: NDM) were ~2 and ~1.4, lower than that for susceptible *E. coli* (S), which displayed a CF of ~5.2. Previous studies have observed differences in bacterial extraction between different bacteria types, which hypothesized electrostatic interaction between positively charged MNPs and negatively charged bacterial cell walls [28,35,68,69]. The chemical nature of bacterial cells and the hydrophilic and hydrophobic groups on cell walls results in differences in the cell surface charge [68].

The zeta potential of the pure bacterial isolates, pure gMNPs, and gMNPs–bacteria conjugations was measured further to understand the effect of surface charge on CF. As seen in Figure 4.2b, the average zeta potential of *E. coli* (S) was found to be around −54 mV, while *E. coli* (R: KPC) and *E. coli* (R: NDM) were −41 mV and −20 mV, respectively. The zeta potential of resistant *E. coli* (R) isolates was less than that of *E. coli* (S). An earlier study observed similar results; colistin-susceptible *Acinetobacter baumannii* cells had a higher zeta potential compared to that of colistin-resistant *Acinetobacter baumannii* [70].

The average zeta potential of gMNPs was positively charged and found to be around 20 mV. Further, the average zeta potential of gMNPs–bacteria conjugate was approximately −29 mV for *E. coli* (S) and *E. coli* (R: KPC) and −25 mV for *E. coli* (R: NDM).

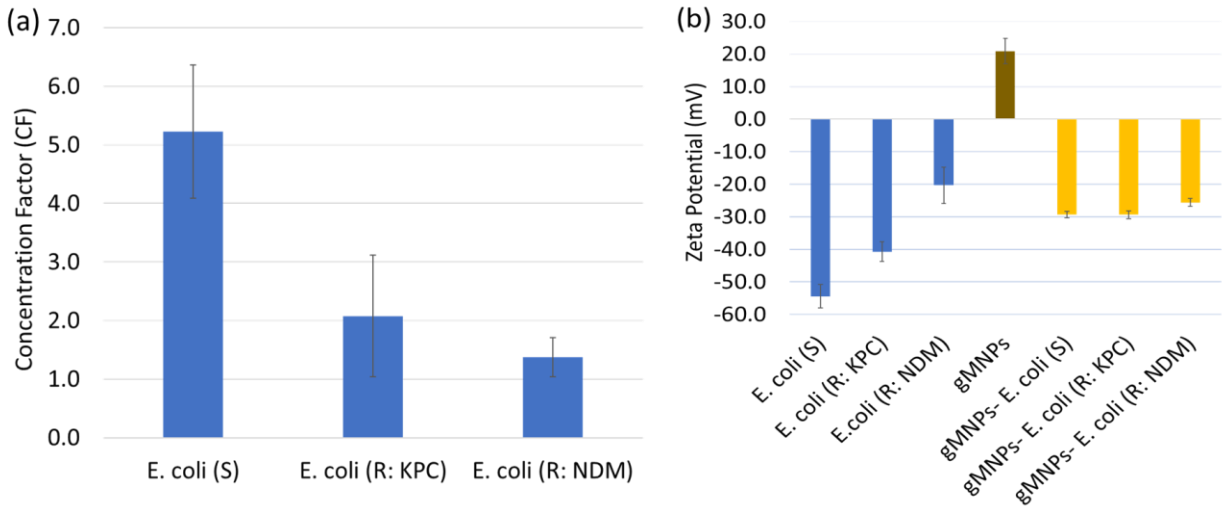

Figure 4.2. (a) The average MNP–bacteria concentration factor, with standard deviations and (b) zeta potential for pure bacteria isolates (blue bars); carbapenem-susceptible *E. coli* (S) and carbapenem-resistant *E. coli* (KPC: R) and *E. coli* (R: NDM), pure gMNPs (brown bar), and gMNPs-bacteria conjugation (yellow bars), with standard deviations.

The positively charged nature of nanoparticles has widely been used in previous studies for the capture of bacterial cells. For example, positively charged gold nanoparticles showed a greater attachment ability to Gram-positive bacteria with higher negative charge than Gram-negative bacteria with lower negative charge [69]. In another recent work, the extraction of Gram-negative *E. coli* O157 was lower (CF = ~4.5) compared to that of Gram-positive *L. monocytogenes* (CF= ~31.6) and *S. aureus* (CF = ~61.2) [60]. Confirming earlier reports, the average zeta potential of *E.coli* O157 is less negative (~−4 mV) than that of *L. monocytogenes* (~−35 mV) and *S. aureus* (~−42 mV) [60]. Similar results were seen in another study, with *S. aureus*, *A. baumanni*, and *P. aeruginosa* displaying a zeta potential of −50.4 mV, −23.9 mV, and −34.6, respectively. Their capture efficiency using polyethyleneimine modified magnetic microspheres (Fe3O4@PEI) was found to be 97.87% for *S. aureus*, 80.57% for *A. baumannii*, and 97.25 for *P. aeruginosa* [71]. The chemical nature of cells or environmental conditions leads to differences in cell wall composition, changes in anionic and cationic species on the cell surface, and electrical potential differences [68,69,72–74]. In accordance with earlier reports, our study confirmed that the MNP-based bacterial concentration is inversely related to the zeta potential.

The MNP-based bacterial extraction does not only depend on the electrostatic interaction but it is also related to receptor–ligand interactions, which may occur on some portions of the

bacterial adhesin surface. Bacterial adherence to surfaces is facilitated by adhesins (polypeptides (fimbrial (pili) or afimbrial) or polysaccharides (usually components of the bacterial cell membrane, cell wall, and capsule)) [75,76]. Each bacteria type has unique components and adhesion mechanisms, regardless of susceptibility status [76–78]. Further, several studies highlighted alterations in the biosynthesis of cell wall material, membrane components, and cytoplasmic contents in ARB, resulting in changes in cell surface characteristics and their adhesion or attachment to host surfaces [42,68,70,74,79,80]. For example, an alteration in the lipid A structure of cell walls reduces its negative charge, resulting in the electrostatic repulsion of cationic peptides to the cell wall [81]. Thus, the lower concentration factor of resistant *E. coli* (R) isolates compared to *E. coli* (S) may be additionally related to alteration or distortion in receptor–ligand interaction. Microscopy was used to elucidate the MNP–bacteria binding interactions further.

4.3.2.2. Microscope Imaging of gMNPs–Bacteria Interaction

The gMNPs–bacteria interaction was characterized using TEM to confirm the binding. Figure 4.3 shows roughly spherical gMNPs successfully attached to bacterial cells. Multiple gMNPs on individual and bacterial cell clusters may have contributed to improved bacterial extraction. Their interaction with flagella was also clearly seen in *E. coli* (S) and *E. coli* (R). Earlier studies showed similar MNP–bacterial cell interaction through microscopic imaging [28,57,82]. Multiple gMNPs interacting with individual cells of *E. coli* O157, and clusters of *S. aureus* and *L. monocytogenes* were seen [60] . The interaction was hypothesized to be related to the differences in cell morphology and cell wall components in each bacteria type. Further, the morphological characteristics of bacteria can impact their Brownian forces and cell attachment to surfaces [28,60,83].

The images also illustrated that gMNPs did not cover the entire surface of bacteria, binding only to some portions of the bacterial surface. This might be the effect of location-specific glycan–protein interaction, The established phenomenon of surface glycan attaching to proteins (e.g., lectins) on the bacterial cell surface may help better understand gMNP binding [27,28,35,67,84]. For example, the adhesin FimH can recognize and bind to terminal mannose residues [85], and sugar moieties can bind to concanavalin A protein [86] and C-type Salmo Salar Lectin (SSL) [87].

As earlier studies highlighted, the binding of gMNPs to bacterial cells is usually achieved through a combination of forces (Figure 4.3d): (1) Brownian motion, which allows random and uncontrolled movement of particles, (2) electrostatic forces, which assist in bringing the positively charged MNPs closer to negatively charged bacterial cells, and (3) in proximity, bacteria can adhere to glycan surface of MNPs through (glycan–protein) hydrogen bonding and van der Waals interaction [28,60,67]. This study showed that these interactions have successfully allowed gMNPs to capture resistant *E. coli* (R) isolates.

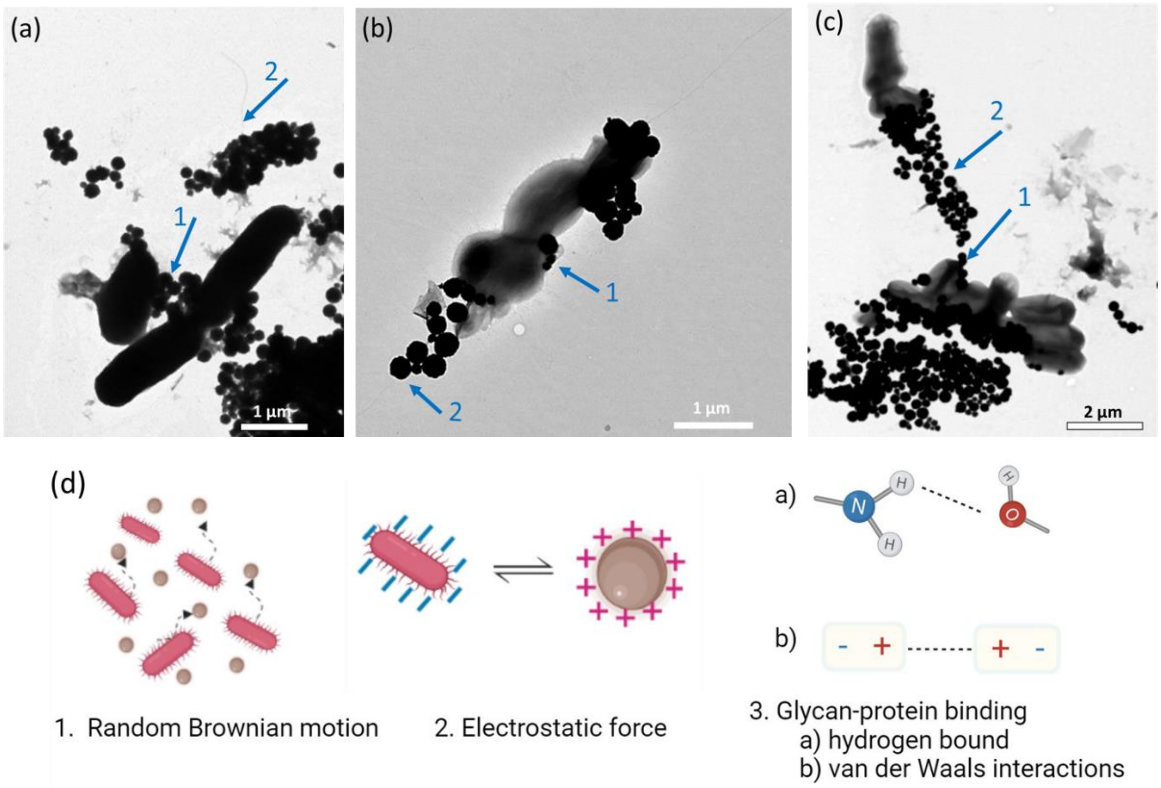

Figure 4.3. TEM images of MNP interactions with the susceptible and resistant E. coli isolates extracted from buffer solution: (a) E. coli (S), (b) E. coli (R: KPC), and (c) E. coli (R: NDM). Arrows show MNP–bacteria interaction: MNP–cell (1) and MNP–flagellum (2). (d) Schematic representation of the underlying hypothesis of the gMNPs interaction (created with BioRender, accessed on 7 August 2023)), which was adapted by a study [28].

The gMNPs interaction with resistant *E. coli* isolates (R: KPC and R: NDM) was seen as clusters, unlike individual cells of *E. coli* (S). Apart from the differences in gMNPs–cell binding, the *E. coli* (R) cells appear smaller and as imperfect rods (bacilli). As previously mentioned, the differences in cell morphology may have resulted from alterations in the cell surface components. In various studies, morphological and ultrastructural changes in bacterial cells under antibiotic exposure were observed and attributed to cell wall synthesis disruption due to

deficiency in cell wall materials and cell lysis [68,80,88–92], resulting in a change of cell morphology [80,83] and leading to alterations in electrostatic surface charge [68,70,93–95]. For example, carbapenems enter the bacteria through outer membrane proteins (porins) and degrade the penicillin-binding proteins (PBPs) at the cell wall, weakening the glycan backbone in the cell wall and resulting in alteration in cell morphology (filament or non-perfect round shapes) and surface components [20,96,97]. Thus, the distortion or alteration in cell components, including surface proteins, may have affected the glycan–protein interaction for carbapenem-resistant bacteria.

Considering the antimicrobial properties of chitosan-coated MNPs on bacteria, a previous study has shown that their antibacterial activity and cell lysis of bacteria occur after exposure of at least 8 h [60,98]. Therefore, the short-term (<15 min) exposure of the MNPs to bacteria may not have impacted their cell viability and properties. CP *E.* coli (R) cells before gMNP exposure also showed similar cell morphology (data not shown). Overall, it should be noted that the morphological nature of the resistant bacteria could have impacted their receptor–ligand (glycan–protein) interaction and the electrostatic repulsion between bacteria and gMNPs.

This study showed that the gMNPs could successfully isolate resistant *E. coli* (R) isolates. The bacterial extraction or isolation from the large-volume samples with varying pH environments and bacterial loads was tested to determine their possible field application.

4.3.2.3. Effect of Bacterial Load and Buffer pH on Concentration Factor

The extraction of *E. coli* (S) and resistant *E. coli* (R: KPC and R: NDM) was further investigated at varying bacterial concentrations and pH levels to elucidate the binding capacity of MNP (Figure 4.4). With varying bacterial concentrations at an approximately neutral pH (7.4) of PBS, the average CF of *E. coli* (S) was higher (>~5) at 10^2–10^3 CFU/mL, following a linearly decreasing trend as bacterial concentration increased ($R^2 = 0.98$) as seen in Figure 4.4a. However, resistant *E. coli* (R: KPC and R: NDM) isolates did not show a strong linear trend with varying bacterial concentrations ($R^2 = 0.68$ and 0.85, respectively). The average CF of *E. coli* (R) isolates was more than 1 at 10^2–10^5 CFU/mL, while a lower CF (<1) was seen at 10^6–10^7 CFU/mL. Notably, *E. coli* (S) and CP *E. coli* (R) isolates displayed the highest CF at low concentrations (10^2–10^3 CFU/mL). Similar results were previously seen in another study where positively charged MNPs successfully captured *E. coli* (90%) at ultra-low concentrations (10–100 CFU/mL) [23]. It was also found that positively charged nanoparticles have a higher

adsorption capacity for bacilli (*E. coli* and *B. subtilis*) than staphylococci (*S. aureus*) and streptococci (*L. lactis*) [23]. The higher bacterial extraction with gMNPs at lower bacterial concentrations could assist their quick detection for preventing outbreaks.

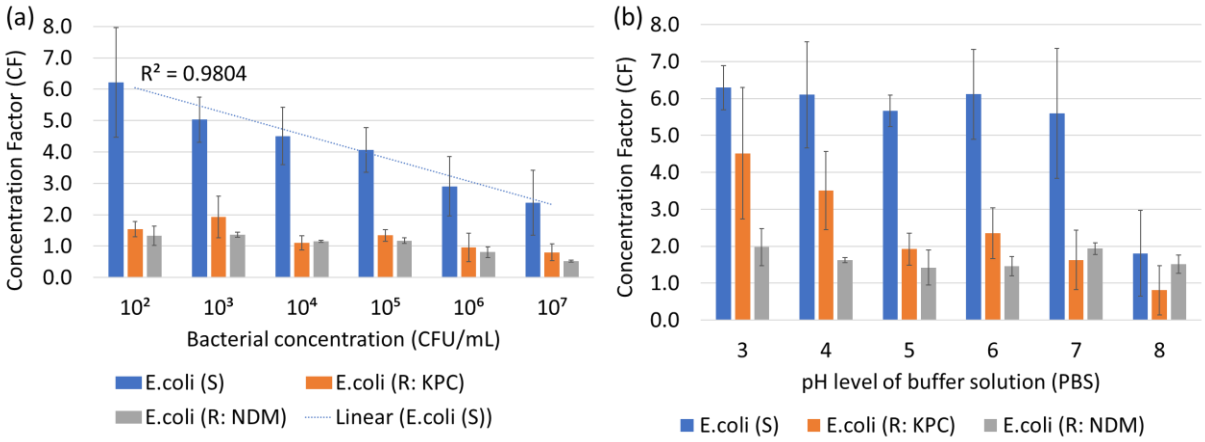

Figure 4.4. MNP–bacteria binding capacity: **(a)** Average concentration factor at varying bacterial concentrations with standard deviations (N:9) and **(b)** pH levels of buffer solutions with standard deviations.

The concentration factor was also tested in different pH environments for *E. coli* (S) and resistant *E. coli* (R) isolates (at ~10^3 CFU/mL). As observed in Figure 4.4b, *E. coli* (S) displayed similar CF (>5) at pH 3–7, while a sharp decrease in CF (~2) at pH 8 was seen. *E. coli* (R: KPC) showed higher CF (~>3) at pH 3–4 level, and the trend became stable (CF = ~2) at pH 5–7 and showed a sharp decrease (CF: <1) at pH 8. However, a similar trend was not observed in *E. coli* (R: NDM); their CF was between 1–2. Overall, these results confirmed earlier reports that reducing environmental pH might impact bacterial extraction. In a previous study, for instance, MNPs in the pH range of 5–8 displayed higher bacterial capture [23,57]. Further, the capture capacity at varying pH levels may also depend on the bacteria type. For example, an earlier report showed that the CF for *E. coli* O157 decreased linearly as the pH level (5–8) increased and remained stable at ~pH 8–10. The same study observed that the CF for *L. monocytogenes* and *S. aureus* did not show a trend and were similar in the pH 6–9 range [60]. Studies have also shown lower pH is generally associated with higher capture [23,57,60]. Since the gMNPs are naturally hydrophilic, the amino groups can be protonated at low pH levels, increasing the charge difference and promoting MNP–bacteria binding capacity [23,57,60].

4.3.3. Bacterial Extraction at Low Concentration from Large-Volume Samples (100 ML)

To evaluate the applicability of the gMNPs for large-volume bacterial extraction at low concentrations (~10^3 CFU/mL), the susceptible and resistant *E. coli* isolates were first tested in 100 mL of PBS. The gMNPs successfully extracted *E. coli* isolates, with an average CF of 6.5 for *E. coli* (S), 1.8 for *E. coli* (R: KPC), and 2.5 for *E. coli* (R: NDM); results are shown in Figure 4.5. Following the large-volume PBS concentration, the applicability of the gMNPs in water and food samples was tested. Magnetic extraction of the bacteria from water and various food types, including lettuce, raw chicken meat, and ground beef, was quantified using CF by selective plating. As seen in Figure 4.5, *E. coli* (S), *E. coli* (R: KPC), and *E. coli* (R: NDM) were successfully extracted from water and the food matrices with a CF > 1. Although *E. coli* (S) showed higher CF in PBS, the CF was lower in the water and food samples. The bacterial extraction was lower in the lettuce sample compared to chicken, beef, and water samples, which could have been due to the high level of natural microflora in the lettuce samples.

The natural microflora from uninoculated food samples (control) was also magnetically extracted, and their capture was quantified by plating on TSA. The CF of natural microflora was variable, as seen in the inset of Figure 4.5. The average CF was the highest in lettuce, followed by chicken and beef samples. Notably, the CF of *E. coli* samples was inversely related to the presence of bacterial loads in the lettuce sample. Although the natural microflora was higher in chicken, the average CF of *E. coli* (S) and *E. coli* (R: KPC) was lower in the beef samples. This could also be related to the physical microstructure and chemical constituents of the food sample. For example, lettuce is rich in cellulose components, while chicken and beef contain higher protein and fat amounts [75]. While the food composition of these tested food samples varies considerably, the food microparticles could also have affected the MNP–bacteria binding. The attachment or binding can differ based on the bacteria type, food matrix, and hydrophobic or hydrophilic surface [75]. An earlier study also stated that negatively charged molecules contaminating plant or animal tissues might interfere with the MNP–bacteria interaction [23,75].

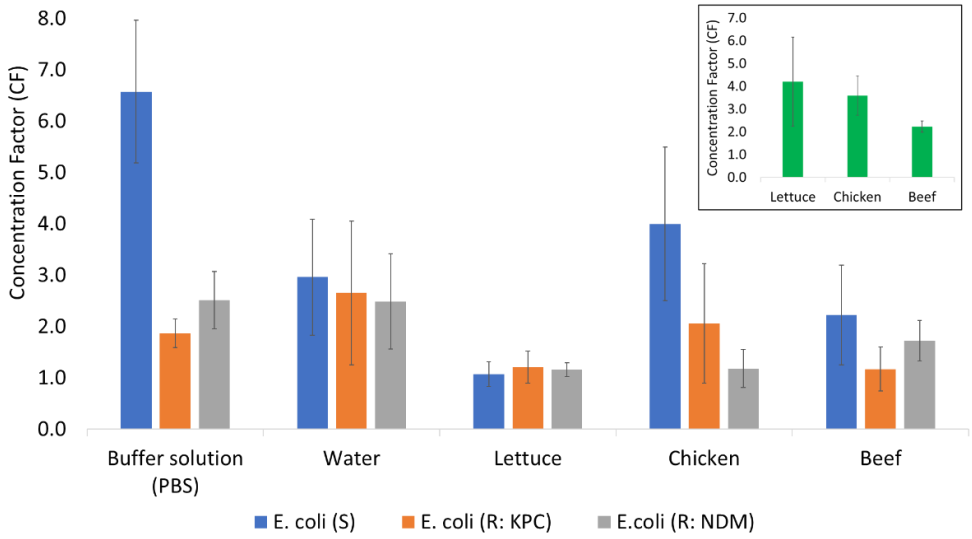

Figure 4.5. The bacterial extraction from food samples: average concentration factor (CF) from large-volume samples, along with inset figure for CF of uninoculated food samples (control), with standard deviations.

TEM images were also taken to confirm the binding of the gMNPs to bacterial cells in foods and are shown in Figure 4.6. The interaction between gMNP and bacterial cells in the presence of food microparticles was confirmed from the micrographs. Images showed that the microparticles (e.g., fat globules, protein fibers, and cellulose) can bind to gMNP and bacteria. In this MNP-based extraction technique, in theory, gMNP–bacteria, bacteria–food matrix, and MNP–food matrix interactions are possible in the liquified sample due to their attachment preferences and electrostatic forces. However, most of the food matrix in the liquefied samples is removed with the supernatant [28]. Magnetic separation using gMNP assists in reducing the remnant food debris from the sample and does not significantly affect the results. Earlier, for example, gMNPs successfully extracted and concentrated several bacteria from large-volume food samples, including milk [57,59], thick and complex liquid (beef juice, apple cider, and homogenized eggs) [58], sausage, deli ham, lettuce, spinach, chicken salad, and flour [60]. Following bacterial extraction from foods using gMNPs, target bacteria were detected, confirming that interferences of the food matrix did not significantly prevent the detection of target DNA [99–101]. Thus, the gMNPs are promising as they offer cost-effective, rapid, and efficient bacterial separation from various food matrices [57,58,60].

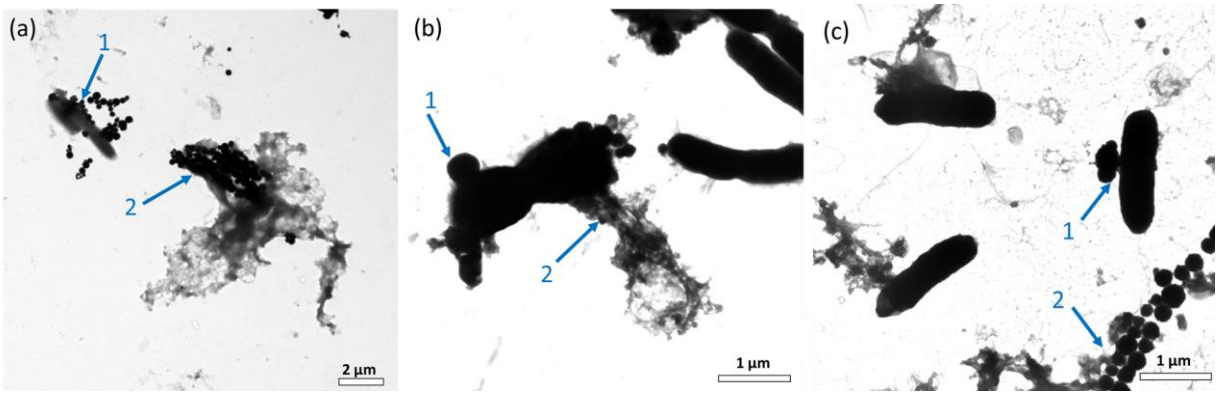

Figure 4.6. TEM images of MNP–bacteria interactions from inoculated food samples: (a) lettuce, (b) chicken, and (c) ground beef. Arrows show MNP–bacteria interaction: MNP–cell (1) and MNP–microparticles (2).

A detection platform can allow identification of the target bacteria following magnetic extraction, as summarized in Table 4.1. For example, the magnetic extraction of bacteria from various food matrices was followed by short enrichment, DNA extraction, and plasmonic biosensor detection: *E. coli* from lettuce and spinach [99], *Salmonella* from melons and cucumbers [100], and *E.coli* 0157 from flour [101]. In another work, the glycan/cysteine-coated MNPs captured *E. coli* O157:H7 from vitamin D milk, and then an electrochemical biosensor was used for detection [67].

Magnetic extraction and detection platforms have been used in clinical samples besides bacterial extraction from food samples. For instance, polyethyleneimine-modified magnetic microspheres (Fe3O4@PEI) were used to capture and enrich bacteria (*S. aureus*, *A. baumannii*, and *P. aeruginosa*) from blood samples by culturing on plates. A single colony from the overnight culture was then used in SERS platforms to identify bacterial type and resistance profile [71]. Elsewhere, vancomycin-modified Fe_3O_3-Au NP captured CRE from urine and detected them using carbapenemase hydrolysis activity by a pH meter [26]. In another example, the antibody-conjugated MNP were used to capture methicillin-resistant *S. aureus* (MRSA) from nasal swab at (10^3–10^5 CFU/mL), and then an electrochemical sensor was used for their detection [25]. As several studies showed that CRE has been found not only in clinical samples but also in foods and water sources [7,62,102–108], their rapid extraction directly from water and food samples has not been documented. This work is the first study for the extraction of CRE, specifically CP *E. coli*, from buffer solution and water and food samples. The differences in gMNP-cell binding capacity of resistant *E. coli* (R) compared to *E. coli* (S) may be due to the differences in cell surface characteristics (e.g., morphology and surface charge) of the resistant

bacteria. This study has offered further insight into the future potential of magnetic extraction of ARB and their extraction from different matrices.

Table 4.1. Summary of several MNP-based extractions of *E. coli* and ARB.

MNP Coating	Bacteria	Matrix	Capture	Detection Method	Ref.
PEI-modified gold-coated microspheres	*E. coli*	Tap water Milk	65%	Raman Spectroscopy	[110]
PEI	*E. coli*	Buffer	90%	Plating	[23]
Biotinylated oligosaccharides	*E. coli* (UPEC)	Buffer	17–34%	Luciferase assay	[111]
Antibody	*E. coli* 0157: H7	Whole milk	20%	Colorimetric biosensor	[112]
Antibody	STEC	Apple juice	39–105%	Multiplex qPCR	[113]
Cysteine-glycan	*E. coli* 0157: H7	Vitamin D Milk	73–90%	Plating	[57]
Cysteine-glycan	*E. coli* 0157: H7	Homogenized Egg Milk Apple cider	70%>	Electrochemical biosensor	[58]
Lyseine-SCGs	*E. coli* 0157: H7	Sausage	90%	Colorimetric biosensor	[114]
Antibody	STEC	Ground beef blueberries	NA	Colorimetric biosensor	[115]
Glycan	*E. coli* O157	Flour	NA	Colorimetric biosensor	[101]
Glycan	*E. coli*	Lettuce Spinach	NA	Colorimetric biosensor	[99]
Glycan	*E. coli* O157	Lettuce Spinach Chicken salad Flour	CF: 0.64–2.54	Plating	[60]*
Lectin-silver	*E. coli* MRSA	Buffer	NA	SERS	[23,24]
Antibody	Carbapenem-resistant *A. baumanni*	Culture Sputum	NA	Lateral flow biosensor	[116]
Vancomycin	CRE: *E. coli* and *K. pneumoniae*	Culture Urine	>70%	pH meter sensing	[26]
Antibody	MRSA	Nasal swab	>90%	Electrochemical biosensor	[25]
Glycan	Carbapenem-resistant *E. coli* (KPC and NDM producing)	Lettuce Chicken breast Ground beef Water	CF: 0.94–4.2	Plating (confirming extraction)	This study *

* The specific rapid detection method is not applied. The plating method is for the confirmation of bacterial extraction. PEI: polyethylemine, STEC: shiga toxin-producing *E. coli*; SCGs: short-chain glucan; MRSA: methicillin-resistant *S. aureus*; CRE: carbapenem-resistant *Enterobacterales*: NA: not applicable.

The non-specific nature of gMNPs may lead to complications in extraction from complex food matrices and those with a high level of natural microflora. The food matrix, in some cases, may affect subsequent detection based on the method employed. In this case, additional washing steps with PBS following supernatant removal can assist in the removal of food particles [28,35,57,84]. However, it should be noted that the non-selective gMNPs allow rapid capturing

of several bacterial types and resistant bacteria and do not require specific affinity binding or specific preparation for each bacterial isolation experiment. The non-selective extraction offers to detect more than one possible target bacteria at once. Thus, their implementation of surveillance programs can be helpful to prevent and control the spread of causative bacteria.

This study showed the applicability of gMNPs for extracting resistant *E. coli* (R) in food samples in the presence of natural microflora and food microparticles. The bacterial capture in these samples was achieved at concentrations as low as 10^3 CFU/mL. Notably, many biochemical separation techniques mostly require a concentration above 10^3 CFU/mL [7]. In addition, this magnetic separation allows accessible and rapid extraction, especially in low-resource settings. The gMNPs can be easily prepared and are chemically stable for three years at room temperature and are cost-effective. For instance, the cost of gMNPs-based extraction was estimated to be as low as USD 0.50 per assay [82,99], compared to IMS, which is USD 5–10 per assay and requires special storage conditions [109]. Further, bacterial extraction and concentration using gMNPs can be achieved within 15 min, while IMS needs longer incubation and extraction time [28].

4.4. Conclusion

Rapid and cost-effective platforms for bacterial extraction from food samples with higher binding efficiency are urgently needed to improve their rapid detection. This study tested glycan-coated MNPs to extract carbapenem-resistant *E. coli* from a buffer solution and large-volume food and water samples. The gMNPs–bacteria binding at varying bacterial concentrations and pH levels was also evaluated. Bacterial extraction from complex food matrices was achieved in the presence of natural microflora and food microparticles and confirmed with microscopic images. This study also showed the potential applicability of gMNPs to extract ARB from various complex solid food matrices. In future work, the applicability and accessibility of this platform can be further tested for the extraction of other ABRs, such as colistin, ampicillin, ESBL, and CRE, and from clinical, environmental, and food samples.

REFERENCES

[1] Ferri, M., Ranucci, E., Romagnoli, P., and Giaccone, V., "Antimicrobial Resistance: A Global Emerging Threat to Public Health Systems," Crit. Rev. Food Sci. Nutr., 2017, 57(13), pp. 2857–2876, DOI: 10.1080/10408398.2015.1077192.

[2] Andersson, D. I., and Hughes, D., "Evolution of Antibiotic Resistance at Non-Lethal Drug Concentrations," Drug Resist. Updat., 2012, 15(3), pp. 162–172.

[3] Wellington, E. M. H., Boxall, A. B. A., Cross, P., Feil, E. J., Gaze, W. H., Hawkey, P. M., Johnson-Rollings, A. S., Jones, D. L., Lee, N. M., and Otten, W., "The Role of the Natural Environment in the Emergence of Antibiotic Resistance in Gram-Negative Bacteria," Lancet Infect. Dis., 2013, 13(2), pp. 155–165.

[4] Sandegren, L., "Selection of Antibiotic Resistance at Very Low Antibiotic Concentrations," Ups. J. Med. Sci., 2014, 119(2), pp. 103–107.

[5] Taggar, G., Rheman, M. A., Boerlin, P., and Diarra, M. S., "Molecular Epidemiology of Carbapenemases in Enterobacteriales from Humans, Animals, Food and the Environment," Antibiotics, 2020, 9(10), pp. 1–22, DOI: 10.3390/antibiotics9100693.

[6] Serwecińska, L., "Antimicrobials and Antibiotic-Resistant Bacteria: A Risk to the Environment and to Public Health," Water, 2020, 12(12), p. 3313, DOI: 10.3390/w12123313.

[7] Caliskan-Aydogan, O., and Alocilja, E. C., "A Review of Carbapenem Resistance in Enterobacterales and Its Detection Techniques," Microorganisms, 2023, 11(6), p. 1491, DOI: 10.3390/microorganisms11061491.

[8] Dankittipong, N., Fischer, E. A. J., Swanenburg, M., Wagenaar, J. A., Stegeman, A. J., and de Vos, C. J., "Quantitative Risk Assessment for the Introduction of Carbapenem-Resistant Enterobacteriaceae (CPE) into Dutch Livestock Farms," Antibiotics, 2022, 11(2), p. 281, DOI: 10.3390/antibiotics11020281.

[9] Antimicrobial Resistance: CDC's Antibiotic Resistance Threats in the United States, 2019. Available online:https://www.cdc.gov/drugresistance/pdf/threatsreport/2019-ar-threats-report-508.pdf (Accessed:06-September-2022).

[10] Mills, M. C., and Lee, J., "The Threat of Carbapenem-Resistant Bacteria in the Environment: Evidence of Widespread Contamination of Reservoirs at a Global Scale," Environ. Pollut., 2019, 255, p. 113143, DOI: 10.1016/j.envpol.2019.113143.

[11] Bonardi, S., and Pitino, R., "Carbapenemase-Producing Bacteria in Food-Producing Animals, Wildlife and Environment: A Challenge for Human Health," Ital. J. Food Saf., 2019, 8(2), DOI: 10.4081/ijfs.2019.7956.

[12] Köck, R., Daniels-Haardt, I., Becker, K., Mellmann, A., Friedrich, A. W., Mevius, D., Schwarz, S., and Jurke, A., "Carbapenem-Resistant Enterobacteriaceae in Wildlife, Food-

Producing, and Companion Animals: A Systematic Review," Clin. Microbiol. Infect., 2018, 24(12), pp. 1241–1250, DOI: 10.1016/j.cmi.2018.04.004.

[13] Woodford, N., Wareham, D. W., Guerra, B., and Teale, C., "Carbapenemase-Producing Enterobacteriaceae and Non-Enterobacteriaceae from Animals and the Environment: An Emerging Public Health Risk of Our Own Making?," J. Antimicrob. Chemother., 2014, 69(2), pp. 287–291, DOI: 10.1093/jac/dkt392.

[14] Guerra, B., Fischer, J., and Helmuth, R., "An Emerging Public Health Problem: Acquired Carbapenemase-Producing Microorganisms Are Present in Food-Producing Animals, Their Environment, Companion Animals and Wild Birds," Vet. Microbiol., 2014, 171(3–4), pp. 290–297, DOI: 10.1016/j.vetmic.2014.02.001.

[15] Capozzi, C., Maurici, M., and Panà, A., "[Antimicrobial Resistance: It Is a Global Crisis, 'a Slow Tsunami']," Ig. Sanita Pubbl., 2019, 75(6), p. 429—450.

[16] Queenan, A. M., and Bush, K., "Carbapenemases: The Versatile β-Lactamases," Clin. Microbiol. Rev., 2007, 20(3), pp. 440–458, DOI: 10.1128/CMR.00001-07.

[17] FDA, "The National Antimicrobial Resistance Monitoring System, NARMS," FDA, 2023, [Online]. Available: https://www.fda.gov/animal-veterinary/antimicrobial-resistance/national-antimicrobial-resistance-monitoring-system.

[18] CDC, "Antimicrobial Resistance;Tracking Antibiotic Resistance," CDC (Centers Dis. Control Prev. Dis. Control Prev., 2021, [Online]. Available: https://www.cdc.gov/drugresistance/tracking.html. [Accessed: 05-May-2022].

[19] ECDC: EARS-Net, "Annual Report of The European Antimicrobial Resistance Surveillance Network (EARS-Net)," Surveill. Report; ECDC, 2017, [Online]. Available: https://www.ecdc.europa.eu/en/publications-data/surveillance-antimicrobial-resistance-europe-2017.

[20] Smith, H. Z., and Kendall, B., "Carbapenem Resistant Enterobacteriaceae," StatPearls [Internet]. StatPearls Publ., 2021.

[21] Decousser, J.-W., Poirel, L., and Nordmann, P., "Recent Advances in Biochemical and Molecular Diagnostics for the Rapid Detection of Antibiotic-Resistant Enterobacteriaceae : A Focus on ß-Lactam Resistance," Expert Rev. Mol. Diagn., 2017, 17(4), pp. 327–350, DOI: 10.1080/14737159.2017.1289087.

[22] Reynoso, E. C., Laschi, S., Palchetti, I., and Torres, E., "Advances in Antimicrobial Resistance Monitoring Using Sensors and Biosensors: A Review," Chemosensors, 2021, 9(8), DOI: 10.3390/chemosensors9080232.

[23] Li, Z., Ma, J., Ruan, J., and Zhuang, X., "Using Positively Charged Magnetic Nanoparticles to Capture Bacteria at Ultralow Concentration," Nanoscale Res. Lett., 2019, 14, DOI: 10.1186/s11671-019-3005-z.

[24] Kearns, H., Goodacre, R., Jamieson, L. E., Graham, D., and Faulds, K., "SERS Detection of Multiple Antimicrobial-Resistant Pathogens Using Nanosensors," Anal. Chem., 2017, 89(23), pp. 12666–12673, DOI: 10.1021/acs.analchem.7b02653.

[25] Nemr, C. R., Smith, S. J., Liu, W., Mepham, A. H., Mohamadi, R. M., Labib, M., and Kelley, S. O., "Nanoparticle-Mediated Capture and Electrochemical Detection of Methicillin-Resistant Staphylococcus Aureus," Anal. Chem., 2019, DOI: 10.1021/acs.analchem.8b04792.

[26] Wang, J., Yang, W., Peng, Q., Han, D., Kong, L., Fan, L., Zhao, M., and Ding, S., "Rapid Detection of Carbapenem-Resistant Enterobacteriaceae Using PH Response Based on Vancomycin-Modified Fe3O4@Au Nanoparticle Enrichment and the Carbapenemase Hydrolysis Reaction," Anal. Methods, 2019, 12(1), pp. 104–111, DOI: 10.1039/c9ay02196e.

[27] Suh, S. H., Jaykus, L. A., and Brehm-Stecher, B., *Advances in Separation and Concentration of Microorganisms from Food Samples*, Woodhead Publishing Limited, 2013, DOI: 10.1533/9780857098740.3.173.

[28] Dester, E., and Alocilja, E., "Current Methods for Extraction and Concentration of Foodborne Bacteria with Glycan-Coated Magnetic Nanoparticles: A Review," Biosensors, 2022, 12(2), p. 112, DOI: 10.3390/bios12020112.

[29] Pitt, W. G., Alizadeh, M., Husseini, G. A., McClellan, D. S., Buchanan, C. M., Bledsoe, C. G., Robison, R. A., Blanco, R., Roeder, B. L., Melville, M., and Hunter, A. K., "Rapid Separation of Bacteria from Blood-Review and Outlook," Biotechnol. Prog., 2016, 32(4), pp. 823–839, DOI: 10.1002/btpr.2299.

[30] Benoit, P. W., and Donahue, D. W., "Methods for Rapid Separation and Concentration of Bacteria in Food That Bypass Time-Consuming Cultural Enrichment," J. Food Prot., 2003, 66(10), pp. 1935–1948, DOI: 10.4315/0362-028X-66.10.1935.

[31] Agoston, R., Soni, K. A., McElhany, K., Cepeda, M. L., Zuckerman, U., Tzipori, S., ... & Pillai, S. D., "Rapid Concentration of Bacillus and Clostridium Spores from Large Volumes of Milk, Using Continuous Flow Centrifugation," J. Food Prot., 2009, 72(3), pp. 666–668, DOI: 10.4315/0362-028X-72.3.666.

[32] Fukushima, H., Katsube, K., Hata, Y., Kishi, R., and Fujiwara, S., "Rapid Separation and Concentration of Food-Borne Pathogens in Food Samples Prior to Quantification by Viable-Cell Counting and Real-Time PCR," Appl. Environ. Microbiol., 2007, 73(1), pp. 92–100, DOI: 10.1128/AEM.01772-06.

[33] Kumar, N., Wang, W., Ortiz-Marquez, J. C., Catalano, M., Gray, M., Biglari, N., Hikari, K., Ling, X., Gao, J., van Opijnen, T., and Burch, K. S., "Dielectrophoresis Assisted Rapid, Selective and Single Cell Detection of Antibiotic Resistant Bacteria with G-FETs," Biosens. Bioelectron., 2020, 156, p. 112123, DOI: 10.1016/j.bios.2020.112123.

[34] Chung, C.-C., Cheng, I.-F., Chen, H.-M., Kan, H.-C., Yang, W.-H., and Chang, H.-C.,

"Screening of Antibiotic Susceptibility to β-Lactam-Induced Elongation of Gram-Negative Bacteria Based on Dielectrophoresis," Anal. Chem., 2012, 84(7), pp. 3347–3354, DOI: 10.1021/ac300093w.

[35] Bohara, R. A., and Pawar, S. H., "Innovative Developments in Bacterial Detection with Magnetic Nanoparticles," Appl. Biochem. Biotechnol., 2015, 176(4), pp. 1044–1058, DOI: 10.1007/s12010-015-1628-9.

[36] Krishna, V. D., Wu, K., Su, D., Cheeran, M. C. J., Wang, J. P., and Perez, A., "Nanotechnology: Review of Concepts and Potential Application of Sensing Platforms in Food Safety," Food Microbiol., 2018, 75, pp. 47–54, DOI: 10.1016/j.fm.2018.01.025.

[37] Lv, M., Liu, Y., Geng, J., Kou, X., Xin, Z., and Yang, D., "Engineering Nanomaterials-Based Biosensors for Food Safety Detection," Biosens. Bioelectron., 2018, 106(January), pp. 122–128, DOI: 10.1016/j.bios.2018.01.049.

[38] Gu, H., Ho, P. L., Tsang, K. W. T., Yu, C. W., and Xu, B., "Using Biofunctional Magnetic Nanoparticles to Capture Gram-Negative Bacteria at an Ultra-Low Concentration," Chem. Commun., 2003, 3(14), pp. 1758–1759, DOI: 10.1039/b305421g.

[39] Mohammed, L., Gomaa, H. G., Ragab, D., and Zhu, J., "Magnetic Nanoparticles for Environmental and Biomedical Applications: A Review," Particuology, 2017, 30, pp. 1–14, DOI: 10.1016/j.partic.2016.06.001.

[40] Xu, M., Wang, R., and Li, Y., "Rapid Detection of Escherichia Coli O157:H7 and Salmonella Typhimurium in Foods Using an Electrochemical Immunosensor Based on Screen-Printed Interdigitated Microelectrode and Immunomagnetic Separation," Talanta, 2016, 148, pp. 200–208, DOI: 10.1016/j.talanta.2015.10.082.

[41] Lai, H., Xu, F., and Wang, L., "A Review of the Preparation and Application of Magnetic Nanoparticles for Surface-Enhanced Raman Scattering," J. Mater. Sci., 2018, 53(12), pp. 8677–8698, DOI: 10.1007/s10853-018-2095-9.

[42] Wang, K., Li, S., Petersen, M., Wang, S., and Lu, X., "Detection and Characterization of Antibiotic-Resistant Bacteria Using Surface-Enhanced Raman Spectroscopy," Nanomaterials, 2018, 8(10), DOI: 10.3390/nano8100762.

[43] Chen, J., and Park, B., "Effect of Immunomagnetic Bead Size on Recovery of Foodborne Pathogenic Bacteria," Int. J. Food Microbiol., 2018, 267(July 2017), pp. 1–8, DOI: 10.1016/j.ijfoodmicro.2017.11.022.

[44] Quintela, I. A., De Los Reyes, B. G., Lin, C. S., and Wu, V. C. H., "Simultaneous Colorimetric Detection of a Variety of Salmonella Spp. In Food and Environmental Samples by Optical Biosensing Using Oligonucleotide-Gold Nanoparticles," Front. Microbiol., 2019, 10(MAY), pp. 1–12, DOI: 10.3389/fmicb.2019.01138.

[45] Sutherland, J. B., Rafii, F., Lay, J. O., and Williams, A. J., "Rapid Analytical Methods to Identify Antibiotic-Resistant Bacteria," *Antibiotic Drug Resistance*, Wiley, September 9,

2019, pp. 533–566, DOI: 10.1002/9781119282549.ch21.

[46] Wu, S., and Hulme, J. P., “Recent Advances in the Detection of Antibiotic and Multi-Drug Resistant Salmonella: An Update,” Int. J. Mol. Sci., 2021, 22(7), DOI: 10.3390/ijms22073499.

[47] Wareham, D. W., Shah, R., Betts, J. W., Phee, L. M., and Momin, M. H. F. A., “Evaluation of an Immunochromatographic Lateral Flow Assay (OXA-48 K -SeT) for Rapid Detection of OXA-48-Like Carbapenemases in Enterobacteriaceae,” J. Clin. Microbiol., 2016, 54(2), pp. 471–473, DOI: 10.1128/JCM.02900-15.

[48] Guntupalli, R., Sorokulova, I., Olsen, E., Globa, L., Pustovyy, O., and Vodyanoy, V., “Biosensor for Detection of Antibiotic Resistant Staphylococcus Bacteria.,” J. Vis. Exp., 2013, (75), pp. 1–11, DOI: 10.3791/50474.

[49] Tawil, N., Mouawad, F., Lévesque, S., Sacher, E., Mandeville, R., and Meunier, M., “The Differential Detection of Methicillin-Resistant, Methicillin-Susceptible and Borderline Oxacillin-Resistant Staphylococcus Aureus by Surface Plasmon Resonance,” Biosens. Bioelectron., 2013, 49, pp. 334–340, DOI: 10.1016/j.bios.2013.05.031.

[50] Wang, Z., Wang, D., Kinchla, A. J., Sela, D. A., and Nugen, S. R., “Rapid Screening of Waterborne Pathogens Using Phage-Mediated Separation Coupled with Real-Time PCR Detection,” Anal. Bioanal. Chem., 2016, 408(15), pp. 4169–4178, DOI: 10.1007/s00216-016-9511-2.

[51] Kretzer, J. W., Schmelcher, M., and Loessner, M. J., “Ultrasensitive and Fast Diagnostics of Viable Listeria Cells by CBD Magnetic Separation Combined with A511::LuxAB Detection,” Viruses, 2018, 10(11), DOI: 10.3390/v10110626.

[52] Bayat, F., Didar, T. F., and Hosseinidoust, Z., “Emerging Investigator Series: Bacteriophages as Nano Engineering Tools for Quality Monitoring and Pathogen Detection in Water and Wastewater,” Environ. Sci. Nano, 2021, 8(2), pp. 367–389, DOI: 10.1039/d0en00962h.

[53] “Gu et Al_2003_Using Biofunctional Magnetic Nanoparticles to Capture Vancomycin-Resistant Enterococci and Other Gram-Positive Bacteria at Ultralow Concentration.Pdf.”

[54] Dwivedi, H. P., and Jaykus, L.-A., “Detection of Pathogens in Foods: The Current State-of-the-Art and Future Directions,” Crit. Rev. Microbiol., 2011, 37(1), pp. 40–63, DOI: 10.3109/1040841X.2010.506430.

[55] Zheng, Q., Liu, H., and Zhu, J., “Amine-Functionalized Fe3O4 Magnetic Nanoparticles for Rapid Capture and Removal of Bacterial Pathogens,” J. Chinese Inst. Food Sci. Technol., 2014, 14(6), pp. 200–207.

[56] Fratila, R. M., Moros, M., and de la Fuente, J. M., “Recent Advances in Biosensing Using Magnetic Glyconanoparticles,” Anal. Bioanal. Chem., 2016, 408(7), pp. 1783–1803, DOI: 10.1007/s00216-015-8953-2.

[57] Matta, L. L., and Alocilja, E. C., “Carbohydrate Ligands on Magnetic Nanoparticles for Centrifuge-Free Extraction of Pathogenic Contaminants in Pasteurized Milk,” J. Food Prot., 2018, 81(12), pp. 1941–1949, DOI: 10.4315/0362-028X.JFP-18-040.

[58] Matta, L. L., Harrison, J., Deol, G. S., and Alocilja, E. C., “Carbohydrate-Functionalized Nanobiosensor for Rapid Extraction of Pathogenic Bacteria Directly from Complex Liquids with Quick Detection Using Cyclic Voltammetry,” IEEE Trans. Nanotechnol., 2018, 17(5), pp. 1006–1013, DOI: 10.1109/TNANO.2018.2841320.

[59] Dester, E. F., “Extraction, Concentration, and Detection of Foodborne Pathogens Using Glycan-Coated Magnetic Nanoparticles and a Gold Nanoparticle Colorimetric Biosensor,” Michigan State University.

[60] Boodoo, C., Dester, E., Sharief, S. A., and Alocilja, E. C., “Influence of Biological and Environmental Factors in the Extraction and Concentration of Foodborne Pathogens Using Glycan-Coated Magnetic Nanoparticles,” J. Food Prot., 2023, 86(4), p. 100066, DOI: 10.1016/j.jfp.2023.100066.

[61] Morrison, B. J., and Rubin, J. E., “Carbapenemase Producing Bacteria in the Food Supply Escaping Detection,” PLoS One, 2015, 10(5), DOI: 10.1371/journal.pone.0126717.

[62] Yao, X., Doi, Y., Zeng, L., Lv, L., and Liu, J.-H., “Carbapenem-Resistant and Colistin-Resistant Escherichia Coli Co-Producing NDM-9 and MCR-1,” Lancet Infect. Dis., 2016, 16(3), pp. 288–289, DOI: 10.1016/S1473-3099(16)00057-8.

[63] Nair, D. V. T., Venkitanarayanan, K., and Johny, A. K., “Antibiotic-Resistant Salmonella in the Food Supply and the Potential Role of Antibiotic Alternatives for Control,” Foods, 2018, 7(10), DOI: 10.3390/foods7100167.

[64] Hamza, D., Dorgham, S., Ismael, E., El-Moez, S. I. A., Elhariri, M., Elhelw, R., and Hamza, E., “Emergence of β-Lactamase- and Carbapenemase- Producing Enterobacteriaceae at Integrated Fish Farms,” Antimicrob. Resist. Infect. Control, 2020, 9(1), p. 67, DOI: 10.1186/s13756-020-00736-3.

[65] Bhusal, N., Shrestha, S., Pote, N., and Alocilja, E., “Nanoparticle-Based Biosensing of Tuberculosis, an Affordable and Practical Alternative to Current Methods,” Biosensors, 2018, 9(1), p. 1, DOI: 10.3390/bios9010001.

[66] Mahmoudi, M., Sant, S., Wang, B., Laurent, S., and Sen, T., “Superparamagnetic Iron Oxide Nanoparticles (SPIONs): Development, Surface Modification and Applications in Chemotherapy,” Adv. Drug Deliv. Rev., 2011, 63(1–2), pp. 24–46, DOI: 10.1016/j.addr.2010.05.006.

[67] Matta, L. L., and Alocilja, E. C., “Emerging Nano-Biosensing with Suspended MNP Microbial Extraction and EANP Labeling,” Biosens. Bioelectron., 2018, 117(July), pp. 781–793, DOI: 10.1016/j.bios.2018.07.007.

[68] Nishino, M., Matsuzaki, I., Musangil, F. Y., Takahashi, Y., Iwahashi, Y., Warigaya, K.,

Kinoshita, Y., Kojima, F., and Murata, S., “Measurement and Visualization of Cell Membrane Surface Charge in Fixed Cultured Cells Related with Cell Morphology,” PLoS One, 2020, 15(7 July), DOI: 10.1371/journal.pone.0236373.

[69] Pajerski, W., Ochonska, D., Brzychczy-Wloch, M., Indyka, P., Jarosz, M., Golda-Cepa, M., Sojka, Z., and Kotarba, A., “Attachment Efficiency of Gold Nanoparticles by Gram-Positive and Gram-Negative Bacterial Strains Governed by Surface Charges,” J. Nanoparticle Res., 2019, 21(8), DOI: 10.1007/s11051-019-4617-z.

[70] Soon, R. L., Nation, R. L., Cockram, S., Moffatt, J. H., Harper, M., Adler, B., Boyce, J. D., Larson, I., and Li, J., “Different Surface Charge of Colistin-Susceptible and -Resistant Acinetobacter Baumannii Cells Measured with Zeta Potential as a Function of Growth Phase and Colistin Treatment,” J. Antimicrob. Chemother., 2011, 66(1), pp. 126–133, DOI: 10.1093/jac/dkq422.

[71] Li, J., Wang, C., Shi, L., Shao, L., Fu, P., Wang, K., Xiao, R., Wang, S., and Gu, B., “Rapid Identification and Antibiotic Susceptibility Test of Pathogens in Blood Based on Magnetic Separation and Surface-Enhanced Raman Scattering,” Microchim. Acta, 2019, 186(7), p. 475, DOI: 10.1007/s00604-019-3571-x.

[72] Yang, D. C., Blair, K. M., and Salama, N. R., “Staying in Shape: The Impact of Cell Shape on Bacterial Survival in Diverse Environments,” Microbiol. Mol. Biol. Rev., 2016, 80(1), pp. 187–203.

[73] Wilson, W. W., Wade, M. M., Holman, S. C., and Champlin, F. R., “Status of Methods for Assessing Bacterial Cell Surface Charge Properties Based on Zeta Potential Measurements,” J. Microbiol. Methods, 2001, 43(3), pp. 153–164, DOI: 10.1016/S0167-7012(00)00224-4.

[74] Ferreyra Maillard, A. P. V., Espeche, J. C., Maturana, P., Cutro, A. C., and Hollmann, A., “Zeta Potential beyond Materials Science: Applications to Bacterial Systems and to the Development of Novel Antimicrobials,” Biochim. Biophys. Acta - Biomembr., 2021, 1863(6), p. 183597, DOI: 10.1016/j.bbamem.2021.183597.

[75] Frank, J. F., “Microbial Attachment to Food and Food Conctact Surfaces,” *Advances Innnnnnn Food and Nutrition Research Vol 43*, Academic press, 2001, ISBN: 0-12-016443-4.

[76] Wilson, J. W., Schurr, M. J., LeBlanc, C. L., Ramamurthy, R., Buchanan, K. L., and Nickerson, C. A., “Mechanisms of Bacterial Pathogenicity,” Postgrad. Med. J., 2002, 78(918), pp. 216–224, DOI: 10.1136/pmj.78.918.216.

[77] Li, B., Zhao, Y., Liu, C., Chen, Z., and Zhou, D., “Molecular Pathogenesis of Klebsiella Pneumoniae Molecular Pathogenesis of Klebsiella Pneumoniae,” 2016, 9(SEPTEMBER 2014), pp. 1071–1081.

[78] Rizi, K. S., Ghazvini, K., and Farsiani, H., “Clinical and Pathogenesis Overview of Enterobacter Infections,” Rev. Clin. Med., 2020, 6(4), pp. 146–154, DOI:

10.22038/RCM.2020.44468.1296.

[79] Galvan, D. D., and Yu, Q., “Surface-Enhanced Raman Scattering for Rapid Detection and Characterization of Antibiotic-Resistant Bacteria,” Adv. Healthc. Mater., 2018, 7(13), pp. 1–27, DOI: 10.1002/adhm.201701335.

[80] Cushnie, T. P. T., O’Driscoll, N. H., and Lamb, A. J., “Morphological and Ultrastructural Changes in Bacterial Cells as an Indicator of Antibacterial Mechanism of Action,” Cell. Mol. Life Sci., 2016, 73(23), pp. 4471–4492, DOI: 10.1007/s00018-016-2302-2.

[81] Hughes, D., and Andersson, D. I., “Environmental and Genetic Modulation of the Phenotypic Expression of Antibiotic Resistance,” FEMS Microbiol. Rev., 2017, 41(3), pp. 374–391.

[82] Briceno, R. K., Sergent, S. R., Benites, S. M., and Alocilja, E. C., “Nanoparticle-Based Biosensing Assay for Universally Accessible Low-Cost Tb Detection with Comparable Sensitivity as Culture,” Diagnostics, 2019, 9(4), DOI: 10.3390/diagnostics9040222.

[83] Young, K. D., “Bacterial Morphology: Why Have Different Shapes?,” Curr. Opin. Microbiol., 2007, 10(6), pp. 596–600.

[84] El-Boubbou, K., Gruden, C., and Huang, X., “Magnetic Glyco-Nanoparticles: A Unique Tool for Rapid Pathogen Detection, Decontamination, and Strain Differentiation,” J. Am. Chem. Soc., 2007, 129(44), pp. 13392–13393, DOI: 10.1021/ja076086e.

[85] Sauer, M. M., Jakob, R. P., Eras, J., Baday, S., Eriş, D., Navarra, G., Bernèche, S., Ernst, B., Maier, T., and Glockshuber, R., “Catch-Bond Mechanism of the Bacterial Adhesin FimH,” Nat. Commun., 2016, 7(1), p. 10738, DOI: 10.1038/ncomms10738.

[86] SAFINA, G., VANLIER, M., and DANIELSSON, B., “Flow-Injection Assay of the Pathogenic Bacteria Using Lectin-Based Quartz Crystal Microbalance Biosensor,” Talanta, 2008, 77(2), pp. 468–472, DOI: 10.1016/j.talanta.2008.03.033.

[87] Mi, F., Guan, M., Hu, C., Peng, F., Sun, S., and Wang, X., “Application of Lectin-Based Biosensor Technology in the Detection of Foodborne Pathogenic Bacteria: A Review,” Analyst, 2021, 146(2), pp. 429–443, DOI: 10.1039/D0AN01459A.

[88] Capita, R., Riesco-Peláez, F., Alonso-Hernando, A., and Alonso-Calleja, C., “Exposure of Escherichia Coli ATCC 12806 to Sublethal Concentrations of Food-Grade Biocides Influences Its Ability to Form Biofilm, Resistance to Antimicrobials, and Ultrastructure,” Appl. Environ. Microbiol., 2014, 80(4), pp. 1268–1280, DOI: 10.1128/AEM.02283-13.

[89] Lorian, V., “Low Concentrations of Antibiotics,” J. Antimicrob. Chemother., 1985, 15(SUPPL. A), pp. 15–26, DOI: 10.1093/jac/15.suppl_a.15.

[90] O’Driscoll, N. H., Cushnie, T. P. T., Matthews, K. H., and Lamb, A. J., “Colistin Causes Profound Morphological Alteration but Minimal Cytoplasmic Membrane Perforation in Populations of Escherichia Coli and Pseudomonas Aeruginosa,” Arch. Microbiol., 2018,

200(5), pp. 793–802, DOI: 10.1007/s00203-018-1485-3.

[91] Furchtgott, L., Wingreen, N. S., and Huang, K. C., “Mechanisms for Maintaining Cell Shape in Rod-shaped Gram-negative Bacteria,” Mol. Microbiol., 2011, 81(2), pp. 340–353.

[92] Chang, T.-W., and Weinstein, L., “Morphological Changes in Gram-Negative Bacilli Exposed to Cephalothin,” J. Bacteriol., 1964, 88(6), pp. 1790–1797.

[93] Domingues, M. M., Silva, P. M., Franquelim, H. G., Carvalho, F. A., Castanho, M. A. R. B., and Santos, N. C., “Antimicrobial Protein RBPI21-Induced Surface Changes on Gram-Negative and Gram-Positive Bacteria,” Nanomedicine Nanotechnology, Biol. Med., 2014, 10(3), pp. 543–551, DOI: 10.1016/j.nano.2013.11.002.

[94] King, T., Osmond-McLeod, M. J., and Duffy, L. L., “Nanotechnology in the Food Sector and Potential Applications for the Poultry Industry,” Trends Food Sci. Technol., 2018, 72(September 2017), pp. 62–73, DOI: 10.1016/j.tifs.2017.11.015.

[95] Fonseca, A. P., and Sousa, J. C., “Effect of Antibiotic-Induced Morphological Changes on Surface Properties, Motility and Adhesion of Nosocomial Pseudomonas Aeruginosa Strains under Different Physiological States,” J. Appl. Microbiol., 2007, 103(5), pp. 1828–1837, DOI: 10.1111/j.1365-2672.2007.03422.x.

[96] Papp-Wallace, K. M., Endimiani, A., Taracila, M. A., and Bonomo, R. A., “Carbapenems: Past, Present, and Future,” Antimicrob. Agents Chemother., 2011, 55(11), pp. 4943–4960, DOI: 10.1128/AAC.00296-11.

[97] Codjoe, F., and Donkor, E., “Carbapenem Resistance: A Review,” Med. Sci., 2017, 6(1), p. 1, DOI: 10.3390/medsci6010001.

[98] Matta, L. L., “Biosensing Total Bacterial Load in Liquid Matrices to Improve Food Supply Chain Safety Using Carbohydrate-Functionalized Magnetic Nanoparticles for Cell Capture and Gold Nanoparticles for Signaling,” 2018.

[99] Sharief, S. A., Caliskan-Aydogan, O., and Alocilja, E., “Carbohydrate-Coated Magnetic and Gold Nanoparticles for Point-of-Use Food Contamination Testing,” Biosens. Bioelectron. X, 2023, 13(November 2022), p. 100322, DOI: 10.1016/j.biosx.2023.100322.

[100] Sharief, S. A., Caliskan-Aydogan, O., and Alocilja, E. C., “Carbohydrate-Coated Nanoparticles for PCR-Less Genomic Detection of Salmonella from Fresh Produce,” Food Control, 2023, 150(January), p. 109770, DOI: 10.1016/j.foodcont.2023.109770.

[101] Dester, E., Kao, K., and Alocilja, E. C., “Detection of Unamplified E. Coli O157 DNA Extracted from Large Food Samples Using a Gold Nanoparticle Colorimetric Biosensor,” Biosensors, 2022, 12(5), p. 274, DOI: 10.3390/bios12050274.

[102] Tanner, W. D., VanDerslice, J. A., Goel, R. K., Leecaster, M. K., Fisher, M. A., Olstadt, J., Gurley, C. M., Morris, A. G., Seely, K. A., Chapman, L., Korando, M., Shabazz, K.-A.,

Stadsholt, A., VanDeVelde, J., Braun-Howland, E., Minihane, C., Higgins, P. J., Deras, M., Jaber, O., Jette, D., and Gundlapalli, A. V., "Multi-State Study of Enterobacteriaceae Harboring Extended-Spectrum Beta-Lactamase and Carbapenemase Genes in U.S. Drinking Water," Sci. Rep., 2019, 9(1), p. 3938, DOI: 10.1038/s41598-019-40420-0.

[103] Sugawara, Y., Hagiya, H., Akeda, Y., Aye, M. M., Myo Win, H. P., Sakamoto, N., Shanmugakani, R. K., Takeuchi, D., Nishi, I., Ueda, A., Htun, M. M., Tomono, K., and Hamada, S., "Dissemination of Carbapenemase-Producing Enterobacteriaceae Harbouring BlaNDM or BlaIMI in Local Market Foods of Yangon, Myanmar," Sci. Rep., 2019, 9(1), p. 14455, DOI: 10.1038/s41598-019-51002-5.

[104] Roschanski, N., Guenther, S., Vu, T. T. T., Fischer, J., Semmler, T., Huehn, S., Alter, T., and Roesler, U., "VIM-1 Carbapenemase-Producing Escherichia Coli Isolated from Retail Seafood, Germany 2016," Eurosurveillance, 2017, 22(43), pp. 1–7, DOI: 10.2807/1560-7917.ES.2017.22.43.17-00032.

[105] Wang, J., Yao, X., Luo, J., Lv, L., Zeng, Z., and Liu, J. H., "Emergence of Escherichia Coli Coproducing NDM-1 and KPC-2 Carbapenemases from a Retail Vegetable, China," J. Antimicrob. Chemother., 2018, 73(1), pp. 252–254, DOI: 10.1093/jac/dkx335.

[106] Touati, A., Mairi, A., Baloul, Y., Lalaoui, R., Bakour, S., Thighilt, L., Gharout, A., and Rolain, J.-M., "First Detection of Klebsiella Pneumoniae Producing OXA-48 in Fresh Vegetables from Béjaïa City, Algeria," J. Glob. Antimicrob. Resist., 2017, 9, pp. 17–18, DOI: 10.1016/j.jgar.2017.02.006.

[107] Liu, B.-T., Zhang, X.-Y., Wan, S.-W., Hao, J.-J., Jiang, R.-D., and Song, F.-J., "Characteristics of Carbapenem-Resistant Enterobacteriaceae in Ready-to-Eat Vegetables in China," Front. Microbiol., 2018, 9(JUN), DOI: 10.3389/fmicb.2018.01147.

[108] Chaalal, N., Touati, A., Bakour, S., Aissa, M. A., Sotto, A., Lavigne, J. P., and Pantel, A., "Spread of OXA-48 and NDM-1-Producing Klebsiella Pneumoniae ST48 and ST101 in Chicken Meat in Western Algeria," Microb. Drug Resist., 2021, 27(4), pp. 492–500, DOI: 10.1089/mdr.2019.0419.

[109] Wang, C., Wang, J., Li, M., Qu, X., Zhang, K., Rong, Z., Xiao, R., and Wang, S., "A Rapid SERS Method for Label-Free Bacteria Detection Using Polyethylenimine-Modified Au-Coated Magnetic Microspheres and Au@Ag Nanoparticles," Analyst, 2016, 141(22), pp. 6226–6238, DOI: 10.1039/C6AN01105E.

[110] Yosief, H. O., Weiss, A. A., and Iyer, S. S., "Capture of Uropathogenic E. Coli by Using Synthetic Glycan Ligands Specific for the Pap-Pilus," ChemBioChem, 2013, 14(2), pp. 251–259, DOI: 10.1002/cbic.201200582.

[111] Lim, M.-C., Park, J. Y., Park, K., Ok, G., Jang, H.-J., and Choi, S.-W., "An Automated System for Separation and Concentration of Food-Borne Pathogens Using Immunomagnetic Separation," Food Control, 2017, 73, pp. 1541–1547, DOI: 10.1016/j.foodcont.2016.11.021.

[112] Triplett, O. A., Xuan, J., Foley, S., Nayak, R., and Tolleson, W. H., “Immunomagnetic Capture of Big Six Shiga Toxin–Producing Escherichia Coli Strains in Apple Juice with Detection by Multiplex Real-Time PCR Eliminates Interference from the Food Matrix,” J. Food Prot., 2019, 82(9), pp. 1512–1523, DOI: 10.4315/0362-028X.JFP-19-134.

[113] You, S.-M., Jeong, K.-B., Luo, K., Park, J.-S., Park, J.-W., and Kim, Y.-R., “Paper-Based Colorimetric Detection of Pathogenic Bacteria in Food through Magnetic Separation and Enzyme-Mediated Signal Amplification on Paper Disc,” Anal. Chim. Acta, 2021, 1151, p. 338252, DOI: 10.1016/j.aca.2021.338252.

[114] Quintela, I. A., de los Reyes, B. G., Lin, C.-S., and Wu, V. C. H., “Simultaneous Direct Detection of Shiga-Toxin Producing Escherichia Coli (STEC) Strains by Optical Biosensing with Oligonucleotide-Functionalized Gold Nanoparticles,” Nanoscale, 2015, 7(6), pp. 2417–2426, DOI: 10.1039/C4NR05869K.

[115] Hu, S., Niu, L., Zhao, F., Yan, L., Nong, J., Wang, C., Gao, N., Zhu, X., Wu, L., Bo, T., Wang, H., and Gu, J., “Identification of Acinetobacter Baumannii and Its Carbapenem-Resistant Gene BlaOXA-23-like by Multiple Cross Displacement Amplification Combined with Lateral Flow Biosensor,” Sci. Rep., 2019, 9(1), p. 17888, DOI: 10.1038/s41598-019-54465-8.

[116] Lau, H. K., Clotilde, L. M., Lin, A. P., Hartman, G. L., and Lauzon, C. R., “Comparison of IMS Platforms for Detecting and Recovering Escherichia Coli O157 and Shigella Flexneri in Foods,” SLAS Technol., 2013, 18(2), pp. 178–183, DOI: 10.1177/2211068212468583.

CHAPTER 5: NANOPARTICLE-BASED PLASMONIC BIOSENSOR FOR THE UNAMPLIFIED GENOMIC DETECTION OF CARBAPENEM-RESISTANT BACTERIA

This chapter has been published in *Diagnostics*, 2023 (10.3390/diagnostics13040656).

5.1. Introduction

Infectious disease outbreaks have killed thousands of people with severe negative global economic impacts. Among these, antimicrobial-resistant (AMR) bacteria are a major growing concern [1]. Due to AMR infections, it is estimated that approximately 700,000 people die each year worldwide [2], with 39% of the cases linked to last-resort AMR bacteria [3]. According to a recent estimate, by the year 2050, AMR infections will result in 10 million deaths per year, along with losses worth USD 100 trillion [4].

Carbapenems, a subclass of β-lactam antibiotics, are the last line of defense against severe multi-resistant infections [1,5]. The incidence and spread of carbapenem-resistant bacteria have increased globally at an alarming rate since early 2010 [5]. Subsequently, carbapenem-resistant *Acinentobacter baumannii, Pseudomonas aeruginosa*, and carbapenem-resistant *Enterobacterales* (CRE) have been listed as critical priority pathogens by the World Health Organization (WHO) since 2017 [6] and the Centers for Disease Control and Prevention (CDC) since 2019 [7]. Particularly, CRE results in 1,100 deaths and 13,100 infections in the USA [7], with a significant fraction of these infections potentially resulting in death due to a lack of alternative antibiotic treatments [5,7].

Carbapenem resistance mainly results from carbapenemase production and the porin gene mutation (non-carbapenemase). The presence of carbapenemase is usually sufficient for carbapenem resistance [8]. Production of carbapenemase can occur by mutations or through horizontal gene transfer (HGT) [9,10]. For example, a subset of bacterial cells from susceptible populations can develop spontaneous mutations in genes, allowing them to survive in the presence of antibiotics (carbapenem). These mutations lead to a selection of the genes that alter antibiotic actions through enzyme (carbapenemase) production [10,11], which are commonly transferable. In HGT, these carbapenemase genes are often located on mobile genetic elements, such as integrons, transposons, and plasmids, which contribute to their spread [1,12,13]. This results in carbapenemase-producing (CP) bacteria cases in humans who are not using the

antibiotic or are hospitalized but interact with environments and hosts colonized with CP bacteria [2]. The most common enzymes are *Klebsiella pneumoniae* carbapenemase (KPC), Metallo-β-lactamases (New Delhi Metallo-lactamase (NDM), Imipenemase (IMP), and Verona integron-encoded Metallo-lactamase (VIM), and Oxacillinase-48 (OXA-48). The CDC routinely tests these common carbapenemase types through the Antibiotic Resistance Laboratory Network [14].

In diagnostic protocols, antibiotic susceptibility tests (AST) are widely used in clinical and public health labs to assess antibiotic resistance profiles of target isolates [7]. AST methods usually require overnight culturing in selective media for species identification, followed by further growth in antibiotic solutions for determining their antibiotic-resistant profile [15–18]. Culture-based tests for identification of the CP bacteria include Modified Hodge Test (MHT) [19] and carbapenemase inactivation methods (CIM) [20,21], which are cost-effective and widely applicable. There have also been specific mediums designed for CP strain screening [22,23]. However, these culture-based tests are labor-intensive and require time-consuming steps for the isolation of pure cultures, taking days to weeks for determining their resistant profile [15,16,18].

Several phenotypic techniques have been developed to shorten the required time to detect CP bacteria based on their carbapenemase hydrolysis activity. For example, an ultraviolet (UV) spectrophotometric method has been developed to measure the imipenem hydrolysis activity of CP bacteria [24]. Further, the combination of automation and a user-friendly interface recently made matrix-assisted laser desorption/ionization time-of-flight mass spectrometry (MALDI-TOF MS) popular in clinical labs. This technique identifies bacteria at the species and genus level from single isolated colonies [25]. Bioluminescence-based assays have also been developed for the detection of CP bacteria within 2.5 h [26]. Recently, a colorimetric assay, the Carba NP test and its commercial kits, have been developed for simple and cost-effective detection within 2 h [20,21,25,27]. However, these assays require pure cultures and depend on the growth rate of bacteria [25]. Many of these rapid phenotypic techniques also require expensive and complex equipment, data analysis, and trained personnel, which reduces their applicability in low-resource settings [16–18,28].

Molecular methods have also been developed as effective techniques to detect specific resistant genes. PCR-based methods, DNA microarray and chips, whole genome sequencing (WGS), loop-mediated isothermal amplification (LAMP), and fluorescence in situ hybridization

(FISH) are used as genotypic techniques for the detection of resistance [17,18,28]. Among these, PCR-based approaches have been used as a gold standard for detecting β-lactam (*bla*) resistant genes. For example, multiplex PCR has been developed to detect 11 acquired carbapenemase genes using three different multiplex reaction mixtures [29]. Numerous automated systems have also been designed to detect and confirm the presence of target genes for bacteria and their resistance [21,25], although associated costs limit their use [25]. LAMP has been used as an alternative to PCR, particularly in low-resource settings, due to its simplicity and cost-efficiency. However, it still has limitations such as complex primer design [17,18,30]. Many genotypic methods offer rapid detection with higher sensitivity and specificity, but require costly reagents, equipment, and need skilled operators [16,18].

Biosensors have emerged as an alternative approach for simple, rapid, and low-cost detection. These analytical devices utilize biological or chemical reactions and convert the recognition event into measurable signals to detect target analyte [31,32]. A few biosensor studies have been developed for CP bacteria detection. For instance, a label-free electrochemical biosensor detected PCR amplified bla_{NDM} gene using impedance spectroscopy [33]. Other voltammetry-based techniques have allowed for bla_{KPC} detection in 45 min [34]. Recently, the Surface-Enhanced Raman Scattering technique (SERS) for carbapenem resistance detection has also been developed using silver nanoparticles [35], gold nanostars [36], and gold and silver nanorods [37] with higher specificity and sensitivity. However, these techniques require multivariate data analysis for detection. In another study, a lateral flow biosensor was developed to identify and differentiate $bla_{OXA\text{-}23\text{-}like}$, by multiple cross displacement amplification [38]. Elsewhere, plasmonic nanosensors were developed using GNPs for colorimetric detection of CP pathogens based on carbapenemase activity and pH changes [39]. However, these biosensors are still costly and require complex techniques for signal measurements and data analysis [28]. Colorimetric gold nanoparticle (GNP) biosensors can offer an ideal solution.

The size-dependent chemical, electric, optical, and physical properties of GNPs are their primary advantages [40–42]. In addition, GNPs are chemically stable and can be easily modified for biosensor applications, stimulating their popularity and use in recent years [41–43]. They have unique optical properties; free electrons of GNPs in colloidal solutions induce coherent oscillation once the frequency of light matches with electron frequency, producing a strong SPR band. The SPR band is strongly distance-dependent and transforms depending on monodispersed

or aggregated state of GNPs in a liquid solution, resulting in a visible color change [40–42]. Small monodispersed GNPs have an SPR absorption peak at around 520 nm, with a red color, which shifts to longer wavelength with aggregation of particles leading to color change to blue or purple [43–45]. Compared to other nanoparticles displaying SPR, which are unstable and toxic, GNPs are stable for a long time, making them cost-effective [46]. The colorimetric nature of this platform is noteworthy, offering rapid and simple visual detection in under one hour without complex and costly equipment [44,47,48].

GNPs have been extensively used to detect target DNA from several bacteria. For instance, thiol-capped GNPs were used to detect *Klebsiella pneumoniae* within one hour using amplified *K2A* gene [47] and unamplified DNA of uropathogenic *E.coli* [49]. However, traditional GNP synthesis and probe functionalization techniques can require labor and take several days [48,49]. Rapid synthesis and functionalization of GNPs are preferable, and dextrin-coated GNPs have shown higher stability and biocompatibility [50]. These GNPs have been used earlier to detect unamplified DNA of *E. coli* O157:H7 [44] and *Pseudoperonospora cubensis* [50] within 30 min. However, their application for detecting AMR including CP bacteria has not been documented.

Rapid detection is a significant step to control and prevent the emergence and spread of infections. For instance, the mortality rate of CRE infections rises by approximately 8% for each hour of delay in obtaining a correct diagnosis and suitable antibiotic treatment [51]. The delayed appropriate therapy in CP-CRE increase the risk of mortality from 0.9% to 3.7%, hospital cost from ~USD 10,000 to ~USD 25,000, and hospital stay from 5.1 days to 8.5 days [34,52]. Thus, this study proposes a rapid and simple plasmonic biosensor platform for detecting CP-bacteria, specifically the KPC-producing bacteria. The KPC is the most prevalent enzyme type among CP bacteria in the US and the world [10,53].

5.1.1. Novelty of This Study

The GNP-based plasmonic biosensor was designed to detect KPC-producing bacteria. This assay only requires dextrin-coated GNPs, DNA probes (bla_{KPC}) for target bacteria, and DNA samples. Colorimetric results were quantified using absorbance spectra measurements by UV-Vis spectrophotometer. This study's novelty is in the following aspects: 1) our GNP plasmonic biosensor using DNA probe is the first study in detecting AMR, including CP bacteria, 2) probe-functionalization protocols are not required, and 3) PCR amplification is not

required for detection. Scheme 5.1 briefly describes the generalized procedure of the plasmonic biosensor employed in this study.

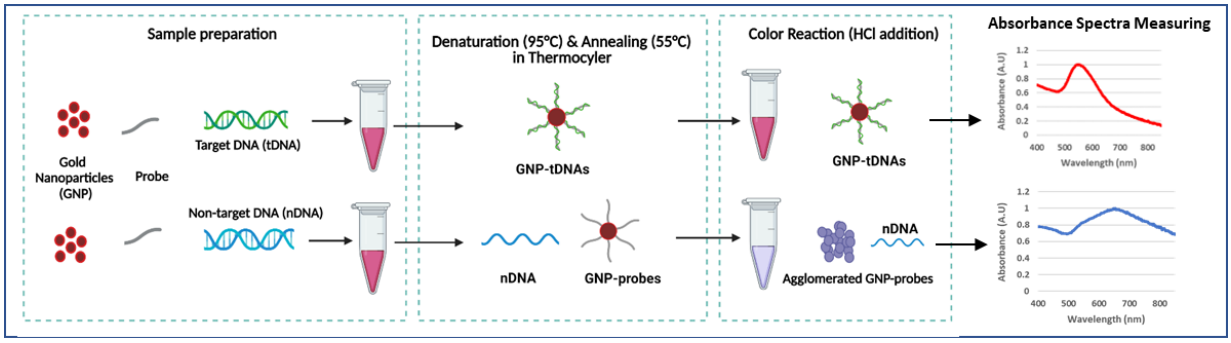

Scheme 5.1**.** Generalized procedure of GNP-based plasmonic biosensor (created with BioRender.com, accessed on December 2022).

5.2. Materials and Methods

5.2.1. Materials

A total of 47 bacterial cultures were used in this study: 3 bacteria from the American Type Culture Collection (ATCC), 38 carbapenemase-producing (CP) bacteria isolates from the Michigan Department of Health and Human Services (MDHHS), and 6 bacteria from Dr. Evangelyn Alocilja's Nano-Biosensors Laboratory at Michigan State University (MSU). DNA extraction kits were purchased from Qiagen (Germantown, MD, USA). NanoDrop One from ThermoFisher Scientific (Waltham, MA, USA) was used to quantify DNA samples and absorption spectra. Oligonucleotide probes were ordered from Integrated DNA Technologies (IDT; Coralville, Iowa). Tryptic Soy Agar (TSA) and Tryptic Soy Broth (TSB), Hydrochloric acid (HCl), gold (III) chloride ($HAuCl_4$), sodium carbonate (Na_2Co_3), 11-mercaptoundecanoic acid (MUDA $HS(CH_2)_{10}CO_2H$), sodium dodecyl sulfate (SDS, $C_{12}H_{25}NaO_4S$), dextrin from potato starch were purchased from Sigma Aldrich (St. Louis, MO, USA).

5.2.2. Bacterial Cultures

Bacterial strains of *E. coli* C-3000 (15597), KPC-producing carbapenem-resistant *E. coli* (BAA-2340), and *Klebsiella pneumoniae* subsp. *pneumoniae* (13883) were obtained from ATCC. Frozen cultures of *Salmonella enterica* serovar Typhimurium, *Salmonella enterica* serovar Enteritidis, *Klebsiella pneumoniae*, and *Enterobacter cloacae*, and carbapenem-resistant *Klebsiella pneumoniae* were obtained from MSU. The CP bacteria isolates from MDHHS included 12 KPC-producing bacteria: *E. coli* (2), *E. cloacae* (1), *K. pneumoniae* (3), *K.*

aerogenes (2), *Raultella ornithinolytica* (2), *Citrobacter amalonaticus* (1), *Citrobacter freundii* (1), and 26 non-KPC (IMP, NDM, OXA-48, VIM)-producing bacteria: *E. coli* (5), *K. pneumoniae* (4), *E. cloacae* (7), *K. oxytoca* (1), *C. freundii* (2), *Providencia rettgeri* (2), *Proteus mirabilis* (2), *Morganella morganii* (2), and *P. aeruginosa* (1). Carbapenem-resistant bacteria isolates from MDHHS were verified by molecular (CARBA-R Cepheid assay and CDC laboratory-developed assay) and growth-based AST methods.

Stock cultures of all isolates were stored at −80 °C. The cultures were refreshed by plating on TSA and incubated at 37 °C for 24–48 h. A single colony of the fresh bacterial cultures on TSA was then transferred into 9 mL of TSB with an overnight incubation at 37 °C before the experiment. The susceptible profile of *E. coli* C-3000, *S.* Typhimurium, *S.* Enteritidis, *E. cloacae*, *K. pneumoniae*, and *K. aerogenes* were confirmed using agar-dilution test (AST) [54].

5.2.3. DNA Extraction

The DNA of the pure bacteria cultures after overnight incubation was extracted using the commercial kit, which removes any interfering materials and was finally suspended in elution buffer (pH 8). The DNA concentration and quality were measured with the NanoDrop. DNA samples with acceptable A_{260}/A_{280} and A_{260}/A_{230} ratios, between 1.8 and 2.2, were used for the designed biosensor assay.

5.2.4. Probe Design and PCR Confirmation

A single-stranded oligonucleotide primer and probe were designed to target specifically KPC-producing bacteria. The primers and probe were designed using the bla_{KPC} gene sequence of carbapenem-resistant *E. coli* (ATCC-2340), utilizing the design tools from NCBI BLAST (National Center for Biotechnology Information Basic Location Alignment Search Tool). Here, E-values were checked to indicate that the gene sequence is specific. The following aminated probe was used: 5′ CGG TGT GTA CGC GAT GGA TAC CGG CTC AGG CGC AAC TGT AAG TTA CCG CGC TGA GGA GCG. The following PCR primer sequence was used: F- 5′ CGGTGTGTACGCGATGGATA and R- 5′ TCCGGTTTTGTCTCCGACTG. The absence and presence of the bla_{KPC} gene in all samples were confirmed by PCR; the protocol was adapted from an earlier study [29]. Amplified products were run on a 2% agarose gel in Tris Acetate EDTA (TAE) buffer at an applied voltage of 120 V for 1 h.

5.2.5. GNP Synthesis and Surface Modification

Dextrin-coated gold nanoparticles (GNPs) were synthesized using the alkaline synthesis method according to the procedure developed previously [55]. Briefly, gold (III) chloride trihydrate was dissolved in water and neutralized with sodium carbonate. Then, dextrin was added and heated at 150 °C under continuous stirring conditions until the solution turned wine red. The synthesis of GNPs was then confirmed by determining their absorption maxima using the NanoDrop at around 520 nm (red color). The GNPs were modified with 25 µM mercaptoundecanoic acid (MUDA) and suspended in 0.1 M borate buffer. As the MUDA-coated GNPs have -COOH groups, they create non-covalent interactions with amine groups on the aminated probe, leading to almost instantaneous GNP-probe functionalization. Batches of the surface-modified, ready-to-use GNPs were stored at 4 °C until further use. Since the GNPs are stable for a long time, new synthesis is not required for everyday analysis.

5.2.6. Biosensor Design and Optimization

The GNP-based plasmonic biosensor assay was developed with the following procedure [44]. Each biosensor trial included the extracted DNA sample (10 µL), 25 µM DNA probe (5 µL), and surface-modified GNPs (5 µL) in a single tube. Samples were then placed in a thermocycler to allow denaturation at 95 °C for 5 min, annealing at 55 °C for 10 min, and cooling to room temperature. This cycle enables target DNA to hybridize with the probe-GNP. Next, 0.1 M HCl was added to the sample, inducing GNP aggregation by distributing the electrostatic repulsion from the GNPs. However, target DNA bound to the GNP-probe prevents GNPs from aggregation. Thus, samples with target DNA remained red, while non-target samples allowed GNP aggregation, resulting in color change (purple or blue). The visual change in color of the GNPs was quantified by measuring their absorbance spectra in the wavelength range of 400–800 nm. Target samples were expected to have maximum absorbance at ~520 nm, while blue/purple samples shifted right, with higher absorption maxima. Quantification of the GNP aggregation was determined using absorbance ratios at 625 nm and 520 nm ($A_{625/520}$), which is based on an earlier reported study [50].

The GNP biosensor optimization variables included the amount of HCl (5–10 µL) and the response time between HCl addition and reading the colorimetric results (5–10 min). The optimum HCl amount and aggregation time were determined through qualitative and quantitative

analysis. Different amounts of 0.1 M HCl (5–10 µL) were separately added to the negative control (nuclease-free water), positive sample (10 ng/µL of KPC-producing *E. coli* BAA-2340), and negative sample (10 ng/µL of *E. coli* C-3000). Tubes were incubated until aggregation of negative samples without aggregation of the positive sample, which was visually observable. Absorbance spectra readings were taken at 5 min intervals after HCL addition. Readings were statistically analyzed at a 95% confidence interval; the optimized procedure had a significant and consistent difference between positive and negative samples, with a visible color change.

5.2.7. Limit of Detection Testing (Analytical Sensitivity)

The analytical sensitivity test was conducted at different DNA concentrations to determine the minimum detectable concentration of DNA. In this test, target and non-target DNA samples were serially diluted to lower concentrations, ranging from 20 to 1 ng/µL. Then, the target DNA sample (KPC-producing *E. coli* (BAA-2340)) was compared with a non-target sample (*E. coli* C-3000) at the same concentrations with a series of nine trials. Their visual color change and absorbance spectra measurements were used to determine the difference in GNP aggregations between the two samples. The $A_{625/520}$ values were statistically analyzed at a 95% confidence interval.

5.2.8. Diagnostic Sensitivity and Specificity Testing

The biosensor was tested with a total of 47 DNA samples: 14 KPC-producing bacteria (target DNA) and 33 non-KPC-producing bacteria (non-target DNA), as listed in Table 5.1. A DNA concentration of 10 ng/µL was used for all samples with a series of nine trials. Each specificity trial included a negative control (DNA-free), target, and non-target samples. Their absorbance spectra measurements and images were collected during the experiment. Differences in $A_{625/520}$ values among target and non-target samples were statistically analyzed at a 95% confidence interval.

The diagnostic sensitivity and specificity of this assay were calculated as described in an earlier study [56]. The sensitivity is the proportion of positive tests (True positive/(True positive + False negative)), and specificity is the proportion of negative tests (True negative/(True negative + False positive)).

Table 5.1. Bacterial isolates tested for specificity test.

Positive (Target) Samples (KPC-Producing Resistant Bacteria)	Non-Target Samples	
	Non-KPC (IMP, NDM, OXA-48, VIM)-Producing Resistant Bacteria	Non-Resistant Bacteria (Susceptible)
E. coli (3)	*E. coli* (5)	*E. coli* C-3000 (1)
K. pneumoniae (4)	*K. pneumoniae* (4)	*K. pneumoniae* (2)
E. cloacae (1)	*E. cloacae* (7)	*E. cloacae* (1)
K. aerogenes (2)	*K. oxytoca* (1)	*K. aerogenes* (1)
C. freundii (1)	*C. freundii* (2)	*Salmonella* (2)
C. amalonaticus (1)	*P. rettgeri* (2)	
R. ornithinolytica (2)	*P. mirabilis* (2)	
	M. morganii (2)	
	P. aeruginosa (1)	

5.2.9. Statistical Analysis

Data were presented with averages and standard deviations in bar graphs. The $A_{625/520}$ values were compared among target and non-target samples using one-way analysis of variance (ANOVA) followed by Tukey's HSD (honestly significant difference) test at a 95% confidence interval.

5.3. Results and Discussion

5.3.1. Characterization of GNPs and Principle of the GNP-Based Plasmonic Biosensor

Dextrin-coated GNPs used in the study were synthesized using an alkaline synthesis route. Successful GNP synthesis was confirmed by their wine-red appearance and a peak of maximum absorbance at ~520 nm, as seen in Figure 5.1a. Earlier reports have stated that the red color of GNPs and the absorbance peak at 520 nm indicate their size to be 10–50 nm in diameter [57]. For their biosensor application, the GNPs were surface-modified with MUDA, enabling their instantaneous non-covalent interaction with the aminated DNA probe [44]. The surface-modified GNPs were not affected by this modification, confirmed by their absorbance spectra (Figure 1a). Following sample DNA addition to GNPs and probe, and placement in the thermocycler, the absorbance spectra were again measured to confirm the stability of the GNPs. As seen in Figure 5.1a, GNPs did not show a shift in wavelength of absorption maxima, indicating that heating cycle or presence of DNA, did not affect the size of nanoparticles. After confirming GNPs' stability, proof-of-concept of the assay was conducted.

As stated earlier, our plasmonic biosensor concept is based on the SPR of GNPs, which can be determined spectrophotometrically. GNP aggregation results from the distribution of the electrostatic repulsion, leading to a shift in their absorption maxima due to the distance-

dependent nature of the SPR [44]. The shift in absorption maxima is associated with the color change from red to blue or violet. Thus, this study utilized GNPs' absorbance spectra at 520 nm and shift in the peak of maximum absorbance following HCl addition for DNA detection. It was hypothesized that DNA-probe-GNPs' conjugation would protect GNP against aggregation, leading to the maintenance of red color in the target DNA sample. In non-target samples, GNP would agglomerate due to a lack of protection by target DNA, changing their color from red to blue or purple. The biosensor thus produced a qualitative and quantitative signal, as seen in Figure 5.1b. The quantifiable signal corresponds to the presence or absence of the target analyte.

Optimization of the plasmonic biosensor using the *bla*$_{KPC}$ probe was initially conducted and resulted in 9 µL of 0.1 M HCl and a 5 min response time for further analysis. It should be noted that the GNPs are prevented from aggregation for at least 30 min. All steps from sample preparation to colorimetric analysis can be completed in approximately 30 min; this short duration is due to instantaneous GNP-probe functionalization.

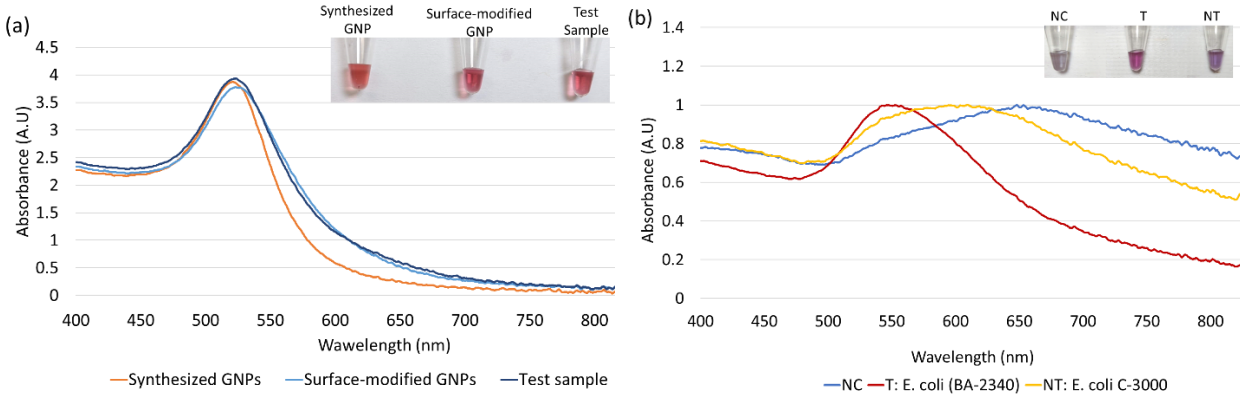

Figure 5.1. The absorbance spectrum of GNP samples along with tube images in the inset: (a) The absorbance spectrum of the synthesized GNPs, surface-modified GNPs, and test sample after the heating cycle and (b) proof-of-concept of the biosensor using the *bla*$_{KPC}$ probe with negative control (NC), target (T), and non-target (NT) samples.

5.3.2. Limit of Detection of the Plasmonic Biosensor

The lowest detection limit of the biosensor for KPC-producing bacteria was determined using the target DNA of KPC-producing *E. coli* (BA-2340) and the non-target DNA of susceptible *E. coli* C-3000. Both target and non-target DNA samples were diluted from 20 to 1 ng/µL by a factor of two. Target and non-target DNA samples at the same concentrations were compared using absorbance spectra measurements; tube images are shown in Figure 5.2. Quantification of GNP aggregation was achieved using $A_{625/520}$. The difference in average

$A_{625/520}$ of target and non-target samples was higher at 20 ng/µL and 10 ng/µL followed by 5 ng/µL and 2.5 ng/µL. The least difference between the target and non-target samples was observed at 1 ng/µL. Statistically significant differences between target and non-target samples for each concentration were assessed using ANOVA followed by Tukey's test**.** The target samples at 20 ng/µL, 10 ng/µL, 5 ng/µL, 2.5 ng/µL, and 1 ng/µL were significantly different from their non-target samples ($p < 0.05$). However, the average $A_{625/520}$ of the target sample at 1 ng/µL overlapped with non-target samples at 20 ng/µL, 10 ng/µL, 5 ng/µL, 2.5 ng/µL, which were all similar ($p > 0.05$). Further, visual detection at 1 ng/µL was also not clearly observed. Thus, the detection limit was found to be 2.5 ng/µL.

Sensitivity results also indicate that the $A_{625/520}$ values of non-target were in a similar range while those of target at various DNA concentrations followed a linear trend. Here, the $A_{625/520}$ of target DNA samples at 20 ng/µL and 10 ng/µL were similar ($p > 0.05$), indicating that DNA concentrations above 10 ng/µL would have a similar absorbance ratio. Previous literature confirmed this observation where a GNP biosensor detected *E. coli* O157 with a similar absorbance peak in target samples at 10 ng/µL and 20 ng/µL [44]. Thus, our plasmonic biosensor can detect and differentiate target and non-target samples at and above 2.5 ng/µL.

The detection limit of our biosensor using unamplified DNA was lower than that of similar colorimetric assays in the literature. For instance, a colorimetric assay using thiolated GNPs for detecting *Staphylococcus epidermis* was achieved with a limit of 20 ng/µL [58]. In another study, *Leishmania* sps. were detected using multiple probes with DNA as low as 11.5 ng/µL [59]. Among other bacteria, uropathogenic *E.coli* was detected from the pure culture with a detection limit of 9.4 ng/µL [49], and *E. coli* O157 was detected with a limit of 2.5 ng/µL [44]. In other examples of GNP-based colorimetric assays, which had a significantly lower detection limit in clinical isolates, amplification of DNA samples was needed. Examples include the detection of *Acinetobacter baumannii* [60] and *Mycobacterium tuberculosis* [61] within 2 h following PCR. Compared to similar assays, the detection limit of our biosensor is reasonable without any PCR amplification and probe-functionalization and can be achieved in 30 min.

The detection limit of our biosensor corresponds to approximately 10^3 CFU/mL. Other studies using lateral-flow immunochromatographic assay and colloidal GNPs successfully detected OXA-48 variants but demonstrated a higher detection limit at 10^6 CFU/mL [62]. Similarly, electrochemical biosensor platforms for bla_{KPC} detection [34] and plasmonic sensors

for CP bacteria detection have all shown detection limits >10^4 CFU/mL [39], with other methods requiring overnight culturing [19,23,25,35,63,64]. Our plasmonic biosensor promises a lower detection limit from unamplified DNA samples, along with a simple, rapid, and cost-effective detection.

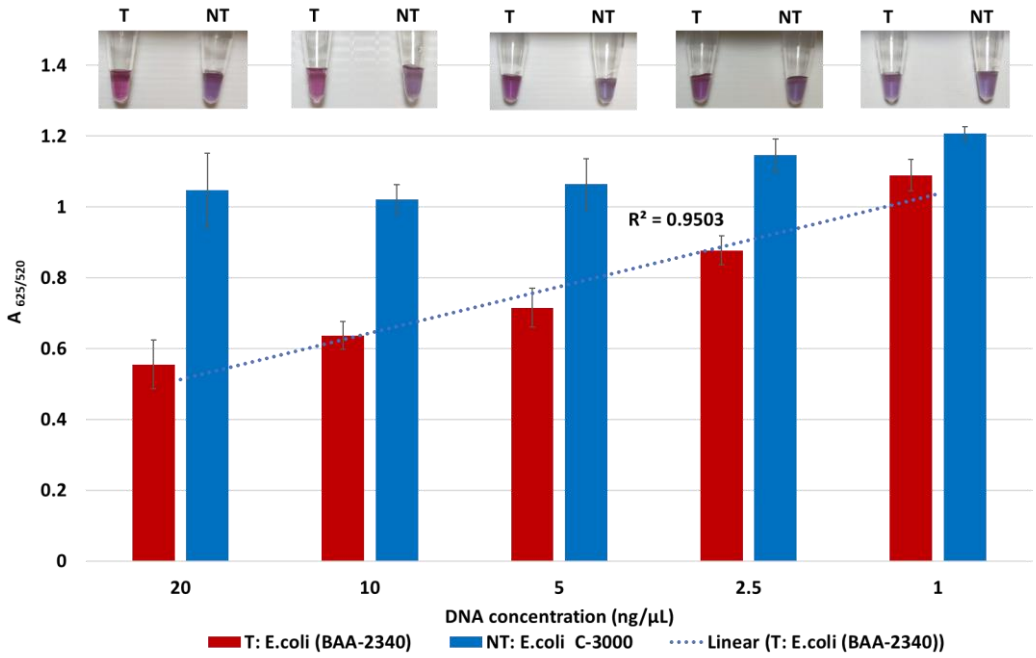

Figure 5.2**.** Limit of detection of the plasmonic biosensor using the *bla*$_{KPC}$ probe. The absorbance ratio at 625 and 520 nm ($A_{625/520}$) of the target (T) and non-target (NT) DNA samples at the different concentrations, along with their visual images.

5.3.3. Diagnostic Sensitivity and Specificity of the Plasmonic Biosensor

A total of 47 isolates were first confirmed for the presence of the *bla*$_{KPC}$ gene in the target (14) and its absence in non-target samples (33) by PCR amplification. Our plasmonic biosensor was then tested on all target and non-target samples. The PCR and biosensor results, with average of $A_{625/520}$ and tube images are shown for all 47 samples in Figures 5.3–7.

Figure 5.3a shows results from *E. coli* samples with three KPC-producing targets and six non-KPC-producing non-target samples. The plasmonic biosensor successfully detected two of three target samples. Sample spectra are also shown in Figure 5.3c. Among KPC-producing *E. cloacae* samples, the target was successfully detected, while none of the non-KPC-producing samples were detected by the biosensor (Figure 5.4a). No cross-reactivity with non-target DNA was observed, resulting in GNP agglomeration. For KPC-producing *K. pneumoniae*, all the target samples were successfully detected. However, one (NDM-producing) of six non-target samples

was also detected by the biosensor (Figure 5.5a). The biosensor was also successful in detecting one of the two KPC-producing *K. aerogenes* samples and differentiated it from non-KPC producing carbapenem-resistant *K. aerogenes*, *K. oxytoca*, *P. rettgeri*, *P. aeruginosa*, and susceptible *K. aerogenes*, *S.* Enteritidis, and *S.* Typhimurium (Figure 5.6a). Lastly, our biosensor detected and differentiated KPC-producing *R. ornithinolytica*, *C. amalonaticus*, and *C. freundii* from non-KPC-producing carbapenem-resistant *C. freundii*, *M. morganii*, *P. mirabilis* (Figure 5.7a). The $A_{625/520}$ values of all detected samples were significantly different than those of the non-detected samples ($p < 0.05$).

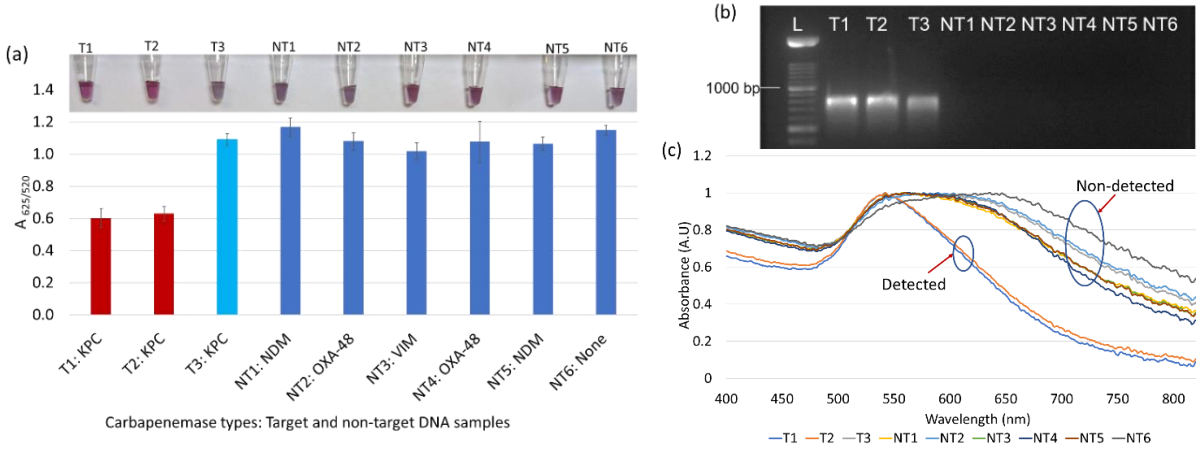

Figure 5.3. Plasmonic biosensor and PCR results of *E. coli* samples: (a) the average absorbance ratio at 625 and 520 nm ($A_{625/520}$) of the target (T) and non-target (NT) samples with colorimetric results in tubes. Detected target samples are shown with red color bars, and non-target samples are shown with blue bars. One of the three target samples was not detected (shown in light blue). (b) PCR amplification results of the same samples along with a 1000 bp ladder. (c) Absorbance spectra of the *E. coli* samples.

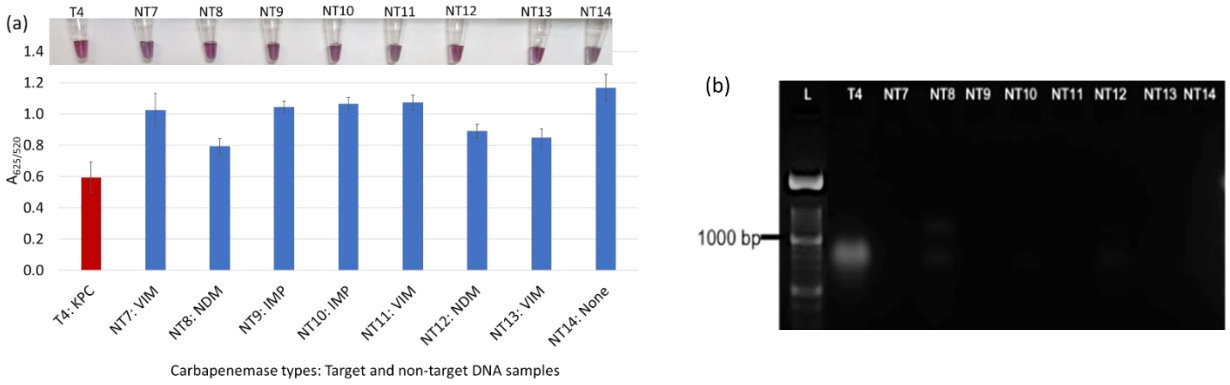

Figure 5.4. Plasmonic biosensor and PCR results of *E. cloacae* samples: (a) the average absorbance ratio at 625 and 520 nm ($A_{625/520}$) of the target (T) and non-target (NT) samples, with colorimetric results in tubes. Detected target samples are shown with red color bars, and non-target samples are shown with blue bars. (b) PCR amplification results of the same samples with a 1000 bp ladder.

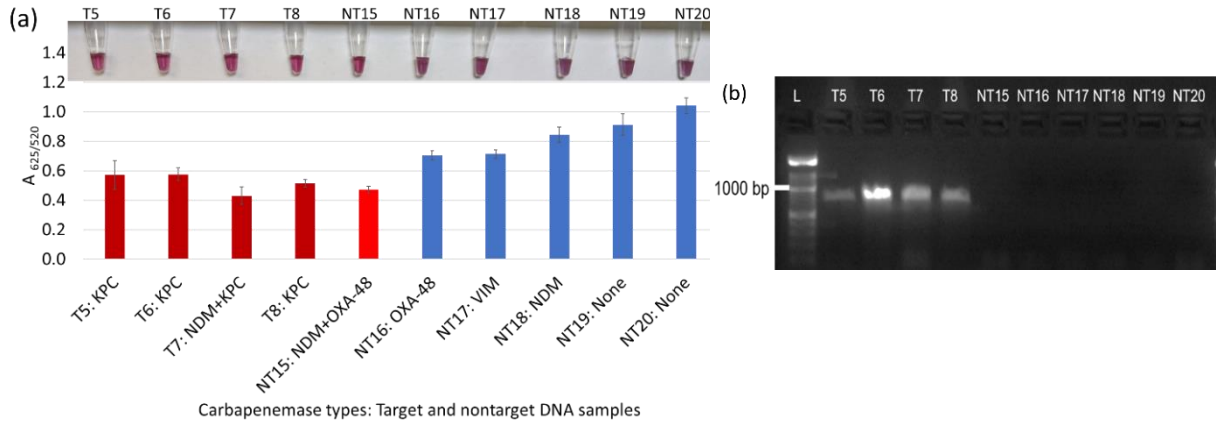

Figure 5.5. Plasmonic biosensor and PCR results of *K. pneumoniae* samples: (a) the average absorbance ratio at 625 and 520 nm ($A_{625/520}$) of the target (T) and non-target (NT) samples, with colorimetric results in tubes. Detected target samples are shown with red color bars, and non-target samples are shown with blue bars. One of the six non-target samples was detected (shown in light red). (b) PCR amplification results of the same samples along with a 1000 bp ladder.

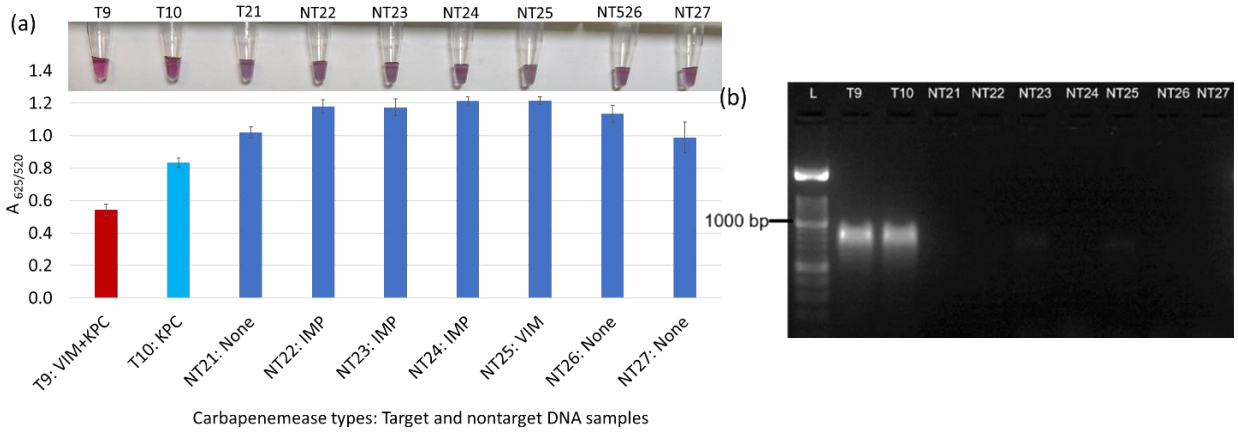

Figure 5.6. Plasmonic biosensor and PCR results of *K. aerogenes* (T9, T10, NT21), *K. oxytocia* (NT22), *P. rettgeri* (NT23 and NT24), *P. aeruginosa* (NT25), *S.* Typhimurium (NT26), and *S.* Enteritidis (NT27): (a) the average absorbance ratio at 625 and 520 nm ($A_{625/520}$) of the target (T) and non-target (NT) samples, with colorimetric results in tubes. The detected target sample is shown with a red bar, and non-target samples are shown with blue bars. One of the two target samples was not detected (shown in light blue). (b) PCR amplification results of the same samples along with a 1000 bp ladder.

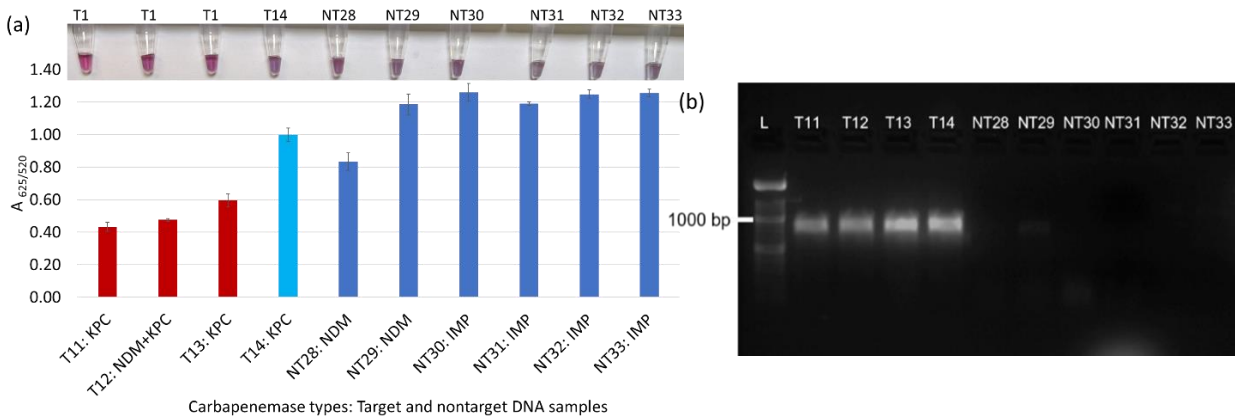

Figure 5.7. Plasmonic biosensor and PCR results of *R. ornithinolytica* (T11, T12), *C. amalonaticus* (T13), *C. freundii* (T14), *C. freundii* (NT28 and NT29), *P. mirabilis* (NT30 and NT31), and *M. morganii* (NT32 and NT33): (a) the average absorbance ratio at 625 and 520 nm ($A_{625/520}$) of the target (T) and non-target (NT) samples, with colorimetric results in tubes. Detected target samples are shown with red bars, and non-target samples are shown with blue bars. One of the four target samples was not detected (shown in light blue). (b) PCR amplification results of the same samples along with a 1000 bp ladder.

Overall, the designed DNA-based plasmonic biosensor used the bla_{KPC} probe to successfully detect and differentiate KPC-producing bacteria from non-KPC-producing bacteria regardless of bacterial types. The rapid biosensor was in almost perfect agreement with the result of PCR amplification as seen in Figures 5.3b, 4b, 5b, 6b, and 7b. The biosensor detected 11 of 14 target DNA samples and one of 33 non-target DNA samples, confirmed statistically. The average $A_{625/520}$ of the detected target DNA samples in all trials was in the range of 0.43–0.63, while the absorbance ratio of non-target DNA detection was between 0.71–1.2 after HCl application (5 min response). The differences in absorbance ratio of all detected samples were significantly ($p < 0.05$) different than those of all non-detected samples.

The diagnostic specificity (true negative) and sensitivity (true positive) of our biosensor were found to be 97% and 79%, respectively (Table 2). These results were in the range of sensitivity and specificity levels of the phenotypic techniques used in clinical labs to detect carbapenem-resistant bacteria. For instance, MALDI-TOF MS detected the resistant bacteria with a range of 72.5–100% sensitivity and 98–100% specificity, along with an issue on OXA-48 identification [20,25]. The sensitivity of the Carba NP test was 73–100%, but it performed poorly in the detection of OXA-48 enzyme type [20,21,27]. Different types of commercial kits: RAPIDEC Carba NP test (first commercial test), β-CARBA test, Rapid CARB screen, Rapid Carb Blue kit, and Neo-CARB kit have been used to detect CP bacteria in the range of 15 min to

2 h with varying sensitivity (89.5–99%) and specificity (70.9–100%) from the pure culture [21,25]. In culture-based methods, sensitivity of the MHT was found to be 69% [65] and 93–98% [20], along with lower performance in the detection of NDM enzymes [20,21]. Lastly, the sensitivity of the CIM method was 98–100% [20,66], and 96.1% [66]. However, the CIM method is labor-intensive and takes days to determine the resistant profile of the bacteria [18,20].

Table 5.2. Diagnostic sensitivity and specificity for KPC detection.

	Sensitivity	**Specificity**
	Positive Samples	Negative Samples
Positive Tests	11	1
Negative Tests	3	32
Total	14	33
	11/14 = 0.7857	32/33 = 0.9696

Among the genotypic methods, the multiplex oligonucleotide ligation-PCR procedure helps to detect β-lactamase genes and their variations with high sensitivity and specificity (100% and 99.4%) in 5 h [25]. The LAMP method using hyfroxynaphtol blue dye (LAMP-HNB) and microarray techniques has also been used to detect carbapenemase enzymes with higher specificity and sensitivity at 100% and > 90%, respectively [18,21]. The RNA-targeted molecular approach, NucliSENS EasyQKPC test, successfully detected bla_{KPC} variants within 2 h, achieving 93.3% sensitivity and 99% specificity [67]. While genotypic methods show higher sensitivity and specificity, they are expensive and therefore limited in their field-application. Alternatively, our GNP biosensor offers cost-effective and rapid detection with good sensitivity and specificity for KPC-producing bacteria.

5.3.4. Improving GNP Plasmonic Biosensor Applicability and Accessibility

Rapid diagnostic techniques with higher specificity and sensitivity help improve diagnosis, disease management, epidemiology, and outbreak investigations [7]. As AMR infections, particularly carbapenem-resistant infections, are a global concern, rapid detection of the causative bacteria is of utmost importance. The GNP-based plasmonic biosensors can become an accessible and rapid detection method, especially in low-resource settings.

This plasmonic biosensor is the first study to detect AMR with KPC-producing bacteria. This study showed the potential of the plasmonic biosensor applicability in detecting the gene of KPC-producing bacteria in a short time. While the designed biosensor is easy, rapid, and cost-effective, its applicability and accessibility can be further developed through future works. For

instance, visual results can also be quantified without requiring absorbance spectra measurements. Smartphone imaging techniques have been used to differentiate the color difference between target and non-target samples [39,68] and can be applied to this assay. Further, our biosensor using the bla_{KPC} probe can be tested on more bacteria isolates to improve its sensitivity and specificity. The biosensor design can be extended to detect other carbapenemase genes using bla_{NDM}, bla_{OXA-48}, bla_{VIM}, and bla_{IMP} probes for broad-range detection. A multiplex GNP biosensor using multiple probes can be designed to detect all carbapenemase genes. The GNP biosensor can be further tested on clinical, environmental, and food samples to increase its real-world applicability. Even though carbapenems are used in human medicine, environmental, microbiological, and clinical investigations show that CP bacteria in the environment (water or soil ecosystems) could widely spread among animals and agricultural products [1,69–73]. Thus, rapid detection of CP bacteria, regardless of their pathogenicity, and its implementation in surveillance programs is important to prevent and control possible future endemics or pandemics.

Besides carbapenem resistance detection, our platform can be extended to other antibiotic-resistant bacteria (colistin, ampicillin, ESBL, etc.). Detection of specific genes with the plasmonic biosensor can be achieved in a simple, rapid, and cost-effective manner allowing it to be applied as an effective screening test in low-resource settings.

The colorimetric nature of this plasmonic biosensor offers rapid and simple visual detection in 30 min. The GNPs are easily prepared and modified and chemically stable for a long time. This assay has only three steps—adding extracted DNA to GNPs, placing the mixture in a thermocycler (acting as a heating block, not for DNA amplification), and HCl application. The estimated material cost of this GNP plasmonic biosensor is affordable at less than USD 2 per test, compared to rapid molecular methods (USD 23–150) and phenotypic methods (USD 2–10) [25]. This GNP biosensor does not require PCR amplification, complex and costly equipment such as a spectrophotometer, mass spectrophotometer or qPCR, and data analysis. Other inexpensive phenotypic methods require overnight culture and are therefore not rapid. Hence, our platform is affordable, rapid, and applicable; this designed plasmonic biosensor can be applied for point-of-care testing and field studies.

5.4. Conclusion

Dextrin-coated GNPs were used to design a DNA-based plasmonic biosensor to detect KPC-producing carbapenem-resistant bacteria in 30 min. This biosensor using the bla_{KPC} probe can successfully visually differentiate between target (KPC-producing bacteria) and non-target samples (non-KPC-producing bacteria). Successful detection was achieved as low as 2.5 ng/µL (~10^3 CFU/mL) from unamplified DNA samples. The diagnostic sensitivity and specificity were found to be 79% and 97%, respectively. In future works, this biosensor can be extended to detect different carbapenemase genes in clinical and biological samples.

REFERENCES

[1] Taggar, G., Rheman, M. A., Boerlin, P., and Diarra, M. S., "Molecular Epidemiology of Carbapenemases in Enterobacteriales from Humans, Animals, Food and the Environment," Antibiotics, 2020, 9(10), pp. 1–22, DOI: 10.3390/antibiotics9100693.

[2] Capozzi, C., Maurici, M., and Panà, A., "[Antimicrobial Resistance: It Is a Global Crisis, 'a Slow Tsunami']," Ig. Sanita Pubbl., 2019, 75(6), p. 429—450.

[3] Serwecińska, L., "Antimicrobials and Antibiotic-Resistant Bacteria: A Risk to the Environment and to Public Health," Water, 2020, 12(12), p. 3313, DOI: 10.3390/w12123313.

[4] Littmann, J., Buyx, A., and Cars, O., "Antibiotic Resistance: An Ethical Challenge," Int. J. Antimicrob. Agents, 2015, 46(4), pp. 359–361, DOI: 10.1016/j.ijantimicag.2015.06.010.

[5] Dankittipong, N., Fischer, E. A. J., Swanenburg, M., Wagenaar, J. A., Stegeman, A. J., and de Vos, C. J., "Quantitative Risk Assessment for the Introduction of Carbapenem-Resistant Enterobacteriaceae (CPE) into Dutch Livestock Farms," Antibiotics, 2022, 11(2), p. 281, DOI: 10.3390/antibiotics11020281.

[6] World Health Organization (WHO), "WHO Publishes List of Bacteria for Which New Antibiotics Are Urgently Needed," WHO, [Online]. Available: https://www.who.int/news/item/27-02-2017-who-publishes-list-of-bacteria-for-which-new-antibiotics-are-urgently-needed. [Accessed: 06-Sep-2022].

[7] Antimicrobial Resistance: CDC's Antibiotic Resistance Threats in the United States, 2019. Available online:https://www.cdc.gov/drugresistance/pdf/threatsreport/2019-ar-threats-report-508.pdf (Accessed:06-September-2022).

[8] CDC, "Healthcare-Associated Infections (HAIs):CRE Technical Information," CDC (Centers Dis. Control Prev., 2019, [Online]. Available: https://www.cdc.gov/hai/organisms/cre/technical-info.html. [Accessed: 08-Jun-2022].

[9] Holmes, A. H., Moore, L. S. P., Sundsfjord, A., Steinbakk, M., Regmi, S., Karkey, A., Guerin, P. J., and Piddock, L. J. V., "Understanding the Mechanisms and Drivers of Antimicrobial Resistance," Lancet, 2016, 387(10014), pp. 176–187, DOI: 10.1016/S0140-6736(15)00473-0.

[10] Munita, J. M., and Arias, C. A., "Mechanisms of Antibiotic Resistance," Virulence Mech. Bact. Pathog., 2016, 4(2), pp. 481–511, DOI: 10.1128/9781555819286.ch17.

[11] Capita, R., and Alonso-Calleja, C., "Antibiotic-Resistant Bacteria: A Challenge for the Food Industry," Crit. Rev. Food Sci. Nutr., 2013, 53(1), pp. 11–48, DOI: 10.1080/10408398.2010.519837.

[12] Codjoe, F., and Donkor, E., "Carbapenem Resistance: A Review," Med. Sci., 2017, 6(1), p. 1, DOI: 10.3390/medsci6010001.

[13] Smith, H. Z., and Kendall, B., “Carbapenem Resistant Enterobacteriaceae,” StatPearls [Internet]. StatPearls Publ., 2021.

[14] CDC, “Antimicrobial Resistance;Tracking Antibiotic Resistance,” CDC (Centers Dis. Control Prev. Dis. Control Prev., 2021, [Online]. Available: https://www.cdc.gov/drugresistance/tracking.html. [Accessed: 05-May-2022].

[15] McLain, J. E., Cytryn, E., Durso, L. M., and Young, S., “Culture-based Methods for Detection of Antibiotic Resistance in Agroecosystems: Advantages, Challenges, and Gaps in Knowledge,” J. Environ. Qual., 2016, 45(2), pp. 432–440.

[16] Syal, K., Mo, M., Yu, H., Iriya, R., Jing, W., Guodong, S., Wang, S., Grys, T. E., Haydel, S. E., and Tao, N., “Current and Emerging Techniques for Antibiotic Susceptibility Tests,” Theranostics, 2017, 7(7), pp. 1795–1805, DOI: 10.7150/thno.19217.

[17] Khan, Z. A., Siddiqui, M. F., and Park, S., “Current and Emerging Methods of Antibiotic Susceptibility Testing,” Diagnostics, 2019, 9(2), p. 49, DOI: 10.3390/diagnostics9020049.

[18] Sutherland, J. B., Rafii, F., Lay, J. O., and Williams, A. J., “Rapid Analytical Methods to Identify Antibiotic-Resistant Bacteria,” *Antibiotic Drug Resistance*, Wiley, September 9, 2019, pp. 533–566, DOI: 10.1002/9781119282549.ch21.

[19] Takayama, Y., Adachi, Y., Nihonyanagi, S., and Okamoto, R., “Modified Hodge Test Using Mueller-Hinton Agar Supplemented with Cloxacillin Improves Screening for Carbapenemase-Producing Clinical Isolates of Enterobacteriaceae,” J. Med. Microbiol., 2015, 64(7), pp. 774–777, DOI: 10.1099/jmm.0.000068.

[20] Lutgring, J. D., and Limbago, B. M., “The Problem of Carbapenemase-Producing-Carbapenem-Resistant-Enterobacteriaceae Detection,” J. Clin. Microbiol., 2016, 54(3), pp. 529–534, DOI: 10.1128/JCM.02771-15.

[21] Cui, X., Zhang, H., and Du, H., “Carbapenemases in Enterobacteriaceae: Detection and Antimicrobial Therapy,” Front. Microbiol., 2019, 10(August), pp. 1–12, DOI: 10.3389/fmicb.2019.01823.

[22] Alizadeh, N., Rezaee, M. A., Kafil, H. S., Barhaghi, M. H. S., Memar, M. Y., Milani, M., Hasani, A., and Ghotaslou, R., “Detection of Carbapenem-Resistant Enterobacteriaceae by Chromogenic Screening Media,” J. Microbiol. Methods, 2018, 153(September), pp. 40–44, DOI: 10.1016/j.mimet.2018.09.001.

[23] Nordmann, P., Girlich, D., and Poirel, L., “Detection of Carbapenemase Producers in Enterobacteriaceae by Use of a Novel Screening Medium,” J. Clin. Microbiol., 2012, 50(8), pp. 2761–2766, DOI: 10.1128/JCM.06477-11.

[24] Bernabeu, S., Poirel, L., and Nordmann, P., “Spectrophotometry-Based Detection of Carbapenemase Producers among Enterobacteriaceae,” Diagn. Microbiol. Infect. Dis., 2012, 74(1), pp. 88–90, DOI: 10.1016/j.diagmicrobio.2012.05.021.

[25] Decousser, J.-W., Poirel, L., and Nordmann, P., “Recent Advances in Biochemical and Molecular Diagnostics for the Rapid Detection of Antibiotic-Resistant Enterobacteriaceae : A Focus on ß-Lactam Resistance,” Expert Rev. Mol. Diagn., 2017, 17(4), pp. 327–350, DOI: 10.1080/14737159.2017.1289087.

[26] van Almsick, V., Ghebremedhin, B., Pfennigwerth, N., and Ahmad-Nejad, P., “Rapid Detection of Carbapenemase-Producing Acinetobacter Baumannii and Carbapenem-Resistant Enterobacteriaceae Using a Bioluminescence-Based Phenotypic Method,” J. Microbiol. Methods, 2018, 147(February), pp. 20–25, DOI: 10.1016/j.mimet.2018.02.004.

[27] Nordmann, P., Poirel, L., and Dortet, L., “Rapid Detection of Carbapenemase-Producing Enterobacteriaceae,” Emerg. Infect. Dis., 2012, 18(9), pp. 1503–1507, DOI: 10.3201/eid1809.120355.

[28] Reynoso, E. C., Laschi, S., Palchetti, I., and Torres, E., “Advances in Antimicrobial Resistance Monitoring Using Sensors and Biosensors: A Review,” Chemosensors, 2021, 9(8), DOI: 10.3390/chemosensors9080232.

[29] Poirel, L., Walsh, T. R., Cuvillier, V., and Nordmann, P., “Multiplex PCR for Detection of Acquired Carbapenemase Genes,” Diagn. Microbiol. Infect. Dis., 2011, 70(1), pp. 119–123, DOI: 10.1016/j.diagmicrobio.2010.12.002.

[30] Wu, S., and Hulme, J. P., “Recent Advances in the Detection of Antibiotic and Multi-Drug Resistant Salmonella: An Update,” Int. J. Mol. Sci., 2021, 22(7), DOI: 10.3390/ijms22073499.

[31] Perumal, V., and Hashim, U., “Advances in Biosensors: Principle, Architecture and Applications,” J. Appl. Biomed., 2014, 12(1), pp. 1–15, DOI: 10.1016/j.jab.2013.02.001.

[32] Ahmed, A., Rushworth, J. V., Hirst, N. A., and Millner, P. A., “Biosensors for Whole-Cell Bacterial Detection,” Clin. Microbiol. Rev., 2014, 27(3), pp. 631–646, DOI: 10.1128/CMR.00120-13.

[33] Huang, J. M.-Y., Henihan, G., Macdonald, D., Michalowski, A., Templeton, K., Gibb, A. P., Schulze, H., and Bachmann, T. T., “Rapid Electrochemical Detection of New Delhi Metallo-Beta-Lactamase Genes To Enable Point-of-Care Testing of Carbapenem-Resistant Enterobacteriaceae,” Anal. Chem., 2015, 87(15), pp. 7738–7745, DOI: 10.1021/acs.analchem.5b01270.

[34] Gordon, N., Bawa, R., and Palmateer, G., “Carbapenem-Resistant Enterobacteriaceae Testing in 45 Minutes Using an Electronic Sensor,” *Current Issues in Medicine: Diagnosis and Imaging*, 2021, pp. 1–18.

[35] Bashir, S., Nawaz, H., Majeed, M. I., Mohsin, M., Abdullah, S., Ali, S., Rashid, N., Kashif, M., Batool, F., Abubakar, M., Ahmad, S., and Abdulraheem, A., “Rapid and Sensitive Discrimination among Carbapenem Resistant and Susceptible E. Coli Strains Using Surface Enhanced Raman Spectroscopy Combined with Chemometric Tools,” Photodiagnosis Photodyn. Ther., 2021, 34(March), DOI: 10.1016/j.pdpdt.2021.102280.

[36] Wong, Y. L., Kang, W. C. M., Reyes, M., Teo, J. W. P., and Kah, J. C. Y., "Rapid Detection of Carbapenemase-Producing Enterobacteriacae Based on Surface-Enhanced Raman Spectroscopy with Gold Nanostars," ACS Infect. Dis., 2020, 6(5), pp. 947–953, DOI: 10.1021/acsinfecdis.9b00318.

[37] Li, J., Wang, C., Kang, H., Shao, L., Hu, L., Xiao, R., Wang, S., and Gu, B., "Label-Free Identification Carbapenem-Resistant Escherichia Coli Based on Surface-Enhanced Resonance Raman Scattering," RSC Adv., 2018, 8(9), pp. 4761–4765, DOI: 10.1039/C7RA13063E.

[38] Hu, S., Niu, L., Zhao, F., Yan, L., Nong, J., Wang, C., Gao, N., Zhu, X., Wu, L., Bo, T., Wang, H., and Gu, J., "Identification of Acinetobacter Baumannii and Its Carbapenem-Resistant Gene BlaOXA-23-like by Multiple Cross Displacement Amplification Combined with Lateral Flow Biosensor," Sci. Rep., 2019, 9(1), p. 17888, DOI: 10.1038/s41598-019-54465-8.

[39] Santopolo, G., Rojo-Molinero, E., Clemente, A., Borges, M., Oliver, A., and de la Rica, R., "Bedside Detection of Carbapenemase-Producing Pathogens with Plasmonic Nanosensors," Sensors Actuators, B Chem., 2021, 329(October 2020), DOI: 10.1016/j.snb.2020.129059.

[40] Aldewachi, H., Chalati, T., Woodroofe, M. N., Bricklebank, N., Sharrack, B., and Gardiner, P., "Gold Nanoparticle-Based Colorimetric Biosensors," Nanoscale, 2018, 10(1), pp. 18–33, DOI: 10.1039/C7NR06367A.

[41] Li, Y., Schluesener, H. J., and Xu, S., "Gold Nanoparticle-Based Biosensors," Gold Bull., 2010, 43(1), pp. 29–41, DOI: 10.1007/BF03214964.

[42] Zeng, S., Yong, K.-T., Roy, I., Dinh, X.-Q., Yu, X., and Luan, F., "A Review on Functionalized Gold Nanoparticles for Biosensing Applications," Plasmonics, 2011, 6(3), pp. 491–506, DOI: 10.1007/s11468-011-9228-1.

[43] Wang, Y., and Alocilja, E. C., "Gold Nanoparticle-Labeled Biosensor for Rapid and Sensitive Detection of Bacterial Pathogens," J. Biol. Eng., 2015, 9(1), pp. 1–7, DOI: 10.1186/s13036-015-0014-z.

[44] Dester, E., Kao, K., and Alocilja, E. C., "Detection of Unamplified E. Coli O157 DNA Extracted from Large Food Samples Using a Gold Nanoparticle Colorimetric Biosensor," Biosensors, 2022, 12(5), p. 274, DOI: 10.3390/bios12050274.

[45] Hua, Z., Yu, T., Liu, D., and Xianyu, Y., "Recent Advances in Gold Nanoparticles-Based Biosensors for Food Safety Detection," Biosens. Bioelectron., 2021, 179(February), p. 113076, DOI: 10.1016/j.bios.2021.113076.

[46] Sabela, M., Balme, S., Bechelany, M., Janot, J.-M., and Bisetty, K., "A Review of Gold and Silver Nanoparticle-Based Colorimetric Sensing Assays," Adv. Eng. Mater., 2017, 19(12), p. 1700270, DOI: 10.1002/adem.201700270.

[47] Ahmadi, S., Kamaladini, H., Haddadi, F., and Sharifmoghadam, M. R., "Thiol-Capped Gold Nanoparticle Biosensors for Rapid and Sensitive Visual Colorimetric Detection of Klebsiella Pneumoniae," J. Fluoresc., 2018, 28(4), pp. 987–998, DOI: 10.1007/s10895-018-2262-z.

[48] Quintela, I. A., De Los Reyes, B. G., Lin, C. S., and Wu, V. C. H., "Simultaneous Colorimetric Detection of a Variety of Salmonella Spp. In Food and Environmental Samples by Optical Biosensing Using Oligonucleotide-Gold Nanoparticles," Front. Microbiol., 2019, 10(MAY), pp. 1–12, DOI: 10.3389/fmicb.2019.01138.

[49] Bakthavathsalam, P., Rajendran, V. K., and Baquir Mohammed, J. A., "A Direct Detection of Escherichia Coli Genomic DNA Using Gold Nanoprobes," J. Nanobiotechnology, 2012, 10(1), p. 8, DOI: 10.1186/1477-3155-10-8.

[50] Baetsen-Young, A. M., Vasher, M., Matta, L. L., Colgan, P., Alocilja, E. C., and Day, B., "Direct Colorimetric Detection of Unamplified Pathogen DNA by Dextrin-Capped Gold Nanoparticles," Biosens. Bioelectron., 2018, 101(August 2017), pp. 29–36, DOI: 10.1016/j.bios.2017.10.011.

[51] Alizadeh, M., Wood, R. L., Buchanan, C. M., Bledsoe, C. G., Wood, M. E., McClellan, D. S., Blanco, R., Ravsten, T. V., Husseini, G. A., Hickey, C. L., Robison, R. A., and Pitt, W. G., "Rapid Separation of Bacteria from Blood – Chemical Aspects," Colloids Surfaces B Biointerfaces, 2017, 154, pp. 365–372, DOI: 10.1016/j.colsurfb.2017.03.027.

[52] Buehler, S. S., Madison, B., Snyder, S. R., Derzon, J. H., Cornish, N. E., Saubolle, M. A., Weissfeld, A. S., Weinstein, M. P., Liebow, E. B., and Wolk, D. M., "Effectiveness of Practices To Increase Timeliness of Providing Targeted Therapy for Inpatients with Bloodstream Infections: A Laboratory Medicine Best Practices Systematic Review and Meta-Analysis," Clin. Microbiol. Rev., 2016, 29(1), pp. 59–103, DOI: 10.1128/CMR.00053-14.

[53] Guerra, B., Fischer, J., and Helmuth, R., "An Emerging Public Health Problem: Acquired Carbapenemase-Producing Microorganisms Are Present in Food-Producing Animals, Their Environment, Companion Animals and Wild Birds," Vet. Microbiol., 2014, 171(3–4), pp. 290–297, DOI: 10.1016/j.vetmic.2014.02.001.

[54] Andrews, J. M., "Determination of Minimum Inhibitory Concentrations," J. Antimicrob. Chemother., 2001, 48(SUPPL. 1), pp. 5–16, DOI: 10.1093/jac/48.suppl_1.5.

[55] Anderson, M. J., Torres-Chavolla, E., Castro, B. A., and Alocilja, E. C., "One Step Alkaline Synthesis of Biocompatible Gold Nanoparticles Using Dextrin as Capping Agent," J. Nanoparticle Res., 2011, 13(7), pp. 2843–2851, DOI: 10.1007/s11051-010-0172-3.

[56] Chu, K., "An Introduction to Sensitivity, Specificity, Predictive Values and Likelihood Ratios," Emerg. Med., 1999, 11(3), pp. 175–181, DOI: 10.1046/j.1442-2026.1999.00041.x.

[57] Ghosh, S. K., and Pal, T., “Interparticle Coupling Effect on the Surface Plasmon Resonance of Gold Nanoparticles: From Theory to Applications,” Chem. Rev., 2007, 107(11), pp. 4797–4862, DOI: 10.1021/cr0680282.

[58] Osmani Bojd, M., Kamaladini, H., Haddadi, F., and Vaseghi, A., “Thiolated AuNP Probes and Multiplex PCR for Molecular Detection of Staphylococcus Epidermidis,” Mol. Cell. Probes, 2017, 34, pp. 30–36, DOI: 10.1016/j.mcp.2017.04.006.

[59] Andreadou, M., Liandris, E., Gazouli, M., Taka, S., Antoniou, M., Theodoropoulos, G., Tachtsidis, I., Goutas, N., Vlachodimitropoulos, D., Kasampalidis, I., and Ikonomopoulos, J., “A Novel Non-Amplification Assay for the Detection of Leishmania Spp. in Clinical Samples Using Gold Nanoparticles,” J. Microbiol. Methods, 2014, 96, pp. 56–61, DOI: 10.1016/j.mimet.2013.10.011.

[60] Khalil, M. A. F., Azzazy, H. M. E., Attia, A. S., and Hashem, A. G. M., “A Sensitive Colorimetric Assay for Identification of Acinetobacter Baumannii Using Unmodified Gold Nanoparticles,” J. Appl. Microbiol., 2014, 117(2), pp. 465–471, DOI: 10.1111/jam.12546.

[61] Soo, P.-C., Horng, Y.-T., Chang, K.-C., Wang, J.-Y., Hsueh, P.-R., Chuang, C.-Y., Lu, C.-C., and Lai, H.-C., “A Simple Gold Nanoparticle Probes Assay for Identification of Mycobacterium Tuberculosis and Mycobacterium Tuberculosis Complex from Clinical Specimens,” Mol. Cell. Probes, 2009, 23(5), pp. 240–246, DOI: 10.1016/j.mcp.2009.04.006.

[62] Wareham, D. W., Shah, R., Betts, J. W., Phee, L. M., and Momin, M. H. F. A., “Evaluation of an Immunochromatographic Lateral Flow Assay (OXA-48 K -SeT) for Rapid Detection of OXA-48-Like Carbapenemases in Enterobacteriaceae,” J. Clin. Microbiol., 2016, 54(2), pp. 471–473, DOI: 10.1128/JCM.02900-15.

[63] Ghafourian, S., Sadeghifard, N., Soheili, S., and Sekawi, Z., “Extended Spectrum Beta-Lactamases: Definition, Classification and Epidemiology,” Curr. Issues Mol. Biol., 2014, 17(1), pp. 11–22, DOI: 10.21775/cimb.017.011.

[64] Sharaha, U., Rodriguez-Diaz, E., Riesenberg, K., Bigio, I. J., Huleihel, M., and Salman, A., “Using Infrared Spectroscopy and Multivariate Analysis to Detect Antibiotics’ Resistant Escherichia Coli Bacteria,” Anal. Chem., 2017, 89(17), pp. 8782–8790, DOI: 10.1021/acs.analchem.7b01025.

[65] Amjad, A., Ia, M., Sa, A., Farwa, U., Malik, N., and Zia, F., “Modified Hodge Test : A Simple and Effective Test for Detection of Carbapenemase Production The Isolates Which Showed Intermediate or Susceptible Zones for Imipenem Were Tested for Carbapenemase Modified Hodge Test , as CL Recommends the MHT to Be Perform,” Iran. J. Microbiol., 2011, 3(4), pp. 189–193.

[66] Saito, K., Nakano, R., Suzuki, Y., Nakano, A., Ogawa, Y., Yonekawa, S., Endo, S., Mizuno, F., Kasahara, K., Mikasa, K., Kaku, M., and Yano, H., “Suitability of Carbapenem Inactivation Method (CIM) for Detection of IMP Metallo-β-Lactamase-

Producing Enterobacteriaceae," J. Clin. Microbiol., 2017, 55(4), pp. 1220–1222, DOI: 10.1128/JCM.02275-16.

[67] McEwan, A. S., Derome, A., Meunier, D., Burns, P. J., Woodford, N., and Dodgson, A. R., "Evaluation of the NucliSENS EasyQ KPC Assay for Detection of Klebsiella Pneumoniae Carbapenemase-Producing Enterobacteriaceae," J. Clin. Microbiol., 2013, 51(6), pp. 1948–1950, DOI: 10.1128/JCM.00057-13.

[68] Zheng, L., Cai, G., Wang, S., Liao, M., Li, Y., and Lin, J., "A Microfluidic Colorimetric Biosensor for Rapid Detection of Escherichia Coli O157:H7 Using Gold Nanoparticle Aggregation and Smart Phone Imaging," Biosens. Bioelectron., 2019, 124–125, pp. 143–149, DOI: 10.1016/j.bios.2018.10.006.

[69] Woodford, N., Wareham, D. W., Guerra, B., and Teale, C., "Carbapenemase-Producing Enterobacteriaceae and Non-Enterobacteriaceae from Animals and the Environment: An Emerging Public Health Risk of Our Own Making?," J. Antimicrob. Chemother., 2014, 69(2), pp. 287–291, DOI: 10.1093/jac/dkt392.

[70] Fernández, J., Guerra, B., and Rodicio, M. R., "Resistance to Carbapenems in Non-Typhoidal Salmonella Enterica Serovars from Humans, Animals and Food," Vet. Sci., 2018, 5(2), DOI: 10.3390/vetsci5020040.

[71] Morrison, B. J., and Rubin, J. E., "Carbapenemase Producing Bacteria in the Food Supply Escaping Detection," PLoS One, 2015, 10(5), DOI: 10.1371/journal.pone.0126717.

[72] Fischer, J., Schmoger, S., Jahn, S., Helmuth, R., and Guerra, B., "NDM-1 Carbapenemase-Producing Salmonella Enterica Subsp. Enterica Serovar Corvallis Isolated from a Wild Bird in Germany," J. Antimicrob. Chemother., 2013, 68(12), pp. 2954–2956, DOI: 10.1093/jac/dkt260.

[73] Mills, M. C., and Lee, J., "The Threat of Carbapenem-Resistant Bacteria in the Environment: Evidence of Widespread Contamination of Reservoirs at a Global Scale," Environ. Pollut., 2019, 255, p. 113143, DOI: 10.1016/j.envpol.2019.113143.

CHAPTER 6: PARALLEL BIOSENSOR PLATFORM FOR THE DETECTION OF CARBAPENEMASE-PRODUCING *E. COLI* IN SPIKED FOOD AND WATER SAMPLES

This chapter has been published in Food Control (10.1016/j.foodcont.2024.110485).

6.1. Introduction

Carbapenem-resistant *Enterobacterales* (CRE) has globally increased at an alarming rate in the last decade [1,2], which is reported as the global priority list of antimicrobial-resistant infections [3,4]. Due to limited antibiotic treatments, many CRE infections potentially result in death [1,3,5]. Their emergence and spread mostly rely on disseminating genes encoding carbapenemases by horizontal gene transfer [2,6,7]. The most prevalent carbapenemases are *Klebsiella pneumoniae* carbapenemase (KPC), New Delhi metallo-β-lactamase (NDM), Verona integron-encoded Metallo-β-lactamase (VIM), and Oxacillinase-48 (OXA-48) [8–10]. Several microbiological, clinical, and environmental studies reported that carbapenemase-producing (CP)-CRE was found in human specimens, hospital and municipal wastewater, agricultural environments, drinking water, surface and groundwater, food animals, and food products [2,8,11–16]. Thus, the presence of CP-CRE in clinical and biological samples is routinely tested [1,17–19].

The global food trade and water sources are one of the major routes for transmitting CP-CRE and the resistant genes, which threaten public health [11,20,21]. Thus, there has been an international ban and zero-tolerance policy on selling CRE-contaminated foods in various countries [8]. In the last two decades, global surveillance programs have targeted animal-based food products that are potential sources of antimicrobial-resistant bacteria (ARB) [19,22,23]. The surveillance programs mostly focus on tracing pathogenic indicator bacteria such as *Salmonella*, *E. coli*, *Campylobacter*, and *Enterococcus* on meat products (e.g., beef, poultry, and pork) and food animals. The surveillance has been extended to tracking CP-CRE in food animals and meat products since 2016 in the U.S. and Europe [1,17–19]. Thus, rapid detection of CP-CRE in the food chain and implementation of surveillance programs are significant to control and prevent future outbreaks.

The current methods for detecting ARB, including CP-CRE, have multiple obstacles in terms of speed and accessibility. For instance, culture-based tests, including standard

antimicrobial susceptibility testing (AST) [24–26], Modified Hodge Test (MHT) [27,28], and modified carbapenemase inactivation methods (mCIM) [29,30] are affordable and widely applicable. However, these tests are cumbersome and require pure cultures, which take days to weeks to identify the resistant profile of pathogens [2,31,32]. Widely implemented rapid phenotypic methods such as matrix-assisted laser desorption/ionization time-of-flight mass spectrometry (MALDI-TOF MS) and colorimetric assays (e.g., CARBA NP test) and genotypic methods have been developed to reduce the diagnostic time from days to hours. However, many of these techniques need pure cultue, advanced equipment, complex data analysis, expensive reagents, and skilled personnel, restricting their use in many limited-resource laboratories [2,26,31–33].

Recently, a few biosensors have been developed to address the global need for a simple, cost-effective, and rapid detection of CP-CRE. For instance, an impedimetric electrochemical biosensor detected NDM-producing bacteria with PCR amplified bla_{NDM} gene [34], and a voltammetry-based electrochemical biosensor allowed KPC-producing bacteria detection [35]. Among other methods, the Surface-Enhanced Raman Scattering (SERS) technique successfully detected CRE with higher specificity and sensitivity using nanoparticles [36–38]. However, these optical and electrochemical biosensors still require PCR amplification and multivariate data analysis, along with costly reagents and equipment [32]. Recently, plasmonic biosensors or gold nanoparticle (GNP)-based colorimetric biosensors have offered rapid, simple, and cost-effective genomic detection without the necessity of costly equipment and reagents and PCR amplification [39,40]. For instance, dextrin-coated GNPs (dGNPs) were utilized to visually detect a resistant gene (bla_{KPC}) harbored in various bacteria regardless of bacterial type [41]. As with many detection methods, the assay was mostly tested with susceptible pathogens, with a few examples from complex matrices. However, the rapid detection of ARB, including CRE, needs further attention. Particularly, direct detection of ARB from real samples has not been studied and requires further studies to improve the applicability and accessibility of this rapid detection technique. Thus, this study aimed to use the plasmonic biosensor to detect ARB, particularly CP-CRE isolates from matrices.

Besides concerns about accessible and applicable detection methods, bacterial extraction and concentration from real samples are often a critical challenge. This is typically necessary to ensure the enough number of bacterial cells required for successful detection [42–44]. The

bacterial isolation or extraction techniques in clinical and biological samples are usually physical methods (e.g., centrifugation and filtration) and biochemical methods (e.g., metal hydroxides, dielectrophoresis, and magnetic nanoparticles) [42,43,45]. However, many of these methods still face some challenges regarding limited volumes, filter clogging, and ineffective separation from complex matrices [42,46,47]. Among some primary alternatives, magnetic nanoparticles (MNPs) have been utilized for rapid and effective isolation of bacteria from clinical and biological samples [42,48–52]. Herein, immunomagnetic separation (IMS) methods have been commonly used to isolate target bacteria based on antigen-antibody conjugation. However, its inefficiency in complex matrices due to the blocking of the antibody by debris and its associated higher costs and specific storage conditions have limited its application [42,43,47]. Recently, carbohydrate-functionalized MNPs have been used as cost-effective and rapid alternatives to IMS. For instance, glycan-coated MNPs (gMNPs) successfully isolated gram-positive and gram-negative bacteria from various foods [53–55], although their use for the extraction of ARB, including CRE, requires attention. While gMNPs do not allow targeted bacterial capture, they could be combined with particular detection assays [39,54,56,57]. One-pot synthesis, long-term stability at room temperature, cost-effectiveness, and compatibility with many detection techniques make gMNPs lucrative alternatives [42,58]. Therefore, this work used gMNPs for the extraction of bacteria from matrices.

This research mainly designed a rapid, simple, and cost-effective platform to detect CP-CRE, specifically KPC-producing *E. coli*, as KPC is the most common carbapenemase type in the US and worldwide [10,16,59]. Further, CP *E. coli* isolates have been commonly found in foods and water sources [8,60–62]; thus, tap water, romaine lettuce, chicken breast, and ground beef were chosen as matrices of focus for the extraction and detection of KPC-producing *E. coli*.

This study hypothesized that carbohydrate-coated nanoparticles can rapidly extract and detect KPC-producing *E. coli* from large-volume samples (foods and water) without PCR amplification and lengthy enrichment steps. To achieve this, tap water and food samples were first artificially contaminated with carbapenem-susceptible and carbapenem-resistant bacteria. The gMNPs were used to extract these bacteria, and their interaction was assessed with TEM. Magnetically extracted bacteria were followed by a short-enrichment step (5 h) and DNA extraction. The detection of target DNAs for *E. coli* isolates, and KPC-producing bacteria was

parallelly achieved by GNP-based plasmonic biosensors using *uidA* and *bla*$_{KPC}$ probes. The overall procedure used in this study was briefly described in Scheme 6.1.

To the best of our knowledge, this study is the first study on the direct detection of CRE from food and water samples, along with magnetic extraction and parallel plasmonic biosensors to detect KPC-producing *E. coli*. This study further explored the implementation of the combined platform on real samples, which aids in increasing its accessibility and applicability in the field.

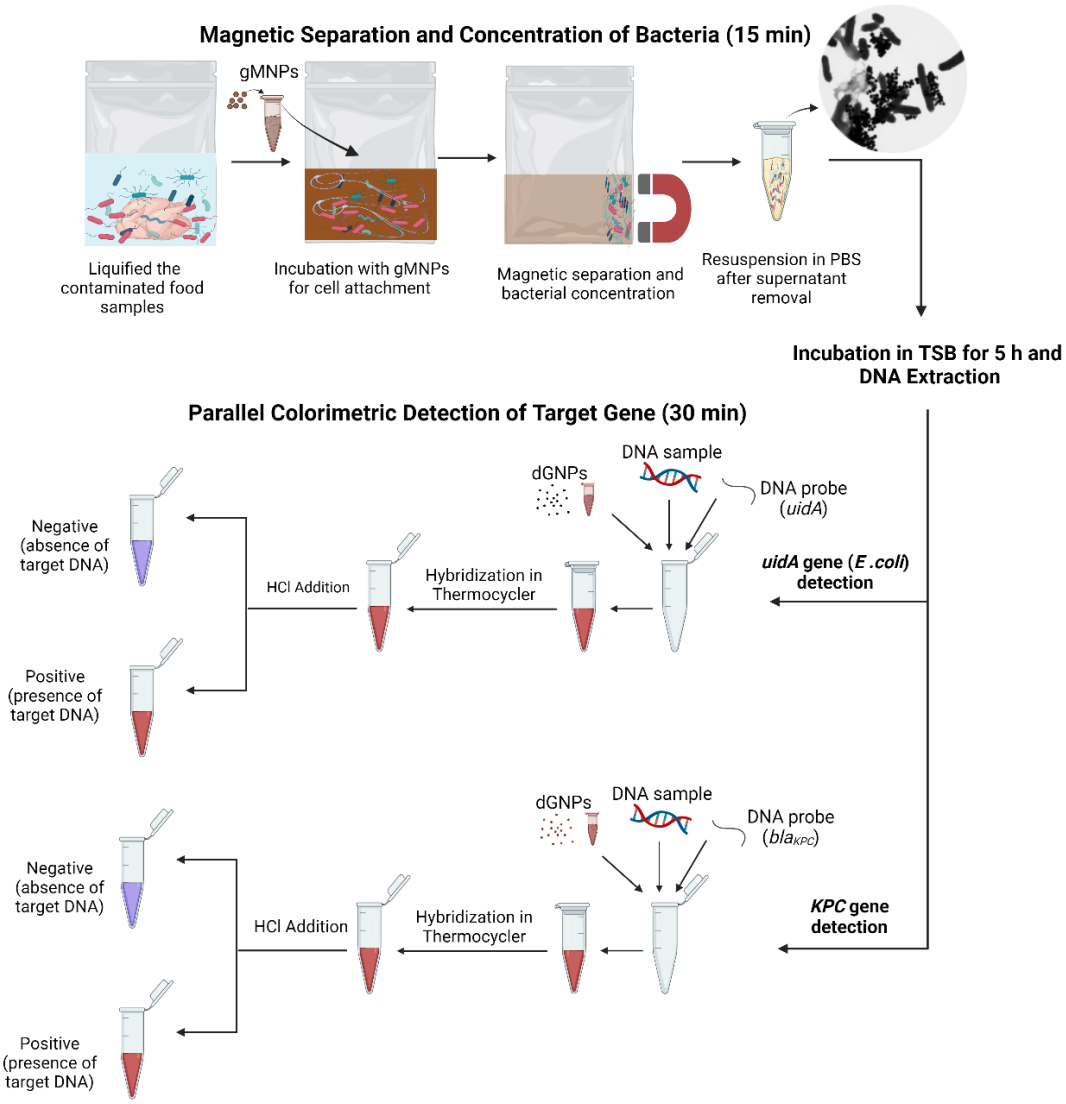

Scheme 6.1. The overall procedure for the extraction and identification of KPC-producing *E. coli* from large-volume complex matrices (created with BioRender, accessed on 7 June 2023).

6.2. Materials and Methods

6.2.1. Materials

Frozen stock cultures of KPC-producing *E. coli* (BAA-2340) and susceptible *E. coli* C-3000 (ATCC 15597) were ordered from the American Type Culture Collection (ATCC). Slant culture of an NDM-producing *E. coli* isolate was provided by the Michigan Department of Health and Human Services (MDHHS). Frozen culture of *Salmonella* enterica serovar Enteritidis, *Salmonella* enterica serovar Typhimurium, *Enterobacter cloacae*, *Klebsiella pneumoniae*, L*isteria monocytogenes*, *Bacillus cereus*, and *Staphylococcus aureus* were received from Dr. Alocilija's Nano-Biosensors Laboratory at Michigan State University (MSU). The commercial kit for genomic DNA isolation was purchased from Qiagen (Germantown, MD, USA), and oligonucleotide primers and probes were ordered from Integrated DNA Technologies (Coralville, IA). A NanoDrop One (ThermoFisher Scientific, Waltham, MA, USA) at Dr. Alolcilja's lab was used to measure wavelengths.

The chemicals of Phosphate Buffered Saline (PBS, pH 7.4), Tryptic Soy Broth (TSB) and Tryptic Soy Agar (TSA), Hydrochloric Acid (HCl), Sodium Carbonate (Na_2Co_3), Gold (III) Chloride ($AuHCl_4$), dextrin from potato starch, Sodium Dodecyl Sulfate (SDS, $NaC_{12}H_{25}SO_4$), and 11-Mercaptoundecanoic Acid (MUDA, $C_{11}H_{22}O_2S$) were provided from Sigma Aldrich (St. Louis, MO, USA). The selective agars, SUPERCARBA for CP bacteria and CHROMagar for *E. coli* were purchased by DRG International (Springfield, NJ). For Transmission Electron Microscopy (TEM) imaging, uranyl acetate stain, glutaraldehyde, and cacodylate buffer were received by the Center for Advanced Microscopy (CAM) at MSU, and TEM grids with formvar/carbon 200 mesh copper were obtained by Electron Microscopy Systems (Hatfield, PA). Further, Whirl-Pak bags (92 oz. and 18 oz.) were ordered from VWR International. Magnetic racks for magnetic separation were ordered from Spherotech (Lake Forest, IL). Food samples: a total of three packages of romaine lettuce, raw chicken breast, and raw ground beef were bought from a local grocery and kept at 4 °C before their use.

6.2.2. Rapid Extraction of Bacterial Cells from Artificially Contaminated Water and Food Samples Using gMNPs

In-house proprietary gMNPs were synthesized following a previously published procedure [63]. The synthesized gMNPs (powder) were kept at room temperature for further use;

5 mg/mL of gMNPs in the sterilized deionized water were sonicated for 30 min prior to experiments. Optimization of the magnetic extraction test was conducted earlier in Dr. Alocilja's Nanobiosensor laboratory; different amounts of gMNPs (0.5-5 mL) in a 100 mL of a buffer solution with a low-level bacterial load (approximate 10^2-10^3 CFU/mL) were tested. The gMNP-treated and non-treated (control) samples for each amount of gMNPs were separately plated and incubated at 37 ^oC for 24h. The number of colonies on the plates for control and test samples was used to calculate the gMNP-bacteria binding capacity, expressed as concentration factor (CF: CFUs in gMNP-treated test sample/CFUs in control sample)[53,58]. The CF values were the highest and consistently similar when $\geq$1 mL of gMNPs were used; thus, the optimum volume of gMNPs was earlier determined as low as 1 mL. This optimized volume has been employed to extract bacteria from food samples.

The method for bacterial extraction at large-volume samples in this study was adapted from earlier studies [53,58]. Overnight bacterial cultures were grown in TSBs for ~5 h in a shaking incubator with agitation at 125 rpm. Following serial dilution, 1 mL of 10^5 CFU/mL of each bacteria was separately inoculated in tap water (25 mL) and the food samples (25 g) in a Whirl-Pak bag: one bag for *E. coli* (S), one bag for *E. coli* (R: NDM), one bag for *E. coli* (R: KPC), and one bag for *S.* Typhimurium for each matrix, with two replicates. After one hour of incubation at room temperature for acclimation, 225 mL of PBS (pH: 7.4) was added, and samples were homogenized in a stomacher for 2 min. Two Whirlpak bags with 100 mL each from the homogenized samples (consisting of approximately 10^3CFU/mL of inoculated bacterium and natural microflora) were separated; one bag was for the control group, referring to initial bacterial load, and the second was used for the gMNP-treated sample, test group. Then, 1 mL of gMNPs were added to the 100 mL test sample, mixed, and incubated for 5 minutes. After 5-minute magnetic separation and supernatant removal, the gMNPs-cells were resuspended in 1 mL PBS. TEM imaging and standard plating method verified bacterial extraction from the final samples (1 mL). For plating, the control and test samples were plated in the selective media (CHROMagar for *Salmonella* and *E. coli* isolates and SUPERCARBA for *E. coli* (R) isolates). Also, uninoculated samples accounted for natural microflora (negative control) were conducted similarly; gMNP-treated and control samples were plated on non-selective (TSA) media to confirm the presence of natural microflora in the food samples. The plates were incubated at 37 ^oC for 24-48 h; colonies on selective and non-selective media were assessed for target bacteria

isolation. Further, the concentrated gMNPs-bacteria mixture after short enrichment was followed by DNA extraction, which was then used for the rapid detection of target bacteria by the plasmonic biosensor. The whole experiment was conducted in triplicates for each matrix.

6.2.3. Microscope Imaging

Observation of pure gMNP solution and the gMNPs-bacteria interaction from buffer solution, water, and food samples employed using TEM (JEM-1400 Flash, Jeol, Tokyo, Japan) using the standard negative-staining procedure [58]. Briefly, the gMNPs-bacteria mixture was suspended in 100 µL of the buffer (2.5% glutaraldehyde + 0.1M cacodylate buffer) after magnetic separation. A drop of 5 µL from the suspension mixture was placed onto the grid, and 5 µL of 0.5 % uranyl acetate was dropped for the staining. The samples were then loaded into the holder and observed under magnification of 1000-25000 x.

6.2.4. Genomic DNA Extraction, Oligonucleotide Probes and Primer Design

Extraction of genomic DNA was achieved using the QIAamp kit following manufacturer instructions. The gMNPs-bacteria mixture (0.5 mL) from inoculated and uninoculated (negative control) samples were first transferred into TSBs (4.5 mL) with two replicates and then incubated for approximately 5 hours at 37 °C for short enrichment. The total volume of 5 mL was then used for the genomic DNA isolation, along with some modifications for removing gMNPs [57]. The extracted DNA samples' quality and quantity were determined using the Nanodrop spectrophotometer, accepting $A_{260/230}$ and $A_{260/280}$ ratios between 1.8 and 2.2 for biosensor assays and PCR tests. The oligonucleotide probes and primers were designed to specifically target *E. coli* (*uidA*) and KPC-producing bacteria (bla_{KPC}), as listed in Table 6.1. The presence and absence of bla_{KPC} and *uidA* genes in the same samples were verified using the PCR method, using the protocol from earlier published studies [64,65].

Table 6.1. The primer and probe sequences.

Gene	Assay	Sequence (5'-3')	Ref.
*uid*A	Biosensor	Probe: CAATGGTGATGTCAGCGTT	[56]
	PCR	Primers: F- GCAGTCTTACTTCCATGATTTCTTTA R- TAATGCGAGGTACGGTAGG	
bla_{KPC}	Biosensor	Probe: GGTGTGTACGCGATGGATACCGGCTCAGGCGCAACTGTA	[41]
	PCR	AGTTACCGCGCTGAGGAGCG Primers: F- CGGTGTGTACGCGATGGATA R- TCCGGTTTTGTCTCCGACTG	

6.2.5. Synthesis of dGNPs and Plasmonic Biosensor Design

The synthesis of dextrin-coated gold nanoparticles (dGNPs) was conducted using an alkaline method procedure [66]. The synthesized dGNPs were first confirmed with their wine-red color and an absorption maxima at around 520 nm, along with their size (diameter) by TEM. The dGNPs were then surface-functionalized by 25 μM MUDA and resuspended in 0.1 M borate buffer. The dGNPs were kept at 4 °C for further use; a new synthesis or surface modification was not necessary prior to each experiment.

The biosensor assay was adapted from the following procedure [39]. The MUDA-coated dGNPs (5 μL), 25 μM aminated DNA probe (5 μL), and genomic DNA sample (10 μL) were mixed in a single tube, followed by DNA denaturation and annealing in a thermocycler (serving as a heating block). After hybridization, 0.1 M HCl was added into the tubes to induce dGNPs' aggregation; dGNPs in the absence of target DNA turn from red to purple or blue, with a right shift in absorption maxima. In the presence of the target gene, dGNPs maintain their red color and absorption maxima at close to 520 nm. The stability and agglomeration (aggregation) of the dGNPs were measured using absorbance spectra in the visible wavelength and quantified utilizing absorbance ratio at 625 nm and 520 nm ($A_{625/520}$) [41,56].

The successfully working biosensor was earlier developed to detect *E. coli* using the *uidA* probe [56] and identify KPC-producing bacteria regardless of bacterial type using the bla_{KPC} probe from pure cultures [41]. This study implemented the two biosensors to detect specific ARB (CP bacteria: KPC-producing *E. coli*) from pure cultures and matrices. This study first tested the *uidA* biosensor on more bacteria types for its specificity to detect *E. coli* isolates; each trial had series of 20 ng/uL of DNA of each target (T) sample (a carbapenem-susceptible *E. coli* (S), two carbapenem-resistant *E. coli* (R: NDM and R: KPC)) and each non-target (NT) sample (*S.* Typhimurium, *S.* Enteritidis, *K. pneumoniae*, *E. cloacae*, *B. cereus*, *L. monocytogenes*, and *S. aureus*), along with negative control (NC: nuclease free-water) sample. Each T, NT, and NC sample was mixed with the dGNPs and the specific probe, followed by the heating cycle for the probe-DNA hybridization. Images of tubes and the absorbance spectra were obtained after 5 min of HCl addition. Following the *uidA* biosensor, the bla_{KPC} biosensor was further used to differentiate KPC-producing *E. coli* from susceptible *E. coli* (S) and non-KPC-producing resistant *E. coli* (R: NDM), along with negative control. The qualitative (tube images) and quantitative results (absorbance spectra) of each biosensor were separately analyzed and then

verified with PCR tests using the *uidA* and bla_{KPC} primers. Experiments were conducted in triplicates.

6.2.6. Parallel biosensing KPC-producing *E. coli* from Water and Food Samples

The *uidA* and bla_{KPC} biosensors were further parallelly implemented to detect KPC-producing *E. coli* from matrices (the contaminated water and food samples) to show the applicability of this platform. As aforementioned, one sample was inoculated with *E. coli* (R: KPC), one with *E. coli* (R: NDM), one with *E. coli* (S), and one with *S.* Typhimurium, and one with no inoculation to account for natural microflora. Bacterial extraction using gMNPs was performed in these samples consisting of approximately 10^3 CFU/mL of inoculated bacterium and natural microflora. Following magnetic extraction, the extracted cells were incubated for 5 h at 37 ^{o}C for their genomic DNA isolation. The extracted DNA samples from each group theoretically comprise DNA of inoculated bacteria and natural microflora (mixed bacteria group). The target DNA concentration in the sample is unknown; all samples' DNA concentrations were standardized based on the lowest DNA concentration or DNA concentrations of uninoculated samples. Then, both *uidA* and bla_{KPC} biosensors were used to detect the KPC-producing *E. coli* (Table 6.2), with three replicates. First, the *uidA* biosensor specific to *E. coli* was used for all DNA samples (each target sample, non-target sample, and natural microflora). Herein, *Salmonella* enterica was used as a non-target due to their close relationship with *E. coli*; both belong to the same family (Enterobacteriaceae) and are associated with foodborne outbreaks [67].

Table 6.2. Target and non-target samples from water and food samples for the parallel biosensor.

***uidA* and bla_{KPC} biosensors**	***uidA* biosensor for *E. coli***		**bla_{KPC} biosensor for KPC-producing bacteria**	
Uninoculated samples (control group)	Inoculated samples		Inoculated samples	
Natural microflora (NF)	Target	Non-target	Target	Non-target
	E. coli (S) *E. coli* (R: NDM) *E. coli* (R: KPC)	*S. Typhimurium*	*E. coli* (R: KPC)	*E. coli* (S) *E. coli* (R: NDM)

Meanwhile, the bla_{KPC} biosensor was tested to identify the target bacteria (*E. coli* (R: KPC)) on the DNA samples. After hybridization steps and HCl addition, visual results and absorbance spectra of dGNP's aggregation were analyzed. The *uidA* and bla_{KPC} biosensor results

were further confirmed with PCR amplification using the uidA and bla_{KPC} primers. The biosensor-based detection assays were conducted in triplicates for each matrix.

6.2.7. Statistical Analysis

In this study, each experiment was conducted in triplicates; quantitative data were presented with mean and standard deviations in each bar graph. Statistical analysis of each biosensor results (absorbance ratio) of the target, negative control, non-target, and natural flora (control) samples were separately performed at a 95% confidence interval, using the Kruskal-Wallis H test followed by post-hoc Dunn's test.

6.3. Results and Discussion

6.3.1. Successful Extraction of *E. coli* from PBS, Water, and Foods using gMNPs

The as-prepared solution of gMNPs in a tube and its electron micrograph is depicted in Figure 6.1a. The characteristics of gMNPs in terms of superparamagnetic properties (particles movement in external magnetic field), particle morphology (roughly spherical and in the range of ~40-300 nm in diameter), and positive surface charge (~20 mV) was further detailed in our previous study [58]. Successful binding between gMNPs and bacteria (*E. coli* (S) and *E. coli* (R)) in PBS was first visualized using TEM, as shown in Figures 6.1b, 1c, and 1d. Multiple gMNPs are seen binding to bacterial cells, possibly enhancing the capture capacity. In addition, gMNPs binding with susceptible and resistant *E. coli* cells was usually observed in some portion along the curved ends of the cell surface, confirming earlier work [58]. Similar binding in various bacterial types, such as *S. Enteritidis*, generic and pathogenic *E. coli* strains, and *L. monocytogenes*, was seen in earlier studies [42,53,56,57,68].

The gMNPs-cell attachment has been hypothesized to be a function of the Brownian motion of cells, electrostatic interactions between negatively charged-bacterial cells and positively charged-gMNPs, and glycan- lectin-based site-specific binding by hydrogen bonds and van der Waals interaction [42,52,68]. The nature of bacterial cells and their cell wall components could affect their surface charge and their cell attachment to surfaces (receptor-ligand interaction); the gMNP-bacteria binding capacity defined as concentration factor (CF) was variable depending on bacterial type [42,53]. For instance, the gMNP-bacteria binding capacity was found to be different in susceptible *E. coli* (CF: 5.2) and resistant *E. coli* (R: KPC and NDM) (CF: 2.1 and 1.3, respectively) from buffer solution, which could be related with

difference in surface charge and cell wall characteristics of resistant cells [58]. In addition, possible factors, such as bacterial load (10^2-10^7 CFU/mL) and environment pH (3-9), on the gMNP-bacteria interaction were also observed; higher CF at lower bacterial load (10^2-10^3 CFU/mL) and ph (<7) environment were displayed [53,58]. Specifically, the mean CF for *E. coli* (S) was above 5 at 10^2–10^3 CFU/mL of bacterial load, following a linearly decreasing trend as bacterial concentration increased, approximately 2 at 10^7 CFU/mL. [58]. On the other hand, the mean CF values of both *E. coli* (R) isolates were above 1 at low bacterial concentrations (10^2–10^3 CFU/mL) but less than 1 at higher concentrations (10^6–10^7 CFU/mL), most likely due to saturation effect. Notably, *E. coli* (S) and *E. coli* (R) isolates displayed the highest CF at low concentrations (10^2–10^3 CFU/mL) [58], promising the applicability of bacterial extraction at low concentrations in matrices.

Confirmation of the successful bacterial isolation from the buffer solution was followed by their isolation from the contaminated chicken breast, ground beef, lettuce, and tap water. TEM micrographs are shown in Figures 6.1e, 1f, 1g, and 1h, respectively. While the tested food samples' microstructures are relatively more complex than PBS and water, they did not prevent the gMNPs-bacterial cell binding. However, the non-specific gMNPs could lead to complications in isolating any bacteria from natural microflora and food microparticles, which can influence the binding capacity of the bacteria of interest. The target bacterial capture from matrices was confirmed with selective plating methods. For instance, lettuce samples were rich in natural microflora, and gMNPs captured lower target bacteria compared to chicken and beef samples, confirming earlier works [53,58]. Elsewhere, higher protein and fat amounts in chicken and beef samples, such as microparticles attached to bacterial cells and gMNPs seen in Figures 6.1e and 1f, could affect the binding. Overall, the average CF of *E. coli* (S) and *E. coli* (R) isolates in the water and food samples was similar, ranging from 1-3 depending on matrix type, as mentioned previously, confirming earlier work [58]. Further, earlier reports have illustrated the binding between gMNPs and bacterial cells in other complex foods: *E. coli* from spinach and lettuce samples [56] and *S.* Enteritidis from cucumber and melon samples [57]. Previous studies have also shown gMNPs to successfully extract *E. coli* O157 from spinach, flour, romaine lettuce, and chicken salad, and *L. monocytogenes* and *S. aureus* from deli ham, romaine lettuce, sausage, and milk [53]. In another study, similar MNPs (glycan-cysteine coated) were used to extract *L. monocytogenes*, *E. coli* O157:H7, and *S.* Enteritidis from apple cider, whole milk, and

homogenized eggs [68]. However, it should be noted that bacterial extraction using gMNPs in these studies was variable, depending on bacterial type and matrix type.

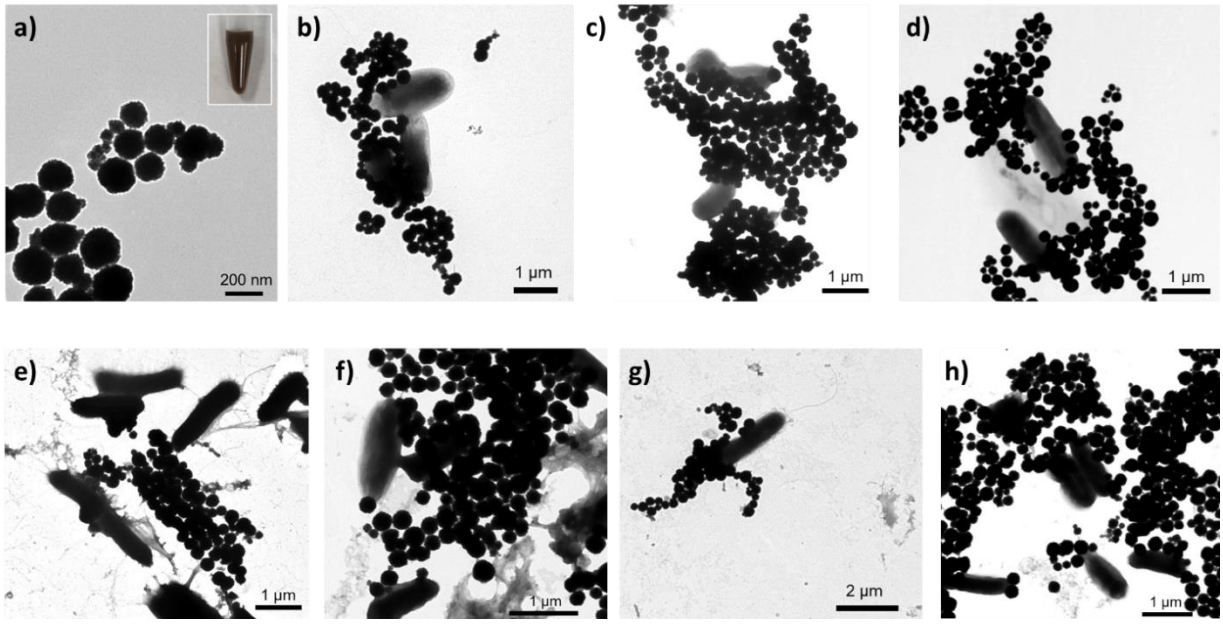

Figure 6.1. TEM images of gMNPs-bacterial cells interaction from buffer and food and water samples: a) pure gMNPs with as prepared solution, b) gMNPs-*E. coli* (S), c) gMNPs- *E. coli* (R: KPC), d) gMNPs- *E. coli* (R: NDM), e) gMNPs-bacteria from chicken breast, f) gMNPs-bacteria from ground beef, g) gMNPs-bacteria from romaine lettuce, and h) gMNPs-bacteria from tap water.

Bacterial extraction using other non-specific MNPs was further seen in the literature. For instance, low concentrations of *E. coli* from buffer solution were extracted using positively charged MNPs [48]. In another study, aminated MNPs were used to extract *E. coli*, *S. lutea*, *S. aureus*, and *P. aeruginosa* from buffer solution, river and lake water, grape juice, and green tea [69]. Apart from pathogen extraction from food samples, a few examples of extraction of ARB from clinical samples have been encountered in the literature but have used recognition ligands. For instance, antibody-based MNPs were used to isolate carbapenem-resistant *A. baumannii* (CRAB) from buffer solution and sputum [70] and methicillin-resistant *S. aureus* (MRSA) from nasal swab [50]. Lectin-silver-coated MNPs extracted *E. coli* and MRSA and *E. coli* from buffer [48,49], and vancomycin-coated MNPs successfully extracted CRE: *K. pneumoniae* and *E. coli* from buffer and urine samples [51].

Overall, bacterial extraction and concentration from different matrices using the non-selective MNPs were variable, which could be associated with MNP coatings, bacterial types, natural microflora, chemical constituents, and physical microstructure of matrices. This work

highlighted the use of gMNPs to isolate susceptible and resistant bacteria from various matrices in the presence of natural microflora and food microparticles, showing their broad applicability. This study further confirmed that gMNPs contribute toward the simple and rapid isolation of ARB, specifically CP *E. coli*. For specific detection of target bacteria, a rapid detection method can be further conducted. Since their affordable and rapid diagnosis is equally significant, along with rapid and efficient extraction. To achieve this, a plasmonic biosensor was designed for feasibility. The following part focused on the identification of *E. coli* (R: KPC) using parallel plasmonic biosensors.

6.3.2. Characterization of dGNPs and Principle of Plasmonic Biosensor

The characteristics of dGNPs and the principle of the plasmonic biosensor are described in Figure 6.2. The synthesis of dGNPs was initially verified by their wine-red appearance, which is a result of their small size of ~30 nm. The size was also confirmed by visualization in TEM (Fig. 2a), which showed the maximum absorbance peak at approximately 520 nm. For the biosensor assay, the synthesized dGNPs were surface-modified with MUDA, which enables their GNP-probe functionalization. The COOH- groups on the surface-modified dGNPs interact with the -NH2 groups of the aminated probe with a non-covalent bound. Notably, the surface modification did not impact their color and size, confirmed with maximum absorbance at around 520 nm. Overall, the dGNPs were stable under the following surface modification and heating cycles or in the presence of DNA, as confirmed in our previous work [41,56].

This biosensor was performed with negative control (NC), target DNA (T), and non-target DNA (NT) at the same DNA concentration (20 ng/µL) using the bla_{KPC} probe. As earlier mentioned, an assay typically included mixing DNA samples, surface-modified dGNPs, and an aminated probe, followed by a heating cycle for probe hybridization. After HCl addition, the stability of dGNPs was used for the detection of target DNA since its conjugation with probes on dGNPs results in the protection of dGNPs against aggregation. This allows the dGNPs to maintain their dispersed state; thereby, the target samples are in red color (Fig. 2b). The absence of a target gene in non-target and negative control samples readily exposes the dGNPs to HCl, resulting in their aggregation and a change of color to blue or purple (Fig. 2c), confirming earlier reports [71,72]. The stability and aggregation of dGNPs associated with a visible color change can be further determined as a quantitative signal spectrophotometrically (Fig. 2d).

The principle of this biosensor is further illustrated in Fig. 2e. This biosensor concept depends on the surface plasmon resonance (SPR) of GNPs as a result of the coherent oscillation of free electrons in a colloidal solution [41]. The GNPs' red color depends on the distribution of the electrostatic repulsion among negatively charged GNPs. The dispersed GNPs give spectra around 520 nm under plasmon excitation [41,71]. GNPs' agglomeration is a result of the distortion of the electrostatic repulsion, which might be due to charge neutralization once GNPs react with the acidic solution [71]. This aggregation leads to a right shift in their absorbance spectrum (~625-630) because of the distance-dependent nature of the SPR [71]. The absorbance ratio at 625 nm and 520 nm ($A_{625/520}$) was further used to quantify the level of dGNPs' aggregation.

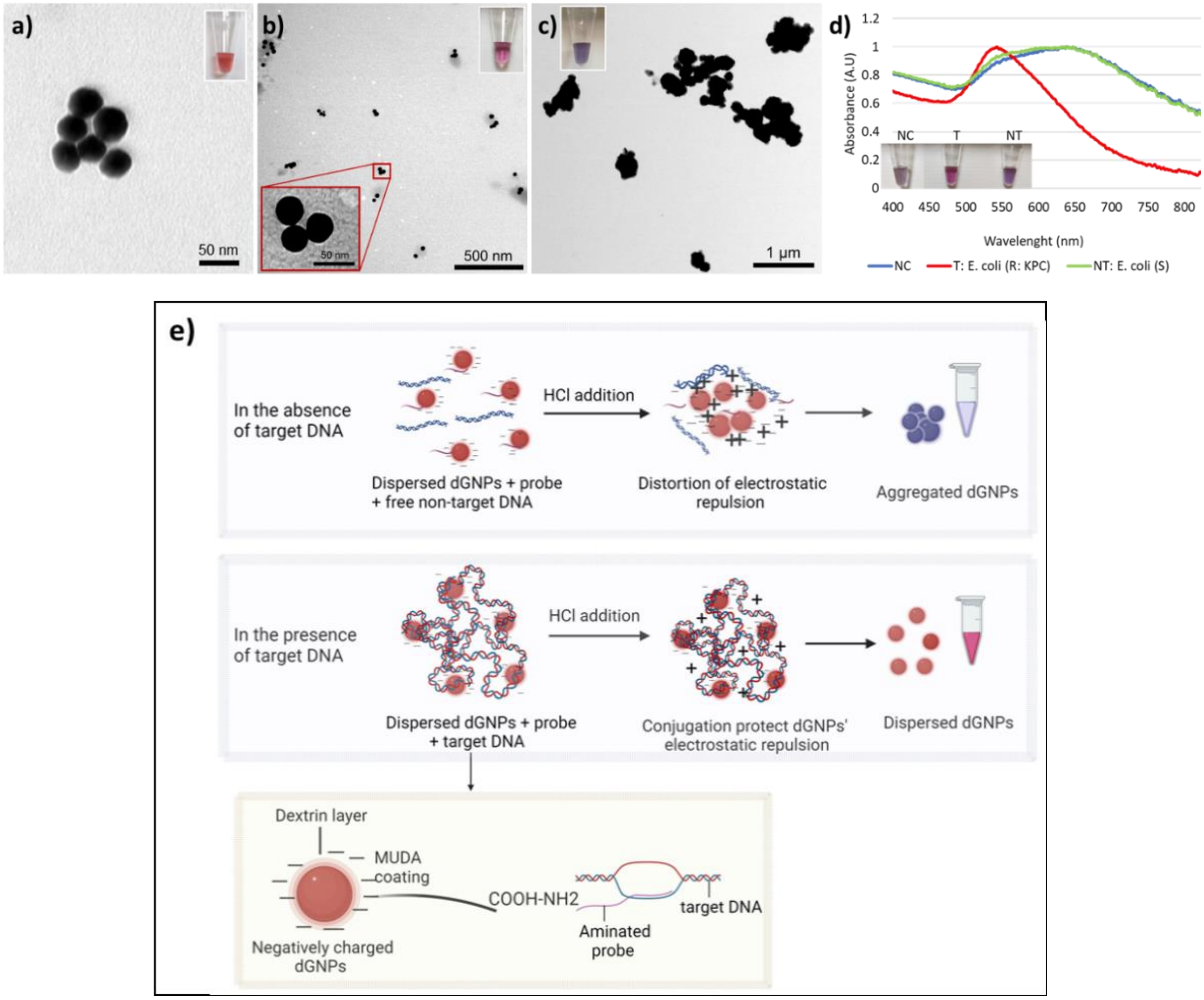

Figure 6.2. The proof-of-concept of the plasmonic biosensor: **a)** TEM images of pure dGNPs, **b)** TEM micrograph of the target (T) samples, **c)** TEM micrograph of non-target (NT) samples, **d)** absorbance spectra result with T, NT, and negative control (NC), **e)** scheme for the principle of this biosensor created with BioRender, accessed on 7 July 2023).

Optimization of the biosensor was conducted in the previous study for the detection of *E. coli* [56] and KPC-producing bacteria [41]. The optimal conditions were found to be 0.1 M HCl with a 5 min response time. Further, our previous studies have shown the successful detection at different target and non-target DNA concentrations (ranging from 20 to 1 ng/µL by a factor of two); a dilution study revealed statistically significant differences between target DNA at as low as 2.5 ng/uL and non-target at 20 ng/uL [39,41]. In addition, the stability of dGNPs was clearly seen at higher target DNA concentrations (10-40 ng/µL), along with the lower absorbance ratio [39,41,56]. These studies further proved that a sufficient level of target DNA protects GNPs' aggregation; the lower detection limit was found to be 10 ng/µL for the *uidA* biosensor [56] and 2.5 ng/µL for the bLa_{KPC} biosensor [41]. This work utilized the two biosensors to detect the KPC-producing *E. coli* from pure cultures and matrices.

6.3.3. Detection of KPC-Producing *E. coli* Using *uidA* and bla_{KPC} Probes

The developed biosensors were separately tested on target (T) and non-target (NT) DNA samples isolated from pure cultures. *E. coli* detection was first tested using the *uidA* probe. This assay included three target samples and seven non-target samples at 20 ng/µL of DNA concentration, along with a negative control (NC) sample. Figure 6.3a illustrates the results from the *uidA* biosensor with the average absorbance ratio, $A_{625/520}$, and tube images. The *uidA* biosensor successfully detected the three target samples (*E. coli* (S), *E. coli* (R: KPC), and *E. coli* (R: NDM)) with the lowest $A_{625/520}$ and minimal dGNP aggregation. In contrast, the non-target samples illustrated relatively higher aggregation, confirmed by higher $A_{625/520}$ and visual results (blue or purple). The $A_{625/520}$ values of each target sample were significantly lower ($p < 0.05$) compared to NC and seven NT samples.

Following *E. coli* identification, the bla_{KPC} biosensor was used to identify the presence of the KPC gene. In this assay, a negative control, a target sample (*E. coli* (R: KPC)), and two non-target samples (*E. coli* (S) and *E. coli* (R: NDM)) at a concentration of 20 ng/µL of DNA were used. Figure 6.3b shows the bla_{KPC} biosensor results with tube images and the average $A_{625/520}$. The bla_{KPC} biosensor successfully detected the target, which was in red appearance and had a lower $A_{625/520}$, while the negative control and non-target samples showed a blue or purple appearance with a higher $A_{625/520}$. The $A_{625/520}$ values of the target sample were significantly lower ($p < 0.05$) than the $A_{625/520}$ values of the NC and NT samples.

The use of two biosensors offered successful detection of KPC-producing *E. coli* within an hour without the necessity of a complex and or tedious process. The biosensor results were further verified with the PCR tests using the *uidA* and bla_{KPC} primers (Fig. 3 (c & d); the band on gel electrophoresis images confirmed the presence of target gene/s in these samples. Our method provides the advantage of rapidity and ease of implementation in low-resource settings.

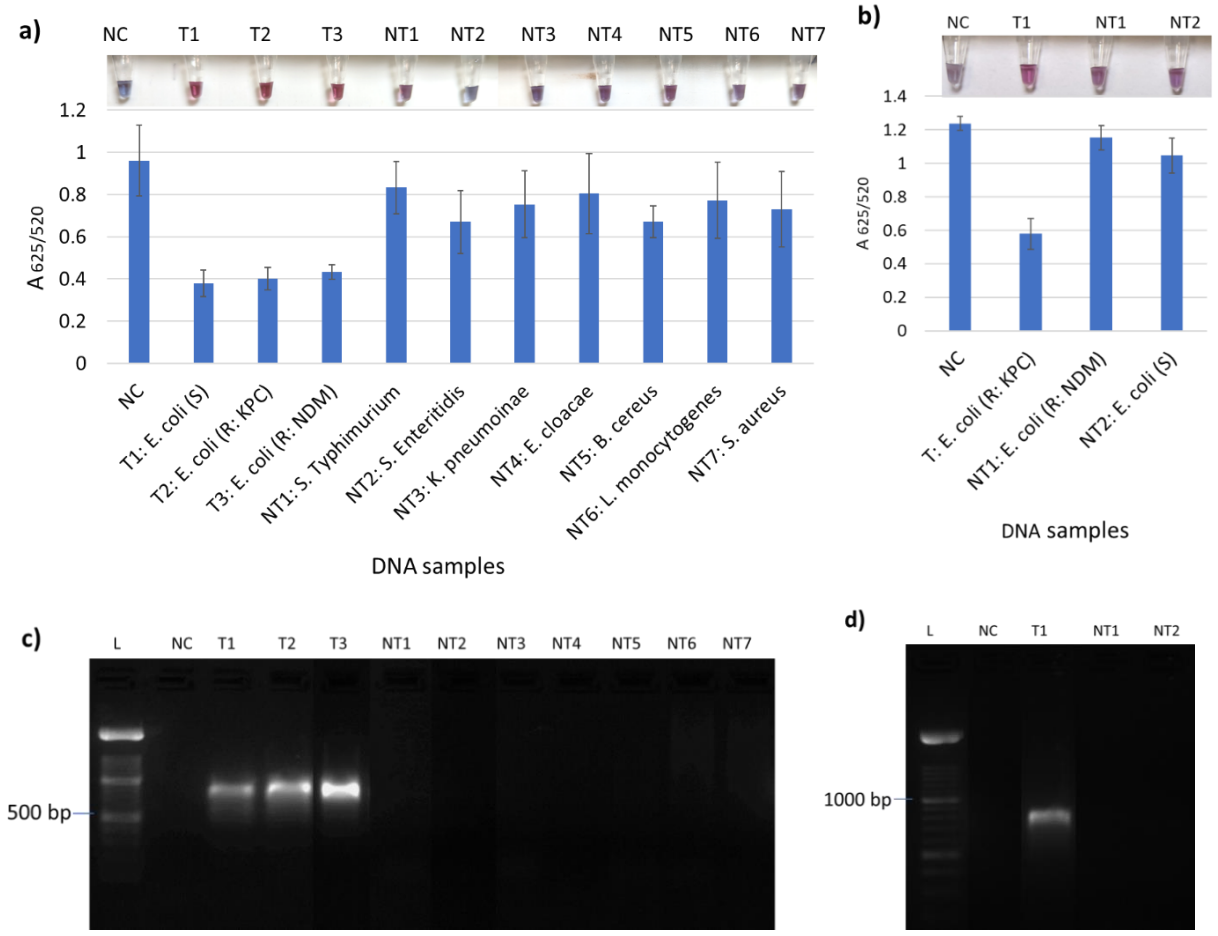

Figure 6.3. Plasmonic biosensor detection: a) mean absorbance ratio at 625 nm and 520 nm ($A_{625/520}$) of the detection of *E. coli* isolates using the *uidA* probe, along with a set of tube images and b) average $A_{625/520}$ of the detection of KPC-producing *E. coli* using the bla_{KPC} probe, along with a set of tube images, c) and d) PCR amplification results of the same samples using *uidA* and bla_{KPC} primers, respectively.

The successful detection using *uidA* and bla_{KPC} probes confirmed our previous works for *E. coli* and KPC-producing bacteria. The *E. coli* C-300 (*E. coli* (S)) was detected using the *uidA* probe against *S.* Enteritidis, *K. pneumoniae*, and *E. cloacae* [56], and 11 KPC-producing bacteria were detected with bla_{KPC} probes against 32 non-target bacteria [41]. Similar colorimetric assay further differentiated *Salmonella* enterica from *E. coli*, *E. cloacae*, *K. pneumoniae*, *L.*

monocytogenes, and B. cereus using an *invA* probe [57], detected *E. coli* O157 against *E. coli* C-3000, *B. cereus*, *S.* Enteritidis, and *L. monocytogenes* using *StxA1* probe [39], and identified *S. aureus* from *B. cereus*, *E. coli* O157, and *S.* Enteritidis using multi-probe [73], without the need for PCR amplification, within 30 min. These studies showed that the plasmonic biosensor is reproducible and repeatable, increasing its applicability and accessibility in the field. To test the applicability of this platform with real samples, matrices with natural microflora and complex microparticles were used. Thus, the following section focuses on the detection of target bacteria in artificially contaminated water and foods.

6.3.4. Parallel Detection of KPC-producing *E. coli* from Foods and Water

Identifying bacteria directly from matrices with a short enrichment of the extracted samples is crucial. Magnetically extracted bacterial cells from the uninoculated and inoculated food and water samples with *S.* Typhimurium, *E. coli* (S), *E. coli* (R: NDM), and *E. coli* (R: KPC), were grown in the TSBs for 5 h and followed by DNA extraction. The extracted DNA samples from each matrix were separately tested with the *uidA* and bla_{KPC} biosensor to identify target bacteria, all *E. coli* isolates and KPC-dependent resistance, respectively. First, Figures 6.4a and 4b shows the *uidA* biosensor results: bar graph with an average of $A_{625/520}$ and standard deviation, along with tube images and PCR results for all food and water samples. Target samples (T1: *E. coli* (S), T2: *E. coli* (R: KPC), and T3: *E. coli* (R: NDM)) for *uidA* biosensor displayed lower $A_{625/520}$, minimal aggregation of dGNPs, with maintenance of red color. However, negative control (NC), non-target (NT), and natural microflora (NF) samples displayed higher $A_{625/520}$, which is a result of significant aggregation of dGNPs and purple or blue color. The $A_{625/520}$ values of each target sample (T1: *E. coli* (S), T2: *E. coli* (R: KPC), and T3: *E. coli* (R: NDM) were found to be significantly different ($p < 0.05$) compared to the $A_{625/520}$ values of NT, NF, and NC for all food and water samples. The *uidA* biosensor successfully detected *E. coli* isolates from water and food samples.

The bla_{KPC} biosensor was parallelly used to identify the KPC-dependent carbapenem resistance among the *E. coli* isolates: *E. coli* (R: KPC), *E. coli* (S), and *E. coli* (R: NDM) for each matrix. DNA samples from NF were also included as a control in this assay. Figures 6.4c and 4d illustrates the bla_{KPC} biosensor results, with average $A_{625/520}$ and standard deviation, along with tube images and PCR results for all food and water samples. The lower $A_{625/520}$ in the target sample (T: *E. coli* (R: KPC), confirmed the minimal aggregation of dGNPs with the remaining

red color. The non-targets (NT1: *E. coli* (R: NDM) and NT2: *E. coli* (S)), NF, and NC all showed significant aggregation of dGNPs, with a color change to purple or blue. The difference of the $A_{625/520}$ between the target sample and that of NT, NF, and NC for all food and water samples was significant ($p < 0.05$). The *bla*$_{KPC}$ biosensor successfully detected the KPC-producing bacteria from water and food samples.

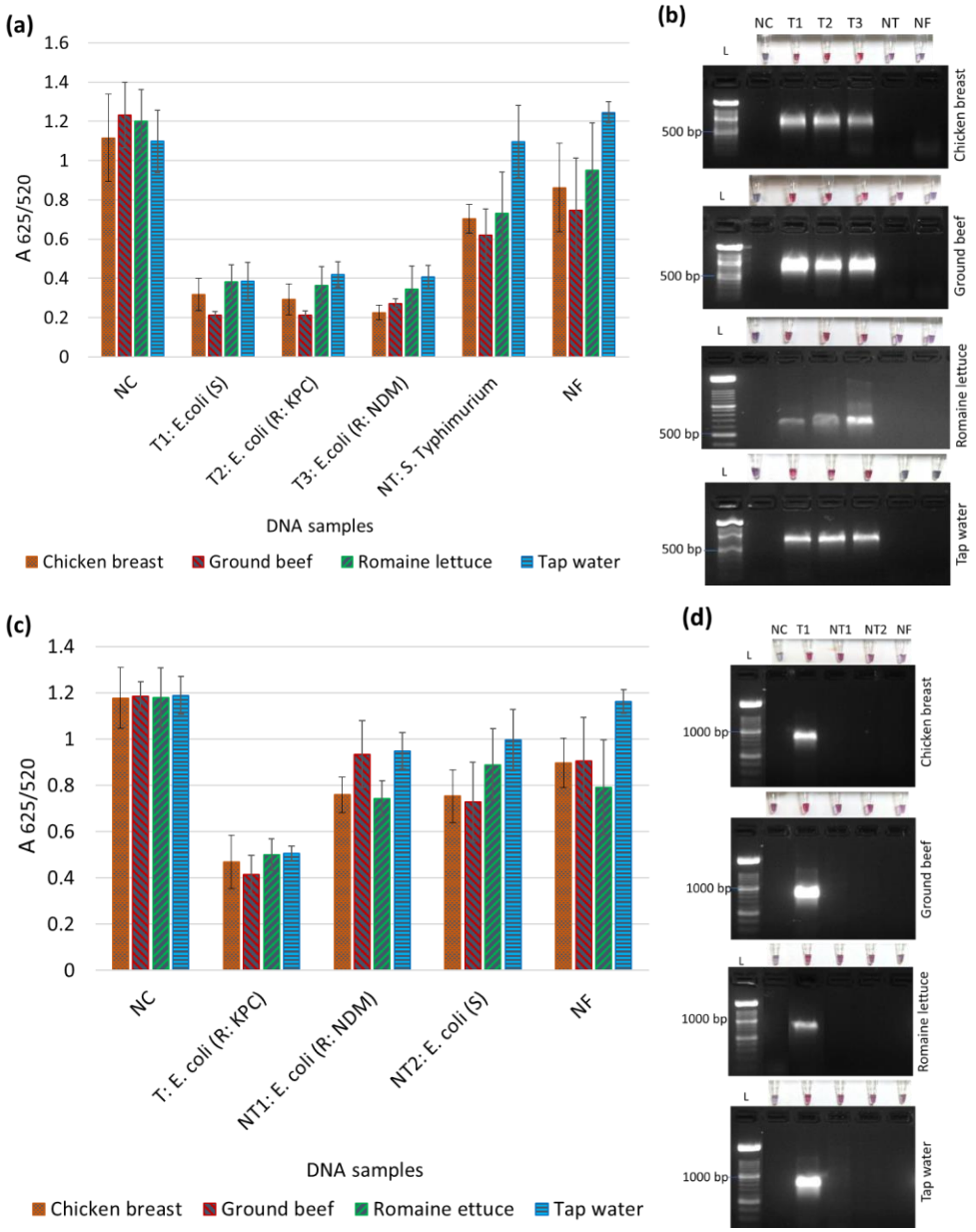

Figure 6.4. Detection of KPC-producing *E. coli* from chicken breast, ground beef, romaine lettuce, and tap water: a) and c) Average absorbance ratio ($A_{625/520}$) of negative control (NC), target (T) and non-target (NT), and natural microflora (NF) from *uidA* and *bla*$_{KPC}$ biosensor, respectively (N: 36); b) and d) biosensor colorimetric results in a set of tubes and gel electrophoresis results of the same sample.

Overall, the use of *uidA* and bla_{KPC} biosensors offered the specific detection of KPC-producing *E. coli* from water and foods. This study further showed that the presence of DNAs from natural microflora did not significantly impact the absorbance ratio in target testing. A lower ratio indicates a lower aggregation level of dGNPs, confirming the presence of sufficient target DNA samples from each matrix. To confirm these biosensor results, the standard PCR tests were conducted on the same DNA samples to determine the absence or presence of the target genes. As seen in Fig. 4 (b & d), images from gel electrophoresis confirmed the presence of target genes, indicating its role in the stability of dGNPs in target samples from food and water samples. Only three target samples (*E. coli* (R: KPC), *E. coli* (S), and *E. coli* (R: NDM) displayed PCR amplification of the *uidA* gene for *E. coli* confirmation, clearly seen with a band. Similarly, only the target sample (*E. coli* (R: KPC) displayed PCR amplification of the bla_{KPC} gene for KPC-producing bacteria confirmation. In contrast, no band can be seen for all NT, NF, and NC samples, confirming no amplification. Overall, the PCR results highlighted that the use of the integrated platform offers successful extraction and detection of the target bacteria in the presence of natural microflora, which further confirmed the specificity of the biosensors.

Our study showed successful detection of KPC-producing *E. coli* from food and water samples using the parallel biosensor within one hour. The integrated gMNP-based extraction and dGNP-based detection were completed within <7 h. This combined assay offers rapid, simple, and efficient detection directly from real samples. Table 6.3 summarizes the techniques used to extract and detect pathogens (specifically *E. coli*) and ARB from matrices and how this work is compared. Many rapid methods require equipment and data analysis, increasing costs and limiting their accessibility and field applicability [34,74–77]. Lateral-flow biosensors have been developed to eliminate costly equipment; however, they still use antibodies for magnetic extraction or need overnight incubation for the detection from matrices, increasing the detection time and cost [70]. In rapid colorimetric tests, some assays still require PCR amplification for the detection of target bacteria [78]. As seen in Table 3, the detection of ARB or CRE from samples has not been well-documented, especially from food and water samples.

Studies show that CRE has been found in water sources and foods [2,8]. For example, CRE (*K. pneumoniae, E. cloacae, E. coli*, and *Citrobacter freundii*) were isolated from river samples [79–83], KPC and VIM-producing *E. coli* in several wastewater treatment plants [84], and OXA-48 producing CRE in tap water samples [83]. Moreover, CP bacteria were found in

meats, seafood, and vegetables [21,85–90]. Bacterial contamination in food varies by type, location, and production; however bacterial concentration is hardly documented in the literature. Further, their direct extraction and detection from water and food samples have not been explored. This may be related to antimicrobial-resistant profiles usually being tested on pure cultures after isolating and identifying pathogens from matrices, which takes several days [2]. Thus, simple, rapid, and efficient extraction of ARB directly from real samples is extremely needed for their quick detection and prevention of possible outbreaks.

Our designed platform is the first study for detecting CP-CRE, including CP *E. coli*, directly from food and water samples. Although food samples are usually associated with a high amount of natural microflora and microparticles, gMNPs successfully captured bacteria. These extracted samples were plated on selective media to verify the successful extraction of target bacterial cells (Fig. A.1), determining the target bacterial capture using average colony counts. This platform successfully detected approximately 10^3 CFU/mL of the target bacteria magnetically extracted from the foods and water after only 5 h incubation. Similar results were seen in earlier studies using the combined assays for successful detection of approximately 10^3 CFU/mL of *E. coli* O157 from flour and *S. aureus* from milk, deli ham, and sausage. However, these studies used a 4 henrichment step following magnetic extraction [39,73]. Notably, our previous studies displayed that the plasmonic biosensor platform successfully detected approximately 10^2 CFU/mL of *E. coli* C-3000 from romaine lettuce and spinach and *S.* Enteritidis from cut-melons and cucumbers after 4 h enrichment step [56,57]. As summarized in Table 6.3, the detection limits of many techniques mostly ranged between 10^1 and 10^6 CFU/mL, with a detection time of one hour to 24 hours. Thus, the detection limit of this study is reasonable with sort enrichment incubation and without the necessity of PCR amplification, which can be completed during workday hours.

The combined platform using carbohydrate-coated nanoparticles is noteworthy, allowing simple and rapid extraction and visual detection without the necessity of costly reagents and equipment. The gMNPs are easily prepared (one-pot synthesis), stable at room temperature for at least three years, and cost-effective; gMNP-based extraction cost was estimated to be as low as US $ 0.50 per assay [56,91], compared to other methods, such as IMS that is $5-10 for each assay and require stringent storage conditions [92]. In addition, dGNPs are easily synthesized and surface-modified, physically and chemically stable for at least three years, and cost-

effective; the material cost of the biosensor was estimated to be approximately $2 per assay, in comparison to rapid phenotypic tests ($ 2–10) and molecular methods ($23–150) per assay [33,41]. Hence, our assay is affordable and widely applicable to low-resource settings; this integrated biosensor platform can be appropriate for field and point-of-need testing studies. This platform offers significant advancement over the current assays and the opportunity for advancements and applications in ARB and their direct extraction and detection from other matrices.

Table 6.3. Techniques used to extract and detect antimicrobial-resistant bacteria (ARB) from different matrices.

Technique	Target	Matrix (Sample)	Separation Method and Time	Detection Limit and Time	Total Assay Time	Equipment Requirement	Ref.
Electrochemical biosensor	NDM-producing *C. freundii* (*bla_{NDM}*)	Pure culture	NA for bacterial separation (DNA extraction)	100 pM, following PCR amplification	NA	Yes	[34]
Electrochemical biosensor	KPC-producing bacteria (*bla_{KPC}*)	Clinical isolates	Streptavidin-coated magnetic particle-based separation (10 min)	10-100 CFU/mL	45 min	Yes	[35]
SERS	*E. coli* MRSA	Culture	Lectin-silver coated MNP-based separation (1 h)	10 CFU/mL ~1h	~2h	Yes	[49]
SERS	MRSA CRAB CRPA	Blood	PEI-modified magnetic microspheres-based separation (15 min), following overnight incubation	10^8 CFU/mL ~1h	> 1 day	Yes	[76]
Lateral flow biosensor	CRAB (*$bla_{OXA\text{-}23\text{-}like}$*)	Sputum	No separation techniques; Culture-based methods	100 fg following PCR amplification. NA for sputum samples	>1 day	No	[70]
CarbaNP test	CRE: *E. coli* and *K. pneumoniae*	Urine	Vancomycin-coated MNP-based separation (1.5 h)	10^3 CFU/mL 2h	~3.5 h	No	[51]
Electrochemical biosensor	MRSA	Nasal swab	Filtration and IMS (1h)	845 CFU/mL	~4.5 h	Yes	[50]
Colorimetric enzyme-based biosensor	MRSA	Blood Wound Swabs	NA for bacterial separation (DNA extraction and isothermal amplification (2h))	10^2-10^3 CFU/mL 1h	~3 h	No	[93]
Plasmonic biosensor	*KPC-producing bacteria (*bla_{KPC}*)*	Clinical isolates	NA for bacterial separation (DNA extraction, no PCR amplification	2.5 ng/µL, ~10^3 CFU/mL 30 min	~1h	No	[41]
MALDI-TOF MS	E. coli O157:H7	Ground beef	IMS, following 20 h pre-enrichment	2x10^6 cells/mL ~25 min	~21 h	Yes	[77]
Multiplex qPCR	*STEC*	Apple juice	Centrifugation and IMS (6.5 h)	3.34 CFU/mL ~3.5 h	~9.5 h	Yes	[75]
Plasmonic biosensor	STEC	Ground beef Blueberries	IMS following 6 h pre-enrichment	9 CFU/g, following PCR amplification	~ 9h	Yes	[78]
Plasmonic biosensor	*E. coli* O157 *E. coli*	Flour Lettuce, Spinach	gMNPs-based extraction, following 4 h pre-enrichment	10^2-10^3 CFU/mL* 30 min	~6-7 h	No	[39,56]

Table 6.3 (cont'd)

Parallel plasmonic biosensor	KPC-producing *E. coli* (bla_{KPC} and *uidA*)	Chicken breast Ground beef Romaine lettuce Tap water	gMNP-based separation (15 min), following 5h pre-enrichment	10^2-10^3 CFU/mL* 1h	<7h	No	This study

* This platform successfully detected approximately 10^2-10^3 CFU/mL of the target bacteria magnetically extracted from the foods and water after only a 4-5 h incubation. A study detailing the limit of detection from matrices was not conducted. MRSA: Methicillin-resistant *Staphylococcus aureus*, CRPA: Carbapenem-resistant *Pseudomonas aeruginosa*, CRAB: Carbapenem-resistant *Acinetobacter baumannii*, CRE: Carbapenem-resistant *Enterobacterales*, STEC: Shiga-toxin producing *E. coli*, IMS: immunomagnetic separation; gMNPs; glycan-coated magnetic nanoparticles, PEI: Polyethyleneimine, SERS: surface-enhanced Raman scattering, MALDI-TOF MS: Matrix-assisted laser desorption ionization–time-of-flight mass spectrometry; qPCR: Rea;l-time or quantitative polymerase chain reaction, NA: Not available.

6.4. Conclusion

Cost-effective, rapid, and simple detection of causative bacteria from clinical and biological matrices can aid in preventing outbreaks. Although ARB, including CRE, are found in food and water samples, their direct detection from these samples has not been explored. This study focused on extracting and detecting KPC-producing *E. coli* from tap water and complex food samples using carbohydrate-coated magnetic and gold nanoparticles. The successful detection of approximately 10^3CFU/mL of target bacteria magnetically extracted from tap water and foods was achieved after five hours of enrichment. The total turn-around time of this assay, including sample processing through gMNPs-based extraction, short enrichment, genomic DNA extraction, and dGNPs-based genomic detection, was only seven hours. This combined platform does not need DNA amplification or specific storage conditions, increasing its accessibility and applicability in limited-resource laboratories. In future studies, bacterial extraction and genomic detection processes can be improved by testing more matrices with mixed contamination and other bacteria types. With such improvements, this combined platform can offer rapid and cost-effective detection of causative bacteria, including ARB, such as extended-spectrum β-lactamase (ESBL)-producing bacteria, colistin-resistant bacteria, and other carbapenem-resistant bacteria from biological and clinical samples.

REFERENCES

[1] Dankittipong, N., Fischer, E. A. J., Swanenburg, M., Wagenaar, J. A., Stegeman, A. J., and de Vos, C. J., "Quantitative Risk Assessment for the Introduction of Carbapenem-Resistant Enterobacteriaceae (CPE) into Dutch Livestock Farms," Antibiotics, 2022, 11(2), p. 281, DOI: 10.3390/antibiotics11020281.

[2] Caliskan-Aydogan, O., and Alocilja, E. C., "A Review of Carbapenem Resistance in Enterobacterales and Its Detection Techniques," Microorganisms, 2023, 11(6), p. 1491, DOI: 10.3390/microorganisms11061491.

[3] Antimicrobial Resistance: CDC's Antibiotic Resistance Threats in the United States, 2019. Available online:https://www.cdc.gov/drugresistance/pdf/threatsreport/2019-ar-threats-report-508.pdf (Accessed:06-September-2022).

[4] WHO, "Antimicrobial Resistance," WHO (World Heal. Organ., 2021, [Online]. Available: https://www.who.int/news-room/fact-sheets/detail/antimicrobial-resistance. [Accessed: 05-Oct-2022].

[5] Rebold, N., Lagnf, A. M., Alosaimy, S., Holger, D. J., Witucki, P., Mannino, A., Dierker, M., Lucas, K., Kunz Coyne, A. J., El Ghali, A., Caniff, K. E., Veve, M. P., and Rybak, M. J., "Risk Factors for Carbapenem-Resistant Enterobacterales Clinical Treatment Failure," Microbiol. Spectr., 2023, 11(1), DOI: 10.1128/spectrum.02647-22.

[6] Capozzi, C., Maurici, M., and Panà, A., "[Antimicrobial Resistance: It Is a Global Crisis, 'a Slow Tsunami']," Ig. Sanita Pubbl., 2019, 75(6), p. 429—450.

[7] Smith, H. Z., and Kendall, B., "Carbapenem Resistant Enterobacteriaceae," StatPearls [Internet]. StatPearls Publ., 2021.

[8] Taggar, G., Rheman, M. A., Boerlin, P., and Diarra, M. S., "Molecular Epidemiology of Carbapenemases in Enterobacteriales from Humans, Animals, Food and the Environment," Antibiotics, 2020, 9(10), pp. 1–22, DOI: 10.3390/antibiotics9100693.

[9] Queenan, A. M., and Bush, K., "Carbapenemases: The Versatile β-Lactamases," Clin. Microbiol. Rev., 2007, 20(3), pp. 440–458, DOI: 10.1128/CMR.00001-07.

[10] CDC, "Healthcare-Associated Infections (HAIs):CRE Technical Information," CDC (Centers Dis. Control Prev., 2019, [Online]. Available: https://www.cdc.gov/hai/organisms/cre/technical-info.html. [Accessed: 08-Jun-2022].

[11] Mills, M. C., and Lee, J., "The Threat of Carbapenem-Resistant Bacteria in the Environment: Evidence of Widespread Contamination of Reservoirs at a Global Scale," Environ. Pollut., 2019, 255, p. 113143, DOI: 10.1016/j.envpol.2019.113143.

[12] Bonardi, S., and Pitino, R., "Carbapenemase-Producing Bacteria in Food-Producing Animals, Wildlife and Environment: A Challenge for Human Health," Ital. J. Food Saf., 2019, 8(2), DOI: 10.4081/ijfs.2019.7956.

[13] Köck, R., Daniels-Haardt, I., Becker, K., Mellmann, A., Friedrich, A. W., Mevius, D., Schwarz, S., and Jurke, A., "Carbapenem-Resistant Enterobacteriaceae in Wildlife, Food-Producing, and Companion Animals: A Systematic Review," Clin. Microbiol. Infect., 2018, 24(12), pp. 1241–1250, DOI: 10.1016/j.cmi.2018.04.004.

[14] Woodford, N., Wareham, D. W., Guerra, B., and Teale, C., "Carbapenemase-Producing Enterobacteriaceae and Non-Enterobacteriaceae from Animals and the Environment: An Emerging Public Health Risk of Our Own Making?," J. Antimicrob. Chemother., 2014, 69(2), pp. 287–291, DOI: 10.1093/jac/dkt392.

[15] Serwecińska, L., "Antimicrobials and Antibiotic-Resistant Bacteria: A Risk to the Environment and to Public Health," Water, 2020, 12(12), p. 3313, DOI: 10.3390/w12123313.

[16] Guerra, B., Fischer, J., and Helmuth, R., "An Emerging Public Health Problem: Acquired Carbapenemase-Producing Microorganisms Are Present in Food-Producing Animals, Their Environment, Companion Animals and Wild Birds," Vet. Microbiol., 2014, 171(3–4), pp. 290–297, DOI: 10.1016/j.vetmic.2014.02.001.

[17] FDA, "The National Antimicrobial Resistance Monitoring System, NARMS," FDA, 2023, [Online]. Available: https://www.fda.gov/animal-veterinary/antimicrobial-resistance/national-antimicrobial-resistance-monitoring-system.

[18] CDC, "Antimicrobial Resistance;Tracking Antibiotic Resistance," CDC (Centers Dis. Control Prev. Dis. Control Prev., 2021, [Online]. Available: https://www.cdc.gov/drugresistance/tracking.html. [Accessed: 05-May-2022].

[19] ECDC: EARS-Net, "Annual Report of The European Antimicrobial Resistance Surveillance Network (EARS-Net)," Surveill. Report; ECDC, 2017, [Online]. Available: https://www.ecdc.europa.eu/en/publications-data/surveillance-antimicrobial-resistance-europe-2017.

[20] Morrison, B. J., and Rubin, J. E., "Carbapenemase Producing Bacteria in the Food Supply Escaping Detection," PLoS One, 2015, 10(5), DOI: 10.1371/journal.pone.0126717.

[21] Yao, X., Doi, Y., Zeng, L., Lv, L., and Liu, J.-H., "Carbapenem-Resistant and Colistin-Resistant Escherichia Coli Co-Producing NDM-9 and MCR-1," Lancet Infect. Dis., 2016, 16(3), pp. 288–289, DOI: 10.1016/S1473-3099(16)00057-8.

[22] FoodNet, "Foodborne Diseases Active Surveillance Network (FoodNet)," CDC (Centers Dis. Control Prev., 2023, [Online]. Available: https://www.cdc.gov/foodnet/index.html. [Accessed: 02-Jun-2023].

[23] CDC, "Antimicrobial Resistance: CDC's Antibiotic Resistance (AR) Laboratory Networks," CDC (Centers Dis. Control Prev., 2021, [Online]. Available: https://www.cdc.gov/drugresistance/laboratories.html. [Accessed: 06-Jun-2022].

[24] McLain, J. E., Cytryn, E., Durso, L. M., and Young, S., "Culture-based Methods for

Detection of Antibiotic Resistance in Agroecosystems: Advantages, Challenges, and Gaps in Knowledge," J. Environ. Qual., 2016, 45(2), pp. 432–440.

[25] Syal, K., Mo, M., Yu, H., Iriya, R., Jing, W., Guodong, S., Wang, S., Grys, T. E., Haydel, S. E., and Tao, N., "Current and Emerging Techniques for Antibiotic Susceptibility Tests," Theranostics, 2017, 7(7), pp. 1795–1805, DOI: 10.7150/thno.19217.

[26] Khan, Z. A., Siddiqui, M. F., and Park, S., "Current and Emerging Methods of Antibiotic Susceptibility Testing," Diagnostics, 2019, 9(2), p. 49, DOI: 10.3390/diagnostics9020049.

[27] Takayama, Y., Adachi, Y., Nihonyanagi, S., and Okamoto, R., "Modified Hodge Test Using Mueller-Hinton Agar Supplemented with Cloxacillin Improves Screening for Carbapenemase-Producing Clinical Isolates of Enterobacteriaceae," J. Med. Microbiol., 2015, 64(7), pp. 774–777, DOI: 10.1099/jmm.0.000068.

[28] Amjad, A., Ia, M., Sa, A., Farwa, U., Malik, N., and Zia, F., "Modified Hodge Test : A Simple and Effective Test for Detection of Carbapenemase Production The Isolates Which Showed Intermediate or Susceptible Zones for Imipenem Were Tested for Carbapenemase Modified Hodge Test , as CL Recommends the MHT to Be Perform," Iran. J. Microbiol., 2011, 3(4), pp. 189–193.

[29] Lutgring, J. D., and Limbago, B. M., "The Problem of Carbapenemase-Producing-Carbapenem-Resistant-Enterobacteriaceae Detection," J. Clin. Microbiol., 2016, 54(3), pp. 529–534, DOI: 10.1128/JCM.02771-15.

[30] Cui, X., Zhang, H., and Du, H., "Carbapenemases in Enterobacteriaceae: Detection and Antimicrobial Therapy," Front. Microbiol., 2019, 10(August), pp. 1–12, DOI: 10.3389/fmicb.2019.01823.

[31] Sutherland, J. B., Rafii, F., Lay, J. O., and Williams, A. J., "Rapid Analytical Methods to Identify Antibiotic-Resistant Bacteria," *Antibiotic Drug Resistance*, Wiley, September 9, 2019, pp. 533–566, DOI: 10.1002/9781119282549.ch21.

[32] Reynoso, E. C., Laschi, S., Palchetti, I., and Torres, E., "Advances in Antimicrobial Resistance Monitoring Using Sensors and Biosensors: A Review," Chemosensors, 2021, 9(8), DOI: 10.3390/chemosensors9080232.

[33] Decousser, J.-W., Poirel, L., and Nordmann, P., "Recent Advances in Biochemical and Molecular Diagnostics for the Rapid Detection of Antibiotic-Resistant Enterobacteriaceae : A Focus on ß-Lactam Resistance," Expert Rev. Mol. Diagn., 2017, 17(4), pp. 327–350, DOI: 10.1080/14737159.2017.1289087.

[34] Huang, J. M.-Y., Henihan, G., Macdonald, D., Michalowski, A., Templeton, K., Gibb, A. P., Schulze, H., and Bachmann, T. T., "Rapid Electrochemical Detection of New Delhi Metallo-Beta-Lactamase Genes To Enable Point-of-Care Testing of Carbapenem-Resistant Enterobacteriaceae," Anal. Chem., 2015, 87(15), pp. 7738–7745, DOI: 10.1021/acs.analchem.5b01270.

[35] Gordon, N., Bawa, R., and Palmateer, G., "Carbapenem-Resistant Enterobacteriaceae Testing in 45 Minutes Using an Electronic Sensor," *Current Issues in Medicine: Diagnosis and Imaging*, 2021, pp. 1–18.

[36] Bashir, S., Nawaz, H., Majeed, M. I., Mohsin, M., Abdullah, S., Ali, S., Rashid, N., Kashif, M., Batool, F., Abubakar, M., Ahmad, S., and Abdulraheem, A., "Rapid and Sensitive Discrimination among Carbapenem Resistant and Susceptible E. Coli Strains Using Surface Enhanced Raman Spectroscopy Combined with Chemometric Tools," Photodiagnosis Photodyn. Ther., 2021, 34(March), DOI: 10.1016/j.pdpdt.2021.102280.

[37] Wong, Y. L., Kang, W. C. M., Reyes, M., Teo, J. W. P., and Kah, J. C. Y., "Rapid Detection of Carbapenemase-Producing Enterobacteriacae Based on Surface-Enhanced Raman Spectroscopy with Gold Nanostars," ACS Infect. Dis., 2020, 6(5), pp. 947–953, DOI: 10.1021/acsinfecdis.9b00318.

[38] Li, J., Wang, C., Kang, H., Shao, L., Hu, L., Xiao, R., Wang, S., and Gu, B., "Label-Free Identification Carbapenem-Resistant Escherichia Coli Based on Surface-Enhanced Resonance Raman Scattering," RSC Adv., 2018, 8(9), pp. 4761–4765, DOI: 10.1039/C7RA13063E.

[39] Dester, E., Kao, K., and Alocilja, E. C., "Detection of Unamplified E. Coli O157 DNA Extracted from Large Food Samples Using a Gold Nanoparticle Colorimetric Biosensor," Biosensors, 2022, 12(5), p. 274, DOI: 10.3390/bios12050274.

[40] Quintela, I. A., de los Reyes, B. G., Lin, C.-S., and Wu, V. C. H., "Simultaneous Colorimetric Detection of a Variety of Salmonella Spp. in Food and Environmental Samples by Optical Biosensing Using Oligonucleotide-Gold Nanoparticles," Front. Microbiol., 2019, 10, DOI: 10.3389/fmicb.2019.01138.

[41] Caliskan-Aydogan, O., Sharief, S. A., and Alocilja, E. C., "Nanoparticle-Based Plasmonic Biosensor for the Unamplified Genomic Detection of Carbapenem-Resistant Bacteria," Diagnostics, 2023, 13(4), DOI: 10.3390/diagnostics13040656.

[42] Dester, E., and Alocilja, E., "Current Methods for Extraction and Concentration of Foodborne Bacteria with Glycan-Coated Magnetic Nanoparticles: A Review," Biosensors, 2022, 12(2), p. 112, DOI: 10.3390/bios12020112.

[43] Suh, S. H., Jaykus, L. A., and Brehm-Stecher, B., *Advances in Separation and Concentration of Microorganisms from Food Samples*, Woodhead Publishing Limited, 2013, DOI: 10.1533/9780857098740.3.173.

[44] Alizadeh, M., Wood, R. L., Buchanan, C. M., Bledsoe, C. G., Wood, M. E., McClellan, D. S., Blanco, R., Ravsten, T. V., Husseini, G. A., Hickey, C. L., Robison, R. A., and Pitt, W. G., "Rapid Separation of Bacteria from Blood – Chemical Aspects," Colloids Surfaces B Biointerfaces, 2017, 154, pp. 365–372, DOI: 10.1016/j.colsurfb.2017.03.027.

[45] Pitt, W. G., Alizadeh, M., Husseini, G. A., McClellan, D. S., Buchanan, C. M., Bledsoe, C. G., Robison, R. A., Blanco, R., Roeder, B. L., Melville, M., and Hunter, A. K., "Rapid

Separation of Bacteria from Blood-Review and Outlook," Biotechnol. Prog., 2016, 32(4), pp. 823–839, DOI: 10.1002/btpr.2299.

[46] Benoit, P. W., and Donahue, D. W., "Methods for Rapid Separation and Concentration of Bacteria in Food That Bypass Time-Consuming Cultural Enrichment," J. Food Prot., 2003, 66(10), pp. 1935–1948, DOI: 10.4315/0362-028X-66.10.1935.

[47] Dwivedi, H. P., and Jaykus, L.-A., "Detection of Pathogens in Foods: The Current State-of-the-Art and Future Directions," Crit. Rev. Microbiol., 2011, 37(1), pp. 40–63, DOI: 10.3109/1040841X.2010.506430.

[48] Li, Z., Ma, J., Ruan, J., and Zhuang, X., "Using Positively Charged Magnetic Nanoparticles to Capture Bacteria at Ultralow Concentration," Nanoscale Res. Lett., 2019, 14, DOI: 10.1186/s11671-019-3005-z.

[49] Kearns, H., Goodacre, R., Jamieson, L. E., Graham, D., and Faulds, K., "SERS Detection of Multiple Antimicrobial-Resistant Pathogens Using Nanosensors," Anal. Chem., 2017, 89(23), pp. 12666–12673, DOI: 10.1021/acs.analchem.7b02653.

[50] Nemr, C. R., Smith, S. J., Liu, W., Mepham, A. H., Mohamadi, R. M., Labib, M., and Kelley, S. O., "Nanoparticle-Mediated Capture and Electrochemical Detection of Methicillin-Resistant Staphylococcus Aureus," Anal. Chem., 2019, DOI: 10.1021/acs.analchem.8b04792.

[51] Wang, J., Yang, W., Peng, Q., Han, D., Kong, L., Fan, L., Zhao, M., and Ding, S., "Rapid Detection of Carbapenem-Resistant Enterobacteriaceae Using PH Response Based on Vancomycin-Modified Fe3O4@Au Nanoparticle Enrichment and the Carbapenemase Hydrolysis Reaction," Anal. Methods, 2019, 12(1), pp. 104–111, DOI: 10.1039/c9ay02196e.

[52] Bohara, R. A., and Pawar, S. H., "Innovative Developments in Bacterial Detection with Magnetic Nanoparticles," Appl. Biochem. Biotechnol., 2015, 176(4), pp. 1044–1058, DOI: 10.1007/s12010-015-1628-9.

[53] Boodoo, C., Dester, E., Sharief, S. A., and Alocilja, E. C., "Influence of Biological and Environmental Factors in the Extraction and Concentration of Foodborne Pathogens Using Glycan-Coated Magnetic Nanoparticles," J. Food Prot., 2023, 86(4), p. 100066, DOI: 10.1016/j.jfp.2023.100066.

[54] Matta, L. L., Harrison, J., Deol, G. S., and Alocilja, E. C., "Carbohydrate-Functionalized Nanobiosensor for Rapid Extraction of Pathogenic Bacteria Directly from Complex Liquids with Quick Detection Using Cyclic Voltammetry," IEEE Trans. Nanotechnol., 2018, 17(5), pp. 1006–1013, DOI: 10.1109/TNANO.2018.2841320.

[55] Matta, L. L., and Alocilja, E. C., "Carbohydrate Ligands on Magnetic Nanoparticles for Centrifuge-Free Extraction of Pathogenic Contaminants in Pasteurized Milk," J. Food Prot., 2018, 81(12), pp. 1941–1949, DOI: 10.4315/0362-028X.JFP-18-040.

[56] Sharief, S. A., Caliskan-Aydogan, O., and Alocilja, E., "Carbohydrate-Coated Magnetic and Gold Nanoparticles for Point-of-Use Food Contamination Testing," Biosens. Bioelectron. X, 2023, 13(November 2022), p. 100322, DOI: 10.1016/j.biosx.2023.100322.

[57] Sharief, S. A., Caliskan-Aydogan, O., and Alocilja, E. C., "Carbohydrate-Coated Nanoparticles for PCR-Less Genomic Detection of Salmonella from Fresh Produce," Food Control, 2023, 150(January), p. 109770, DOI: 10.1016/j.foodcont.2023.109770.

[58] Caliskan-Aydogan, O., Sharief, S. A., and Alocilja, E. C., "Rapid Isolation of Low-Level Carbapenem-Resistant E. Coli from Water and Foods Using Glycan-Coated Magnetic Nanoparticles," Biosensors, 2023, 13(10), p. 902, DOI: 10.3390/bios13100902.

[59] Munita, J. M., and Arias, C. A., "Mechanisms of Antibiotic Resistance," Virulence Mech. Bact. Pathog., 2016, 4(2), pp. 481–511, DOI: 10.1128/9781555819286.ch17.

[60] Guerra, B., Fischer, J., and Helmuth, R., "An Emerging Public Health Problem: Acquired Carbapenemase-Producing Microorganisms Are Present in Food-Producing Animals, Their Environment, Companion Animals and Wild Birds," Vet. Microbiol., 2014, 171(3–4), pp. 290–297, DOI: 10.1016/j.vetmic.2014.02.001.

[61] Nair, D. V. T., Venkitanarayanan, K., and Johny, A. K., "Antibiotic-Resistant Salmonella in the Food Supply and the Potential Role of Antibiotic Alternatives for Control," Foods, 2018, 7(10), DOI: 10.3390/foods7100167.

[62] Hamza, D., Dorgham, S., Ismael, E., El-Moez, S. I. A., Elhariri, M., Elhelw, R., and Hamza, E., "Emergence of β-Lactamase- and Carbapenemase- Producing Enterobacteriaceae at Integrated Fish Farms," Antimicrob. Resist. Infect. Control, 2020, 9(1), p. 67, DOI: 10.1186/s13756-020-00736-3.

[63] Bhusal, N., Shrestha, S., Pote, N., and Alocilja, E., "Nanoparticle-Based Biosensing of Tuberculosis, an Affordable and Practical Alternative to Current Methods," Biosensors, 2018, 9(1), p. 1, DOI: 10.3390/bios9010001.

[64] Poirel, L., Walsh, T. R., Cuvillier, V., and Nordmann, P., "Multiplex PCR for Detection of Acquired Carbapenemase Genes," Diagn. Microbiol. Infect. Dis., 2011, 70(1), pp. 119–123, DOI: 10.1016/j.diagmicrobio.2010.12.002.

[65] Srinivasan, S., Aslan, A., Xagoraraki, I., Alocilja, E., and Rose, J. B., "Escherichia Coli, Enterococci, and Bacteroides Thetaiotaomicron QPCR Signals through Wastewater and Septage Treatment," Water Res., 2011, 45(8), pp. 2561–2572, DOI: 10.1016/j.watres.2011.02.010.

[66] Anderson, M. J., Torres-Chavolla, E., Castro, B. A., and Alocilja, E. C., "One Step Alkaline Synthesis of Biocompatible Gold Nanoparticles Using Dextrin as Capping Agent," J. Nanoparticle Res., 2011, 13(7), pp. 2843–2851, DOI: 10.1007/s11051-010-0172-3.

[67] Abd El-Atty, N. S., and Meshref, A. M. S., "Prevalence of Salmonella and E.Coli O157 in

Some Foods," J. Vet. Med. Res., 2008, 18(1), pp. 73–78, DOI: 10.21608/jvmr.2008.77848.

[68] Matta, L. L., and Alocilja, E. C., "Emerging Nano-Biosensing with Suspended MNP Microbial Extraction and EANP Labeling," Biosens. Bioelectron., 2018, 117(July), pp. 781–793, DOI: 10.1016/j.bios.2018.07.007.

[69] Huang, Y.-F., Wang, Y.-F., and Yan, X.-P., "Amine-Functionalized Magnetic Nanoparticles for Rapid Capture and Removal of Bacterial Pathogens," Environ. Sci. Technol., 2010, 44(20), pp. 7908–7913, DOI: 10.1021/es102285n.

[70] Hu, S., Niu, L., Zhao, F., Yan, L., Nong, J., Wang, C., Gao, N., Zhu, X., Wu, L., Bo, T., Wang, H., and Gu, J., "Identification of Acinetobacter Baumannii and Its Carbapenem-Resistant Gene BlaOXA-23-like by Multiple Cross Displacement Amplification Combined with Lateral Flow Biosensor," Sci. Rep., 2019, 9(1), p. 17888, DOI: 10.1038/s41598-019-54465-8.

[71] Jin, N. Z., Anniebell, S., Gopinath, S. C. B., and Chen, Y., "Variations in Spontaneous Assembly and Disassembly of Molecules on Unmodified Gold Nanoparticles," Nanoscale Res. Lett., 2016, 11(1), p. 399, DOI: 10.1186/s11671-016-1615-2.

[72] Sohn, J. S., Kwon, Y. W., Jin, J. Il, and Jo, B. W., "DNA-Templated Preparation of Gold Nanoparticles," Molecules, 2011, 16(10), pp. 8143–8151, DOI: 10.3390/molecules16108143.

[73] Boodoo, C., Dester, E., David, J., Patel, V., KC, R., and Alocilja, E. C., "Multi-Probe Nano-Genomic Biosensor to Detect S. Aureus from Magnetically-Extracted Food Samples," Biosensors, 2023, 13(6), p. 608, DOI: 10.3390/bios13060608.

[74] Vaisocherová-Lísalová, H., Víšová, I., Ermini, M. L., Špringer, T., Song, X. C., Mrázek, J., Lamačová, J., Scott Lynn, N., Šedivák, P., and Homola, J., "Low-Fouling Surface Plasmon Resonance Biosensor for Multi-Step Detection of Foodborne Bacterial Pathogens in Complex Food Samples," Biosens. Bioelectron., 2016, 80, pp. 84–90, DOI: 10.1016/j.bios.2016.01.040.

[75] Triplett, O. A., Xuan, J., Foley, S., Nayak, R., and Tolleson, W. H., "Immunomagnetic Capture of Big Six Shiga Toxin–Producing Escherichia Coli Strains in Apple Juice with Detection by Multiplex Real-Time PCR Eliminates Interference from the Food Matrix," J. Food Prot., 2019, 82(9), pp. 1512–1523, DOI: 10.4315/0362-028X.JFP-19-134.

[76] Li, J., Wang, C., Shi, L., Shao, L., Fu, P., Wang, K., Xiao, R., Wang, S., and Gu, B., "Rapid Identification and Antibiotic Susceptibility Test of Pathogens in Blood Based on Magnetic Separation and Surface-Enhanced Raman Scattering," Microchim. Acta, 2019, 186(7), p. 475, DOI: 10.1007/s00604-019-3571-x.

[77] Ochoa, M. L., and Harrington, P. B., "Immunomagnetic Isolation of Enterohemorrhagic Escherichia c Oli O157:H7 from Ground Beef and Identification by Matrix-Assisted Laser Desorption/Ionization Time-of-Flight Mass Spectrometry and Database Searches," Anal.

Chem., 2005, 77(16), pp. 5258–5267, DOI: 10.1021/ac0502596.

[78] Quintela, I. A., de los Reyes, B. G., Lin, C.-S., and Wu, V. C. H., "Simultaneous Direct Detection of Shiga-Toxin Producing Escherichia Coli (STEC) Strains by Optical Biosensing with Oligonucleotide-Functionalized Gold Nanoparticles," Nanoscale, 2015, 7(6), pp. 2417–2426, DOI: 10.1039/C4NR05869K.

[79] Poirel, L., Barbosa-Vasconcelos, A., Simões, R. R., Da Costa, P. M., Liu, W., and Nordmann, P., "Environmental KPC-Producing Escherichia Coli Isolates in Portugal," Antimicrob. Agents Chemother., 2012, 56(3), pp. 1662–1663, DOI: 10.1128/AAC.05850-11.

[80] Zhang, X., Lü, X., and Zong, Z., "Enterobacteriaceae Producing the KPC-2 Carbapenemase from Hospital Sewage," Diagn. Microbiol. Infect. Dis., 2012, 73(2), pp. 204–206, DOI: 10.1016/j.diagmicrobio.2012.02.007.

[81] Isozumi, R., Yoshimatsu, K., Yamashiro, T., Hasebe, F., Nguyen, B. M., Ngo, T. C., Yasuda, S. P., Koma, T., Shimizu, K., and Arikawa, J., "Bla NDM-1 –Positive Klebsiella Pneumoniae from Environment, Vietnam," Emerg. Infect. Dis., 2012, 18(8), DOI: 10.3201/eid1808.111816.

[82] Lepuschitz, S., Schill, S., Stoeger, A., Pekard-Amenitsch, S., Huhulescu, S., Inreiter, N., Hartl, R., Kerschner, H., Sorschag, S., Springer, B., Brisse, S., Allerberger, F., Mach, R. L., and Ruppitsch, W., "Whole Genome Sequencing Reveals Resemblance between ESBL-Producing and Carbapenem Resistant Klebsiella Pneumoniae Isolates from Austrian Rivers and Clinical Isolates from Hospitals," Sci. Total Environ., 2019, 662, pp. 227–235, DOI: 10.1016/j.scitotenv.2019.01.179.

[83] Tanner, W. D., VanDerslice, J. A., Goel, R. K., Leecaster, M. K., Fisher, M. A., Olstadt, J., Gurley, C. M., Morris, A. G., Seely, K. A., Chapman, L., Korando, M., Shabazz, K.-A., Stadsholt, A., VanDeVelde, J., Braun-Howland, E., Minihane, C., Higgins, P. J., Deras, M., Jaber, O., Jette, D., and Gundlapalli, A. V., "Multi-State Study of Enterobacteriaceae Harboring Extended-Spectrum Beta-Lactamase and Carbapenemase Genes in U.S. Drinking Water," Sci. Rep., 2019, 9(1), p. 3938, DOI: 10.1038/s41598-019-40420-0.

[84] Hoelle, J., Johnson, J. R., Johnston, B. D., Kinkle, B., Boczek, L., Ryu, H., and Hayes, S., "Survey of US Wastewater for Carbapenem-Resistant Enterobacteriaceae," J. Water Health, 2019, 17(2), pp. 219–226, DOI: 10.2166/wh.2019.165.

[85] Sugawara, Y., Hagiya, H., Akeda, Y., Aye, M. M., Myo Win, H. P., Sakamoto, N., Shanmugakani, R. K., Takeuchi, D., Nishi, I., Ueda, A., Htun, M. M., Tomono, K., and Hamada, S., "Dissemination of Carbapenemase-Producing Enterobacteriaceae Harbouring BlaNDM or BlaIMI in Local Market Foods of Yangon, Myanmar," Sci. Rep., 2019, 9(1), p. 14455, DOI: 10.1038/s41598-019-51002-5.

[86] Roschanski, N., Guenther, S., Vu, T. T. T., Fischer, J., Semmler, T., Huehn, S., Alter, T., and Roesler, U., "VIM-1 Carbapenemase-Producing Escherichia Coli Isolated from Retail Seafood, Germany 2016," Eurosurveillance, 2017, 22(43), pp. 1–7, DOI: 10.2807/1560-

7917.ES.2017.22.43.17-00032.

[87] Wang, J., Yao, X., Luo, J., Lv, L., Zeng, Z., and Liu, J. H., “Emergence of Escherichia Coli Coproducing NDM-1 and KPC-2 Carbapenemases from a Retail Vegetable, China,” J. Antimicrob. Chemother., 2018, 73(1), pp. 252–254, DOI: 10.1093/jac/dkx335.

[88] Touati, A., Mairi, A., Baloul, Y., Lalaoui, R., Bakour, S., Thighilt, L., Gharout, A., and Rolain, J.-M., “First Detection of Klebsiella Pneumoniae Producing OXA-48 in Fresh Vegetables from Béjaïa City, Algeria,” J. Glob. Antimicrob. Resist., 2017, 9, pp. 17–18, DOI: 10.1016/j.jgar.2017.02.006.

[89] Liu, B.-T., Zhang, X.-Y., Wan, S.-W., Hao, J.-J., Jiang, R.-D., and Song, F.-J., “Characteristics of Carbapenem-Resistant Enterobacteriaceae in Ready-to-Eat Vegetables in China,” Front. Microbiol., 2018, 9(JUN), DOI: 10.3389/fmicb.2018.01147.

[90] Chaalal, N., Touati, A., Bakour, S., Aissa, M. A., Sotto, A., Lavigne, J. P., and Pantel, A., “Spread of OXA-48 and NDM-1-Producing Klebsiella Pneumoniae ST48 and ST101 in Chicken Meat in Western Algeria,” Microb. Drug Resist., 2021, 27(4), pp. 492–500, DOI: 10.1089/mdr.2019.0419.

[91] Briceno, R. K., Sergent, S. R., Benites, S. M., and Alocilja, E. C., “Nanoparticle-Based Biosensing Assay for Universally Accessible Low-Cost Tb Detection with Comparable Sensitivity as Culture,” Diagnostics, 2019, 9(4), DOI: 10.3390/diagnostics9040222.

[92] Lau, H. K., Clotilde, L. M., Lin, A. P., Hartman, G. L., and Lauzon, C. R., “Comparison of IMS Platforms for Detecting and Recovering Escherichia Coli O157 and Shigella Flexneri in Foods,” SLAS Technol., 2013, 18(2), pp. 178–183, DOI: 10.1177/2211068212468583.

[93] Mohamed A. Abdou Mohamed, Kozlowski, H. N., Kim, J., Zagorovsky, K., Kantor, M., Feld, J. J., Mubareka, S., Mazzulli, T., and Chan, W. C. W., “Diagnosing Antibiotic Resistance UsingNucleic Acid Enzymes and Gold Nanoparticles,” 2021.

CHAPTER 7: CONCLUSIONS AND FUTURE WORKS

7.1. Conclusions

The information and data collected throughout this dissertation indicate the potential of the nanoparticle-based biosensing platform for simple, rapid, and cost-effective extraction and detection of carbapenem-resistant bacteria, specifically carbapenemase-producing (CP) *E. coli*. The glycan-coated magnetic nanoparticles (gMNPs) were used for bacterial isolation, and the dextrin-coated gold nanoparticles (dGNPs) were used for genomic detection as a plasmonic (colorimetric) biosensor. This study further elaborated on the use of the combined platform for the detection of target bacteria from water and food samples within a seven-hour workday.

The experimental design integrated the gMNP and dGNP platform (Chapter 2). The properties and characteristics of the nanoparticles were assessed in the extraction and detection of target bacteria. Specifically, gMNPs were first evaluated for isolation of several CP *E. coli* isolates from buffer solution, along with an analysis of bacterial cell surface characteristics (Chapter 3). The interaction of gMNPs with CP *E. coli* was confirmed through plating and microscopy. The gMNPs-bacteria binding capacity (Concentration Factor: CF) of CP *E. coli* isolates was found to be different from carbapenem-susceptible *E. coli*, which could be due to differences in the cell surface characteristics (cell morphology and cell surface charge). Further, the applicability of gMNPs was tested in large-volume biological samples (Chapter 4). This study notably illustrated that the gMNPs successfully extracted the CP *E. coli* from artificially contaminated tap water and food samples (raw chicken breast, ground beef, and romaine lettuce) in the presence of natural microflora and food microparticles, confirmed using the selective plating method. Herein, it was noted that target bacterial extraction and concentration among the tested food matrices were lower from buffer solution and variable, which could be associated with bacterial types, natural microflora, chemical constituents, and physical microstructure of the tested matrices. This study further confirmed that non-selective gMNPs contribute toward the simple and rapid isolation of antimicrobial-resistant bacteria (ARB), specifically CP *E. coli*, showing their broad applicability. For specific detection of target bacteria, a rapid detection method was further conducted.

A plasmonic biosensor assay using dGNPs was first specifically designed for feasible rapid detection (Chapter 5). The proof-of-concept of the biosensor was achieved using a bla_{KPC} probe to detect CP bacteria, specifically *Klebsiella pneumoniae* carbapenemase (KPC)-producing

bacteria from pure cultures, confirmed with PCR tests. The stability of dGNPs (red in color) indicated the presence of target DNA, while the agglomeration of dGNPs (blue or purple in color) resulted in the absence of target DNA. The designed plasmonic biosensor successfully detected the KPC gene in several bacteria regardless of bacterial type, with 79% sensitivity and 97% specificity. For specific bacterial detection, the previously developed biosensor using the *uidA* probe for *E. coli* detection was further assessed (Chapter 6). The use of two biosensors offered successful detection of KPC-producing *E. coli*, which were further verified with the standard PCR tests. The plasmonic biosensor provided visual detection within 30 minutes without the necessity of PCR amplification and complex equipment and data analysis, displaying their broad accessibility. The applicability of the biosensor platform with real samples was further tested.

Finally, this study integrated magnetic extraction and plasmonic biosensor to identify KPC-producing *E. coli* from matrices (contaminated tap water and the food samples) in the presence of food microparticles and natural microflora (Chapter 6). First, magnetically extracted bacterial cells from the selected matrices were followed by short enrichment and DNA extraction. Then, the developed plasmonic biosensor assay successfully detected KPC-producing *E. coli* by simultaneously detecting *uidA* and bla_{KPC} genes. Biosensor results were further confirmed with the standard PCR tests. The combined platform (magnetic extraction (15 min), short enrichment time (5 h), and genomic detection (<1 h) proved the capabilities for accessible and affordable detection within a seven-hour workday. The integrated platform is noteworthy, allowing for simplicity, affordability, and accessibility in resource-limited settings.

7.2. Future Works

This dissertation offers several opportunities to be extended in future works. The extensive literature review (Chapter 1) acknowledges many challenges in the detection of antimicrobial-resistant bacteria, specifically CRE, and insufficient studies and information on the isolation of these bacteria from real samples, along with their cell surface characteristics. This work shares a rich database of experiments and concepts on bacterial cell surface characteristics, bacterial isolation, and detection of carbapenem-resistant bacteria, which is a priority for future studies. Although this study establishes only proof-of-concept of the magnetic extraction and biosensor-based detection of carbapenem-resistant *E. coli*, future works are required to optimize this technology to prepare for real-world applicability and accessibility, as discussed below.

This work assessed the interaction of gMNPs with several CP *E. coli* isolates, along with their cell surface characteristics; the observed cell surface characteristics and gMNP-cell interaction shed light on their attachment properties, although only one susceptible *E. coli* isolate as reference bacteria (control) was used. To further elucidate and differentiate the behavior of resistant and susceptible *E. coli* cells, the inclusion of more susceptible *E. coli* types/serotypes such as non-pathogenic, intestinal pathogenic *E. coli*, and extraintestinal pathogenic *E. coli* (ExPEC) should be explored. Additionally, biofilm-forming *E. coli* types, regardless of susceptibility status, should be further explored to determine whether the biofilm matrix hinders the interaction of gMNP with the bacteria. Further, the gMNPs need to be tested on other CREs, such as *Enterobacter* and *Klebsiella* species, as well as other common ARB isolates (methicillin-resistant Staphylococcus aureus, vancomycin-resistant *Enterococcus*, etc.) which can assist in a deeper understanding of the gMNP-bacteria interaction. Last but not least, to improve the efficacy of gMNPs, particles may be further functionalized with biomolecules such as amine groups to increase their positive surface and improve their interaction with bacterial species.

Another progression of this work is to assess the applicability of gMNPs in large-volume biological samples, as there is no existing study in the literature on the extraction of ARB from foods, including CRE. However, this study displayed the successful bacterial extraction in water and food samples inoculated with only one inoculum level (10^5 CFU/mL) of the bacterial species; further studies are required to optimize the gMNP-based magnetic extraction. Such studies may include 1) assessment of target bacterial concentration from contaminated matrices with different inoculum levels and 2) evaluation of the attachment capacity of gMNPs with other bacterial species (natural microflora) using different selective media to determine which bacterial type(s) may out-compete the target bacteria for MNP adhesion. Further, this study can be extended to test more solid or liquid food samples or samples directly from farms and animals. Moreover, this study can be expanded to extract different types of CRE, other ARB, and pathogens from various matrices (clinical, biological, and environmental samples). However, it should be noted that background microflora and matrix type, in some cases, could interfere with the success of bacterial extraction and detection. Herein, optimization of the gMNP-based magnetic extraction may be improved through modification of the upstream concentration process, such as 1) washing the extracted sample in buffer solution (PBS) and repeating magnetic extraction might reduce the particulates, 2) enrichment in selective media or antibiotic-

added TSBs may be used to dominate the growth of bacteria interests and suppress background microflora, and 3) gMNPs may be aminated for more efficient bacterial capture as earlier mentioned, or species-specific glycan may be used to capture the target bacteria selectively. Although successful magnetic extraction is conducted in matrices, the presence of natural microflora and microparticles might impact the efficiency and success of many detection assays. The magnetically extracted bacteria from complex matrices may be further used in different detection assays to ensure their compatibility.

While simple procedures and low-cost materials are already utilized in this assay, further applications may optimize the assay. For example, although the sensitivity of the biosensor was tested by comparing the target and non-target at a concentration of 1-20 ng/μL, further sensitivity tests can be conducted to compare the target at 1 ng/μL to the non-target at higher concentrations, up to 100 ng/μL. In addition, the biosensor specificity tests can be extended to include more bacterial types and a mixed population of target and non-target DNA samples. While this assay showed higher specificity (97%) and good sensitivity (79%) using a probe for the most common type of KPC variant in the USA, this platform's accuracy can be further improved by designing a more specific probe for the KPC variant. Also, there are possibly more than 80 KPC variants worldwide, as mentioned in the literature; specific probes for different KPC variants, depending on their prevalence in the geographical area, can be designed and tested. Further, this assay can be extended to design specific probes for other carbapenemase variants (NDM, VIM, OXA-48, etc.) and other antibiotic-resistant bacteria (colistin, ampicillin, ESBL, etc.). Last but not least, the assay can also be developed for multiplex detection of several target genes, which might offer broad-range detection of other carbapenemase variants.

Further studies can optimize this platform to detect target bacteria from contaminated matrices with different inoculum levels (dilution series of 10-10^7 CFU/mL), along with the relationship between inoculum level (log CFU/mL) and corresponding target DNA concentration. Further, this platform can be extended to test more matrices, such as samples from wastewater plants, farms, slaughterhouses, and clinical samples. While this developed integrated platform offers rapid and simple detection without complex and costly equipment, significant supplies and equipment still needed in this assay were DNA extraction kits, a thermocycler, and NanoDrop. These obstacles may be addressed with the following options: 1) DNA extraction kits can be replaced using chemical lysis or heat treatment, 2) thermocycler can be replaced with a

programmable heating block or water bath, and 3) a smartphone application can replace the NanoDrop. Further, the prepared large-volume batches of gMNPs, dGNPs, and probes can be transported to points as needed for the field-based application of this assay. The platform is not designed as a self-contained detection kit but takes advantage of easy and rapid preparation as well as a yes/no response (visual results), which would highly assist limited-resource settings.

In closing, with future works, the rapid biosensing platform developed in this dissertation has the potential to improve food and water safety, leading to healthy people and a sustainable economy.